The Handbook of Environmental Chemistry 88
Series Editors: Damià Barceló · Andrey G. Kostianoy

Pankaj Pathak
Dharmendra K. Gupta *Editors*

Strontium Contamination in the Environment

Springer

The Handbook of Environmental Chemistry

Founding Editor: Otto Hutzinger

Volume 88

More information about this series at http://www.springer.com/series/698

Strontium Contamination in the Environment

Volume Editors: Pankaj Pathak · Dharmendra K. Gupta

With contributions by

S. Chatterjee · I. A. Cheshyk · D. Garbaruk · D. K. Gupta · N. Ilyas · S. Ilyas · S. A. Kalinichenko · G. Keceli · N. Koshy · M. Kudzin · L. N. Mikhailovskaya · S. Mishra · A. Mitra · T. A. Nedobukh · A. N. Nikitin · P. Pathak · V. N. Pozolotina · V. S. Semenishchev · S. Sharma · O. A. Shurankova · R. R. Srivastava · A. Uhlianets · A. V. Voronina · C. Walther · V. Zabrotski

Springer

Editors
Pankaj Pathak
Marwadi University
Department of Environmental Science & Engineering
Rajkot, Gujarat, India

Dharmendra K. Gupta
Institut für Radioökologie und Strahlenschutz (IRS)
Gottfried Wilhelm Leibniz Universität Hannover
Hannover, Germany

ISSN 1867-979X ISSN 1616-864X (electronic)
The Handbook of Environmental Chemistry
ISBN 978-3-030-15313-7 ISBN 978-3-030-15314-4 (eBook)
https://doi.org/10.1007/978-3-030-15314-4

This Springer imprint is published by the registered company Springer Nature Switzerland AG
The registered company address is: Gewerbestrasse 11, 6330 Cham, Switzerland

The Handbook of Environmental Chemistry Also Available Electronically

The Handbook of Environmental Chemistry is included in Springer's eBook package *Earth and Environmental Science*. If a library does not opt for the whole package, the book series may be bought on a subscription basis.

For all customers who have a standing order to the print version of *The Handbook of Environmental Chemistry*, we offer free access to the electronic volumes of the Series published in the current year via SpringerLink. If you do not have access, you can still view the table of contents of each volume and the abstract of each article on SpringerLink (www.springerlink.com/content/110354/).

You will find information about the

– Editorial Board
– Aims and Scope
– Instructions for Authors
– Sample Contribution

at springer.com (www.springer.com/series/698).

All figures submitted in color are published in full color in the electronic version on SpringerLink.

Aims and Scope

Since 1980, *The Handbook of Environmental Chemistry* has provided sound and solid knowledge about environmental topics from a chemical perspective. Presenting a wide spectrum of viewpoints and approaches, the series now covers topics such as local and global changes of natural environment and climate; anthropogenic impact on the environment; water, air and soil pollution; remediation and waste characterization; environmental contaminants; biogeochemistry; geoecology; chemical reactions and processes; chemical and biological transformations as well as physical transport of chemicals in the environment; or environmental modeling. A particular focus of the series lies on methodological advances in environmental analytical chemistry.

Series Preface

With remarkable vision, Prof. Otto Hutzinger initiated *The Handbook of Environmental Chemistry* in 1980 and became the founding Editor-in-Chief. At that time, environmental chemistry was an emerging field, aiming at a complete description of the Earth's environment, encompassing the physical, chemical, biological, and geological transformations of chemical substances occurring on a local as well as a global scale. Environmental chemistry was intended to provide an account of the impact of man's activities on the natural environment by describing observed changes.

While a considerable amount of knowledge has been accumulated over the last four decades, as reflected in the more than 150 volumes of *The Handbook of Environmental Chemistry*, there are still many scientific and policy challenges ahead due to the complexity and interdisciplinary nature of the field. The series will therefore continue to provide compilations of current knowledge. Contributions are written by leading experts with practical experience in their fields. *The Handbook of Environmental Chemistry* grows with the increases in our scientific understanding, and provides a valuable source not only for scientists but also for environmental managers and decision-makers. Today, the series covers a broad range of environmental topics from a chemical perspective, including methodological advances in environmental analytical chemistry.

In recent years, there has been a growing tendency to include subject matter of societal relevance in the broad view of environmental chemistry. Topics include life cycle analysis, environmental management, sustainable development, and socio-economic, legal and even political problems, among others. While these topics are of great importance for the development and acceptance of *The Handbook of Environmental Chemistry*, the publisher and Editors-in-Chief have decided to keep the handbook essentially a source of information on "hard sciences" with a particular emphasis on chemistry, but also covering biology, geology, hydrology and engineering as applied to environmental sciences.

The volumes of the series are written at an advanced level, addressing the needs of both researchers and graduate students, as well as of people outside the field of "pure" chemistry, including those in industry, business, government, research

establishments, and public interest groups. It would be very satisfying to see these volumes used as a basis for graduate courses in environmental chemistry. With its high standards of scientific quality and clarity, *The Handbook of Environmental Chemistry* provides a solid basis from which scientists can share their knowledge on the different aspects of environmental problems, presenting a wide spectrum of viewpoints and approaches.

The Handbook of Environmental Chemistry is available both in print and online via www.springerlink.com/content/110354/. Articles are published online as soon as they have been approved for publication. Authors, Volume Editors and Editors-in-Chief are rewarded by the broad acceptance of *The Handbook of Environmental Chemistry* by the scientific community, from whom suggestions for new topics to the Editors-in-Chief are always very welcome.

Damià Barceló
Andrey G. Kostianoy
Editors-in-Chief

Preface

Strontium (Sr) is a common earth metal found in rocks, in soil water and in air. Generally, strontium is found as a non-radioactive metal in natural origin and has four stable isotopes, i.e. ^{84}Sr, ^{86}Sr, ^{87}Sr and ^{88}Sr. Additionally, there are 28 unstable radioactive isotopes; amongst them ^{90}Sr is most significant one; it emits β rays with a half-life of 28.9 years. ^{90}Sr is produced in nuclear reactors and during the explosion of nuclear weapons. In nature, Sr is found as a mineral ore, such as celestite ($SrSO_4$) and strontianite ($SrCO_3$). After Sr is extracted from the ore, it is concentrated into strontium carbonate or other chemical forms by a sequence of chemical processes, and further it may be used in various industries including ceramics, paint pigments, fluorescent lights and medicines.

The study on Sr contamination became more important after two major nuclear power plants accidents, i.e. Chernobyl Power Plant accident in 1986 (about 30,000 km^2 of agricultural and forest land were contaminated with >10 kBq/m^2 of ^{90}Sr) and Fukushima Nuclear Power Plant accident in year 2011 (the total activity of ^{90}Sr in seawater reached up to 1,500,000 Bq/m^3 at the Fukushima plant port). Apart from major nuclear power plant accidents till 1980, due to atmospheric nuclear weapon testing, roughly 6×10^{17} Bq of ^{90}Sr were produced and worldwide dispersed [1].

The detrimental properties of radioactive Sr are mainly due to high radiation energy. Sr is amalgamated into the human bones by exchanging calcium ions in the hydroxyapatite crystal lattice, as both Ca and Sr are homologous alkaline earth metals and of course act likewise in the atmosphere. It is also a well-known fact that Sr is highly available in plants due to the formation of water-soluble complexes. The basic way of regulatory movement of radionuclides (and additional trace constituents) in soil involves convective transportation by flowing water, distribution caused by spatial variations of convection velocities, diffusive crusade within the liquid and occasionally physicochemical interactions with soil matrix [2]. Once radionuclides are deposited on the soil surface, their movement and relocation in the soil can be determined by elementary soil properties which include pH, texture, interchangeable Ca and K and organic matters which are present in the soil [1]. Further these radionuclides which adhered onto soil ultimately enter into the soil

network and then taken up by plants through food chain and finally relocate to animals including humans [3].

The utmost remarkable structures of this book are associated with how strontium comes into the environment and its translocation from soil to plants and lastly to animals including humans. Chapters 'Strontium: Source, Occurrence, Properties, and Detection' and 'Isotopes of Strontium: Properties and Applications' deal with different isotopes of strontium and its presence in the environment, detection and application. Chapters 'Strontium Extraction from the Geo-environment' and 'Biosorption of Strontium from Aqueous Solutions' emphasize different modes of strontium extraction from the environment. Chapter 'Plant Response Under Strontium and Phytoremediation' focuses on strontium toxicity and its responses in animals and in plants. Chapters 'Uptake, Transport, and Remediation of Strontium', 'Spatial Distribution of ^{90}Sr in the Ecosystems of Polesye State Radiation-Ecological Reserve', 'Spatial Distribution of ^{90}Sr from Different Sources in Soils of the Ural Region, Russia' and '^{90}Sr in the Components of Pine Forests of Belarusian Part of Chernobyl NPP Exclusion Zone' give attention to uptake mechanism and different remediation methods, with three experimental project statements on Polesie State Radioecological Reserve, Belarus; Urals region of Russia; and Belarusian part of exclusion zone of Chernobyl Nuclear Power Plant. Last but not least, the last three chapters ['Removal of Strontium by Physicochemical Adsorptions and Ion Exchange Methods', 'Use of Sorption Method for Strontium Removal' and 'Assessment of the Alkaline Earth Metals (Ca, Sr, Ba) and Their Associated Health Impacts'] discuss different methods of strontium removal from the environment, assessment of other alkaline earth metals and their associated problems along with risk assessment factors. Nevertheless, the material collected in this volume will convey deep knowledge of strontium and its associated problems.

On the whole, the material composed in this book will bring in-depth understanding and extension of knowledge in the field of radionuclide toxicity and its possible remediation techniques. Dr. Pankaj Pathak and Dr. Dharmendra K. Gupta individually acknowledge authors and reviewers for contributing their precious time, knowledge and interest to bring this book into the present shape.

References

1. Gupta DK, Walther C (2018) Behaviour of strontium in plants and the environment. Springer
2. Walther C, Gupta DK (2015) Radionuclides in the environment: influence of chemical speciation and plant uptake on radionuclide migration. Springer
3. Gupta DK, Walther C (2014) Radionuclide contamination and remediation through plants. Springer

Rajkot, India Pankaj Pathak
Hannover, Germany Dharmendra K. Gupta

Contents

Strontium: Source, Occurrence, Properties, and Detection

Tatiana Alexeevna Nedobukh and Vladimir Sergeevich Semenishchev

Contents

Abstract This chapter gives an overview of the properties of strontium as a chemical element, the methods of its determination, data on its abundance in the environment, and its impact on the human organism in daily life. Strontium is one of the alkaline earth group elements, two of which, calcium and magnesium, are among the ten most abundant elements in the Earth's crust. Chemical properties of strontium are analyzed in comparison with properties of other group II elements. The chemical properties of strontium are quite similar to those of calcium and barium, resulting in similar behavior in the environment and biological objects, and also making determination of strontium by chemical methods difficult, especially in environmental samples. Therefore, traditional chemical methods of strontium determination are replaced by modern physical and physicochemical analytical methods that lower the detection limit and simplify sample treatment techniques. This chapter is not focused on radioactive isotopes of strontium, for example, ^{90}Sr, a long-lived beta-emitting fission product causing long-term environmental contamination.

T. A. Nedobukh · V. S. Semenishchev (✉)
Radiochemistry and Applied Ecology Department, Physical Technology Institute, Ural Federal University, Ekaterinburg, Russia
e-mail: vovius82@mail.ru

P. Pathak, D. K. Gupta (eds.), *Strontium Contamination in the Environment*,
The Handbook of Environmental Chemistry 88,
https://doi.org/10.1007/978-3-030-15314-4_1

Because the stable and radioactive isotopes of an element act identically in most physical, chemical, and biological processes, the methods for pre-concentration and separation of strontium in the analytical techniques described here can be used successfully for determination of the radioisotopes of strontium.

Keywords Alkaline earth elements · Chemical properties of strontium · Strontium · Strontium determination · Strontium in the environment

1 Introduction

Strontium was discovered at the end of the eighteenth century. A new mineral that was later called strontianite was found in lead ores near Strontian Village in Scotland. For a long time, it was assumed to be a type of fluorite CaF_2 or witherite $BaCO_3$. In 1790, Adair Crawford and William Cruickshank showed that the strontianite constituted a new "earth," an oxide of an unknown element. In 1791, Thomas Charles Hope determined separately compounds of barium, strontium, and calcium by using, among other methods, typical flame colors: yellow-green for barium, red for strontium, and orange-red for calcium. At the same time, the German chemist Martin Heinrich Klaproth reported the discovery of a new "earth," and the Russian chemist Lovitz separated strontium from barite ($BaSO_4$) and identified it as another element according to the typical color of its flame. Thus, it was demonstrated for the first time that strontium can present as an impurity in minerals of its analogues [1].

Strontium metal was first obtained in 1808 by Humphry Davy, the famous English scientist. Considering the new element to be a reactive alkaline earth, he used electrolysis of the mixture of humidified strontium oxide with HgO for synthesis of strontium metal, that is, by the same method as for obtaining calcium, magnesium, and barium. Strontium metal generated at the cathode interacted with mercury, resulting in formation of an amalgam. By thermal decomposition of the amalgam, Davy obtained pure strontium metal.

Strontium compounds were used in pyrotechnics for red flames even before the discovery of strontium. At the end of the nineteenth century, it had found a wide application as a hydroxide in sugar technology, resulting in significant increase in production and treatment. However, strontium compounds were later replaced by analogue calcium compounds in sugar production. Today, the main applications of strontium are in production of special glass for TV sets and computer monitors (53%), pyrotechnics (14%), and magnetic materials (11%) [2].

2 The Main Chemical Properties of Strontium and Its Compounds

2.1 Common Characteristics

Strontium (Sr) is a chemical element of the second group (Group II: alkaline earth metals) of the periodic table. Its atomic number is 38, and its standard atomic weight is 87.62. Natural strontium consists of four stable isotopes: ^{84}Sr (0.56%), ^{86}Sr (9.86%), ^{87}Sr (7.00%), and ^{88}Sr (82.58%) [3]. The percentage of isotopes in natural strontium varies because of the formation of ^{87}Sr after β-decay of a natural long-lived isotope, ^{87}Rb ($T_{1/2} = 4.75 \times 10^{10}$ years). Therefore, the exact isotopic composition of natural strontium in a rock or a mineral is conditioned by its age and the Rb:Sr ratio in the rock or mineral. Other strontium isotopes are radioactive and are not naturally present in the environment. Electron capture or β^+-decay are typical for isotopes with atomic weights of 85 or less, whereas isotopes with an atomic weight of 89 and more decay by the β-mechanism. The most important of these isotopes are ^{85}Sr and ^{89}Sr, which find application in nuclear medicine; ^{90}Sr is a long-lived fission product that causes environmental contamination as a result of nuclear weapon testing and radiation accidents. The detailed analysis of stable and radioactive isotopes of strontium is given in the corresponding chapter of this book (chapter "Isotopes of Strontium: Properties and Applications").

Strontium is one of the alkaline earth metals, an analogue of beryllium, magnesium, calcium, barium, and radium. Radium is a natural radioactive element; usually, the properties of radium are described separately from other alkaline earth elements and compared with stable elements of this group. Strontium is a typical representative of alkaline earth metals, possessing very similar chemical properties to calcium and barium. Therefore, the individual properties of strontium are often ignored, and its properties are analyzed based on the properties of its analogues. However, comparison of the properties of strontium with other representatives of the alkaline earth elements group is very interesting as it allows finding the tendencies of change in the main properties within the group as related to differences in the chemical properties of strontium. These differences give the basis for technological operations, analytical methods, study of physicochemical behavior in the environment, and participation in biochemical processes.

Table 1 shows the main characteristics of the group II elements, excluding radium. Atomic and ionic radii increase from beryllium to barium, whereas ionization energies and electro-negativity decrease in this series. However, as can be seen from Fig. 1, these characteristics change dramatically from beryllium to calcium and less markedly from calcium to barium. This tendency is repeated in the comparative analysis of the chemical properties of the alkaline earth elements.

Table 1 Main characteristics of the group II elements

Characteristic	^{4}Be	^{12}Mg	^{20}Ca	^{38}Sr	^{56}Ba
Period	2	3	4	5	6
Atomic radius M, Å	1.12	1.60	1.97	2.15	2.22
Ionic radius of M^{2+}, Å	0.27	0.72	1.00	1.18	1.35
Ionization energy I1, eV	9.33	7.63	6.12	5.68	5.20
Ionization energy I2, eV	18.2	15.0	11.9	11.0	10.0
Electronegativity, χ_P	1.57	1.31	1.00	0.95	0.89
Oxidation states	0, 2+	0, 2+	0, 2+	0, 2+	0, 2+

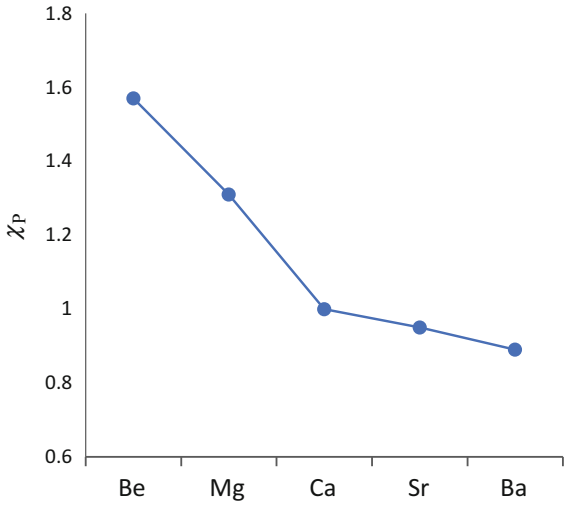

Fig. 1 Electronegativity of group II elements (according to Pauling)

2.2 Strontium Metal

Strontium is a soft silvery-white metal with a pale yellow tinge. At room temperature, strontium has a face-centered cubic crystal lattice (α-Sr); it transforms to hexagonal modification (β-Sr) at 231°C and to body-centered cubic modification (γ-Sr) at 623°C [4]. Table 2 shows some properties of strontium metal compared with other alkaline earth metals. There is a strong difference of properties between beryllium and other elements of the group. Comparison of the melting points shows a sharp difference of these temperatures for beryllium and magnesium in contrast to similarities for calcium, strontium, and barium. Density of metals decreases slightly from beryllium to calcium and then dramatically increases from calcium to barium. The reduction potential of beryllium significantly differs from other metals, whereas potentials of calcium, strontium, and barium are similar (Fig. 2). Thus, calcium, strontium, and barium metals show very similar physical properties or a nearly linear tendency in changes. Strontium is one of the most electronegative metals, showing a

Table 2 Properties of alkaline earth metals

Properties	Be	Mg	Ca	Sr	Ba
Melting point (°C)	1,289	650	842	769	729
Boiling point (°C)	2,472	1,090	1,494	1,382	1,805
Density (g/cm^3)	1.85	1.74	1.55	2.63	3.59
Reduction potential (E°), V $M^{2+}_{aq} + 2\bar{e} \rightarrow M$	−1.97	−2.35	−2.84	−2.89	−2.92
Structural type of crystal lattice at room temperature	Hexagonal		Cubic face-centered		Cubic body-centered

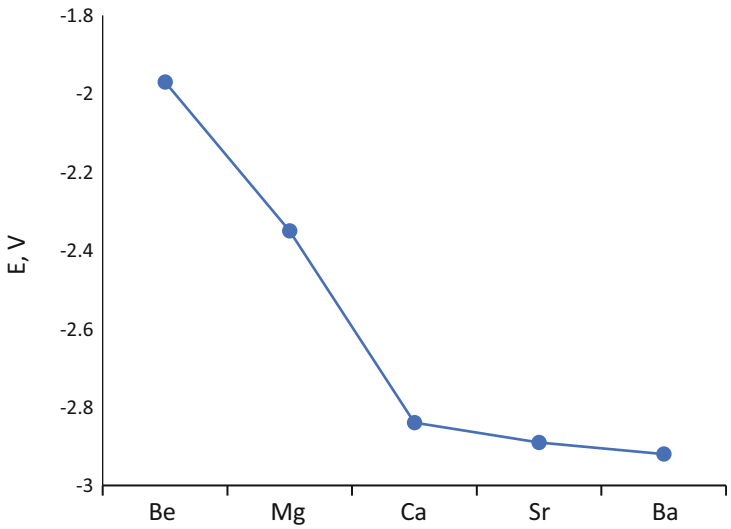

Fig. 2 Reduction potential of alkaline earth elements

high chemical reactivity. The standard electrode potential of −2.89 V indicates that strontium is a strong reducing agent. It is able to displace hydrogen from diluted acids and water as well as reduce most metals from their salts. At room temperature, strontium metal is rapidly oxidized by air, resulting in formation of a yellowish layer on the surface consisting of strontium oxide, SrO, and in lesser degree peroxide, SrO_2, and nitride, Sr_3N_2. Heating strontium in air results in inflammation. Dispersed strontium metal as a powder can ignite in air even at room temperature [4]. Strontium is very resistant against concentrated alkali solutions. Concentrated sulfuric and nitric acids passivate strontium metal, which is rapidly dissolved in diluted acids forming corresponding salts. Among strontium mineral salts, chloride, bromide, iodide, and nitrate are readily soluble in water, whereas fluoride, sulfate, carbonate, and phosphate are sparingly soluble salts. Strontium salts, similar to calcium and barium but in contrast to beryllium and magnesium, are dissolved in liquid ammonia, resulting in formation of dark blue solutions. By evaporation of ammonia, it is

possible to obtain lustrous strontium ammine $Sr(NH_3)_6$ with a copper color, which slowly decomposes to strontium amide $Sr(NH_2)_2$; the decomposition process is accelerated by a catalyst such as platinum metal [2].

Strontium metal can be obtained by electrolysis of a mixture of melted strontium chloride (85%) and potassium or ammonium chloride (15%) on a nickel or iron cathode at 800°C. Strontium obtained by this method usually contains 0.3–0.4% potassium. The high-temperature reduction of strontium oxide can be achieved using aluminum and silicone and ferrosilicon are also used in its high-temperature reduction. The process is conducted at 1,000°C in a steel tube under vacuum. Strontium chloride is reduced by magnesium metal in a hydrogen atmosphere. Similar to other alkaline earth metals, strontium can decontaminate iron alloys from undesirable gases and impurities. Furthermore, strontium is an addition to magnesium, aluminum, lead, nickel, and copper alloys. As strontium metal can adsorb some gases, it is used as a getter in electro-vacuum devices.

2.3 The Most Important Compounds of Strontium

Strontium oxide, SrO, is a white high-melting compound obtained by calcination of carbonate at 1,100°C or by dehydration of hydroxide. Strontium oxide is used as a component of oxide cathodes of electron emitters in electro-vacuum devices as well as in high-temperature superconductors and pyrotechnical mixtures. It was previously added to the glass of CRT monitors and kinescopes for adsorption of X-ray emissions; today, these devices are replaced by LED technologies. Strontium oxide is also used as a raw material to produce strontium metal. Together with calcium and zinc oxides, strontium oxide is used in mat glaze. Strontium glazes are less toxic and cheaper than lead glazes. Products covered by these glazes exhibit additional hardness and thermal and chemical stability. Some enamel is produced using silicone and strontium oxides with the addition of titanium and zinc oxides to increase their opacity. Porcelains may be covered by crackle glazes based on strontium oxide [1].

Strontium peroxide, SrO_2, is formed via oxidizing strontium oxide with oxygen at elevated pressure. Strontium peroxide octahydrate, $SrO_2 \cdot 8H_2O$, can be obtained by interaction of strontium hydroxide solution with hydrogen or sodium peroxide. Heating to 100–130°C results in dehydration of strontium peroxide octahydrate; decomposition of peroxide to oxide with oxygen release is observed at 700–800°C.

Strontium hydroxide, $Sr(OH)_2$, is a moderately strong base obtained by interaction of amorphous strontium oxide with water accompanying heat release. Having a moderate solubility, strontium hydroxide can be also precipitated from salt solution by a concentrated alkali solution, such as NaOH or KOH. Strontium hydroxide forms hydrates in excess of water. Dehydration of monohydrate occurs at 100°C; heating to 400°C results in decomposition of hydroxide and formation of SrO. The solubility of strontium hydroxide in water increases as temperature increases. An

aqueous solution of strontium hydroxide adsorbs CO_2 from air, resulting in the precipitation of strontium carbonate.

Comparison of strontium hydroxide with other alkaline earth hydroxides shows increase of solubility and basicity from Be to Ba: beryllium hydroxide, $Be(OH)_2$, is sparingly soluble and amphoteric; magnesium hydroxide, $Mg(OH)_2$, is a sparingly soluble weak base; calcium and strontium hydroxides, $Ca(OH)_2$ and $Sr(OH)_2$, are moderate bases; and barium hydroxide, $Ba(OH)_2$, is a strong base near to alkalis. Solubility in water at room temperature increases significantly from $Be(OH)_2$ to $Ba(OH)_2$ (Fig. 3). Crystal structures of alkaline earth hydroxides also follow general regularities: the coordination numbers of the central atoms are 4 in beryllium hydroxide, 6 in magnesium and calcium hydroxides, and 7 in strontium hydroxide. These changes of coordination numbers indicate a special structure of corresponding compounds [2].

Strontium halides are formed from the interaction of strontium with halogens or by dissolving strontium hydroxide or carbonate in the corresponding hydrogen halide acid. Among halides, strontium fluoride, SrF_2, takes a special place because of its low solubility in water (nearly 0.12 g l^{-1}) and diluted mineral acids. Strontium fluoride can be dissolved in hot concentrated hydrochloric acid. Other strontium halides dissolve well in water, the solubility increases from chloride to iodide.

Strontium chloride is crystallized from a solution as different hydrates depending on temperature. Hexahydrate $SrCl_2 \cdot 6H_2O$ is stable below 60°C; it loses water with increasing temperature and becomes anhydrous above 250°C. In contrast to calcium chloride hexahydrate, strontium chloride hexahydrate is weakly soluble in ethanol (3.64% wt at 6°C), which can be used for their separation. Strontium bromide and iodide dissolve well in both water and ethanol. As the atomic size of a metal increases, interesting regularities of changes in the crystal structures of the alkaline

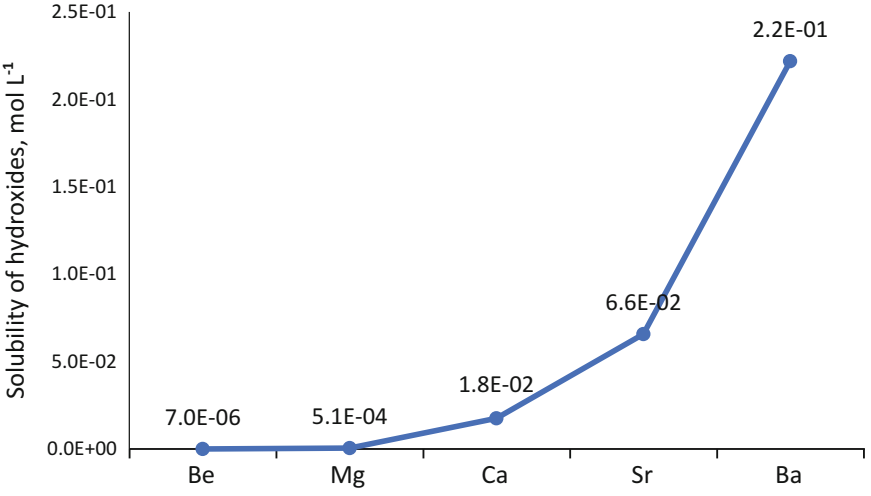

Fig. 3 Solubility of alkaline earth hydroxides in water

earth halides appear [2]. In fluorides, increase in atomic size of a metal results in increase of the coordination number: 4 for beryllium, 6 for magnesium, and 8 for calcium, strontium, and barium. Strontium halides have found applications as optic materials (fluoride and bromide), components of special glass, and luminophores. Strontium iodide is used in scintillation counters, and strontium chloride is added to pyrotechnic compositions for red flame coloring.

Strontium sulfide, SrS, is obtained by heating strontium metal with sulfur or by reduction of strontium sulfate with coal, hydrogen, or other reducing agents. Its colorless crystals are decomposed by water. Strontium sulfide is used as a component of luminophores and fluorescent compounds. Ultrapure strontium sulfides for luminophores are obtained by reaction of strontium carbonate with hydrogen sulfide at 900°C.

Strontium also forms a number of other binary compounds besides halides and sulfide. Strontium metal interacts with coal, forming strontium carbide, Sr_2C, which, like calcium carbide, reacts violently with water, releasing acetylene. Colorless crystals of strontium hydride, SrH_2, are decomposed at 800°C; heating strontium hydride in a nitrogen atmosphere results in its conversion to yellow imide, SrNH. Strontium nitride, Sr_3N_2, is a black crystalline compound that is easily decomposed by water to strontium hydroxide.

Among the salts of oxyacids the most important are carbonate, sulfate, and nitrate. *Strontium nitrate*, $Sr(NO_3)_2$, is a soluble salt that can be obtained by dissolving strontium metal, oxide, hydroxide, or carbonate in nitric acid. It is crystallized as tetrahydrate from aqueous solutions at low temperature; the tetrahydrate easily loses water when heated. Anhydrous strontium nitrate decomposes to strontium oxide at calcination above 600°C. Strontium nitrate is weakly soluble in ethanol and even less so in a mixture of ethanol and diethyl ether, a property used to separate strontium from calcium. Strontium nitrate is widely used as a component of pyrotechnic compounds for signals, lighting, and incendiary rockets. It colors the flame carmine-red. Although all strontium compounds stain the flame in the same color, strontium nitrate is preferable for pyrotechnics because it also works as an oxidizing agent. Thermal decomposition of strontium nitrate results first in strontium nitrite formation, followed by strontium and nitrogen oxide formation with oxygen release [1].

Strontium carbonate, $SrCO_3$, is formed as colorless rhombic crystals by precipitation from strontium salts solutions by sodium or ammonium carbonate. Strontium carbonate is weakly soluble in water; however, its solubility significantly increases in presence of carbon dioxide with the formation of strontium bicarbonate, $Sr(HCO_3)_2$. Strontium carbonate dissolves well in solutions of ammonia salts and is easily decomposed by mineral acids. Heating results in decomposition of strontium carbonate to strontium oxide and carbon dioxide. Decomposition temperatures of alkaline earth carbonate increase with the increase of ionic radius of M^{2+}. The main applications of strontium carbonate are glass for CRT monitors (has become less usual), ceramic ferrite magnets, ceramic glazes, anticorrosion and fluorescent paints, hi-tech ceramics, and pyrotechnics. Furthermore, it is used as a semi-product for synthesis of other strontium compounds.

Strontium sulfate, $SrSO_4$, is a colorless rhombic crystal salt obtained by precipitation from strontium salts solution by sodium sulfate. This is a sparingly soluble salt forming barely soluble double salts with alkaline elements sulfates. Strontium sulfate is used as a filling material in production of paints and rubber.

Strontium chromate, $SrCrO_4$, is precipitated as yellow crystals after mixing solutions of strontium hydroxide and chromic acid. Strontium bichromate, being formed by the impact of acids on chromate, dissolves well in water. Even as weak an acid as acetic acid is sufficient for strontium chromate conversion to bichromate. This quality allows strontium separation from rather less soluble barium chromate, which is converted to soluble bichromate only under the impact of strong acids. Strontium chromate is a lightfast and temperature-resistant pigment (up to 1,000°C) possessing good passivating properties with respect to steel, magnesium, and aluminum. It is used as a yellow pigment, so-called strontianiferous yellow, in the production of lacquers and paints. It is included in the composition of primers based on water-soluble resins and especially primers based on synthetic resins for light metals and alloys in aircraft building.

Strontium titanate, $SrTiO_3$, is a sparingly soluble salt that dissolves in hot concentrated sulfuric acid. It is obtained by sintering strontium and titanium oxides at 1,200–1,300°C. Strontium titanate is used as a ferroelectric material and as a component of piezo-ceramics. In ultrahigh-frequency techniques it serves as a material for dielectric antennas, phase shifters, and other devices. Strontium titanate films are used in the production of nonlinear capacitors and infrared sensors for creation of "dielectric-semiconductor-dielectric-metal" layered structures, which are used in photo-detectors, memory devices, and other devices. Because of its low solubility in water and high thermal and radiation stability, strontium titanate is used as the main form of ^{90}Sr in radioactive sources and radioisotope thermoelectric generators [5] and is considered as a prospective matrix for immobilization of radioactive strontium and actinides.

Strontium hexaferrite, $SrO{\cdot}6Fe_2O_3$, is obtained by sintering strontium and iron (III) oxides. This compound is used as a magnetic material.

Table 3 shows the solubility products of the important sparingly soluble strontium compounds, which determine its behavior in the environment as compared with the

Table 3 Solubility products of the sparingly soluble compounds of the alkaline earth elements

Compound	Solubility product			
	Mg^{2+}	Ca^{2+}	Sr^{2+}	Ba^{2+}
MCO_3	2.1×10^{-5}	3.8×10^{-9}	1.1×10^{-10}	4.0×10^{-10}
MF_2	6.5×10^{-9}	4×10^{-11}	2.5×10^{-9}	1.1×10^{-6}
$M(OH)_2$	6.0×10^{-10} Freshly precipitated	5.5×10^{-6}	3.2×10^{-4}	5.0×10^{-3}
$M_3(PO_4)_2$	1×10^{-13}	2.0×10^{-29}	1×10^{-31}	6×10^{-39}
MSO_4	–	2.5×10^{-5}	3.2×10^{-7}	1.1×10^{-10}

Adopted from [6]
M = Mg^{2+}, Ca^{2+}, Sr^{2+}, or Ba^{2+}

analogue compounds of other alkaline earth elements. The decrease of solubility products of carbonates, sulfates, and phosphates is observed in the series from magnesium to barium; however, these values are quite similar for calcium, strontium, and barium. The reverse dependencies are observed for fluorides and hydroxides. Among sparingly soluble strontium salts, sulfate and carbonate are the most important for technology and strontium behavior in the environment.

Overall, comparative study of the chemical properties of the group II elements confirms that strontium is very similar to calcium and barium and differs significantly from magnesium. Beryllium strongly differs from other alkaline earth metals and shows properties similar to aluminum.

2.4 Complex Compounds of Strontium

Strontium forms a significant number of complex compounds with inorganic and organic ligands; however, there is no unique specific compound for strontium or very stable complexes with high stability constants. Table 4 shows the values of stability constants of strontium complex compounds in comparison with the same compounds of the other alkaline earth elements, excluding beryllium. Complexes of strontium with ethylenediaminetetraacetic acid (EDTA) and polyphosphates have significant importance in analytical chemistry and water treatment technology. Stability constants of the complexes decrease in the series from magnesium to barium for polyphosphates and from calcium to barium for EDTA complexes. It is known that stability of complex compounds is conditioned by many factors simultaneously; therefore, it is difficult observe regularities even within analogue

Table 4 Stability constants of complex compounds of the alkaline earth elements

	Stability constant at the first stage, lgK_1			
Ligands	Mg	Ca	Sr	Ba
OH^-	2.6	1.46	0.82	0.85
NO_3^-		0.28	0.54	0.92
PO_4^{3-}		6.3	4.18	
$P_2O_7^{4-}$	7.2	5.6	5.4	4.64
SO_4^{2-}	2.36	2.31	1.14	2.36
$S_2O_3^{2-}$	1.79	1.91	2.04	2.33
Salts of organic acids				
Acetic	1.25	0.98	1.19	1.15
Oxalic	2.55	1.66	1.25	2.3
Tartaric	1.91	2.98	1.8	2.54
Citric	3.96	4.68	2.9	2.89
Ethylenediaminetetraacetic acid	9.12	10.59	8.8	7.78
8-Oxyquinoline	4.74	3.27	2.56	2.07

Adopted from [6]

elements. If the geometry of an ion is not significant for a complex molecule, small ions form more stable complex compounds. In some cases, especially in formation of complex compounds with macrocyclic ligands, a steric factor may become the main factor affecting stability of the complex, as appears in a high degree in the process of complexes formation with crown ethers [7]. Table 5 presents a comparison of diameters of alkaline earth cations and cavities of some crown ethers. From the aspect of the corresponding sizes of ion and cavity, strontium should form the most stable complexes with 18-crown-6. The stability constants of strontium with crown complexes are lgK = 3.24 for 18-crown-6 and only lgK = 1.95 for 15-crown-5 [2]. 4′,4″(5″)-di-(*tert*-Butylcyclohexano)-18-crown-6 forms more stable complexes with strontium and barium than with magnesium, calcium, or alkaline ions (see Fig. 4). Application of crown ethers is possible with both liquid extraction and extraction chromatography. Complex compounds of alkaline earth metals with cryptands are also known; the stability constants depend on agreement between ion diameter and cavity size. As a rule, the stability of cryptates increases from magnesium to barium [2].

Table 5 Diameters of alkaline earth cations and cavities of crown ethers

Cation	Ion diameter (nm)	Crown cycle	Cavity size (nm)
Mg^{2+}	0.144	14-crown-4	0.120–0.150
Ca^{2+}	0.200	15-crown-5	0.170–0.220
Sr^{2+}	0.236	18-crown-6	0.260–0.320
Ba^{2+}	0.270	21-crown-7	0.340–0.430

Adopted from [2]

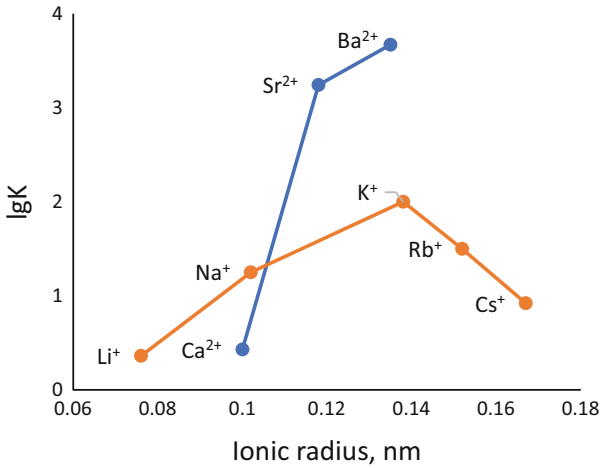

Fig. 4 Constants of complex formations of group I and II ions with dicyclohexane-18-crown-6 (adopted from [2])

3 Determination of Strontium

Analysis of the chemical properties of strontium and its analogues indicates the main requirements for methods of strontium determination. There are no selective reactions and reagents for strontium; therefore, analysis of stable strontium is based mainly on physicochemical methods. Analysis of radioactive isotopes of strontium is based on radiometric and spectrometric techniques. Among radioactive isotopes, ^{90}Sr and ^{89}Sr are the most important relatively long-lived fission products (half-lives are 28.9 years and 50.5 days, respectively), being controlled routinely in environmental samples. These two isotopes are pure β-emitters; therefore, their separation from all other β-emitting radionuclides is required for successful determination because the identification of β-emitters is a very difficult task. Alternatively, ^{90}Sr can be measured via mass spectrometry; in this case, elimination of isobaric interferences is necessary [8]. Furthermore, calcium and magnesium are macroconstituents in all environmental samples, and typical concentrations of strontium and barium are very similar. Thus, most of the analytical methods for strontium are multistage; they commonly include stages of sample pretreatment (if necessary), pre-concentration and group separation of alkaline earth elements, and strontium separation from alkaline earths and determination.

3.1 The Main Methods of Strontium Pre-concentration and Separation

The main methods of strontium pre-concentration and separation are based on its chemical properties as already described. After strontium pre-concentration from a large water sample or leaching from a soil/rock/cement sample, the first task is strontium and the alkaline earth group separation from the third, fourth, and fifth group elements, which can be precipitated as chlorides, sulfides, hydroxides, and other sparingly soluble salts in the analytical method: this is especially necessary in low strontium concentrations as compared with concentrations of interfering elements. The next task is purification of the alkaline earth group and further selective separation of strontium from other alkaline earths. The necessity of the realization of each step depends on the possible detection method and the requirements of a method.

Precipitation methods were the first methods used for pre-concentration and collective separation of alkaline earth elements and sometimes for calcium/strontium/barium separation [2]. Formation of strontium nitrate, being hardly soluble in strong nitric acid or organic solvents, is used for the separation of strontium from various matrices and for selective separation of strontium from calcium. Pure strontium separation can be achieved by this method if the Ca:Sr concentrations ratio does not exceed 100. Alcohol and ketone media are commonly used for this separation. It is interesting to note that precipitation of strontium nitrate from 15 M

nitric acid was one of the methods for pure ^{90}Sr separation from radioactive wastes at radiochemical enterprises in the process of ^{90}Sr isotope production [9]. Precipitation of carbonates is used for collective pre-concentration of alkaline earth elements. It is also possible to use this process for selective strontium separation if other alkaline earth elements are absent in the sample. Use of EDTA allows strontium/calcium separation because a stronger complex compound is formed of EDTA with calcium. Calcium carbonate or phosphates are used for co-precipitation of trace amounts of strontium including its radioactive isotopes. Sulfate precipitation is a classic method for collective separation of alkaline earth elements; furthermore, it can be used for elimination of calcium and magnesium from the strontium fraction. The last method is based on the fact that calcium is not precipitated by $(NH_4)_2SO_4$ solutions. However, calcium/strontium is not pure, and some loss of strontium occurs in this method. The sulfate separation can be improved in presence of complexing agents such as EDTA. In methods of strontium analysis in rocks and minerals using the flame photometry technique, strontium can be separated by co-precipitation with barium sulfate. Co-precipitation with lead (II) sulfate is used for joint separation of micro-amounts of strontium and barium with further detection by spectral methods. Strontium precipitation as the oxalate is used for separation together with calcium and barium in minerals analysis. The strontium yield depends on calcium concentration in this case. Despite some differences in solubility products of calcium, strontium, and barium phosphates, it is not possible to organize their pure separation. Therefore, precipitation of phosphates is used for collective separation of alkaline earth elements from alkaline elements. Co-precipitation of strontium with hydroxides of polyvalent metals such as iron (III), titanium, and manganese (IV) is commonly used for pre-concentration of strontium micro-amounts including ^{90}Sr from large water samples.

Ion-exchange chromatography is used for concentrating strontium micro-amounts and for strontium separation from other alkaline earths and other metals. In the case of strong acid cation-exchange resins, such as Dowex 50WX8, distribution coefficients increase from beryllium to barium and decrease with the increase in acidity. Pure separation is possible with eluent chromatography based on use of eluting solutions with different concentrations and different complexing agents. Lactic and citric acids as well as ethylenediaminetetraacetate are used as the complexing agents. For example, Greenwood and Earnshaw [2] described a method for strontium separation from seawater using the Dowex 50X12 resin in calcium form with further flame photometry determination of strontium in the eluate containing diaminocyclohexanetetraacetic acid. Strong et al. [10] described a method for strontium determination in environmental samples via atomic emission spectroscopy: this was followed by its ion-exchange resin separation on Dowex 50 resin from EDTA solution at pH 5.1 and further consequent stripping of alkaline earths and strontium by 0.5 M and 3 M hydrochloric acid, respectively. Application of anion-exchange resins is conditioned by elimination of interfering elements forming negatively charged complex compounds. Inorganic sorbents, such as phosphates, molybdophosphates, and phosphotungstates, can be used for pre-concentration of strontium micro-amounts and for elimination of some interfering

elements. Separation of alkaline and alkaline earth elements can be performed by sorption on sorbents based on zirconium and titanium oxides, molybdates, and tungstates. Methods of strontium pre-concentration from water samples by silica gel are also known.

Extraction techniques for strontium include extraction by tributyl phosphate from perchlorate, iodide, and thiocyanate solutions, by β-diketones with various diluents from alkaline solutions, by alkyl phosphoric acids, 8-oxyquinoline, and some other extractants. However, these extractants are mostly used for nonselective pre-concentration of alkaline earth elements or for separation of impurities of groups III–V of the periodic table. Selective separation of strontium is based on extraction by macrocyclic extractants based on 18-crown-6 ethers [11], which are used in both liquid extraction and extraction chromatography. Ryabukhin et al. [12] described a method for selective separation of radio-strontium using the liquid–liquid extraction by dicyclohexano-18-crown-6 in chloroform for radio-strontium determination in soil samples. The detection limit of strontium in water samples as low as 5 μg l^{-1} was achieved using the method of liquid microextraction by 4′,4″(5″)-di-(*tert*-butylcyclohexano)-18-crown-6 in presence of tetraphenyl borate [13]. Extractants based on 18-crown-6 are used as extraction chromatographic resins for pre-concentration and separation of strontium (or ^{90}Sr) in methods of its determination in various environmental and technogenic samples. Triskem International produces extraction chromatographic SR resin-based 4′,4″(5″)-di-(*tert*-butylcyclohexano)-18-crown-6 [14, 15]. SR resin, containing 40% w/w of 1.0 M 4′,4″(5″)-di-(*tert*-butylcyclohexano)-18-crown-6 in 1-octanol, is used in the methods for strontium determination in strong acidic solutions being formed as a result of solid sample leaching [16] and in such samples and steel [17], cement, and concrete [18].

3.2 *Methods of Strontium Detection*

Any analytical method should be adopted for a specific object and the final purpose of analysis. Therefore, variations of analytical technique depend on analyzed matrices such as environmental and biological samples, water, rocks, etc., as well as on the value to be determined, such as overall concentration, ^{87}Sr:^{86}Sr isotopic ratio, or activity concentration of ^{90}Sr. However, the techniques of strontium pre-concentration and separation and elimination of interfering elements can be common for all methods. Spectral methods of strontium detection have found application in strontium analysis in minerals, ores, and soils. Determination of strontium in waters of various mineralization and origin exploits different methods such as atomic absorption spectroscopy, spectrophotometry, and inductively coupled plasma atomic emission spectroscopy (ICP-MS). The same techniques and also ICP-MS, neutron activation, and X-ray fluorescent spectroscopy are used for strontium determination in biological samples, depending on the sample type and possibilities of the laboratory [19].

The principal methods of strontium detection and examples of their use for analysis of environmental samples are described next.

Gravimetric methods of strontium determination can be used only after separation from other alkaline earth elements. These methods are quite time- and labor consuming. Separation of sparingly soluble compounds of alkaline earth elements exploits the difference of solubility products and varying pH value, salinity, and complexing agents. Sulfate, carbonate, oxalate, and tartrate are used as sparingly soluble salts of strontium [2]. Precipitation of strontium sulfate is suggested for analysis of highly mineralized water; sequential selective precipitation of alkaline earth elements as sulfates is performed in presence of ammonium salts and EDTA at various pHs. Barium can be first precipitated as chromate; then, strontium sulfate is precipitated in the presence of EDTA for calcium concealment. Precipitation by ammonium carbonate in the presence of ammonia as a pH modifier is performed in the method of strontium carbonate gravimetric. Strontium is completely precipitated by ammonium oxalate from a solution containing 20% ethanol.

Titrimetric methods can be used after the separation of strontium from most of the interfering elements. Titration by EDTA solutions is the most common titrimetric method [20]. Titration is usually conducted in alkaline media where strontium carbonate can precipitate; therefore, displacement or back-titration is used. Eriochrome black, methylthymol blue, eriochromazurol S, and some other indicators are applied for determination of equivalence point. Physicochemical methods such as spectrophotometry, potentiometry, or conductometry can be used for determination of equivalence point. Spectrophotometric titration of strontium by EDTA after chromatographic separation with eriochrome black indicator is described by Greenwood and Earnshaw [2].

Spectrophotometric methods are based on reactions resulting in formation of color compounds with strontium ions. Strontium can be determined in ore samples by spectrophotometry with chlorphosphonazo III in the presence of EDTA after acidic leaching and calcium separation through acetone treatment. A spectrophotometric method using alizarin complexion is developed for simultaneous determination of SrO, MgO, and CaO in Portland cement [21]. Spectrophotometry is also used for strontium determination in water samples [22].

Among *electrochemical methods* for strontium detection, we can mention the polarographic determination of strontium in ethanol with tetraethyl ammonium iodide in presence of low barium concentrations; calcium interferes with the determination of strontium. It is necessary to eliminate Ba, Ca, Na, and K if their concentrations significantly exceed strontium concentration. Inversion polarography allows determining very low strontium concentrations (10^{-5}–10^{-9} mol l^{-1}) in case of preliminary strontium concentration in a mercury drop and further anodic dissolving [2]. The method of capillary electrophoresis is validated by Russian State Standard 31869-12 [23] for determination of concentrations of some cations including strontium in drinking water, natural (surface and underground) waters, and wastewater.

Spectrographic methods are widely used for strontium determination in water, soil, rocks, and plants [2]. Strontium has the most intensive peaks in the optical

spectrum: 4,607.33 Å, 4,077.71 Å, and 4,215.52 Å; the last two peaks are less suitable for use in analysis of electric arc with carbon electrodes. The peak at 4,607.33 Å is characterized by a strong self-absorption; therefore, it is recommended for determination of low strontium concentrations, less than 0.1%. The peaks at 3,464.46 Å, 4,811.88 Å, and 4,832.08 Å are used for determination of high strontium concentrations. Various interferences caused by superposition of strontium peaks with peaks of other elements should be taken into account. The arc of direct or alternating current as well as spark and high-frequency discharge is used as a spectrum excitation source. The sensitivity of strontium determination in the arc is 5×10^{-5} to 1×10^{-4}%; use of pulsed arc discharge allows decreasing the detection limit to 8×10^{-12} g. The sensitivity of strontium determination in the spark is $(1–5) \times 10^{-4}$%. The spectrographic method is used for direct strontium determination of minerals and ores. The standards are prepared using rocks with similar chemical composition as the sample to be analyzed. Chrome, vanadium, and cobalt are used as internal standards. The method of additions is applicable for consideration of the matrix effect.

Atomic emission spectroscopy: The method of flame photometry is widely used for strontium quantitative analysis in rocks, natural waters, and wastewater. It is applied for high precision and sensitive determination in cases of both low and high concentrations. As a rule, this method allows direct determination of strontium without its separation from other elements. The resonance line of strontium atom at 460.7 nm is used. High-temperature flames such as acetylene–air, propane–butane–oxygen, acetylene–oxygen, and acetylene–nitrous oxide flames are required for strontium excitation. In case of the impulse method of evaporation in acetylene–nitrous oxide flame, the absolute detection limit of strontium is 1×10^{-13} to 2×10^{-12} g. In case of a relative large sample (~10 mg), the relative detection limit decreases to 1×10^{-7}%. A number of ions affect the intensity decrease of strontium emission. Elimination of the influence of quenching cations and anions is possible by two methods: (1) separation of these ions from the analyzed solution using the methods of precipitation, ion exchange, extraction, and, in the case of volatile compounds, evaporation; and (2) addition of agents preventing formation of nonvolatile strontium compounds. The methods for strontium determination in water samples by flame emission photometry usually include ion-exchange separation of alkaline and alkaline earth elements and interfering anions, or alternatively, strontium separation by oxalate precipitation. Determination of strontium in seawater is possible after ion-exchange separation of interfering ions without pre-concentration and purification. Popov et al. [24] described a method for direct strontium determination in seawater and various mineral waters containing 1–20 mg l^{-1} of strontium via laser spark emission spectrometry. The method for strontium determination in environmental samples after ion-exchange recovery on the Dowex-50 resin is developed [10]. The method of inductively couple plasma atomic emission spectroscopy is recommended for quantitative determination of strontium in drinking and natural (surface and underground) water including tap water [25]. Strontium concentration in drinking water can also be analyzed by emission flame photometry [26]. Flame photometry is used for strontium determination in rocks and minerals.

Interfering elements are eliminated by ion exchange or co-precipitation with trivalent hydroxides after the sample leaching or dissolving. It is reported that the flame photometry method is adopted for determination of strontium in chalky minerals [27] and in feldspar after fusion of sodium and potassium carbonates followed by dissolving strontium carbonate in hydrochloric acid [24]. Analysis of strontium in foods is performed after sample ashing, dissolving, and strontium separation from the matrix. The method for determination of strontium and some other elements in coffee is suggested using the extraction chromatographic and ion-exchange separation of the elements with further detection by inductively coupled plasma optical emission spectrometry [28].

The *atomic absorption method* is often used in analytical methods [2]. Determination of strontium is based on measurement of light absorption by its atoms. The most suitable strontium atomic line is 460.7 nm; it can be also determined with lower sensitivity using the lines at 242.8, 256.9, 293.2, and 689.3 nm. Use of high-temperature flame opens the possibility of strontium determination by its ionic absorption line of 407.8 nm (ionic absorption spectroscopy). The sensitivity of this method depends on spectrometer quality and on the type of flame. Acetylene–air flame provides the sensitivity of 0.01–0.2 mg l^{-1}, whereas acetylene–nitrous oxide flame provides 0.006–0.04 mg l^{-1}. Pre-treatment of ore samples is performed by acidic leaching or fusion depending on ore type. After sample pretreatment, strontium can be separated from the matrix by ion exchange. In case of strontium analysis in ash of food products or bioassays, the sample is dissolved, and the solution is decontaminated by anion-exchange resin. Direct measurement is possible for seawater samples. Use of atomic adsorption spectroscopy for strontium analysis in water samples in described in ASTM methods [29].

The *neutron activation method* has found application for strontium analysis in various samples. The method is based on sample irradiation in a nuclear reactor and further determination of activity of ^{87m}Sr ($T_{1/2} = 2.84$ h, $E_\gamma = 0.391$ MeV), which is formed from three of four natural isotopes of strontium according to the following nuclear reactions: ^{86}Sr(n,γ)^{87m}Sr, ^{87}Sr(γ,γ')^{87m}Sr, and ^{88}Sr(n,2n)^{87m}Sr. As a rule, measurement of ^{87m}Sr activity is performed after radiochemical separation of strontium from the irradiated sample based on the methods of precipitation, extraction, and ion exchange. Use of a high-energy resolution gamma spectrometer allows increasing accuracy of the method and uses it as a nondestructive technique or reduces the number of operations before and after irradiation. This method is used for determination of strontium in seawater and mineral water, rocks, minerals, and biosamples. The sensitivity of the method reaches 2×10^{-5} g g^{-1} depending on many factors. Versieck et al. [30] applied the neutron activation analysis for strontium quantification in human blood. Instrumental photons activation analysis (IPAA) was used for determination of the Sr:Ca ratio of a human tooth sample [31].

Mass spectrometry is a high-precision instrument for determination of the isotopic composition of strontium in geochronology, archaeology, and isotope signature tracing as well as for analysis of micro-amounts of strontium in various samples by the isotopic dilution method. Determination of strontium concentration in seawater is based on quantification of ^{84}Sr and ^{88}Sr. Mass spectrometry is widely used for

strontium analysis in biosamples. Ulanova et al. [32] reported the results of mass spectrometric determination of strontium in blood and urine of children living near the celestite ore deposit containing up to 20% strontium sulfate. The laser ablation inductively coupled plasma mass spectrometry (LA-MC-ICP-MS) is used for determination of ^{87}Sr:^{86}Sr isotopic ratio in speleothems [33]. Stable ^{88}Sr was determined in rice by the ICP-MS method by Srinuttrakul and Yoshida [34]. Souza et al. [35] used ICP-MS determination of the strontium isotopic ratio for revealing pollution sources in a mangrove food web. The strontium isotopic ratio was analyzed in wheat for determination of its geographic origin [36]; thermal ionization mass spectrometry (TIMS) was used for determination of ^{87}Sr:^{86}Sr isotopic ratio in tomatoes to confirm their geographic origin [37].

The advantages of the *X-ray fluorescent spectroscopy method* is the possibility of rapid nondestructive determination and high sensitivity for strontium (10^{-3}–10^{-4}%) that is sufficient for most purposes. The X-ray fluorescent (XRF) spectroscopy method is based on analysis of the spectrum obtained by irradiation of the sample by X-rays. This irradiation results in excitation of atoms and ionization of α- and β-electron levels. Further relaxation of the atom results in photons emission with a certain energy depending on the electron structure of the atom. The quantification of strontium is usually based on its $K_\alpha = 0.877$ Å. Application of internal standards decreases matrix effects. Yttrium ($K_\alpha = 0.831$ Å), rubidium ($K_\alpha = 0.926$ Å), and also molybdenum and arsenic are used as internal standards. The effect of matrix composition is very important for XRF spectroscopy because of absorption of X-rays in the sample. This effect can be taken into consideration by using standard samples or the additions method. The XRF spectroscopy method is widely applicable for strontium analysis in water of different mineralization, rocks, minerals, ores, soils, and biological materials. XRF spectroscopy is used for strontium determination in sedimentary rocks of oil deposits after the sample is crushed to 200 mesh and mixed with the matrix [2]. Strontium in the bones of animals is usually analyzed after sample ashing. It is possible to determine strontium in bones in vivo using XRF spectroscopy with a detection limit of 0.25 mg strontium per gram of calcium [38]. Shurupova and Golubtsov [39] developed a procedure for rapid determination of low strontium concentrations in sea bottom sediments using XRF spectroscopy without preliminary concentration or destruction of the sample. Determination of strontium in pyrotechnical devices such as fireworks and firecrackers by the energy-dispersive X-ray fluorescence method (EDXRF) was suggested by Wu [40].

4 Strontium in the Environment and Biological Systems

The Clarke number of strontium in the Earth's crust is 3.8×10^{-2}, which is near to the Clarke number of barium. The average content of strontium decreases in the following series of rocks types: intermediate igneous rocks (8.0×10^{-2}%), sedimentary rocks (4.5×10^{-2}%), mafic igneous rocks (4.4×10^{-2}%), felsic igneous rocks (3×10^{-2}%), and ultramafic igneous rocks (1×10^{-3}%) [41]. In geochemical

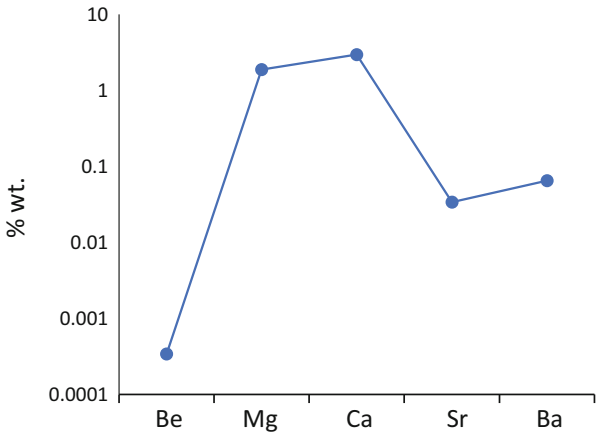

Fig. 5 Clarke numbers of second group elements (adopted from [41])

processes, strontium behavior is very similar to that of calcium, which is the fifth abundant element in the Earth's crust. Figure 5 shows Clarke numbers of alkaline earth elements excluding radium, which presents as a trace element. The most important minerals of strontium are celestite ($SrSO_4$) and strontianite ($SrCO_3$). Strontium can also present as an isomorphic admixture in the crystal lattice of calcium, barium, and potassium minerals. A certain amount of strontium is present in ores and sedimentary rocks containing gypsum, anhydrite, halite, chalkstone, and dolomite.

The specific characteristics of strontium geochemistry are the following:

- Change of isotopic composition during the Earth evolution from radiogenic formation of ^{87}Sr;
- Accumulation in sediments together with gypsum as a result of evaporation mechanism
- Accumulation in low-sulfate waters
- More intensive migration of strontium from lithosphere to hydrosphere (the ocean) as compared with calcium
- Lower affinity to biota as compared with calcium
- Content of strontium in the ocean is higher than in the lithosphere
- Relatively low need in technology: the ratio between annual production of strontium to its Clarke number is approximately 1,000 times lower than the same characteristic of calcium

Strontium migrates to the atmosphere as a result of natural processes such as weathering of rocks, migration of dust particles with wind, and resuspension processes [42]. The air in coastal regions contains elevated strontium from seawater aerosols. Strontium appearance in surface and underground waters is conditioned by the processes of rocks and soils weathering [43]. Technogenic dispersion of natural strontium isotopes is conditioned by coal burning, use of phosphoric fertilizers, and pyrotechnical devices.

The average concentration of strontium in soils (0.035%) is very similar to its Clarke number in the Earth's crust; however, it can increase significantly, to 0.2% in some regions [42]. Strontium is characterized by moderate mobility in soils and sediments because it is adsorbed by components of soils such as oxides, clay minerals, and organic matter [44]. Organic compounds strongly affect strontium mobility in soils and transfer to groundwaters. The average concentrations of strontium in seawater and surface freshwater are 8 and 0.08 mg l^{-1}, respectively [45, 46]. A part of the strontium in the ocean is accumulated in ferromanganese concretions. The average concentrations of strontium in the dry biomass of terrestrial flora and fauna are 8×10^{-2}% and 10^{-3} to 10^{-2}%, respectively. Aquatic organisms accumulate strontium more intensively than those terrestrial: sea algae contain 2.6 to 14×10^{-2}% (dry weight) and sea animals contain 2 to 50×10^{-2}% of strontium. Strontium is the fourth most common element accumulated by the biota of the ocean after Cu, Zn, and Ba [42].

Strontium is not a biogenic element, but it is easily consumed by plants because of its similar chemistry to calcium [19]. Accumulation of strontium in plants being used for food by people and cattle depends on both strontium content in soils and the type of a plant. Concentrations up to 600 mg of strontium kg^{-1} of a soil are assumed as normal. Redundant strontium concentrations of 600–1,000 mg kg^{-1} may result in elevated concentrations of strontium in agricultural plants. Typical concentrations of strontium in food and fodder agricultural plants are (in mg kg^{-1}) wheat, 3.0; rye, 7.8–70.2; barley, 43.2; buckwheat, 2.7–6.8; peas, 6.5–39; corn, 0.0008–0.02; potatoes, 0.05; beetroot, 0.02–0.14; oats, 0.46; grass, 0.5–7.8; clover, 1.3; mangel, 33.0; soya, 138.0; and silage, 63.1 [42, 47]. Some species such as dill and parsley also contain much strontium. Besides professional risk such as working at strontium mining and treatment enterprises, the main natural sources of strontium intake by organisms are drinking water and food, especially crops, leafy vegetables, and milk products. Daily intake of strontium by adults is assessed to be as much as 4 mg day^{-1}. Drinking water and foods contribute nearly 0.7–2 and 1.2–2.3 mg day^{-1}, respectively. The contribution of strontium uptake through the air is insignificant. Daily intake may be significantly higher in areas with elevated concentrations of strontium in drinking water or in soil. The typical quantity of strontium in a human body is 0.3–0.4 g; 99% of strontium is located in bone tissue [19]. Salts and compounds of strontium are low in toxicity; however, regular elevated uptake of strontium results in disorders of bone tissue, liver, and brain. Strontium is very similar to calcium as a chemical element, but the behavior of these elements in an organism is quite different. Redundant intake of strontium ions with water slowly results in calcification disorders of bone tissue in humans and animals, leading to deformation in bones and joints. This disorder is called strontium rachitis, or urov disease, after the Urov River in Transbaikalia, which has an abnormally high strontium concentration [42]. The degree of calcium replacement by strontium in bone tissue depends on the age and sex of a person as well as individual metabolism and daily calcium intake.

5 Conclusions

The similar properties of strontium and other alkaline earth metals, especially calcium and barium, determine their similar behavior in the environment. The slight differences in chemical properties are used for strontium separation in analytical methods. Among the most effective methods, ion exchange and extraction by macrocyclic compounds, especially by 4′,4″(5″)-di-(*tert*-butylcyclohexano)-18-crown-6, can be realized by liquid–liquid extraction or extraction chromatography. The physical methods of atomic absorption spectroscopy, inductively coupled plasma atomic emission spectroscopy, X-ray fluorescent spectroscopy, and especially inductively coupled plasma mass spectrometry (ICP-MS) are widely used for strontium determination in various samples. ICP-MS is used for determination of both concentration and isotopic composition of strontium. Although strontium compounds are of low toxicity, the similarity of strontium to calcium results in strontium accumulation in bones that may lead to calcification disorders in cases of regular high intake, especially in children. This possibility requires the control of strontium in water and food as well as the study of its metabolism and content in organs and tissues. Moreover, chemical properties of stable strontium and its physicochemical behavior are the basis for analysis of radioactive strontium behavior in the environment, its migration, and the impact on humans.

References

1. Petryanov-Sokolov IV (1983) Popular library of chemical elements, vol 1. Nauka, Moscow, pp 478–486
2. Greenwood NN, Earnshaw A (1997) Chemistry of the elements, 2nd edn. Butterworth Heinemann, Oxford
3. Magill J, Pfenning G, Dreher R, Soti Z (2012) Chart of the nuclides (Karlsruher Nuclidkarte), 8th edn. Nucleonica GmbH, Karlsruher
4. Poluektov NS, Mishchenko VT, Kononenko LI, Beltyukova SV (1978) Analytical chemistry of strontium. Nauka, Moscow
5. Shaurina AM, Yakovlev VV (2015) Creation and consequences of use of radiological warfare as a terrorists' weapon. Proceedings of international conference, Days of Science of Peter the Great St. Petersburg Polytechnic University, pp 140–144
6. Lur'e YY (1989) Handbook on analytical chemistry. Chemistry, Moscow, p 448
7. Hiraoka M (1982) Crown compounds: their characteristics and applications. Elsevier, Amsterdam
8. Takagai Y, Furukawa M, Kameo Y, Suzuki K (2014) Sequential inductively coupled plasma quadrupole mass-spectrometric quantification of radioactive strontium-90 incorporating cascade separation steps for radioactive contamination rapid survey. Anal Method 6:355–362
9. Mishina NE, Zilberman BY, Lumpov AA, Koltsova TI, Puzikov EA, Ryabkov DV (2015) Nitric acid adduct formation during crystallization of barium and strontium nitrates and their co-precipitation from nitric acid media. J Radioanal Nucl Chem 304:387–393
10. Strong AB, Rehnberg GL, Moss UR (1968) Determination of strontium in environmental media. Talanta 5:73–77

11. Surman JJ, Pates JM, Zhang H, Happel S (2014) Development and characterization of a new Sr selective resin for the rapid determination of ^{90}Sr in environmental water samples. Talanta 129:623–628
12. Ryabukhin VA, Volynets MP, Myasoedov BF, Rodionova IM, Tuzova AM (1991) Determination of strontium radioisotopes in soils. J Anal Chem 341:636–637
13. Wang CY, Chang DA, Shen Y, Sun YC, Wu CH (2017) Vortex-assisted liquid–liquid microextraction of strontium from water samples using 4′,4′′(5′′)-di-(*tert*-butylcyclohexano)-18-crown-6 and tetraphenylborate. J Sep Sci 40:3866–3872
14. Horwitz EP, Chiarizia R, Dietz ML (1992) A novel strontium-selective extraction chromatographic resin. Solvent Extr Ion Exch 10:313–336
15. TKI (2015) Direct strontium determination in aqueous samples – Version 1.0 – 14/09/15 – TKI analytical methods. http://www.triskem-international.com/scripts/files/59e32e826d5652.55245802/direct_strontium_determination_in_aqueous_samples_v10_en.pdf
16. McLain DR, Liu C, Sudowe R (2018) Using Sr resin with mixed acid matrices. J Radioanal Nucl Chem 316:485–490
17. McLain DR, Amato V, Sudowe R (2017) Effects of urban debris material on the extraction chromatographic separation of strontium: part I: steel. J Radioanal Nucl Chem 314:2585–2590
18. McLain DR, Liu C, Sudowe R (2017) Effects of urban debris material on the extraction chromatographic separation of strontium: part II: cement and concrete. J Radioanal Nucl Chem 314:2591–2596
19. WHO (2010) Strontium and strontium compounds (Concise international chemical assessment document; 77) World Health Organization 2010. http://www.who.int/ipcs/publications/cicad/cicad77.pdf
20. Schwarzenbach G, Flaschka H (1969) Complexometric titrations, 2nd English edn. Methuen and Co. Ltd., London
21. Idriss KA, Sedaira H, Ahmed SS (2009) Determination of strontium and simultaneous determination of strontium oxide, magnesium oxide and calcium oxide content of Portland cement by derivative ratio spectrophotometry. Talanta 78:81–87
22. AOAC (1990) Methods 911.03, 973.66, 974.37. In: Official methods of analysis of the Association of Official Analytical Chemists, 15th edn. Association of Official Analytical Chemists, Gaithersburg
23. Russian State Standard 31869-12 (2012) Water: methods for the determination of cations (ammonium, barium, potassium, calcium, lithium, magnesium, sodium, strontium) content using capillary electrophoresis. http://gostexpert.ru/gost/gost-31869–2012
24. Popov AM, Drozdova AN, Zaytsev SM, Biryukova DI, Zorova NB, Labutin TA (2016) Rapid, direct determination of strontium in natural waters by laser-induced breakdown spectroscopy. J Anal Atom Spectrom 31:1123–1130
25. Russian State Standard 31870-2012 (2012) Drinking water: determination of elements content by atomic spectrometry methods. http://gostexpert.ru/gost/gost-31870–2012
26. Soviet State Standard 23950-88 (1988) Drinking water: method for determination of strontium mass concentration. http://gostexpert.ru/gost/gost-23950-88
27. Rains TC, Zittel HE, Ferguson M (1962) Flame spectrophotometric determination of micro concentrations of strontium in calcareous material. Anal Chem 34:778–781
28. Pohl P, Szymczycha-Madeja A, Welna M (2018) Simple ICP-OES based method for determination of selected elements in brewed ground and soluble coffees prior to evaluation of their intake and chemical fractionation. Food Chem 263:171–179
29. ASTM (1999) Methods D3352, D3920, D4185. In: 1999 annual book of ASTM standards: water and environmental technology. vol. 11.02. American Society for Testing and Materials, Philadelphia
30. Versieck J, Vanballenberghe L, Wittoek A, Vanhoe H (1993) The determination of strontium in human blood-serum and packed blood-cells by radiochemical neutron-activation analysis. J Radioanal Nucl Chem 168:243–248

31. Kavun Y, Boztosun I, Dapo H, Maraş I, Segebade C (2018) Determination of the Sr/Ca ratio of tooth samples by photoactivation analysis in Southern Turkey. Radiochim Acta 106:759–768
32. Ulanova TS, Gileva OB, Steno EB, Weichmann GA, Nedoshitova AB (2015) Determination of strontium in whole blood and urine using the inductively coupled plasma mass spectrometry. Biomed Chem 61:613–616
33. Weber M, Wassenburg JA, Jochum KP, Breitenbach SF, Oster J, Scholz D (2017) Sr-isotope analysis of speleothems by LA-MC-ICP-MS: high temporal resolution and fast data acquisition. Chem Geol 468:63–74
34. Srinuttrakul W, Yoshida S (2017) Determination of stable cesium and strontium in rice samples by inductively coupled plasma mass spectrometry. IOP Conf Ser J Phys Conf Ser 860:12–13
35. Souza IC, Arrivabene HP, Craig CA, Midwood AJ, Thornton B, Matsumoto ST, Elliott M, Wunderlin DA, Monferrán MV, Fernandes MN (2018) Interrogating pollution sources in a mangrove food web using multiple stable isotopes. Sci Total Environ 640-641:501–511
36. Liu H, Wei Y, Lu H, Wei S, Jiang T, Zhang Y, Banc J, Guoa B (2017) The determination and application of $^{87}Sr/^{86}Sr$ ratio in verifying geographical origin of wheat. J Mass Spectrom 52:248–253
37. Trincherini PR, Baffi C, Barbero P, Pizzoglio E, Spalla S (2014) Precise determination of strontium isotope ratios by TIMS to authenticate tomato geographical origin. Food Chem 145:349–355
38. Pejovic-Milic A, Stromach IM, Gyorffy J, Webber CE, Chettle DR (2004) Quantification of bone strontium levels in humans by in vivo X-ray fluorescence. Med Phys 31:528–538
39. Shurupova TI, Golubtsov IV (2004) X-ray fluorescence determination of strontium in marine bottom sediments. J Anal Chem 59:564–565
40. Wu JY (2017) Determination of strontium content in pyrotechnics used for fireworks and firecrackers based on energy dispersive X-ray fluorescence spectrometry (EDXRF). Advances in Engineering Research (AER) 148, 3rd Workshop on Advanced Research and Technology in Industry Applications (WARTIA 2017), pp 413–417
41. Perelman AI (1989) Geochemistry. High School, Moscow, p 528
42. Filov VA (1988) Toxic chemical compounds. Inorganic compounds of elements I–IV groups. Khimiya, Leningrad, pp 124–132
43. ATSDR (2004) Toxicological profile for strontium. United States Department of Health and Human Services, Public Health Service, Agency for Toxic Substances and Disease Registry, Atlanta. http://www.atsdr.cdc.gov/toxprofiles/tp159.html
44. Sahai N, Carroll SA, Roberts S, O'Day PA (2000) X-ray absorption spectroscopy of strontium (II) coordination: II. Sorption and precipitation at kaolinite, amorphous silica, and goethite surfaces. J Coll Interf Sci 222:198–212
45. Angino EE, Billings GK, Andersen N (1966) Observed variations in the strontium concentration of sea water. Chem Geol 1:145
46. Kogel JE, Trivedi NC, Barker JM, Krukowski ST (2006) Industrial minerals & rocks: commodities, markets, and uses. Society for Mining, Metallurgy and Exploration, Ltd., Littleton, p 927
47. Kabata-Pendias A, Mukherjee AB (2007) Trace elements from soil to human. Springer, Berlin

Isotopes of Strontium: Properties and Applications

Vladimir Sergeevich Semenishchev and Anna Vladimirovna Voronina

Contents

Abstract The chapter gives an overview of properties and application of stable and radioactive isotopes of strontium. Natural strontium consists of the following four stable isotopes: ^{84}Sr (0.56%), ^{86}Sr (9.86%), ^{87}Sr (7.00%), and ^{88}Sr (82.58%). Among them, ^{87}Sr is a radiogenic isotope being the decay product of the long-lived natural beta-emitting isotope ^{87}Rb; it is widely used in geology for rocks and minerals dating as well as for systematization of origin of various rock formations. A unique ^{87}Sr/^{86}Sr ratio in each region became a useful tool for tracing geographical origin of water, archaeological artifacts, and foods. Besides stable isotopes, a number of radioactive isotopes of strontium from ^{73}Sr to ^{107}Sr are also known; among them, relatively long-lived isotopes are ^{90}Sr, ^{89}Sr, ^{82}Sr, and ^{85}Sr. The most long-lived radioactive isotope ^{90}Sr with the half-life of 28.9 years is one of the most contaminants of the environment because of radiation accidents. Being a significant component of irradiated nuclear fuel and radioactive waste after spent fuel reprocessing, ^{90}Sr is used in production of radioisotope thermoelectric generators, as beta radiation sources for radiometric and dosimetry applications, as well as in nuclear medicine as a mother nuclide for isotopic generators of ^{90}Y being used for

V. S. Semenishchev (✉) · A. V. Voronina
Radiochemistry and Applied Ecology Department, Ural Federal University,
Physical Technology Institute, Ekaterinburg, Russia
e-mail: vovius82@mail.ru

P. Pathak, D. K. Gupta (eds.), *Strontium Contamination in the Environment*,
The Handbook of Environmental Chemistry 88,
https://doi.org/10.1007/978-3-030-15314-4_2

therapy in oncology. Applications of ^{82}Sr and ^{85}Sr in nuclear imaging and ^{89}Sr in radiotherapy are described in the chapter.

Keywords Nuclear medicine · RITEG · Rubidium-strontium dating · Strontium isotopes · Strontium isotope signature: Strontium-90

1 Introduction

Strontium is an alkaline earth metal, the 38th element of the periodic table. Totally, 35 isotopes of strontium are known from ^{73}Sr to ^{107}Sr [1]. In contrast to odd elements consisting usually of one or two stable isotopes, natural strontium consists of stable isotopes ^{84}Sr, ^{86}Sr, ^{87}Sr, and ^{88}Sr. Among them, ^{87}Sr is a radiogenic isotope being the decay product of the long-lived natural beta-emitting isotope ^{87}Rb. Different ratios between concentration of strontium and rubidium in rocks as well as different ages of these rocks result in a unique percentage of ^{87}Sr at each geographic region, whereas the proportion between ^{84}Sr, ^{86}Sr, and ^{88}Sr remains the same. This gives us a useful tool for rocks dating and determination of geographic origin of strontium-containing substances such as foods and archaeological artifacts. Table 1 shows a brief overview of properties of stable strontium isotopes. The average neutron cross section of strontium 1.2 barn makes it useless for nuclear reactors: this is too much for construction materials (materials with $<$0.2 barn are commonly used) and too low for control rods (materials with $>$100 barn are used).

Other 34 isotopes of strontium are radioactive with the half-lives from 230 ns to 28.9 years; the overview of their properties is given in Table 2.

Among radioactive isotopes, only four isotopes, ^{90}Sr, ^{89}Sr, ^{85}Sr, and ^{82}Sr, are used. Other 30 radioactive isotopes have too short half-lives and have no long-lived parent radionuclides for practical use. Two of useful radioactive strontium isotopes, ^{90}Sr and ^{89}Sr, are neutron excess nuclei decaying by β^- decay mechanism, whereas ^{85}Sr and ^{82}Sr are proton excess nuclei resulting in electron capture mechanism of radioactive decay. Use of these isotopes is conditioned only by their radioactive properties such as type of radiation (beta, gamma), energy of decay, and formation of useful daughter radionuclides.

Table 1 Properties of stable isotopes of strontium (adopted from [1])

Isotope	Average abundance, %	Neutron cross section, barns	Origin
^{84}Sr	0.56	0.6	Non-radiogenic
^{86}Sr	9.86	0.81	Non-radiogenic
^{87}Sr	7.0	16	Radiogenic
^{88}Sr	82.58	0.0058	Non-radiogenic

Table 2 Properties of radioactive isotopes of strontium with half-lives more than 1 min (adopted from [1])

Isotopes	Decay mode	Half-life	β^+/β^- energy, MeV	γ energy, keV
^{78}Sr	β^+	2.65 m	–	104, 243, 268, 212 …
^{79}Sr	β^+	2.3 m	4.2	39, 105, 219
^{80}Sr	EC[a]	1.8 h	No β^+	589, 175, 553, …
^{81}Sr	β^+	22.2 m	2.7, 3.0	154, 148, 443, 188, …
^{82}Sr	EC	25.34 day	No β^+	No γ
^{83}Sr	EC, β^+	32.4 h	1.2	763, 381, 418, …
^{85}Sr	EC	64.85 day	No β^+	514
^{89}Sr	β^-	50.5 day	1.5	909
^{90}Sr	β^-	28.9 year	0.5	No γ
^{91}Sr	β^-	9.5 h	1.1, 2.7	1,024, 750, 653, …
^{92}Sr	β^-	2.71 h	0.6, 1.9	1,384
^{93}Sr	β^-	7.43 m	1.5, 3.4	590, 876, 888, 710, 169, …
^{95}Sr	β^-	74 s	2.1, 3.5	1,428

[a]EC is electron capture

2 Use of Stable Isotopes of Strontium

2.1 Rubidium-Strontium Dating

The rubidium-strontium dating method was suggested by German radiochemists Fritz Strassmann and Otto Hahn in the 1930s. Today it became a routine technique for minerals and rocks dating along with K-Ar, U-Pb, Sm-Nd, and some other dating methods. The method is based on radioactive decay of long-lived primordial radionuclide ^{87}Rb with the half-life of 4.89×10^{10} [1] years decaying to stable ^{87}Sr isotope. In a mineral containing rubidium, concentration of ^{87}Sr increases during time, whereas ^{87}Rb decays according to Eq. (1):

$$N = N_0 \times e^{-\lambda t} \tag{1}$$

where N and N_0 are initial and current number of ^{87}Rb; t is time, years; and λ is radioactive decay constant of ^{87}Rb, 1.417×10^{-11} years^{-1}. All atoms of ^{87}Rb decay to ^{87}Sr and therefore the number of ^{87}Sr atoms ingrowths according to Eq. (2):

$$N_{\text{Sr-87}} = N_{\text{Rb-87}} \times \left(e^{\lambda t} - 1\right) \tag{2}$$

The mineral or rock should meet the following requirements for correct determination of its age:

1. The mineral/rock should be closed for both rubidium and strontium meaning that no addition or loss of these elements occurred since mineral/rock formation.
2. All atoms of ^{87}Sr in the mineral/rock were formed due to ^{87}Rb decay.

The first requirement is satisfied or not depending on a mineral. Decay of ^{87}Rb results in formation of hot atom ^{87}Sr with a kinetic energy of several electron volts; therefore, ^{87}Sr appears in defects of the mineral's crystal lattice. In addition, there is a significant difference of strontium and rubidium ionic radii (1.13 Å and 1.48 Å, respectively) complicating isomorphic replacement. Any loss of strontium results in undervaluation of the mineral's age. The most suitable minerals for Rb/Sr dating are as follows: biotite > fengite > muscovite > chlorite > potassium feldspar [2]. Radiogenic ^{87}Sr leached from biotite is usually adsorbed by the nearest Ca-containing minerals; therefore, it is possible to determine the age of the rock at whole; samples of around 30 kg are recommended for these cases. In addition, it is preferable to use minerals with a high Rb/Sr ratio.

The second requirement is not usually satisfied because initial magma contains some quantity of radiogenic ^{87}Sr. In this case, Eq. (2) should be corrected to Eq. (3):

$$N_{\text{Sr-87}} = N_{\text{Sr-87}}{}^{0} + N_{\text{Rb-87}} \times \left(e^{\lambda t} - 1\right) \tag{3}$$

where $N_{\text{Sr-87}}{}^{0}$ is initial number of ^{87}Sr atoms being captured by the mineral during crystallization. The initial number of ^{87}Sr atoms is an unknown value; however, it is possible to determine also the content of non-radiogenic ^{86}Sr and transform Eq. (3) to Eq. (4):

$$\frac{N_{\text{Sr-87}}}{N_{\text{Sr-86}}} = \left(\frac{N_{\text{Sr-87}}}{N_{\text{Sr-86}}}\right)_{0} + \frac{N_{\text{Rb-87}}}{N_{\text{Sr-86}}} \times \left(e^{\lambda t} - 1\right) \tag{4}$$

Analysis of several rock samples with different Rb/Sr ratios gives the possibility of plotting isochrone in coordinates "^{87}Sr/^{86}Sr – ^{87}Rb/^{86}Sr." The isochrone has the linear appearance where slope depends on the age of the rock ($tg\alpha = e^{\lambda t} - 1$) and the point of intersection with the axis indicates initial ^{87}Sr/^{86}Sr isotopic ratio at the moment of the rock formation. A theoretical example of initial data and plotting isochrone is shown in Table 3 and Fig. 1.

According to the isochrone, the age of 3.47 Ga and the initial ^{87}Sr/^{86}Sr ratio of 0.7062 can be found.

Fluctuations of isotopic ratios for non-radiogenic isotopes of strontium are very low: $\delta^{88/86}$Sr varies from 0.16 to 0.97‰ [3]. The similar results obtained for glacial waters and soils [4, 5] also showed low strontium fractionation in the environment. Thus, no significant separation of strontium occurs in the environment. Therefore, the systematization of values of initial ^{87}Sr/^{86}Sr ratio in various points of the Earth crust is a very interesting instrument for study of history of geochemical formations.

Table 3 Raw data for an isochrone plotting

Sample	^{86}Sr, %	^{87}Sr, %	^{87}Rb, %	^{87}Sr/^{86}Sr	^{87}Rb/^{86}Sr
1	0.0043	0.00339	0.00687	0.788	1.598
2	0.00099	0.00107	0.00712	1.081	7.192
3	0.00128	0.00131	0.00838	1.023	6.547

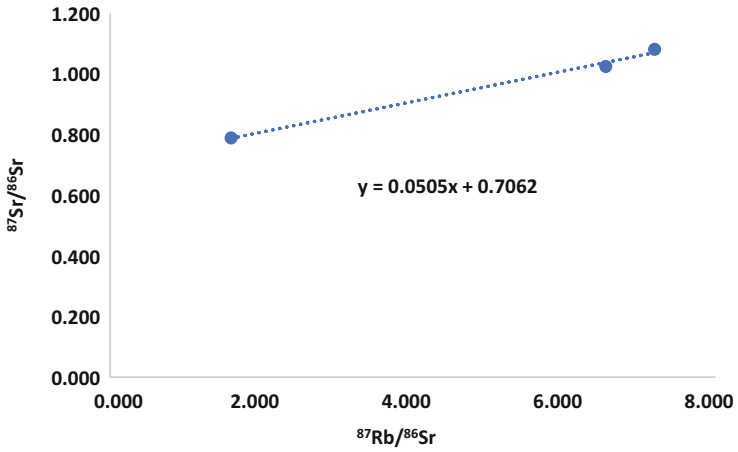

Fig. 1 A theoretical example of Rb/Sr isochrones

The initial $^{87}Sr/^{86}Sr$ ratio in Earth 4.55 Ga ago was assessed to be 0.69898 using meteorites study. The modern ratio in mantle is calculated to be 0.7045, and continental value is near to 0.7090 [6].

2.2 Use of Strontium Isotopic Ratio for Geographic Tracing

A relatively recent application of strontium isotopic ratio is based on simultaneous difference of Rb/Sr ratios and ages of rocks in each geological province. This results in a unique $^{87}Sr/^{86}Sr$ ratio in each region that can be used for geographic tracing of foods and various archaeologic artifacts. Strontium can be easily found in natural water as well as in calcium-rich organic matter such as bones, milk products, wine, etc. The first idea of $^{87}Sr/^{86}Sr$ ratio used for geographic tracing belongs to Chaudhuri [7] that studied the possibility of application of $^{87}Sr/^{86}Sr$ to investigate the origin of groundwater. It was the main application field for strontium isotope signature until 1990; however, it is still valid today. Sahib et al. [8] used strontium isotope signature for determination of salinity sources of groundwater in Iraq and found it to be a very powerful tool in distinguishing between mixing of groundwater with oil field brines or water from another formation. This method was also successful for tracing landfill leachate in groundwater from southeastern France. It was shown that natural groundwater and landfill leachate contamination were characterized by different $^{87}Sr/^{86}Sr$ ratios of 0.708175 and 0.708457, respectively. The evaluation of mixing ratios indicated that fertilizers were additional source of groundwater contamination [9]. Among the recent activities, there are applications of slight seasonal variations of $^{87}Sr/^{86}Sr$ ratios (0.18–0.31‰) for study of chemical weathering processes in glacier and river landscapes [10, 11].

Since the 1990s, the strontium isotope signature tracing is intensively used in archaeology. It was reported that strontium presenting in bones of humans or animals is transferred from soil through water, vegetation, and other foods; therefore, $^{87}Sr/^{86}Sr$ ratio in bones may indicate the origin of food and thus possible migration of bones owner [12]. It should be noted that continual replacement of inorganic phase undergoes bones. Therefore, measurements of bone strontium reflect the later years of the life of the individual, as well as an average composition of all nutrients ingested during the last 5–10 years of life depending on the type of bone [13]. Gan et al. [14] described a combined study based on determination of $^{87}Sr/^{86}Sr$, $\delta^{18}O$, and $\delta^{13}C$ in tooth enamel from cattle mandibles excavated from Roman deposits (second to fourth century AD) in Worcester, Worcestershire, England. Combination of these useful archaeological tools allowed proving that none of these was born in the deposition place. Hughes et al. [15] used strontium tracing for evaluation of contribution of German migrants to Anglo-Saxon settlement of Britain in fourth to seventh centuries by analysis of 19 individuals from the early Anglo-Saxon cemetery at Eastbourne, Sussex. Another interesting case is described by Sheridan and Gregoricka [16]. The authors have determined $^{87}Sr/^{86}Sr$ ratio in teeth of 22 individuals from the Byzantine monastery of St. Stephen's (Jerusalem) and found that 9 of them arrived at the monastery from other regions, hypothetically from Levant and Europe. The similar archaeological studies performed in Peru [17, 18] showed intensive migration of Incas. Teeth and bones are the most used objects in studies; however, some archaeologists used the strontium isotope signature method to study artifacts of inorganic origin also. For example, Ganio et al. [19] used combined tests of $^{87}Sr/^{86}Sr$ and $^{143}Nd/^{144}Nd$ ratios for determination of origin of 31 glass fragments, dated to the third to seventh century AD and excavated in the same deposit in Iraq, and showed that at least two different sources of wood ash were used for glass melting.

Finally, the strontium isotope signature is used for tracing food origin. It is mainly important for determination of falsification of expensive products such as elite wine and cheese. Several recent publications describe systematization of $^{87}Sr/^{86}Sr$ ratios in original wines from Italy [20–23] and Canada [24]. Marchionni et al. [25] have proved that $^{87}Sr/^{86}Sr$ ratio remains stable during the winemaking processes based on the study of wines, grape juices, soils, and rocks from six selected vineyards of "Cesanese" wine area. A technology and first results of determination of "Pecorina di Farindola" cheese, a unique product from Farindola village, Italy, are also reported [26]. Strontium presenting in natural surface water and groundwater shows the maximal bioavailability; therefore, $^{87}Sr/^{86}Sr$ ratio in foods corresponds mainly to this in water. Thus, mapping $^{87}Sr/^{86}Sr$ ratios in natural water of various regions would simplify the task of systematization of $^{87}Sr/^{86}Sr$ ratios in foods [27].

3 Properties and Applications of Radioactive Isotopes of Strontium

As we have mentioned before, only four radioactive isotopes of strontium, ^{90}Sr, ^{89}Sr, ^{85}Sr, and ^{82}Sr, have found practical applications that are conditioned by their relatively long half-lives. ^{82}Sr is interesting only due to formation of very short-lived ^{82}Rb, a positron emitter with the half-life of 1.27 min. As all positron emitters, ^{82}Rb emits annihilation 511 keV gamma quants. The main field of its application is positron emission tomography (PET) of cordial system.

^{85}Sr is pure gamma emitter with gamma energy of 514 keV. Sometimes it is used as a radiotracer in radiochemical studies. Being a pure gamma emitter, it is appropriate tracer for determination of strontium chemical yield in analysis of ^{90}Sr in various samples [28] because its radiation does not interfere detection of beta radiation of ^{90}Sr. Imaging in nuclear medicine is another important field of application of ^{85}Sr.

^{89}Sr is used mostly in nuclear medicine for palliative therapy of bone tumors.

^{90}Sr is the most usable radioactive isotope of strontium. Being a long-lived fission product with yield of nearly 5%, it is the only one radioactive strontium isotope that is produced from spent nuclear fuel and corresponding radioactive wastes. Strictly speaking, ^{89}Sr is also a fission product, but it totally decays during cooling of spent fuel before reprocessing (it usually takes at least 3–5 years); therefore, raffinates of PUREX process contain ^{90}Sr with insignificant impurities of stable isotopes. According to data of IAEA [29], the total electricity supply at nuclear power plants in 2017 was 2,502.9 TW(e) h. Average efficiency coefficient is 35%; therefore, the energy production was nearly 7,150 TW h. Fission of one ton of ^{235}U results in energy release of 22.8 TW h. Therefore, all world nuclear power reactors spend approximately 313.6 tons of ^{235}U. Assuming yield of ^{90}Sr to be 5%, we can easily calculate that nuclear reactors produce nearly 15.7 tons of ^{90}Sr annually that corresponds to activity of 8×10^{19} Bq. Significant part of produced ^{90}Sr decays during storage of appears vitrificated with other high-level radioactive, whereas a little part less than 1% is used. Combination of pure beta emission of ^{90}Sr and formation of hard beta-emitting daughter ^{90}Y conditions dualism of its application fields: it is used as beta emitter in beta sources and energy sources and as parent nuclide for ^{90}Y generators in nuclear medicine. Beta sources based on ^{90}Sr are very popular as calibration sources for radiometers and dosimeters because ^{90}Sr requires significantly less shielding as compared with other popular gamma-emitting sources containing ^{137}Cs or ^{60}Co. Kelley [30] mentioned that ^{90}Sr is used by US Navy in the In-flight Blade Inspection System for monitoring the structural condition of rotor blades of helicopters. Applications of strontium isotopes in energy sources and medicine are described below.

3.1 Energy Sources Based on ^{90}Sr

The energy released as a result of radioactive decay is able to heat the environment. This effect was used for creation of radioisotope thermoelectric generators (RTG or RITEG), where heat energy is transformed into electricity by the Seebeck effect. As a rule, RITEGs have low electrical power, up to several hundred watts (because of low efficiency coefficient, 3–7%), and generate ionizing radiation; however, these power sources do not require any service and can work for a long time depending on half-life of a radionuclide. Therefore, their field of application is traditionally limited to power sources in space probes, satellites, unmanned lighthouses in Arctic, some scientific installations in Antarctica, as well as small batteries in cardioaccelerators. The USSR and USA were leaders in RITEGs production.

Several radionuclides were used or tested for RITEGs production. The three most used isotopes are ^{238}Pu, ^{90}Sr, and ^{244}Cm; besides them, ^{210}Po, ^{137}Cs, ^{147}Pm, ^{60}Co, and some other nuclides were studied or exploited in limited applications. Table 4 gives a comparison of properties of radionuclides being used in RITEGs. Nuclear properties were taken from Magill et al. [1]; power densities were calculated by authors based on nuclear properties.

Table 4 Physical properties of radionuclides being used in RITEGs

Radionuclides	Half-life	Decay mode	Power density, W/g	α/β energy, MeV	γ energy, keV	Production source
^{90}Sr	28.9 year	β^-	0.46	0.5, 2.27 (^{90}Y)	No γ	Spent fuel, radioactive waste
^{238}Pu	87.74 year	α	0.54	5.5	43, 100 low yield	Irradiated Np targets
^{244}Cm	18.1 year	α	2.8	5.8	43, low yield	Irradiated Pu targets
^{210}Po	138.38 day	α	141	5.3	No γ	Natural
^{241}Am	432.2	α	0.11	5.48	60, low yield	Spent fuel, radioactive waste
^{147}Pm	2.62 year	β^-	0.2	0.2	121, low yield	Spent fuel, radioactive waste
^{137}Cs	30.08 year	β^-	0.38	0.5	662, high yield	Spent fuel, radioactive waste
^{60}Co	5.27 year	β^-	8.4	0.3, 1.5	1,332, 1,173, high yield	Irradiated Co targets

Radionuclides should meet the following requirements to be used in RITEGs:

- Appropriate half-life. On the other hand, long half-life results in a long life of the corresponding energy source and low decrease of power per year. On the other hand, long half-life results in lower specific activity and lower power density of the source. It can be seen from Table 3 that short-lived ^{210}Po provides the highest power density. The optimal half-life should be within several years to several decades; ^{90}Sr meets this requirement.
- High decay energy providing high power density. ^{90}Sr itself is a relatively soft beta emitter, but its short-lived daughter nuclide ^{90}Y is one of the hardest beta emitters with maximal beta energy of 2.27 MeV. Due to this, power density of ^{90}Sr is quite high.
- Low shielding requirements. The type of radiation should require as light shielding as possible. Alpha emitters are preferable due to very short tracks of alpha particles in solid materials and absence of secondary radiation; for example, ^{210}Po does not require significant shielding due to absence of gamma radiation. Gamma radiation requires thick lead or depleted uranium shields depending on gamma energy; therefore, hard gamma emitters such as ^{137}Cs or ^{60}Co cannot be used in cardioaccelerators or space power sources. Neutron radiation is undesirable because it requires thick complex shields consisting of hydrogen-rich substance for neutron moderation, cadmium shield for neutrons absorption, and lead shields for absorption of secondary gamma radiation being produced by cadmium. Path of beta particles in metals is short (up to a few mm); however, they generate bremsstrahlung X-ray radiation that requires lead or depleted uranium shielding for absorption. Thus, although ^{90}Sr has no gamma radiation, RITEGs being powered by this radionuclide need a thick shielding. Shaurina and Yakovlev [31] reported that radiation shielding at soviet RITEGs RIT-90 containing 1,500 TBq of ^{90}Sr provided the dose rate of 2 mSv h^{-1} at the surface and 0.1 mSv h^{-1} at 1 m from the container.
- Price and availability of the radionuclide. Isotopes presenting in spent nuclear fuel and radioactive waste after spent fuel treatment are always cheaper and more available than other radionuclides being produced by targets irradiation. It is very difficult to say exactly the price of ^{238}Pu, the most used radionuclide in RITEGs, but it is something around several thousand dollars per gram [32]. As compared with plutonium, ^{90}Sr is very abundant component of radioactive waste, and its production cost is conditioned only by its separation from waste.

Two serious programs of production of ^{90}Sr-based RITEGs were realized in the twentieth century: one is SNAP-21 in the USA [33] and another is RIT-90 series in the Soviet Union. Nearly one thousand ^{90}Sr-based RITEGs were produced in the USSR. Most of them were used in arctic unmanned lighthouses and navigation beacons at the Northeast Passage [34], approximately 40 RITEGs were located in Antarctica [35]. The RITEGs contained initial strontium activity from 1.32×10^{15} to 1.72×10^{16} Bq. Active rods contained strontium was as chemical form of strontium titanate or strontium-doped borosilicate glass [31]. The devices had assigned resource of 10 years with possibility of prolongation for 5 years. Since all soviet

RITEGs significantly exceeded their design operational lives at the beginning of twenty-first century, the program of their decommissioning and utilization started in 2001 according to Norway's initiative [34]. In 2015 Sergey Kirienko, the former head of Rosatom Company, reported at Russian Government's session that all RITEGs were collected and transported for further utilization including four last RITEGs in Antarctica. Additionally, two RITEGs were raised from sea bottom where they were accidentally drowned in the 1980s [36].

Nearly 20 accidents occurred with ^{90}Sr-based RITEGs in Russia, Georgia, Kazakhstan, and Tajikistan including cases of loss, damage, and theft of sources [31]. Loborev et al. [37] calculated that attempt of extraction of the ^{90}Sr source from RITEG results in lethal irradiation of a person and death during disassembling. Some of lost RITEGs are still not found. Maximov et al. [38] described a search expedition in Okhotsk Sea that was aimed to find a lost IEU-1 ^{90}Sr-based RITEG with the initial activity of radiostrontium of 1.72×10^{16} Bq. The RITEG was accidentally dropped from a transport helicopter to the sea near east coast of Sakhalin Island. The search area is 8×12 km; the depth fluctuates from 1.5 to 70 m. Several unsuccessful search expeditions were performed from 1987 to 2014. The last of them tried to find the RITEG by monitoring heat field in bottom layer of sea based on the calculated heat power of the source in 2014 as high as 1,100 W. Ten possible locations with increased temperatures were detected; however, the RITEG is still not found [38].

Heavy ^{90}Sr-based RITEGs are not produced more (but several are still in use); however, work in the field of ^{90}Sr application as an energy source is still in progress. The recent studies are focusing mainly on using ^{90}Sr in betavoltaic cells [39–42]. The betavoltaic cells are based on direct conversion of kinetic energy of beta particles to electricity in a semiconductor. Si, SiC, GaP, GaN, and AlGaAs are suggested as radiation-resistant semiconductors for these systems [43, 44]. The new systems provide higher efficiency as compared with RITEGs: Steinfelds et al. [42] reported that ^{90}Sr-based Radioisotope Energy Conversion Systems can attain electric power generation efficiencies greater than 18%.

3.2 Application of Radioactive Isotopes of Strontium in Nuclear Medicine

Today, nuclear medicine is the most important application field of radioactive isotopes of strontium. There are two independent directions existing in nuclear medicine: nuclear imaging and nuclear therapy. Both directions require short-lived radionuclides allowing fast decay of activity immediately in patient; this is the only one common requirement for all medical radionuclides. Nuclear imaging uses gamma-emitting isotopes, preferably pure gamma emitters, providing as low dose of internal irradiation as possible. This type of diagnostics was developed in the 1950s and became widely used in the 1970s–1980s. Radionuclides with EC and β^- decay modes are commonly used in single-photon emission computed tomography

(SPECT), whereas β^+ emitters are used in rather more prospective positron emission tomography (PET) which is based on detection of pairs of annihilation 511 keV gamma quants. Low beta energy is mandatory for this type of isotopes since it affects internal dose for patient. Optimal value of gamma rays energy is nearly 150–500 keV; lower energy results in increase of gamma rays adsorption in a patient's body and thus low efficiency, whereas higher energy result in undesirable high irradiation dose. Among radioactive isotopes of strontium, ^{85}Sr and ^{82}Sr are suitable isotopes for nuclear imaging.

^{82}Sr is interesting due to its short-lived daughter ^{82}Rb. This isotope has the half-life of 1.27 min and decays by β^+ mode; thus, it can be used in PET. Being an alkaline metal, the nearest analogue of potassium, it is intensively concentrated by the cardiomyocytes via the Na+/K+/ATPase. ^{82}Rb has been approved by the FDA in 1989 for the diagnosis of coronary artery disease. At present, it has become the most commonly applied PET myocardial perfusion tracer in the USA [45]. As compared with two other diagnostic isotopes being used in cardiology, ^{99m}Tc ($T_{1/2} = 6$ h) and ^{201}Tl ($T_{1/2} = 3$ days), rubidium-82 has two significant advantages. At first, ^{82}Rb is used in PET, whereas ^{99m}Tc and ^{201}Tl are used in SPECT providing worse image quality than PET. At second, ^{82}Rb has much shorter half-life resulting in a less internal irradiation dose; furthermore, a patient should not stay in a hospital for a long time until activity decays to acceptable level. Besides cardiology, ^{82}Rb is also successfully used for diagnosis of some neurological and oncological diseases [46]. Being a proton excess nucleus, ^{82}Sr can be produced using a cyclotron or linear accelerator [47]. The most efficient method for producing ^{82}Sr is proton irradiation of metallic natural rubidium by the following nuclear reactions ^{85}Rb$(p,4n)^{82}$Sr and ^{87}Rb$(p,6n)^{82}$Sr with further sorption of strontium from molten rubidium at 300°C [48]. Artun [49] reported that 45–55 MeV protons showed the highest cross sections for ^{85}Rb$(p,4n)^{82}$Sr nuclear reaction. Fitzsimmons et al. [50] reported that the purified preparation of ^{82}Sr contains 10–20.7% of ^{82}Sr, 0–0.05% of ^{83}Sr, 35–48.5% of ^{84}Sr, 16–25% of ^{85}Sr, 12.5–23% of ^{86}Sr, and 0–10% of ^{88}Sr. Among them, ^{84}Sr, ^{86}Sr, and ^{88}Sr are stable nuclides; ^{85}Sr decays to stable ^{85}Rb. Insignificant quantities of ^{83}Sr ($T_{1/2} = 32.4$ h) decay to ^{83}Rb ($T_{1/2} = 86.2$ days), but its activity is much less than activity of ^{83}Sr. Thus, ^{82}Sr/^{82}Rb generators produce almost pure ^{82}Rb with insignificant traces of ^{83}Rb. The generator of ^{82}Rb is a simple sorption column containing hydrated tin(IV) dioxide loaded with up to 5.92 GBq of ^{82}Sr and encased in a tungsten (21 kg) or lead (26 kg) shielding container. ^{82}Rb can be periodically eluted from the column by isotonic solution (0.9% NaCl). The significant activity allows for self-sterilization of the eluting solution [51]. Among other sorbents used in ^{82}Sr/^{82}Rb generators, there are aluminum oxide, phosphates, and organic resins. In the future, the importance of ^{82}Rb in nuclear medicine will be increasing because coronary artery disease causes 17.3 million deaths per year remaining the leading global cause of death [52].

^{85}Sr is 514 keV gamma emitter used in nuclear medicine for diagnostics as strontium-85 dichloride. Strontium is analogue of calcium; therefore, the main field of application of ^{85}Sr is diagnosis of skeletal diseases due to replacing calcium on bones. The method was developed by Flemming et al. [53]. ^{85}Sr has relatively

long half-life; therefore, administered doses are limited to 100 μCi (3.7 MBq) to patients with confirmed malignant diseases and 50 μCi (1.85 MBq) to those only suspected of having a tumor [54]. Significant percent of ^{85}Sr is accumulated in soft tissues and blood during the diagnostic procedure resulting in a high irradiation dose to healthy organs and making the results difficult to interpret. In addition, the long half-life limits the repeated use of ^{85}Sr that is sometimes necessary for refining the diagnosis [55]. Today in the practice of imaging bone tumors and metastases, ^{85}Sr is replaced by phosphates and pyrophosphates labelled by ^{99m}Tc, although it was the most used radionuclide in nuclear medicine imaging until the beginning of the 1970s [56]. Synthesis of ^{85}Sr is quite similar to that of ^{82}Sr; however, ^{85}Sr is used as it is. Besides bone neoplasms, ^{85}Sr was successfully used for the diagnosis of carcinoma of the prostate [57].

Nuclear therapy is another prospective direction of radionuclides application in medicine. Alpha or beta emitters are introduced into a tumor resulting in a very high irradiation dose in the tumor and relatively low dose in all body due to short travel of beta and especially alpha particles in biological tissues. Thus, the main requirements for therapeutic radionuclides are short half-life, high energy of beta/alpha particles, and low yield of gamma radiation. Strontium does not have any alpha-emitting isotopes, but two beta emitters, ^{89}Sr and ^{90}Sr, are used in medicine.

^{89}Sr is used as $^{89}SrCl_2$ in a targeted palliative therapy of painful bone metastasis of various primary tumors [58, 59]. As a rule, repeated doses are administered intravenous or intracavitary. Introduction of ^{89}Sr into a tumor results in destruction and death of a tumor's cells. Storto et al. [60] reported that ^{89}Sr-based palliative therapy was especially effective in combination with use of zoledronic acid. Based on studies with 49 patients, they have found that in patients with painful bone metastases from prostate or breast cancer, the combined therapy with $^{89}SrCl_2$ and zoledronic acid is significantly more effective in treating pain and improving the overall performance status than $^{89}SrCl_2$ and zoledronic acid used separately. ^{89}Sr is also used in combination with ^{85}Sr for monitoring distribution of ^{89}Sr because both isotopes of strontium have the same behavior in human's body and very similar half-lives. However, addition of gamma-emitting ^{85}Sr increases irradiation of healthy tissues. Owaki et al. are developing the technology for direct nuclear medicine imaging distribution of ^{89}Sr dichloride via its own bremsstrahlung X-ray radiation. Although generating efficiency of bremsstrahlung radiation is low, it can be increased by using a lead collimator with optimal thickness of 1.0–1.9 mm and hole length of 40–66 mm [61–63]. The main methods of production of ^{89}Sr for medical purposes are irradiation of a target of highly enriched ^{88}Sr (>99.9%) by thermal neutrons due to $^{88}Sr(n,\gamma)^{89}Sr$ reaction and irradiation of yttrium target by fast neutrons due to $^{89}Y(n,p)^{89}Sr$ reaction. Cross sections of these reactions are quite low, 6×10^{-3} and 0.3×10^{-3} barns for the first and the second reactions, respectively; therefore, yields of ^{89}Sr are also low: 0.4 and 0.01 MBq/(g kW). The RRC "Kurchatov Institute" (Russia) in collaboration with TCI Medical (Albuquerque, USA) has developed a technology for ^{89}Sr synthesis in a 20 kW solution nuclear reactor "Argus." The proposed technology is based on the presence of noble gas isotope ^{89}Kr ($T_{1/2} = 190.7$ s) in the decay chain $^{89}Se \rightarrow {}^{89}Br \rightarrow {}^{89}Kr \rightarrow {}^{89}Rb \rightarrow {}^{89}Sr$.

In this method, ^{89}Kr flows off through an air loop and then stored for ^{89}Kr decay and ^{89}Sr ingrowth. Thus, the technology allows avoiding undesirable impurities of ^{90}Sr in the ^{89}Sr product. The expected annual productivity of the "Argus" reactor is (1.5–1.8) × 10^3 GBq of ^{89}Sr; in addition, it allows to generate and produce ^{99}Mo, ^{133}Xe, and some other valuable products [64]. Production of ^{89}Sr in a subcritical aqueous homogenous reactor driven by a 30-MeV proton accelerator is also considered [65]. Separation of ^{89}Sr from highly enriched uranium targets irradiated in nuclear reactor is another alternative for ^{89}Sr generation. ^{89}Sr can be separated by sorption by polyantimonic acid from 4M HNO_3 medium and then eluted by 1M $AgNO_3$ and 8M HNO_3 at 75°C [66]. In the future, ^{89}Sr will be probably replaced by ^{223}Ra possessing significant advantages as compared with strontium: it is an alpha emitter with four alpha-emitting daughters providing a significantly higher dose in a tumor and it has a shorter half-life, 11.4 days vs. 50 days of ^{89}Sr [67].

^{90}Sr itself is not suitable for nuclear medicine because of too long half-life; however, its short-lived daughter ^{90}Y ($T_{1/2}$ = 64.1 h) is utilized in therapy of various tumors. The high effectiveness of ^{90}Y-labelled radiopharmaceuticals use was shown for tumors in the liver [68] and brain [69], gastroenteropancreatic NETs and glioblastoma [70], breast cancer and prostate cancer [71], and neuroendocrine tumors [72]. In a number of cases, ^{90}Y is used in combination with other radionuclides, i.e., ^{111}In [70] or ^{177}Lu [73]. ^{90}Sr is always separated from spent nuclear fuel or corresponding radioactive waste. The main problem of ^{90}Sr/^{90}Y generator is necessity of clear Y/Sr separation because long-lived ^{90}Sr is highly radiotoxic. Maximal acceptable activity of ^{90}Sr is 74 kBq in bones and 28 kBq in lungs. Thus, the desirable content of ^{90}Sr in ^{90}Y should be 10^{-6}% or less. Sorption and extraction chromatography are commonly used for Y/Sr separation in ^{90}Sr/^{90}Y generators. Extraction chromatographic resins containing crown ether (4,4′(5′)-di-t-butylcyclohexano-18-crown-6) highly selective for strontium are the most promising for this separation [74]. Lee et al. [75] reported that one-column ^{90}Sr/^{90}Y generator based on functionalized silica allows for 92% recovery of ^{90}Y with a contamination ratio ^{90}Sr/^{90}Y of 1.2 × 10^{-5} and 70% with the ratio of 1.2 × 10^{-5}. Happel et al. [76] showed the possibility of Y/Sr separation using nuclear track micro filters impregnated by an appropriate extractant, i.e., crown ether or a 1:1 mixture of bis-(2-ethylhexyl)-phosphate and tributylphosphate.

In addition, other two non-used radioactive strontium isotopes were studied for nuclear medicine applications. ^{87m}Sr ($T_{1/2}$ = 2.81 h, pure gamma emitter, $E\gamma$ = 388 keV) can be used in diagnostic techniques for various skeletal diseases. It isn't applicated for diagnosis because of high body background of the patient during the first days after injection of the isotope and the very short half-life, which does not allow obtaining easily interpreted results [55]. ^{83}Sr ($T_{1/2}$ = 32.4 h) is another potentially useful β^+-emitting radionuclide for therapy planning before use of ^{89}Sr [77].

4 Conclusions

Thus, strontium isotopes, both stable and radioactive, are very useful and important for various spheres of science and technology: from fundamental geological and archaeological researches to diagnostics and therapy of patients in nuclear medicine. The use of stable isotopes of strontium is based on radioactive decay of the long-lived natural ^{87}Rb to stable ^{87}Sr that allows dating Rb-rich rocks. During the last two decades, a unique ^{87}Sr/^{86}Sr ratio in each region is studied as a useful tool for tracing geographical origin of archaeological artifacts and determination of falsification of expensive products such as elite wine and cheese.

Radioactive isotopes of strontium are widely used in nuclear medicine. Among them, ^{85}Sr and ^{89}Sr are used as strontium chlorides for nuclear imaging and palliative therapy of bone tumors and metastases, respectively. Another two are interesting as sources of their valuable daughter radionuclides: ^{82}Rb (daughter of ^{82}Sr) is the main radionuclide for PET diagnostics in cardiology and ^{90}Y (daughter of ^{90}Sr) is used for radiotherapy. While relatively short-lived ^{82}Sr, ^{85}Sr, and ^{89}Sr should be produced in cyclotrons, accelerators, and reactors, the long-lived ^{90}Sr is obtained from irradiated nuclear fuel and corresponding wastes as a by-product. Due to its availability and low price, it has found application for production of beta radiation sources and energy sources as well as in some other spheres.

The analysis of properties and application of stable and radioactive strontium isotopes allow us for the assessment and future potential of their use. Rubidium-strontium dating has become already a routine method in geochronology. Like this, we expect that the use of ^{87}Sr/^{86}Sr ratio as a geographic signature of origin of foods and archaeological artifact will become a routine method during the next several decades. This method probably has a potential for application in some other similar spheres such as criminalistics and tracing animals' migration in biology. Use of radioactive isotopes of strontium has also increasing potential. Among the described applications, use of ^{90}Sr in power sources and use of ^{85}Sr in nuclear imaging show negative dynamics in the twenty-first century. ^{90}Sr-based power sources are replaced by safe and green solar and wind power sources in the whole Arctic region, whereas in the case of space probes and satellites, these sources have given way to ^{238}Pu-based ones. More than 50-year experience of RITEG use resulted in a certain contamination of the environment by radiostrontium as a result of accidents; however, this contamination seems to be insignificant as compared with global dispersion of ^{90}Sr and other fission products as a result of nuclear weapons tests. In other spheres such as production of beta sources and ^{90}Y generators, ^{90}Sr has quite stable or even developing market. By contrast, use of ^{89}Sr and especially ^{82}Sr in nuclear medicine has a very good potential; therefore, we expect that production and use of these radionuclides will increase in the nearest future.

References

1. Magill J, Pfenning G, Dreher R, Soti Z (2012) Chart of the nuclides (Karlsruher Nuclidkarte)8th edn. Nucleonica GmbH, Karlsruhe
2. Titaeva NA (2000) Nuclear geochemistry2nd edn. MSU Publisher, Moscow
3. Amsellem E, Moynier F, Day JMD, Moreira M, Puchtel IS, Teng FZ (2018) The stable strontium isotopic composition of ocean island basalts, mid-ocean ridge basalts, and komatiites. Chem Geol 483:595–602
4. Gregory FS, Reynolds BC, Kiczka M, Bourdon B (2010) Evidence for mass-dependent isotopic fractionation of strontium in a glaciated granitic watershed. Geochim Cosmochim Acta 74:2596–2614
5. Halicz L, Segal I, Fruchter N, Stein M, Lazar B (2008) Strontium stable isotopes fractionate in the soil environments? Earth Planet Sci Lett 272:406–411
6. De Paolo DJ, Wasserburg GJ (1976) Inferences about magma sources and mantle structure from variations of $^{143}Nd/^{143}Nd$. Geophys Res Lett 13:743–746
7. Chaudhuri S (1978) Strontium isotopic composition of several oilfield brines from Kansas and Colorado. Geochim Cosmochim Acta 42:329–332
8. Sahib LY, Marandi A, Schüth C (2016) Strontium isotopes as an indicator for groundwater salinity sources in the Kirkuk region, Iraq. Sci Total Environ 562:935–945
9. Vilomet JD, Angeletti B, Moustier S, Ambrosi JP, Wiesner M, Bottero JY, Snidaro LCH (2001) Application of strontium isotopes for tracing landfill leachate plumes in groundwater. Environ Sci Technol 35:4675–4679
10. Stevenson EI, Aciego SM, Chutcharavan P, Parkinson IJ, Burton KW, Blakowski MA, Arendt CA (2016) Insights into combined radiogenic and stable strontium isotopes as tracers for weathering processes in subglacial environments. Chem Geol 429:33–43
11. Wei G, Ma J, Liu Y, Xie L, Lu W, Deng W, Ren Z, Zeng T, Yang Y (2013) Seasonal changes in the radiogenic and stable strontium isotopic composition of Xijiang River water: implications for chemical weathering. Chem Geol 343:67–75
12. Bentley RA (2006) Strontium isotopes from the earth to the archaeological skeleton: a review. J Archaeol Method Theory 13:135–187
13. Degryse P, Muynck D, Delporte S, Boyen S, Jadoul L, Winne JD, Ivaneanu T, Vanhaecke F (2012) Strontium isotopic analysis as an experimental auxiliary technique in forensic identification of human remains. Anal Method 4:2674–2677
14. Gan YM, Towers J, Bradley RA, Pearson E, Nowell G, Peterkin J, Montgomery J (2018) Multi-isotope evidence for cattle droving at Roman Worcester. J Archaeol Sci Rep 20:6–17
15. Hughes SS, Millard AR, Chenery CA, Nowelld G, Pearson DG (2018) Isotopic analysis of burials from the early Anglo-Saxon cemetery at East Bourne, Sussex, UK. J Archaeol Sci Rep 19:513–525
16. Sheridan SG, Gregoricka LA (2015) Monks on the move: evaluating pilgrimage to byzantine St. Stephen's monastery using strontium isotopes. Am J Phys Anthropol 158:581–591
17. Slovak NM, Paytan A, Rick JW, Chien CT (2018) Establishing radiogenic strontium isotope signatures for Chavín de Huántar, Peru. J Archaeol Sci Rep 19:411–419
18. Turner BL, Kamenov GD, Kingston JD, Armelagos GJ (2009) Insights into immigration and social class at Machu Picchu, Peru based on oxygen, strontium, and lead isotopic analysis. J Archaeol Sci 36:317–332
19. Ganio M, Gulmini M, Latruwe K, Vanhaecke F, Degryse P (2013) Sasanian glass from Veh Ardasır investigated by strontium and neodymium isotopic analysis. J Archaeol Sci 40:4264–4270
20. Durante C, Baschieri C, Bertacchini L, Cocchi M, Sighinolfi S, Silvestri M, Marchetti A (2013) Geographical traceability based on $^{87}Sr/^{86}Sr$ indicator: a first approach for PDO Lambrusco wines from Modena. Food Chem 141:2779–2787

21. Durante C, Baschieri C, Bertacchini L, Bertelli D, Cocchi M, Marchetti A, Manzini D, Papotti G, Sighinolfi S (2015) An analytical approach to Sr isotope ratio determination in Lambrusco wines for geographical traceability purposes. Food Chem 173:557–563
22. Durante C, Bertacchini L, Bontempo L, Camin F, Manzini D, Lambertini P, Marchetti A, Paolini M (2016) From soil to grape and wine: variation of light and heavy elements isotope ratios. Food Chem 210:648–659
23. Petrini R, Sansone L, Slejko FF, Buccianti A, Marcuzzo P, Tomasi D (2015) The $^{87}Sr/^{86}Sr$ strontium isotopic systematics applied to Glera vineyards: a tracer for the geographical origin of the Prosecco. Food Chem 170:138–144
24. Vinciguerra V, Stevenson R, Pedneault K, Poirier A, Hélie JF, Widory D (2015) Strontium isotope characterization of wines from the Quebec (Canada) terroir. Proc Earth Planet Sci 13:252–255
25. Marchionni S, Buccianti A, Bollati A, Braschi E, Cifelli F, Molin P, Parotto M, Mattei M, Tommasini S, Conticelli S (2016) Conservation of $^{87}Sr/^{86}Sr$ isotopic ratios during the winemaking processes of 'red' wines to validate their use as geographic tracer. Food Chem 190:777–785
26. Di Vacri ML (2014) Use of Sr-resin for cheese geographical origin classification. Triskem users group meeting, Bath. http://www.triskem-international.com/scripts/files/59cf52569048b5.48524333/use_of_sr-resin_for_cheese_geographical_origin_classification.pdf. Accessed 05 July 2018
27. Voerkelius S, Lorenz GD, Rummel S, Quetel CR, Heiss G, Baxter M, Brach-Papa C, Deters-Itzelsberger P, Hoelzl S, Hoogewerff J, Ponzevera E, Van BM, Ueckermann H (2010) Strontium isotopic signatures of natural mineral waters, the reference to a simple geological map and its potential for authentication of food. Food Chem 118:933–940
28. Voronina AV, Betenekov ND, Semenishchev VS, Nedobukh TA (2015) Analysis of radionuclides in environmental samples. In: Walther C, Gupta DK (eds) Radionuclides in the environment. Influence of chemical speciation and plant uptake on radionuclide migration. Springer, Berlin, pp 231–253
29. IAEA (2018) Nuclear power reactors in the world. Reference data series No. 2. 2018 edition. IAEA, Vienna. https://www-pub.iaea.org/MTCD/Publications/PDF/RDS-2-38_web.pdf. Accessed 02 July 2018
30. Kelley KK (2005) Wireless blade monitoring system and process, US patent number US7176812B1
31. Shaurina AM, Yakovlev VV (2015) Creation and consequences of use of radiological warfare as a terrorists' weapon. Proceedings of international conference on days of science of Peter the Great. St. Petersburg Polytechnic University, St. Petersburg, pp 140–144
32. Adams R (1996) RTG heat sources: two proven materials. https://atomicinsights.com/rtg-heat-sources-two-proven-materials/. Accessed 01 July 2018
33. Technical Report (1968) SNAP-21 program, phase II. Deep sea radioisotope-fueled thermoelectric generator power supply system. Quarterly report No. 9, July 1, 1968–September 30, 1968
34. IAEA (2013). https://www.iaea.org/OurWork/ST/NE/NEFW/Technical-Areas/WTS/CEG/documents/CEG-Workshop-Vienna-2013/Russian/2.7._Russian_RTG_program_Rus.pdf. Accessed 01 July 2018 (In Russian)
35. Serebryakov BE (2017) RITEGs in Antarctica. http://www.proatom.ru/modules.php?name=News&file=article&sid=7515. Accessed 01 July 2018 (In Russian)
36. Kirienko SV (2015) Report at Russian Government's session from 16.11.2015. http://government.ru/news/20580/. Accessed 01 July 2018 (In Russian)
37. Loborev VM, Pertsev SF, Fortov VE, Shilobreev BA (2014) Physics of nuclear blast. Development of blast, vol 1. Physical and Mathematical Literature, Moscow
38. Maximov AA, Gichev DV, Vysotsky VL, Filippov AS, Tagiltsev AA, Cheranev MY, Goncharov RA (2016) Search of an accidentally drowned radioisotope thermoelectric generator based on heat field in bottom layer of sea. Subaquat Stud Robototech 1:56–65

39. Luo N, Ulmen B, Miley GH (2010) Nanopore/multilayer isotope batteries using radioisotopes from nuclear wastes. In: Proceedings of the 8th annual international energy conversion engineering conference. AIAA 2010-7003
40. Miley GH, Lou N (2011) A nanopore multilayer isotope battery using radioisotopes from nuclear wastes. In: Proceedings of the 9th annual international energy conversion engineering conference, IECEC 2011
41. Oh K, Prelas MA, Rothenberger JB, Lukosi ED, Jeong J, Montenegro DE (2012) Theoretical maximum efficiencies of optimized slab and spherical beta voltaic systems utilizing Sulfur-35, Strontium-90, and Yttrium-90. Nucl Technol 179:234–242
42. Steinfelds EV, Prelas MA, Loyalka SK, Tompson RV (2006) A comparison of the performance capabilities of radioisotope energy conversion systems, beta voltaic cells, and other nuclear batteries. Proceedings of the 2006 International Congress on Advances in Nuclear Power Plants, ICAPP'06, pp 2696–2706
43. Özkeçeci S, Koç R (2017) An experimental setup for study direct charge battery based on Sr-90. AIP Conf Proc 1815:060018
44. Theirrattanakul S, Prelas M (2017) A methodology for efficiency optimization of beta voltaic cell design using an isotropic planar source having an energy dependent beta particle distribution. Appl Radiat Isotop 127:41–46
45. Rischpler C, Paschali A, Anagnostopoulos C, Nekolla SG (2015) Cardiac PET for translational imaging. Curr Cardiol Rep 17:28
46. Zhuikov BL (2014) Production of medical radionuclides in Russia: status and future – a review. Appl Radiat Isotop 84:48–56
47. Do NV, Thanh KT, Khue PD, Hien NT, Kim G, Kim K, Shin SG, Cho MH, Kye YU (2018) Yield ratios of the isomeric pair ^{85m,g}Sr formed in ^{nat}Sr(γ,xn) reactions. Radiat Phys Chem 149:54–60
48. Zhuikov BL (2016) Successes and problems in the development of medical radioisotope production in Russia. Phys Usp 59:481–486
49. Artun O (2018) Calculation of productions of PET radioisotopes via phenomenological level density models. Radiat Phys Chem 149:73–83
50. Fitzsimmons JM, Medvedev DG, Mausner LF (2016) Specific activity and isotope abundances of strontium in purified strontium-82. J Anal Atom Spectrom 31:458–463
51. Chudakov VM, Zhuikov BL, Ermolaev SV, Kokhanyuk VM, Mostova MI, Zaitsev VV, Shatik SV, Kostenikov NA, Ryzhkova DV, Tyutin LA (2014) Characterization of a ^{82}Rb generator for positron emission tomography. Radiochemistry 56:535–543
52. Mangla A, Oliveros E, Williams KA, Kalra DK (2017) Cardiac imaging in the diagnosis of coronary artery disease. Curr Probl Cardiol 42:316–366
53. Flemming WH, McIlraith JD, King ER (1961) Photoscanning of bone lesions utilizing strontium-85. Radiology 77:635–636
54. Goldsmith SJ, Mihailovic J (2015) Guest editorial: skeletal nuclear medicine. Semin Nucl Med 45:2
55. Nalapko TV, Skvortsov VG, Kharitonov YY, Epstein NB (2010) Radiopharmaceuticals for radionuclidic diagnostics of bone pathology (review). Pharm Chem J 44:504–506
56. Mihailović J, Freeman L (2012) Bone: from planar imaging to SPECT & PET/CT. Arch Oncol 20:117–120
57. Williams DF, Blahd W (1967) The diagnostic and prognostic value of strontium-85 photoscanning in carcinoma of the prostate. J Urol 97:1070–1071
58. Audi G, Wapstra AH, Thibault C, Blachot J, Bersillon O (2003) The NUBASE evaluation of nuclear and decay properties. Nucl Phys A 729:3–128
59. Bauman G, Charette M, Reid R, Sathya J (2005) Radiopharmaceuticals for the palliation of painful bone metastases – a systematic review. Radiother Oncol 75:258.E1–258.E13
60. Storto G, Klain M, Paone G, Liuzzi R, Molino L, Marinelli A, Soricelli A, Pace L, Salvatore M (2006) Combined therapy of Sr-89 and zoledronic acid in patients with painful bone metastases. Bone 39:35–41

61. Cipriani C, Atzei G, Argiro G, Boemi S, Shukla S, Rossi G, Sedda AF (1997) Gamma camera imaging of osseous metastatic lesions by strontium-89 bremsstrahlung. Eur J Nucl Med 24:1356–1361
62. Oda H, Hara H, Ueda O, Kawamata H, Sakai H, Katou Y, Kida T, Kubota M (2010) Underlying examination in the imaging of ^{89}Sr bremsstrahlung radiation. Jpn J Radiol Technol 66:764–773
63. Owaki Y, Inoue K, Narita H, Tsuda K, Fukushi MR (2017) Characteristic X-ray imaging for palliative therapy using strontium-89 chloride: understanding the mechanism of nuclear medicine imaging of strontium-89 chloride. Radiol Phys Technol 10:227–233
64. Chuvilin DY, Khvostionov VE, Markovskij DV, Pavshook VA, Ponomarev-Stepnoy NN, Udovenko AN, Shatrov AV, Vereschagin YI, Rice J, Tome LA (2007) Production of ^{89}Sr in solution reactor. Appl Radiat Isotop 65:1087–1094
65. Gholamzadeh Z, Feghhi S, Mirvakili SM, Joze-Vaziri A, Alizadeh M (2015) Computational investigation of ^{99}Mo, ^{89}Sr, and ^{131}I production rates in a subcritical $UO_2(NO_3)_2$ aqueous solution reactor driven by a 30-MeV proton accelerator. Nucl Eng Technol 47:875–883
66. Varma RN, Rao KLN, Chavan GN, Balasubramanian KR, Murthy KS (1982) Separation of ^{89}Sr from irradiated uranium using polyantimonic acid. In: Radiochem Rad Chem Symposium, Pune
67. Bombardieri E, Evangelista L, Ceresoli GL, Boccardo F (2016) Nuclear medicine and the revolution in the modern management of castration-resistant prostate cancer patients: from ^{223}Ra-dichloride to new horizons for therapeutic response assessment. Eur J Nucl Med Mol Imaging 43:5–7
68. Teo JY, Allen JC, Ng DC, Choo SP, Tai DWM, Chang JPE, Cheah FK, Chow PKH, Goh BKP (2016) A systematic review of contralateral liver lobe hypertrophy after unilobar selective internal radiation therapy with Y90. HPB 18:7–12
69. Zalutsky MR (2004) Targeted radiotherapy of brain tumours. Br J Cancer 90:1469–1473
70. Ambrosini V, Fani M, Fanti S, Forrer F, Maecke HR (2011) Radiopeptide imaging and therapy in Europe. J Nucl Med 52:42S–55S
71. Denardo SJ, Denardo GL (2006) Targeted radionuclide therapy for solid tumors: an overview. Int J Radiat Oncol Biol Phys 66:S89–S95
72. Bodei L, Cremonesi M, Grana CM, Chinol M, Baio SM, Severi S, Paganelli G (2012) Yttrium-labelled peptides for therapy of NET. Eur J Nucl Med Mol Imaging 39(Suppl 1):S93–S102
73. Chong HS, Sun X, Chen Y, Sin I, Kang CS, Lewis MR, Liu D, Ruthengael V, Zhong Y, Wu N, Song HA (2015) Synthesis and comparative biological evaluation of bifunctional ligands for radiotherapy applications of ^{90}Y and ^{177}Lu. Bioorg Med Chem 23:1169–1178
74. Pichestapong P, Sriwiang W, Injarean U (2016) Separation of Yttrium-90 from Strontium-90 by extraction chromatography using combined Sr resin and RE resin. Energy Procedia 89:366–372
75. Lee JS, Park UJ, Son KJ, Han HS (2009) One column operation for 90Sr/90Y separation by using a functionalized-silica. Appl Radiat Isot 67:1332–1335
76. Happel S, Streng R, Vater P, Ensinger W (2003) Sr/Y separation by supported liquid membranes based on nuclear track microfilters. Radiat Meas 36:761–766
77. Tárkányi F, Hermanne A, Ditrói F, Takács S, Szücs Z, Brezovcsik K (2017) Investigation of activation cross sections for deuteron induced reactions on strontium up to 50 MeV. Appl Radiat Isotop 127:16–25

Strontium Extraction from the Geo-environment

Rajiv Ranjan Srivastava and Sadia Ilyas

Contents

Abstract Strontium, a highly reactive alkaline earth metal, is very stable in natural occurrence minerals; however, the mobility of its isotope ^{90}Sr produced from the nuclear fallout is one of the deadly fission products. Celestite, $SrSO_4$, is the most important primary source of it following the exploitation via either the black ash or direct leach process. For which, the illustration of the thermal and aqueous chemistry of strontium is very crucial. In the case of ^{90}Sr, its separation from the other radionuclide, most specifically over the ^{137}Cs from the high-level waste (HLW) of fission products, is vital, converting the HLW to low-level waste (LLW). Liquid-liquid (solvent) extraction technology has been widely accepted for the efficient separation and recovery of strontium from the fission products, as the radionuclide already remains in its soluble form therein the waste solution. Interaction strategy between the metal ion and dipole from the donor atom of crown ether is prominently being used, whereas the poorly hydrated anions of dicarbollide, a boron cluster with

R. R. Srivastava (✉)
Center for Environmental Technology, Institute of Research and Development, Duy Tan University, Da Nang, Vietnam
e-mail: r2.srivastava@gmail.com

S. Ilyas (✉)
Mineral and Material Chemistry Lab, Department of Chemistry, University of Agriculture Faisalabad (UAF), Faisalabad, Pakistan
e-mail: sadiailyas1@yahoo.com

P. Pathak, D. K. Gupta (eds.), *Strontium Contamination in the Environment*,
The Handbook of Environmental Chemistry 88,
https://doi.org/10.1007/978-3-030-15314-4_3

a π-bonded trivalent cobalt ion, form ion-pair neutral compounds in the extraction process. In this chapter, the extraction processes of strontium from both natural mineral and synthetic source of the waste fission solution are being discussed, which includes the process technology, adopted techniques behind the technology, crucial points, and key parameters.

Keywords Geo-environment · Mineral · Recovery · Solvent extraction · Strontium

1 Introduction

Strontium (Sr) is a highly reactive alkaline earth metal. The occurrence of natural strontium is stable, but the mobility of its synthetic isotope ^{90}Sr obtained from the nuclear fallout is one of the most harmful fission products [1, 2]. Therefore, the extraction of strontium can also be divided mainly into two parts: (1) minerals, commonly the celestite and strontianite (as shown in Fig. 1), and (2) spent fuels of nuclear fission containing ^{90}Sr [3, 4], which has been focused primarily in this chapter.

2 Extraction from the Primary Minerals

Celestite or say celestine ($SrSO_4$) is the main mineral source of strontium that commonly exists in highly gypsiferous soils. The preferential occurrence in decalcified parts of the groundmass suggests its resultant formation of calcite dissolution without getting affected by the conditions resulting in the dehydration and rehydration of gypsum minerals [3]. The carbonate mineral, strontianite ($SrCO_3$), is another principal mineral of strontium albeit limited and sometimes mixed with celestite. Strontium predominantly as its carbonate salt is largely produced from Sr concentrates by following either black ash or direct leach process.

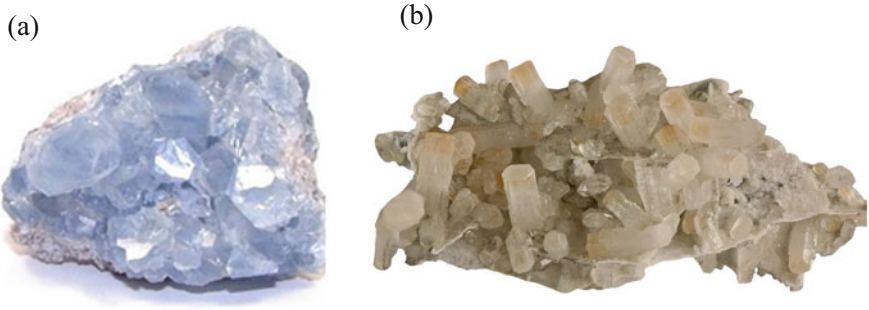

Fig. 1 A pictorial representation of the two major natural minerals of strontium

2.1 Extraction by a Black Ash Process

In the first process, the water-soluble species of strontium sulfide is formed via calcinating the celestite with coal fines in a rotary kiln at a higher temperature ~1100°C to expel out oxygen by forming the CO_2. Thus obtained soluble sulfide of strontium is subjected to dissolve in water and filtered, where the residue contains most of the metal impurities as their insoluble sulfides. The presence of silicon and iron compounds has found to be problematic in this process as they can form water-insoluble silicates and ferrites, respectively, during the calcination process [5–7]. The filtrate is treated with soda ash or carbon dioxide to yield the precipitates of $SrCO_3$ product. Nevertheless, this is the most widely used process, treating approximately 3 lakh tonnes annually [8]; the formation of $SrCO_3$ during calcination causing the insoluble loss of strontium during water leaching is the major disadvantage of this process. Moreover, an energy-intensive process generating the undesirable pollution by-products such as CO_2 and H_2S is also not favorable from operational and environmental aspects [9].

The occurrence of calcination reactions in the black ash process can be given as:

$$SrSO_4 + 2C \xrightarrow{\Delta} SrS + 2CO_2 \quad (1)$$

$$SrSO_4 + 3C \xrightarrow{\Delta} SrS + 2CO + CO_2 \quad (2)$$

However, the Gibbs free energy versus temperature data as shown in Fig. 2 for Eqs. (1) and (2) is thermodynamically possible at approximately 500°C; but if corroborated by the formation of CO and CO_2 from carbon, it can be depicted that

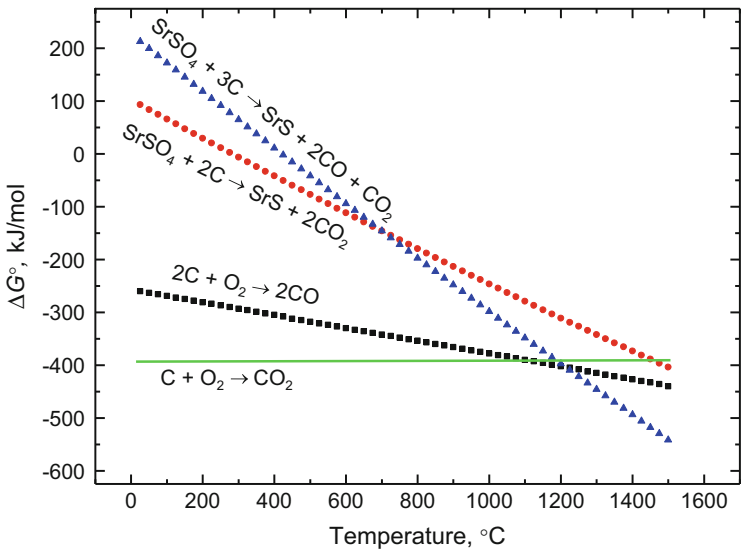

Fig. 2 Gibbs free energy versus temperature plot for celestite calcination with carbon

the occurrence of Eq. (2) is relatively more favorable than Eq. (1) at a temperature slightly below the 1200°C. Thus the formation of the calcined product according to Eq. (1) can be mainly due to often an increased temperature zone than the maintained value while dealing with carbon at high temperature.

The dissolution reaction of calcined product in water can be written as follows:

$$SrS + CO_2 + H_2O \rightarrow SrCO_3 + H_2S \tag{3}$$

Actually Eq. (3) occurs in two steps:

$$SrS + H_2O \rightarrow Sr(OH)_2 + H_2S \tag{3a}$$

$$Sr(OH)_2 + CO_2 \rightarrow SrCO_3 + H_2O \tag{3b}$$

Therefore, it has been found that the progress of Eq. (3) mainly depends on the solubility of $Sr(OH)_2$ by easier decomposition of SrS into hot water (as Eq. 3). The use of CO_2 instead of Na_2CO_3 and the introduction of oxygen in carbonation column can increase the yield and purity of the product within a shorter carbonation time [10].

2.2 *Extraction by Direct Leach Process*

Using the direct leach process in the commercial production of $SrCO_3$, the beneficiation of celestite simply involves crushing, sizing, acid washing (for dissolving impurities of $CaCO_3$, $BaCO_3$, and iron oxide), and sometimes flotation to obtain the concentrates that contain more than 90% $SrSO_4$ [5]. A typical example of celestite beneficiation is given in Table 1 [11]. Thereafter the concentrates are directly leached in carbonate solution using a mechanically stirred tank at moderate temperatures (90–95°C) to yield the $SrCO_3$.

Depending upon the celestite grade and the application, $SrCO_3$ can be used directly or subjected to further purification [6, 11, 12]. Dissolution in HCl followed by pH neutralization of the solution is carried out for removal of iron impurity as its precipitate along with silica. After filtration, the $SrCl_2$ solution is subjected to another precipitation with soda ash to yield $SrCO_3$ of high purity [7]. Alternatively, the impure $SrCO_3$ is calcined at 1400°C to obtain SrO, which is then dissolved in water to separate SiO_2, Fe_2O_3, $Ca(OH)_2$, and Al_2O_3. The filtered solution of $Sr(OH)_2$

Table 1 A typical composition of celestite mineral and concentrate after beneficiation works

Compound	Wt.% in raw mineral	Wt. % in concentrates
$SrSO_4$	76.43	97.85
$SrCO_3$	13.24	<0.01
$CaCO_3$	8.04	<0.01

Small quantities of $BaSO_4$, Fe_2O_3, Al_2O_3, K_2O, and MgO also remain with the mineral

is treated with carbon dioxide to yield the $SrCO_3$ product. In the latter process of purification, the barium carbonate with a little tendency to decompose during calcination can also be eliminated. However, the direct leach process yields a relatively impure product (~95% $SrCO_3$) as compared to the black ash process; it has been considered the simpler process of low cost with by-products of commercial interest [6, 11]. The reactions involved in a direct conversion of celestite to carbonate species followed by purification steps can be given as below:

For leaching:

$$SrSO_4 + Na_2CO_3 \rightarrow SrCO_3 + Na_2SO_4 \tag{4}$$

For purification via acid treatment:

$$SrCO_3 + 2HCl \rightarrow SrCl_2 + H_2CO_3 \tag{5a}$$

$$SrCl_2 + Na_2CO_3 \rightarrow SrCO_3 + 2NaCl \tag{5b}$$

For purification via calcination:

$$SrCO_3 \xrightarrow{\Delta} SrO + CO_2 \tag{6a}$$

$$SrO + H_2O \rightarrow Sr(OH)_2 \tag{6b}$$

$$Sr(OH)_2 + CO_2 \rightarrow SrCO_3 + H_2O \tag{6c}$$

Further, the strontium metal can be produced either by the thermal reduction of strontium oxide and aluminum metal and distillation of elemental strontium on a cooled plate or by the electrolysis of a fused bath of $SrCl_2$ and ammonium/potassium chloride following the reactions [8, 13]:

$$Sr^{2+} + 2e^- \rightarrow Sr \tag{7a}$$

$$2Cl^- \rightarrow Cl_2 + 2e^- \tag{7b}$$

It needs to be mentioned here that low recovery and purity are the main reasons for comparatively being the less industrial use of the direct leach process; hence, this process is widely being studied to understand the direct conversion phenomena of celestite to its high-yield product. Below some of the most influential factors are briefly discussed.

2.2.1 Aqueous Chemistry for Leaching the Strontium

A difference in solubility products between $SrSO_4$ (3.2×10^{-7}) and $SrCO_3$ (1.1×10^{-10}) is the main driving force for the leaching reaction of Eq. (4) [14]; hence, their apparent solubility in terms of Sr ion concentration can be expressed as:

$$\left[Sr^{2+}\right] = \frac{3.2 \times 10^{-7}}{\left[SO_4^{2-}\right]} \tag{8a}$$

$$\left[Sr^{2+}\right] = \frac{1.1 \times 10^{-10}}{\left[CO_3^{2-}\right]} \tag{8b}$$

The solubility calculated for a reaction system of Na_2CO_3: $SrSO_4$ from 1.0 to 1.2 (mole ratio) given in Fig. 3 indicates that regardless of the value of mole ratio, the solubility of $SrSO_4$ is maximum in absence of SO_4^{2-} ions and decreases with an increase in sulfate with the progress of leaching [11]. In contrast, the solubility of $SrCO_3$ increases with consuming the CO_3^{2-} ions. Leaching proceeds to the end of the reaction; the solubility of CO_3^{2-} eventually becomes similar to the SO_4^{2-} ions, which substantially decreases the driving force of leaching reaction. It can be handled by an excess of Na_2CO_3 in solution to keep leaching in progress.

The studies by Iwai and Toguri [15] and Sutarno et al. [7] have clearly established that the stoichiometric conversion of celestite to $SrCO_3$ (at Na_2CO_3: $SrSO_4 = 1{:}1$) occurs only above solution pH 9.0 (as shown in Fig. 4). The influential pH for carbonate leaching has been corroborated by the dissociation constant values of H_2CO_3 [7, 11, 15, 16]:

$$H_2CO_3 \leftrightarrow H^+ + HCO_3^- \quad K_1 = 10^{-6.35} \tag{9a}$$

$$HCO_3^- \leftrightarrow CO_3^{2-} + H^+ \quad K_2 = 10^{-10.33} \tag{9b}$$

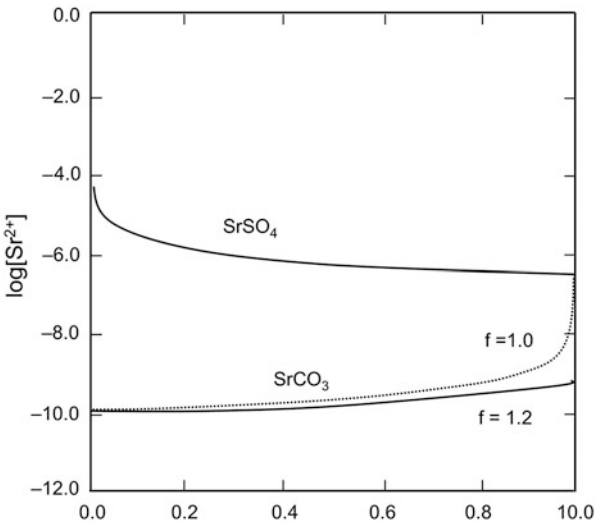

Fig. 3 Apparent solubility of celestite and $SrCO_3$ as a function of sulfate species by reaction with Na_2CO_3 and $SrSO_4$ at different molar ratios (Adopted with permission from Carrillo et al. [11])

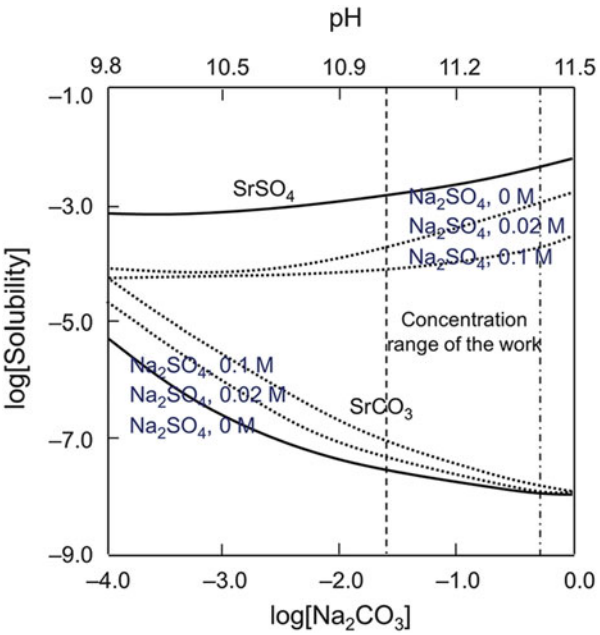

Fig. 4 Relationship between the apparent solubility of $SrCO_3$ and $SrSO_4$ with pH (Adopted with permission from Iwai and Toguri [15])

2.2.2 Parametric Influences on Direct Leach Process of Celestite

Castillejos and co-workers [16] have shown that the rate of reaction significantly increases with increasing carbonate concentration in solution. The fitted parabolic rate constants indicated the leaching is controlled by the diffusion of $NaCO_3^-$ into the pores of the thickening product layer. Notably, leaching celestite in >0.1 M Na_2CO_3 solution at 10 g L^{-1} pulp density caused a decrease in reaction rate due to a lower diffusivity with an increased dense product layer [15, 16]. It has been observed that under a stoichiometric Na_2CO_3 dosage and mild temperature, large conversion fractions are achievable, but not all. An entire conversion has found to be possible with a risen temperature (from 25 to 75°C) under the similar condition (as shown in Fig. 5). The calculated activation energy of 64.1 and 70.05 kJ $mole^{-1}$ in different studies has revealed the transport through chemically controlled conversion reaction [17] and the effective diffusivity of carbonate ions fell in the range of 1.2×10^{-9} to 6.7×10^{-8} cm^2 s^{-1}. Studies on the effect of stirring speed and particle size have favorably demonstrated a high speed (>550 rpm) and small particle size (58 μm) follows shrinking-core model leaching is controlled by product layer reaction [16].

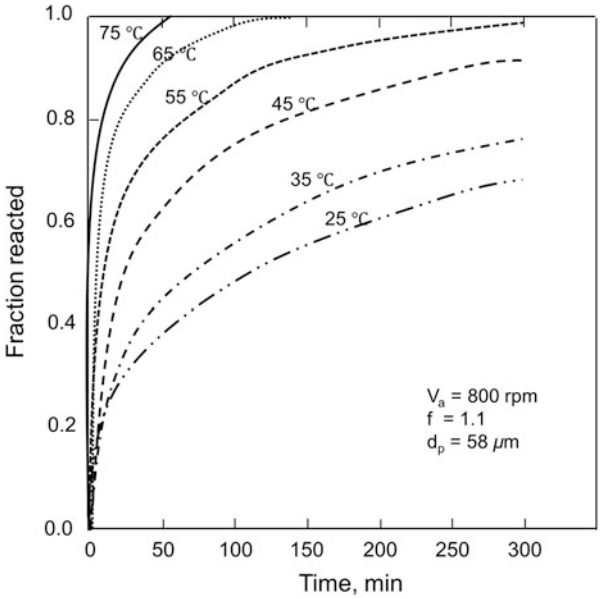

Fig. 5 Rate curve for the conversion of celestite to strontium carbonate as a function of time with different temperatures (Adopted with permission from Castillejos et al. [16])

2.2.3 Other studies

Besides the direct soda ash leach process of celestite, several alternatives have been explored either to increase the yield or purity of $SrCO_3$ product. HCl leaching of celestite showed the activation energy of 68.8 kJ $mole^{-1}$ for the process in 8.25×10^{-3} M $BaCl_2$ solution equilibrated with 0.5 M HCl, and the reaction rate has found to be inversely proportional to the particle size which increases as 0.19, 0.70, and 0.73 powers of the Ba^{2+}, Cl^-, and H^+, respectively [18]. A high purity of 98% celestite has been achieved by Dogan et al. [19], while a Turkish concentrate (~95% $SrSO_4$) cleaning was performed with 50% H_2SO_4 and 1–3% HNO_3 at 40–50°C. Using dry mechanochemical conversion of celestite with Na_2CO_3 in a planetary-type ball mill indicated the degree $SrCO_3$ formation increased (>90%) with milling time above 30 min [20]. The milled powders leached in water at room temperature followed by washing with 1 M HCl give a desirable product of $SrCO_3$, whereas Bingol et al. [21] used the activated $SrSO_4$–$(NH_4)_2CO_3$ mixtures to yield the conversion product of 98.1% $SrCO_3$ [21].

3 Extraction of Radionuclide ^{90}Sr from the HLW of Fission Products

In the processing of spent fuel of nuclear fission, the majority of heat load and radiation in the repository is mainly due to the high-level waste (HLW) of fission products. Approximately 27 tonnes of spent fuel is taken annually from the core of 1000 MWe nuclear reactor [22] that can be regarded entirely as waste (in the USA and Canada) or can be reprocessed (up to 97% in Europe and Japan). ^{137}Cs and ^{90}Sr with their relatively short half-lives of 30 and 28.8 years, respectively, contribute a larger heat load in HLW [23–25]. Therefore, the separation of ^{137}Cs and ^{90}Sr is potentially required to allow their management as a single product with reduced waste volume, saving repository capacity, and shortened the time for subsurface storage until they have decayed sufficiently to be disposed of as low-level waste (LLW). Additionally, the recovered ^{137}Cs and ^{90}Sr can be used as a radiation source in radiotherapy and micropower generator [26, 27]. Various methods (like solvent extraction, ion exchange, adsorption, precipitation, and membrane technology) have been studied and upscaled for the separation of ^{137}Cs and ^{90}Sr from HLW [24, 26–30]. Each of them has own limitations in their application, as given in Table 2 [31, 32]. In terms of stability and applicability for handling a large amount of radionuclide waste, below the prominent one, solvent extraction is being discussed in this chapter (for biosorption studies on strontium, please see Chap. 4).

Table 2 Features and limitations of each process applicable to radioactive waste treatments (After [31, 32])

Technique	Key features	Operational limitations
Precipitation	Handling of large volume and high salt content waste is non-expensive	Low decontamination factor and efficiency is dependent on the filtration rate
Evaporation	Suitable for a variety of radionuclides with decontamination factor $>10^4$ to 10^6	High operational cost with scaling, corrosion, and volatility problems
Ion exchange	The high chemical and thermal stability of long-range resin beads ensure high selectivity	Higher salt concentration affects adversely with blockage and poisoning effect of resin beads
Reverse osmoses	Economical for large-scale operation with decontamination factor 10^2 to 10^3	Fouling and high-pressure system
Ultra filtration	Higher separation ability even for colloidal material	Fouling and radiation damage of membrane are possible
Microfiltration	High recovery, low fouling	Very sensitive to impurity types
Solvent extraction	Large volume operation with high selectivity yields; removal, recovery, and recycling of actinides and solvent itself	Generates aqueous effluent after metal removal often needed a treatment step

3.1 Solvent Extraction

The flexibility in stage design and regeneration of organic, convenience in combining with other processes, and easiness to be scaled up are the inherent properties of solvent extraction (SX) to gain more attention in fuel reprocessing, which in fact is invariably being used at present [33]. Selection of appropriate extractant is the vital factor of SX; hence, below the SX of ^{90}Sr is divided on the basis of extractant used in the separation and recovery process. The compounds developed and widely used in strontium extraction have been given in Fig. 6 [30].

3.1.1 Crown Ethers

Crown ethers are highly selective compounds to interact with metal ions, which arise due to the interactions between the charged metal ion and dipole from the donor atom of crown ether [33]. The selectivity is primarily dependent on the suitability of the size of metal ions with the cavity of particular crown ether. The effect of electrostatic induction as the additional electron withdrawing or donating groups, the presence of altering heteroatoms (P, S, N, and O) within the crown ether, and types of solvents have the major role in the extraction process. Various electron donating and withdrawing substituents, including the alkyl groups (like halogen, methyl, nitro, and amine groups), have been introduced to modify the properties (like solubility and electronic property) of crown ether and are used in the extraction of ^{90}Sr [25, 34]. For instance, 15-crown-5 (15C5) or 18-crown-6 (18C6) are strongly hydrophilic; hence, aryl or alkyl group must be added to enhance their lipophilicity for making them suitable to be used in SX, e.g., dicyclohexano-18-crown-6 (DC18C6) or dibenzo-21-crown-7 (DB21C7) [35]. The extraction of strontium from a nitrate solution by crown ethers can commonly be presented as below (where m and n are an integer value):

$$\mathrm{Sr(NO_3)_2} + \overline{m\mathrm{C}n} \rightarrow \overline{\mathrm{Sr(NO_3)_2} \cdot m\mathrm{C}n} \tag{10}$$

The rigid benzocrown ethers are effective in the extraction of monovalent cations, whereas the cyclohexano crowns are more suitable for divalent cations. The cis-syn-cis, cis-anti-cis, and trans-syn-trans isomers of DC18C6 exhibited the most efficient extractant ($D_{\mathrm{Sr}} = 24.8$) from nitric acid solution. The trans-syn-trans of DC 18C6 yields maximum extraction at a higher acidity, however, with only a 14.3 value of distribution coefficient. Using DC18C6 (0.1 M in chloroform) and DB21C7 (0.1 M in nitrobenzene with the addition of phosphomolybdic acid), the extraction of strontium and cesium could be quantitatively achieved, respectively [36]. The value of distribution coefficient decreases more with an increase in nitric acid concentration in the aqueous solution, as the D_{Cs} and D_{Sr} with *bis*-(4,4′(5′)-[1-hydroxy-2-ethylhexyl]-benzo)-18-crown-6 and *bis*-(4,4′(5′)-[1-hydroxyheptyl] cyclohexano)-18-crown-6 (0.02 M concentration of both crown ether in the mixture

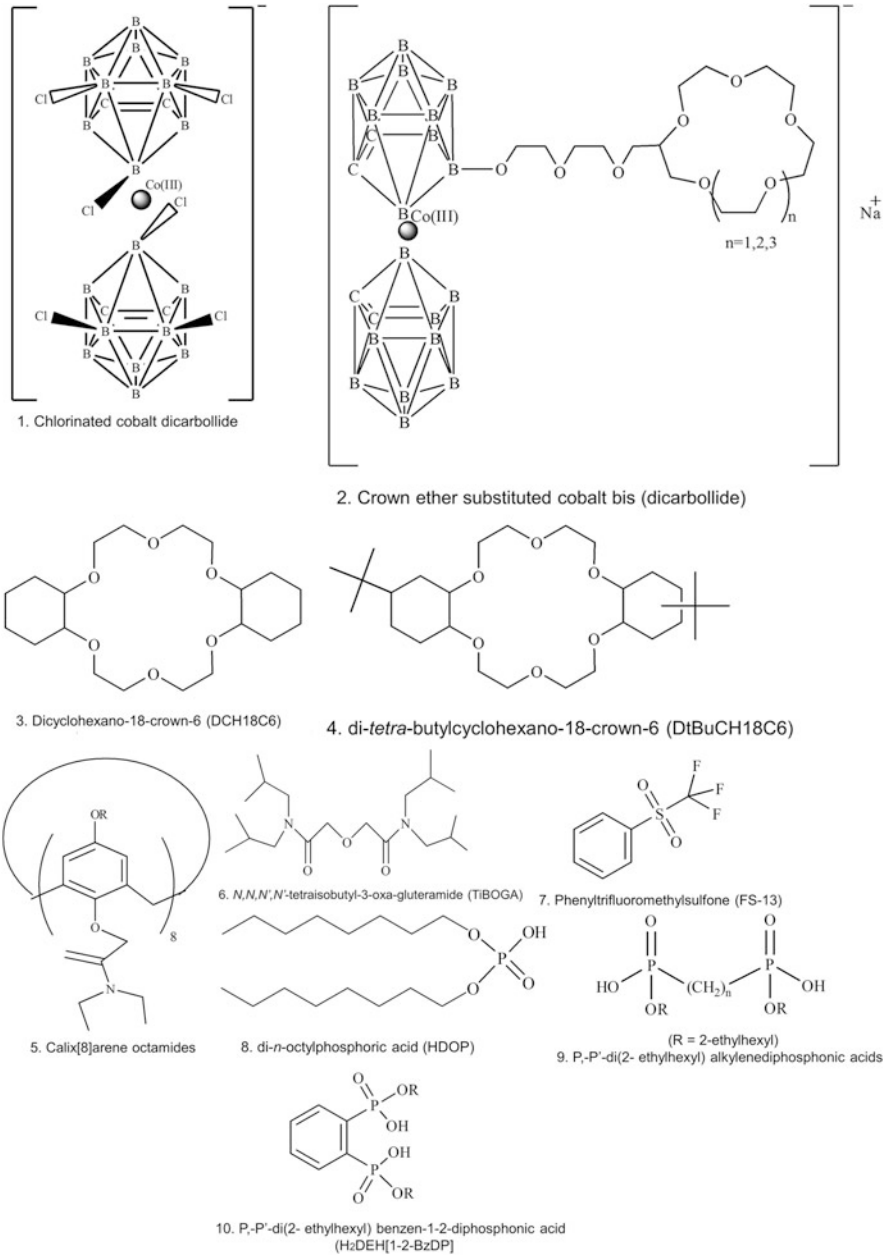

Fig. 6 Various compounds used for solvent extraction of strontium extraction (Adopted with permission from Xu et al. [30])

of 0.1 M nonyl-naphthalenesulfonic acid or TBP–kerosene) were only 1.6 and 1.98 from a 3 M HNO_3 solution. The back-extraction of both metals required multiple stages of stripping with a dilute HNO_3 solution [37–39]. In a similar type of studies by Dietz et al. [40, 41] with a higher acidic solution (4 M HNO_3), the most efficient result ($D_{Cs} = 4$) was with 0.1 M di-*tert*-butyl-benzo-21C7 diluted in methylpentanone and, as for the strontium, evidenced the role of dissolved water therein the diluents. The highest selectivity for cesium over sodium was with 21C7 derivatives; however, the efficient extractant was 4,4′-(5′)-di-[(1-hydroxy-ethylhexyl)-benzo]-18C6 associated with 0.2 M TBP, yielding $D_{Cs} = 30$. It showed that none of the investigated compounds gave the desired combination of selectivity, efficiency, solubility, and stability. The examined dependency on nitrate ion for strontium extraction with various crown ethers revealed the contribution of two moles NO_3^- and the relation with associated cations found in the order of $Mg^{2+} > Al^{3+} > Na^+$ [42]. The extraction behavior of crown ethers from a lower 1.0 HNO_3 solution to the higher 10.0 M HNO_3 solution is given in Table 3.

Horwitz et al. [43–45] used DC18C6 and its dimethyl or di-*tert*-butyl derivatives in various oxygenated and aliphatic diluents, for the SX of strontium from acidic solutions. The highest D_{Sr} obtained with *n*-pentanol and *n*-hexanol could be corroborated to the metal cation extraction with the water contents combined in the diluent. Due to this, the diluent does not require the complete removal of the hydration shell of the nitrate associated with strontium for its mass transfer in the organic phase. Subsequently, the process, namely, "SREX" (stands for strontium extraction) was proposed using the di-*tert*-butyl-cyclohexano-18C6 diluted in 0.2 M 1-octanol from >1 M HNO_3 solution. A good chemical and radiochemical stability showed by the organic constituents required three extraction stages for quantitative extraction (99.7%) of strontium in the SREX process. A trial on Na-bearing waste solution revealed that the interferences caused by the alkali and alkaline earth cations (like Na^+, K^+, Ca^{2+}) did not affect the extraction efficiency of Sr^{2+}. Nevertheless taking the di-*tert*-butyl-cyclohexano-18C6 (0.15 M) in 1.2 M TBP/Isopar L as (diluents), the co-extraction of strontium and lead followed by their selective stripping (using 16 centrifugal contactors) did not give the desired results. A poor selectivity and low extraction were observed due to the building up of metal cations into the organic phase as their insufficient stripping from the loaded organic after the extraction stages.

Combining the Cs extraction (CSEX) with SREX process using the *bis*-4,4′(5′)[(2-hydroxy-alkyl)-benzo]-18-crown-6 and *bis*-4,4′(5′)[(*tert*-butyl)cyclohexano]-18-crown-6 diluted in the mixture of 1.2 M TBP, lauryl nitrile, and Isopar-L, the

Table 3 The behavior of Sr^{2+} extraction by different crown ethers from the feed aqueous solution of 1.0 and 10.0 M HNO_3

	Distribution ratio (D_{Sr}) in acidic solution	
Crown ether	1.0 M HNO_3	10.0 M HNO_3
12C4	0.0009	0.0038
15C5	0.026	0.089
18C6	0.114	0.63
DB18C6	0.0036	0.013

process enables 99.99% cesium and strontium recovery from the waste solution containing 3.78 M HNO_3, 0.486 M Al, 0.778 M Ca, 0.225 M Zr, and 0.015 M Na [46]. Lumetta et al. [47, 48] used di-*tert*-butyl-cyclohexano-18C6 in octanol for selective extraction of strontium after the extraction of lanthanides and actinides by CMPO (Octyl-phenyl-*N*,*N*-diisobutyl carbamoyl methyl phosphine oxide) yielding the decontamination factors that exceeded 7800. A relation between D_{Sr} and water contents into the various organic phases (constituted of DC18C6 in alcohols and DB18C6 derivatives in nitrobenzene 4,4′(5′)-dinonaoyl-dibenzo-18C6, 4,4′(5′)-dihexanoyl-benzo-18C6, 4,4′(5′)-di-acetyl-benzo-18C6, di-*tert*-butylbenzo-18C6, dibenzo-18C6) revealed the highest D_{Sr} with the mixture of butanol and octanol in a ratio of 80:20 [49, 50], whereas the highest D_{Cs} could be achieved with di*tert*-benzo-18C6 in addition with phosphotungstic acid albeit the low solubility of it in nitrobenzene is disadvantageous. Strontium extraction carried out with 15C5/dicarbollide diluted in nitrobenzene from $HClO_4$ with dibenzo-18C6/dicarbollide also diluted in $C_6H_5NO_2$ enabled to get the extraction constants of metal-organic complexes [51, 52]. Also, the highest D_{sr} and selectivity on the extraction of strontium over calcium was obtained with 15-crown-5 and with 15-benzo- and dibenzocrown-5; 12C4 and 18C6 have found to be less effective.

Extraction Influenced by the Diluents and Irradiation Effect

In most of the cases, the diluents comprise the larger part of a solvent. Therefore, proper selection of diluents is almost as crucial as selecting a suitable extractant because of the physical and chemical effects that the diluents can exhibit and also meet the environmental and safety requirements in an SX process [53]. Using the DtBuCH18C6, Mohapatra et al. [54] have investigated the effects of several diluents (including toluene, *n*-octanol, benzene, *t*-butyl benzene, *o*-dichlorobenzene, *n*-dodecane, chloroform, *n*-hexane, and the binary mixtures) on strontium extraction from a nitrate solution. A correlation between the Sr extraction and Schmidt's diluent parameter has been determined, which is formulated by the various physical properties of the diluents (polarizability, H-bonding, viscosity, polarity, Hildebrand's solubility parameter, etc.). Using DCH18C6 with several diluents (chlorobenzene, chloroform, dichloroethane, carbon tetrachloride, *n*-octanol, nitrobenzene, and its mixtures with benzene), Gupta et al. [55] found higher D_{Sr} values for aromatic and chlorinated diluents with their higher dielectric constants. But due to safety concern in the nuclear process, these diluents are not recommended to be used, and, alternatively, a diluent mixture of TBP + dodecane + *n*-octanol (in the proportionate ratio of 30:20:50 vol.%) can be used. Use of dinitriles (glutaronitrile, succinonitrile, malononitrile, and adiponitrile) and diluents with DCH18C6 leads to form the solvated cationic complexes into the organic phase, resulting in an increased efficiency of strontium extraction [56].

The strong radiation by the ^{90}Sr, ^{137}Cs, and other radionuclide elements of the nuclear waste solution, exhibiting the irradiation effect on SX system during the operation, must be addressed [57]. The extractant and diluents in contact with the

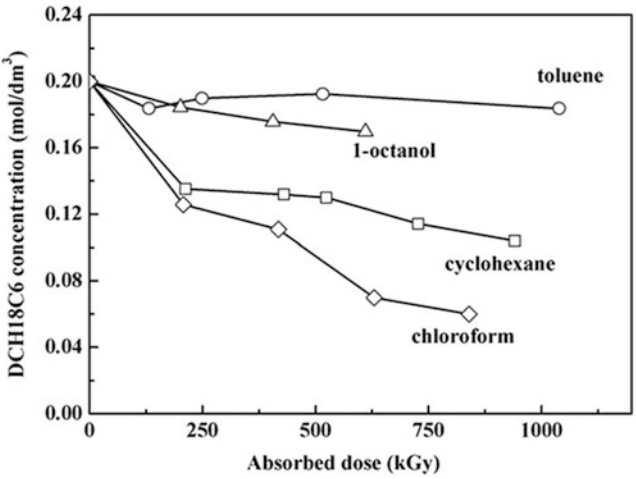

Fig. 7 DCH18C6 concentrations remaining in selected solvents after irradiation (Adopted with permission from Takagi et al. [58])

radioactive waste adversely affect the performance of organic that includes the efficiency, distribution, and separation factors and the recyclability of the organic solvents. The investigated irradiation effect on DCH18C6 with different diluents (chloroform, *n*-octanol, toluene, and cyclohexane) has been given in Fig. 7 [58]. The radiolytic degradation of DCH18C6 in all of the diluents, certainly with different degree, was observed, in which it was least in toluene and highest in chloroform. Exposure to γ-radiation could cause a darkening of solvent (0.12 M HCCD and 0.027 M PEG-400 in phenyltrifluoromethylsulfone) due to the formation of a water-soluble radiolytic product [59]. The value of D_{Sr} gets decreased with an increasing absorbed dosage; however, stripping was unaffected. In a study with the organic phase (0.025 M DtBuCH18C6 in *n*-octanol or in the mixture of 20:80 vol% *n*-octanol/toluene), the irradiated organic phase with diluent mixture showed an improvement in strontium extraction up to a dose of 40 mrad, due to the increased uptake of acid into the organic phase [60]. A reduction in partitioning of Sr^{2+} to crown ether ionic liquids, [C(4)mim][PF6] and [C(4)mim][NTf2] phase, has been observed due to the formation of proton ion during γ-radiation of the ionic liquids, which can be handled by additional water washing step [61–63]. Interestingly, all the removal of Sr^{2+} ions from nuclear waste solution occurs via the irradiated [C_4mim][NTf_2] and via precipitation not by extraction with the organic phase. The precipitates as irradiation product identified as $SrSO_3$ and/or $SrSO_4$, depending on the contact time [63].

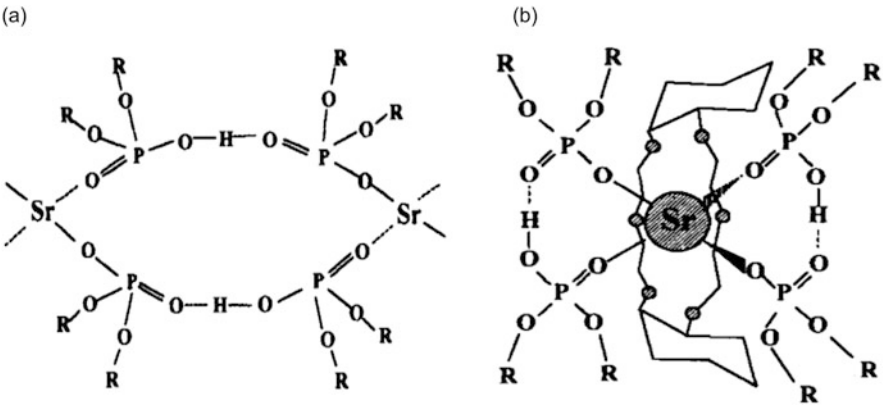

Fig. 8 The structure of Sr complexes (Adopted with permission from Thiyagarajan et al. [65])

Complexed Structure into the Organic Phase

For a better understanding of extraction mechanism, the study on structure formation of metal ion complexed with the organic extractant can be helpful. Adopting the small-angle neutron scattering (SANS) methodology, Chiarizia et al. [64] investigated the extraction behavior of strontium from a $LiNO_3$ solution by using the di-*n*-octylphosphoric acid (HDOP) and compared with HDOP/DCH18C6 mixture in toluene. The addition of DCH18C6 showed a synergistic effect on extraction with increased efficiency than that of with HDOP alone. The SANS analysis revealed that the extraction with HDOP alone in large stoichiometric excess predominantly forms the $Sr(H(DOP)_2)_2$ complex solvated into the organic phase (as shown in Fig. 8a). It is similar to the structure that was reported for the aggregates formation with HDEHP [65]. When Sr^{2+} is wrapped by the DCH18C6 ligand, its interaction with the next two dimmers of HDOP becomes more difficult and prefers to reorient itself as the mononuclear complex schematically is shown in Fig. 8b for the *cis-syn-cis* isomer of DCH18C6. Hence, the addition of crown ether takes part in the complex formation in the ratio of 1:2 for DCH18C6: HDOP while extracting one molecule of Sr^{2+}. The large aggregates by HDOP alone could not be observed in both the *cis-syn-cis* and *cis-anti-cis* isomers of DCH18C6. The structure shown in Fig. 8b is quite supporting to that of the structural study carried out by Burns and Kessler [66] for the bis(dibutylphosphato)aquastrontuim-18crown-6, in which, the 9-coordinated Sr^{2+} ion is revealed to be complexed with six oxygen atoms of the crown ether, two monodentate dibutyl phosphato ions, and one molecule of H_2O. Although a 10-coordinated Sr^{2+} can be found in $[Sr(cis\text{-}syn\text{-}cis\text{-DCHI8C6})(NO_3)_2]\cdot CCI_4$ and $[Sr(cis\text{-}syn\text{-}cis\text{-DCHI8C6})(TMA)_2]\cdot H_2O$ [67], the 9-coordinated Sr^{2+} ion appears to be more suitable for accounting the orientational flexibility of solution complexes [64].

3.1.2 Dicarbollides

Dicarbollide is a boron cluster with a π-bonded cobaltic ion. It was originally prepared by Hawthorne in 1965 and studied for cesium extraction, later used in the extraction of strontium by adding the polyethylene glycols (PEGs) to yield the synergistic effect [23, 29, 30]. The chemical and radiation stability possess the uses of dicarbollides in radionuclide's extraction even from the waste solution of very high acid concentration [68]. The poorly hydrated anions of dicarbollide associated with cations forming the ion-pair neutral compounds have greater solubility in polar-dissociating diluents like nitrobenzene than the water [30]. Its lipophilic anion is difficult to protonate and allows metal cations to be discriminated by their Gibbs energies of transfer. The extraction of strontium from a highly acidic solution can commonly be presented as below (where, m and n are an integer value):

$$\mathrm{Sr^{2+}} + \overline{n\mathrm{H^{+}}} + \overline{n\mathrm{CoB_2^{-}}} \rightarrow n\mathrm{H^{+}} + \overline{\mathrm{Sr^{2+}}} + \overline{n\mathrm{CoB_2^{-}}} \tag{11}$$

The extraction of ^{90}Sr from the nitric acid medium is carried out by dicarbollide anion $\{[\pi\text{-}(3)\text{-}1,2\text{-}\mathrm{B_9C_2H_{11}}]_2\mathrm{Co}\}$ diluted in polar nitrobenzene. The addition of polyethylene glycol (PEG, $\mathrm{HO–(C_2H_4O)}_n\mathrm{–H}$ mainly the lipophilic p-nonylphenyl-nonaethylene glycol, Slovafol 909 $\mathrm{HO–(C_2H_4O)_9–C_6H_4–C_9H_{19}}$) to the dicarbollide can remove the water molecules surrounding the metal cations to improve its transfer to the organic phase. Dicarbollides display good stability toward irradiation; however, only effective in diluents of toxic nature like nitrobenzene and releasing halides during the reprocessing can raise the corrosion problem for the system. Using a diluent without nitro group, diethylene glycol ditetrafluoropropyl is proposed; Slovafol addition can lead to the extraction of ^{90}Sr and ^{137}Cs from 2 M $\mathrm{HNO_3}$ solution. Tetrahexyl-dicarbollide in aromatic hydrocarbon diluents exhibits comparable distribution coefficients to that of the dicarbollide in nitrobenzene. With a negligible loss into the aqueous phase, the equilibrium constant value of 1.7 was obtained for strontium, which was 800 and 0.5 for cesium and sodium ions, respectively [69–71]. Using tetrahexyl-dicarbollide in diethylbenzene for extracting the cesium and strontium from alkaline media yielded a diminished distribution coefficient with respect to increasing alkalinity of the solution. The value of D_{Sr} could be changed from 30 to 7 when NaOH concentration varied from 0.01 to 1.0 M. Using the chlorinated cobalt dicarbollide in nitrobenzene and carbon tetrachloride mixture, with the addition of 1 vol.% Slovafol 909, a 99.8% recovery for ^{90}Sr yielded the decontamination factor of above 500 [72].

Notably, the extracted ^{90}Sr and ^{137}Cs from the HLW are usually taken together for the final geological disposal; hence, their co-extraction can be advantageous [30]. The Universal Extraction (UNEX) process is a relatively well studied co-extraction process using dicarbollide and phosphorylated polyethylene glycols (PPEGs) diluted in m-nitrobenzotrifluoride (MNBTF) [73–75]. The organic phase constituted of the mixture of dicarbollide, PEG, and carbamoylmethyl phosphine oxide (CMPO) diluted in phenyltrifluoromethyl sulfone can be adopted for the simultaneous extraction of ^{90}Sr and ^{137}Cs from highly acidic media, along with the lanthanides and

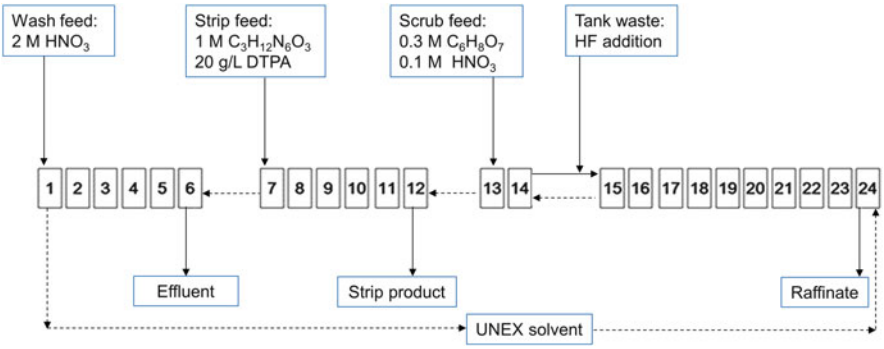

Fig. 9 Flowsheet for the demonstration of the UNEX process. (Adopted with permission from Law et al. [77])

actinides. Diethylenetriaminepentaacetic acid (DTPA) or the guanidine carbonate solution can be used for the effective stripping of extracted metals [76]. Law et al. [77] demonstrated the improved UNEX process with simulated and genuine acidic liquid tank waste, as shown in Fig. 9, in which the suppression iron and zirconium in co-extraction with the strontium and cesium was achieved by adding a certain amount of HF, yielding efficiencies of 99.4% ^{90}Sr and 99.99% ^{137}Cs along with >99% actinides. But looking on the requirement of actinide separation for transmutation in the process of advanced nuclear fuel cycling, the co-extraction of actinides is not preferable; hence, the later use of FS-13 with 0.08 M dicarbollide +0.6 vol.% PEG-400 could significantly suppress the actinide over co-extraction of 99.9% strontium and 97.4% cesium [78].

4 Conclusions

Celestite ($SrSO_4$) and strontianite ($SrCO_3$) are the main mineral source of strontium and predominantly being recovered as its carbonate salt by following the black ash or direct leach process. Nevertheless, the black ash process is widely used; the formation of $SrCO_3$ during calcination leads to the strontium loss, while leaching in water is found to be disadvantageous for the energy-intensive process. On contrary, the direct leach process yields a relatively impure product (~95% $SrCO_3$) as compared to the black ash process, but it is a low-cost simple process with by-products of commercial interests. There has been a plenty of researches devoted to strontium extraction from minerals; however, a high yield with the increased purity has still many scopes for new research to extract strontium from geo-environment.

At the same time, removal of radioactive and heat-emitting ^{90}Sr and ^{137}Cs from nuclear wastes and spent-fuel solutions is of great importance not only for the spent-fuel reprocessing and sustainable management of nuclear but also for the recovery of these two metals. As the requirement of radionuclide removal is still under

discussion with respect to its economic aspects, the R&D on their recovery as value-added products will surely be beneficial for a further technical road map of the spent-fuel reprocessing. The solvent extraction has been potentially demonstrated for the simultaneous separation of cesium and strontium, mainly the CSEX/SREX process, and a combined crown ether/calixarene process. The stability of CSEX crown ether in HNO_3 solution, however, limits its use in an industrial process, and without any further development, the CSEX/SREX process is not a feasible option for advanced fuel cycle initiatives. An improved stability of the extractant in presence of HNO_3 must be addressed by the new research on these processes. In summary, the solvent extraction is a reasonable choice for strontium separation and recovery in advance fuel cycling, and more developments in this area can be well-expected in the near future.

References

1. Pathak P, Singh DN, Pandit GG, Rakesh RR (2016a) Guidelines for quantification of geomaterial-contaminant interaction. J Hazard Toxic Radioact Waste 20:04015012
2. Pathak P, Singh DN, Apte PR, Pandit GG (2016b) Statistical analysis for prediction of distribution coefficient (k_d) of soil-contaminant system. J Environ Eng 142:1–11
3. Mees F, Tursina TV (2010) Salt minerals in saline soils and salts crusts. In: Stoops G, Marcelino V, Mees F (eds) Interpretation of micromorphological features of soils and Regoliths. Elsevier, pp 441–469
4. Ober J (2014) Mineral resource of the month: strontium. Earth, American Geosciences Institute. Retrieved from https://www.earthmagazine.org/article/mineral-resource-month-strontium
5. Collings RK, Andrew PRA (1988) Summary Report No. 2: Celestite. In: CANMET Rep. 88-3E
6. Stein DL (1973) Extraction of strontium values from celestite concentrate at the Kaiser plant in Nova Scotia. In: Gray TJ (ed) International Conference on Strontium Containing Compounds, Atlantic Industrial Research Inst, Halifax, Canada, pp 1–8
7. Sutarno, R Lake, RH, Bowman WS (1970) The extraction of strontium from the mineral celestite. Mineral Sciences Division, Department of Energy, Mines and Resources, Ottawa, Res Rep R-223, pp l–20
8. MacMillan JP, Park JW, Gerstenberg R, Wagner H, Köhler K, Wallbrecht P (2002) Strontium and strontium compounds. Ullmann's Encyclopedia of industrial chemistry. Wiley-VCH, Weinheim
9. Kemal M, Arslan V, Akar A, Canbazoglu M (1996) Production of $SrCO_3$ by black ash process: determination of reductive roasting parameters. In: Kemal M, Arslan V, Canbazoglu M (eds) Changing scopes mineral processing. CRC press, Boca Raton, p 401
10. Erdemoglua M, Canbazoglub M (1998) The leaching of SrS with water and the precipitation of $SrCO_3$ from leach solution by different carbonating agents. Hydrometallurgy 49:135–150
11. Carrillo FR, Uribe A, Castillejos AH (1995) A laboratory study of the leaching of celestite in a Pachuca tank. Miner Eng 8:495–509
12. Trew LJ (1973) Purification of strontium carbonate. US Patent 3741691
13. Grover AK, Joshi MN (1983) Aluminothermic preparation of strontium metal. In: Bose DK, Krishnamurthy N, Mehta OK (eds) Proceedings of the symposium on metallothermic processes in metal and alloy extraction, Nagpur, India, pp 65–78
14. Bard AJ (1966) Chemical equilibrium. Harper and Row, New York
15. Iwai M, Toguri JM (1989) The leaching of celestite in sodium carbonate solutions. Hydrometallurgy 22:87–100

16. Castillejos AHE, Cruz del FPB, Uribe AS (1996) The direct conversion of celestite to strontium carbonate in sodium carbonate aqueous media. Hydrometallurgy 40:207–222
17. Habashi F (1969) Extractive metallurgy, general principles, vol 1. Science Publishers, Paris
18. Aydogan S, Erdemoğlu M, Aras A, Uçar G, Özkan A (2006) Dissolution kinetics of celestite ($SrSO_4$) in HCl solution with $BaCl_2$. Hydrometallurgy 84:239–246
19. Dogan H, Koral M, Kocakusak S (2004) Acid leaching of Turkish celestite concentrate. Hydrometallurgy 71:379–383
20. Setoudeh N, Welham NJ, Azami SM (2010) Dry mechanochemical conversion of $SrSO_4$ to $SrCO_3$. J Alloy Compd 492:389–391
21. Bingol D, Aydoğan S, Bozbaş SK (2012) Production of $SrCO_3$ and $(NH_4)_2SO_4$ by the dry mechanochemical processing of celestite. J Ind Eng Chem 18:834–838
22. Pathak P, Sharma S (2018) Sorption isotherms, kinetics, and thermodynamics of contaminants in Indian soils. J Environ Eng 10:1–9
23. Dozol JF, Dozol M, Macias RM (2000) Extraction of strontium and cesium by dicarbollides, crown ethers and functionalized calixarenes. J Incl Phenom Macrocycl Chem 38:1–22
24. Pathak P (2017) An assessment of strontium sorption onto bentonite buffer material in waste repository. Environ Sci Pollut Res 24:8825–8836
25. Todd TA, Batcheller TA, Law JD, Herbst RS (2004) Cesium and strontium separation technologies: literature review, INEEL/EXT-04-01895. Idaho National Engineering and Environmental Laboratory, Idaho Falls
26. Fukushima S, Inoue T, Ozeki S (1999) Postoperative irradiation of pterygium with Sr-90 eye applicator. Int J Radiat Oncol Biol Phys 43:597–600
27. Gemmill WJ (1971) Miniaturized radioisotope generator. US Patent No. 3566124
28. IAEA-International Atomic Energy Agency (1993) Feasibility of separation and utilization of cesium and strontium from high level liquid waste. Technical Report Series No. 356, Vienna
29. Schulz WW, Bray LA (1987) Solvent extraction recovery of by product ^{137}Cs and ^{90}Sr from HNO_3 solutions. Sep Sci Technol 22:191–214
30. Xu C, Wang J, Chen J (2012) Solvent extraction of strontium and cesium: a review of recent progress. Solvent Extr Ion Exch 30:623–650
31. Rahman ROA, Ibrahium HA, Hung YT (2011) Liquid radioactive wastes treatment: a review. Water 3:551–565
32. Rana D, Matsuura T, Kassim MA, Ismail AF (2013) Radioactive decontamination of water by membrane processes — a review. Desalination 321:77–92
33. Tachimori S (2010) Overview of solvent extraction chemistry for reprocessing. In: Moyer BA (ed) Ion exchange and solvent extraction, vol 19. CRC Press, Boca Raton, pp 1–63
34. Pannell KH, Yee W, Lewandos GS, Hambrich DC (1977) Electronic substituent effects upon the selectivity of synthetic ionophores. J Am Chem Soc 99:1457–1461
35. McDowell WJ, Moyer BA, Case GN, Case FI (1986) Metal ions by organic cation exchangers synergized by macrocycles: factors relating to macrocycle size and structure. Solvent Extr Ion Exch 4:217–236
36. Bryan JC, Sachleben RA, Lavis JM, Davis MC, Burns JH, Hay BP (1998) Structural aspects of rubidium ion selectivity by tribenzo-21-crown-71a. Inorg Chem 37:2749–2755
37. Gerow IH, Davis MW (1979) The use of 24-crown-8's in the solvent extraction of $CsNO_3$ and $Sr(NO_3)_2$. Sep Sci Technol 14:395–414
38. Gerow IH, Smith JE, Davis MW (1981) Extraction of Cs^+ and Sr^{2+} from HNO_3 solution using macrocyclic polyethers. Sep Sci Technol 16:519–548
39. Shuler RG, Bowers CB, Smith Jr JE, Van Brunt V, Davis Jr MW (1985) The extraction of cesium and strontium from acidic high activity nuclear waste using a PUREX process compatible organic extractant. Solvent Extr Ion Exch 3:567–604
40. Dietz ML, Horwitz EP, Jensen MP, Rhoads S, Bartsch RA, Palka A, Krzykewski J (1996b) Substitution effects in the extraction of cesium from acidic nitrate media using macrocyclic polyethers. Solvent Extr Ion Exch 14:357–384

41. Dietz ML, Horwitz EP, Rhoads S, Bartsch RA, Krzykewski J (1996a) Extraction of cesium from acidic nitrate media using macrocyclic polyethers: the role of organic phase water. Solvent Extr Ion Exch 14:1–12
42. Shehata FA (1994) Extraction of strontium from nitric acid solutions by selected crown ethers. J Radioanal Nucl Chem 185:411–417
43. Horwitz EP, Dietz ML, Fisher DE (1990a) Extraction of strontium from nitric acid solutions using dicyclohexano-18-crown-5 and its derivatives. Solvent Extr Ion Exch 8:557–572
44. Horwitz EP, Dietz ML, Fisher DE (1990b) Correlation of the extraction of strontium nitrate by a crown ether with the water content of the organic phase. Sol Extr Ion Exch 8:199–208
45. Horwitz EP, Dietz ML, Fisher DE (1991) SREX: a new process for the extraction and recovery of strontium from acidic nuclear waste streams. Sol Extr Ion Exch 9:1–25
46. Horwitz EP, Dietz ML, Leonard RA (1997) Advanced integrated solvent extraction systems. In: Gephart JM (ed) Efficient separations and processing (ESP) crosscutting program FY 1991 technical exchange meeting, Gaithersburg, MD, USA
47. Lumetta GJ, Wagner MJ, Carlson CD (1996) Actinide, strontium, and cesium removal from Hanford radioactive tank sludge. Solvent Extr Ion Exch 14:35–60
48. Lumetta GJ, Wagner MJ, Jones EO (1995) Separation of strontium-90 from Hanford high-level radioactive waste. Sep Sci Technol 30:1087–1101
49. Kumar A, Mohapatra PK, Pathak PN, Manchanda VK (1997) Dicyclohexano 18 crown 6 in butanol-octanol mixture: a promising extractant of Sr(II) from nitric acid medium. Talanta 45:387–395
50. Kumar A, Mohapatra PK, Manchanda VK (1998) Extraction of cesium-137 from nitric acid medium in the presence of macrocyclic polyethers. J Radioanal Nucl Chem 229:169–172
51. Novy P, Vanura P, Makrlik E (1998) Extraction of 85Sr by the nitrobenzene solution of bis-1,2-dicarbollylcobaltate in the presence of dibenzo-18-crown-6. J Radioanal Nucl Chem 231:65–68
52. Valentova Z, Vanura P, Makrlik E (1997) Extraction of microamounts of strontium by a nitrobenzene solution of bis-1,2-dicarbollylcobaltate in the presence of 15-crown-5. J Radioanal Nucl Chem 224:45–48
53. Ritcey GM, Ashbrook AW (1984) Solvent extraction part I. Elsevier, Amsterdam
54. Mohapatra PK, Lakshmi DS, Manchanda VK (2006) Diluent effect on Sr(II) extraction using di-*tert*-butyl cyclohexano 18 crown 6 as the extractant and its correlation with transport data obtained from supported liquid membrane studies. Desalination 198:166–172
55. Gupta KK, Achuthan PV, Ramanujam A, Mathur JN (2003) Effect of diluents on the extraction of Sr^{2+} from HNO_3 solutions with dicyclohexano-18-crown-6. Solvent Extr Ion Exch 21:53–71
56. Lamb JD, Nazarenko AY, Hansen RJ (1999) Novel solvent system for metal ion separation: improved solvent extraction of strontium(II) and lead(II) as dicyclohexano-18-crown-6 complexes. Sep Sci Technol 34:2583–2599
57. Mincher BJ, Modolo G, Mezyk SP (2009) Review article: the effects of radiation chemistry on solvent extraction: 2. A review of fission-product extraction. Solvent Extr Ion Exch 27:331–353
58. Takagi N, Izumi Y, Ema K, Yamamoto T, Nishizawa K (1999) Radiolytic degradation of a crown ether for extractability of strontium. Solvent Extr Ion Exch 17:1461–1471
59. Mincher BJ, Herbst RS, Tillotson RD, Mezyk SP (2007) Gamma-radiation effects on the performance of HCCD–PEG for Cs and Sr extraction. Solvent Extr Ion Exch 25:747–755
60. Raut DR, Mohapatra PK, Manchanda VK (2010) Extraction of radio-strontium from nitric acid medium using di-*tert*-butyl cyclohexano18-Crown-6 (DTBCH18C6) in toluene-1-octanol diluent mixture. Sep Sci Technol 45:204–211
61. Yuan LY, Peng J, Xu L, Zhai ML, Li JQ, Wei GS (2008) Influence of gamma-radiation on the ionic liquid [C(4)mim][PF6] during extraction of strontium ions. Dalton Trans 45:6358–6360
62. Yuan LY, Peng J, Xu L, Zhai ML, Li JQ, Wei GS (2009a) Radiation effects on hydrophobic ionic liquid [C(4)mim][NTf2] during extraction of strontium ions. J Phys Chem B 113:8948–8952

63. Yuan LY, Xu C, Peng J, Xu L, Zhai ML, Li JQ, Wei GS, Shen XH (2009b) Identification of the radiolytic product of hydrophonic ionic liquid [C(4)mim][NTf2] during removal of Sr^{2+} from aqueous solution. Dalton Trans 38:7873–7875
64. Chiarizia R, Urban V, Thiyagarajan P, Bond AH, Dietz ML (2000) Small angle neutron scattering investigation of the species formed in the extraction of Sr(II) by mixtures of di-*n*-octylphosphoric acid and dicyclohexano-18-crown-6. Solvent Extr Ion Exch 18:451–478
65. Thiyagarajan P, Diamond H, Danesi PR, Horwitz EP (1987) Small-angle neutron-scattering studies of cobalt(II) organophosphorus polymers in deuteriobenzene. Inorg Chem 26:4209–4212
66. Burns JH, Kessler RM (1986) Structural and molecular mechanics studies of bis (dibutylphosphato)aquastrontuim-18crown-6 and analogous alkaline-earth-metal complexes. Inorg Chem 26:1370–1375
67. Burns JH, Bryan SA (1988) Complexes of strontium and barium dimethylpropanoates with dicyclohexano-18-crown-6(A) ether. Acta Cryst C 44:1742–1749
68. Romanovsky VN (2002) Management of accumulated high level waste at the Mayak Production Association in the Russian Federation. In: Issues and trends in radioactive waste management, Proceedings of an International Conference, International Atomic Energy Agency, Vienna, pp 359–372
69. Miller RL, Pinkerton AB, Abney KD, Kinkead SA (1997) US Patent No 5603074
70. Miller RL, Pinkerton AB, Hurlburt PK, Abney KD (1995a) Extraction of cesium and strontium into hydrocarbon solvents using tetra-C-alkyl cobalt dicarbollide. Solvent Extr Ion Exch 13:813–827
71. Miller RL, Pinkerton AB, Hurlburt PK (1995b) 209th ACS national meeting. American Chemical Society, Washington, DC, 2088, p 823
72. Galkin BY, Esimantovskii VM, Lazarev LN, Lyubtsev RI, Romanovskii VN, Shishkin L, Kyrsh KM, Rais I, Selucky P (1998) Abstract in International Solvent Extraction Conference (ISEC 88) Moscow, USSR
73. Esimantovski VM, Galkin BY, Lazarev LN, Lyubtsev RI, Romanovskii VN, Shishkin DN, Dzekun EG (1992) Technological tests of HAW partitioning with the use of chlorinated cobalt dicarbolyde (CHCODIC). Management of Secondary Wastes. In: Proceedings of the International Symposium on Waste Management—92, Tucson, AZ, pp 801–804
74. Herbst RS, Law JD, Todd TA, Romanovskiy VN, Smirnov IV, Babain VA, Esimantovskiy VN, Zaitsev BN (2003) Development of the universal extraction (UNEX) process for the simultaneous recovery of Cs, Sr, and actinides from acidic radioactive wastes. Sep Sci Technol 38:2685–2708
75. Luther TA, Herbst RS, Peterman DR, Tillotson RD, Garn TG, Babain VA, Smirnov IV, Stoyanov ES, Antonov NG (2006) Some aspects of fundamental chemistry of the universal extraction (UNEX) process for the simultaneous separation of major radionuclides (cesium, strontium, actinides, and lanthanides) from radioactive wastes. J Radioanal Nucl Chem 267:603–613
76. Romanovskiy VN, Smirnov IV, Babain VA, Todd TA, Herbst RS, Law JD, Brewer KN (2001) The universal solvent extraction (UNEX) process. I. Development of the UNEX process solvent for the separation of cesium, strontium, and the actinides from acidic radioactive waste. Solvent Extr Ion Exch 19:1–21
77. Law JD, Herbst RS, Todd TA, Romanovskiy VN, Babain VA, Esimantovskiy VM, Smirnov IV, Zaitsev BN (2001) The universal solvent extraction (UNEX) process. II. Flowsheet development and demonstration of the UNEX process for the separation of cesium, strontium, and actinides from actual acidic radioactive waste. Solvent Extr Ion Exch 19:23–36
78. Herbst RS, Law JD, Todd TA, Romanovskii VN, Babain VA, Esimantovski VM, Zaitsev BN, Smirnov IV (2002) Development and testing of a cobalt dicarbollide based solvent extraction process for the separation of cesium and strontium from acidic tank waste. Sep Sci Technol 37:1807–1831

Biosorption of Strontium from Aqueous Solutions

Sadia Ilyas, Rajiv Ranjan Srivastava, and Nimra Ilyas

Contents

Abstract The migration of strontium to the geosphere is one of the major concerns in a proper handling of radionuclide waste solutions. The costly chemical reagents of toxic nature, generating secondary pollution with low efficiency for a minute concentration of metal ions, make their physicochemical separation rather limited in the application. Adsorption onto solid substances like activated carbon, kaolinite, montmorillonite, and colloidal silica is simpler in operation and the most robust; however, their ineptitude at high sodium concentration and very acidic pH are the principal disadvantages of it. The microbial techniques using various biomaterials have been identified as the potential alternative because of being effective to uptake

S. Ilyas (✉)
Mineral and Material Chemistry Lab, Department of Chemistry, University of Agriculture Faisalabad (UAF), Faisalabad, Pakistan
e-mail: sadiailyas1@yahoo.com

R. R. Srivastava (✉)
Center for Environmental Technology, Institute of Research and Development, Duy Tan University, Da Nang, Vietnam
e-mail: r2.srivastava@gmail.com

N. Ilyas
Institute of Microbiology, University of Agriculture Faisalabad (UAF), Faisalabad, Pakistan

P. Pathak, D. K. Gupta (eds.), *Strontium Contamination in the Environment*,
The Handbook of Environmental Chemistry 88,
https://doi.org/10.1007/978-3-030-15314-4_4

lower content of radionuclides, inexpensive, free of secondary pollution, and exhibition of electronegative characteristics through the different organic functional group present therein. The passive removal of metals, termed biosorption, requires the selectivity and high metal uptake capacity of substrates for the applied remediation scenarios. A detailed description of cell wall constituents of fungi, bacteria, and algae is provided in order to explain the selective sorption and/or accumulation of strontium from the radiotoxic waste solutions. The influential role of cellular structure, cell wall, storage, and extracellular polysaccharides is evaluated for the strontium sequestration. Furthermore, the binding mechanisms are discussed, including the involvement of key functional groups and the exhibited ion-exchange process.

Keywords Algae · Bacteria · Biomass · Biosorption · Fungi · Strontium

1 Introduction

Sr^{90}, a product of nuclear fission, has been considered as one of the most radiotoxic substances to the environment and living cells. With long life ($t_{1/2}$ 28.9 years), fair solubility in the aqueous systems, and the utility of Sr^{90} as heat/irradiation source, considerable efforts have been directed toward the separation and recovery of strontium from nuclear waste solutions with particular attention [1–3]. The removal of radionuclides, including Sr^{90} from waste streams, is usually achieved by physicochemical processes, viz., precipitation, coagulation, resin ion exchange, electrochemical processes, solvent extraction, and membrane technology [4]. Decontamination of Cs^+ and Sr^{2+} at a pH 8.0–8.5 using the chemical precipitation method by adding $CuSO_4$,$Fe(NO_3)_3$, $K_4[Fe(CN)_6]$, $BaCl_2$, and Na_2SO_4 as precipitants has been extensively studied [5]. Surface adsorption including ion-exchange process using natural zeolites (along with mordenite, erionite, chabazite, and clinoptilolite), bentonite, granite, and various phenolic resins has been widely investigated [6–11].

In recent times, the adsorption into biomasses has remained in particular interests. The biological systems are identified to have great potential for waste remediation because of their easy availability in abundance, less costly operation, and prevention from further chemical pollution to the environment [12]. The microorganisms, whether prokaryotic or eukaryotic, employ metal species for the structural and/or catalytic functions. Their interactions with metal ions depend in part on whether the microbes are prokaryotic or eukaryotic and also with which (multi)metal system they are supposed to interact. Nevertheless, both microbes can bind with metal ions present in the external environment at the cell surface or their transportation into the cell, for leading various intracellular functions.

In order to have in-depth understanding on the biosorption system which deals with strontium removal from waste streams, this chapter discusses the use of various biosorbents (e.g., algae, fungi, bacteria, plants, and/or plant-derived agro-wastes).

A detailed description of cell wall constituents of fungi, bacteria, and algae is provided in order to explain the selectivity for strontium. The role of cellular structure and associated functional groups is evaluated in terms of their potential for strontium sequestration. Furthermore, the biosorption mechanisms are also explained with respect to various biomasses.

1.1 Defining Biosorption

Biosorption is rather onerous to define due to the simultaneous contribution of several mechanisms controlling the overall process, which usually depends on the characteristics of the (metal)sorbate, (bio)sorbent, environmental factors (pH, medium, etc.), and the absence/presence of metabolic process (involved in the case of living organisms). The prefix "bio" represents the activity of a biological entity (i.e., either the living organism or the component derived from a living organism), whereas "sorption" is a physicochemical expression used for both absorption and adsorption. Notably, absorption is the incorporation of a substance in one state into another substance of different state (e.g., liquids being absorbed onto solid or gaseous molecules, which are a three-dimensional matrix). On the other side, an adsorption is a physical adherence or bonding of ions and molecules onto the surface of another molecular substance (i.e., onto a two-dimensional surface). Adsorption is the most common form of sorption traditionally used and a preferred term unless it is clearly defined about which process (absorption or adsorption) is operative. In particular, the biosorption is a physicochemical property of living (or dead) biomass and the excreted/derived products, which was previously categorized as metabolism-dependent and metabolism-independent biosorption [13]. However, metabolism-dependent processes have now termed as bioaccumulation, and metabolic-independent processes are only taken as the biosorption [14, 15]. For understanding, bioaccumulation is an active biosorption through the attachment of metal ions (sorbates) to the biomass surface followed by the transportation of metal ions into cells [16], on contrary; the passive nature of biosorption process is materialized at a faster rate than that of the bioaccumulation (Fig. 1).

1.2 Biosorption Mechanism

All the biological material has an affinity for metal ions; hence, biomasses potentially available as biosorbents are enormous. A verity of microbial, animal, and plant biomass (inactive, living, or dead) and derived products including synthetic, plants, or agriculture wastes have received attention in a various forms and in relation to different metal ions [19, 20]. However, the biological materials are complex, exhibiting several mechanisms under given conditions. The kind of structural components present in biomass indicates to the functional groups (e.g.,

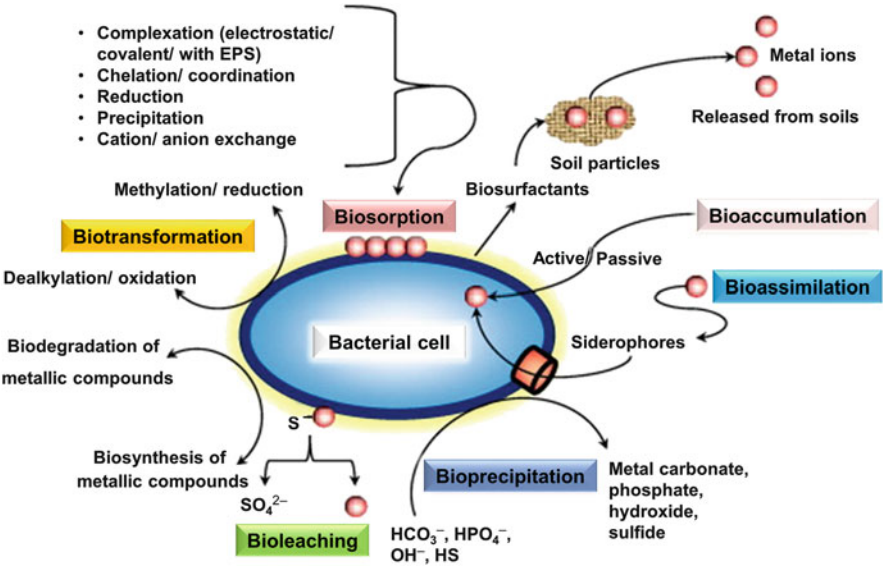

Fig. 1 A typical representation for the various modes of microbial interactions with metal ions (Adopted from the sources: [17, 18])

carboxyl, phosphate, hydroxyl, amino, thiol, etc.) those can interact and bind the metal species [21]. In a biological context, relevant schemes consider ligand preferences, a property that can underline the biological activity: type A (hard acids) preferentially combine with the oxygen-containing ligands (hard bases) predominantly of ionic nature, while type B (soft acids) preferentially combine with the S- and N-containing ligands (soft bases) of covalent characteristics (Fig. 2). The borderline cations can be associated with various atoms from both categories of ligands. Nevertheless, the bonding type can vary with the characteristics of biomass as well. For example, Sr^{2+} binds to denatured yeast biomass through ionic bond, but interaction with the cell wall of living yeast exhibited covalent bonding [22]. The involvement of amine and sulfhydryl functional groups, active on the cell surfaces of living cells and denatured in dead biomass (wherein the carboxylate and phosphate groups are more significant), can be possible reasons behind such phenomena [14].

The coordination of metal (M) ions with O-donor atoms and proton release can be understood by Eq. (1), while the bidentate surface complex by Eq. (2), as below (where S represents a surface site and S-S represents interconnected surface sites).

$$S - OH + M^{2+} \leftrightarrow S - OM^{+} + H^{+} \tag{1}$$

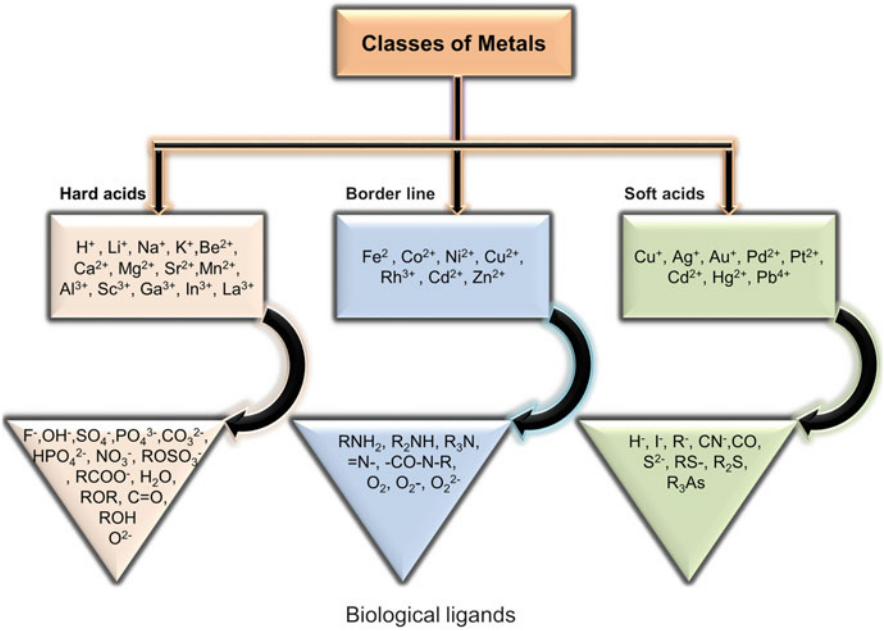

Fig. 2 The hard and soft acid base schemes for ligand preferences in the biological context

$$\begin{matrix} -S-OH \\ I \\ -S-OH \end{matrix} + M^{2+} \leftrightarrow \begin{matrix} -S-O \\ I \\ -S-O \end{matrix} \!\!\diagdown\!\!\diagup\!\!: M + 2H^{+} \qquad (2)$$

1.3 Influential Factors to an Efficient Biosorption Activity

As stated earlier that biosorption comprises many factors which simultaneous contribution of several mechanisms controlling the overall process, the same in the case of strontium biosorption. The main factors are discussed below.

1.3.1 The Type, Nature, and Pretreatment of Biosorbent

The type of biomass, its characteristics, and pre-treatment process are vital including the nature of its application. The physicochemical treatments (viz., boiling, drying, autoclaving, and mechanical disruption) affect the binding properties, while chemical treatments (viz., alkali/acid treatment) are often employed to modify the surface seeking the improvement in biosorption capacity [23, 24]. The growth and nutrition factors can also influence biosorption due to the changes in size and composition

of cell wall, extracellular product formation, etc. (e.g., provision of nutrients and optimal growth conditions are essential requirements to living cell systems).

1.3.2 Solid/Liquid Ratio and Biomass Concentration

The exposed surface area to the volume ratio is important for individual cells/sorbent particles. Additionally, the biomass population may also affect the sorption yield with a decrease in sorption per unit weight occurring with increasing biomass in the pulp.

1.3.3 pH of the System

Among the physicochemical factors, pH is possibly the most important that has in situ effects on both the sorbent and sorbate. Competition between metal cations (sometimes anionic species as well) and protons for binding sites always varies with pH variance of the solution. Hence, the sorption of metal cations (including Sr^{2+}) often declined at low pH values [25, 26]. The extent of sorption may also vary depending on the speciation with respect to pH variation, which in turn affects both solubility and mobility of the metal species [27].

1.3.4 Coexisting and Competing Ions

The preference of metals' sorption onto the available sites is dependent on the competition between the metal ions influenced by their valance and ionic radii. Various selectivity series have been published which reflect such competition, e.g., Al^{3+}, $Ag^{+} > Cu^{2+} > Cd^{2+} > Ni^{2+} > Pb^{2+} > Zn^{2+}$, $Co^{2+} > Cr^{3+}$ for *Chlorella vulgaris* and $Cu > Sr^{2+} > Zn^{2+} > Mg^{2+} > Na^{+}$ for *Vaucheria* sp. [28]. In some cases, cations may increase biosorption of anionic species of metals via binding enhancement of the anions. Anions like CO_3^{2-} and PO_4^{2-} may clearly affect sorption due to exhibiting the reverse solubility or precipitation.

1.3.5 Effect of Temperature

Over modest physiological-type ranges, the temperature has little influence on biosorption; nonetheless high temperatures (e.g., 50 °C) may increase metal uptake; thereafter at a higher temperature, usually the sorption declined. The low temperature will, however, affect living cell systems and any auxiliary metabolism-dependent processes that aid the biosorption [27].

2 Biosorption by Algae

Algae are relatively simple eukaryotic photoautotrophs that lack the tissue (roots, stem, and leaves) of plants which can be unicellular and multicellular with/without the cell wall. The cell wall is usually fibrillar skeleton cellulosic material that also contains hemicellulose, mucilage, pectin, and other substances like alginic acid, fucoidin, fucin, calcium carbonate, silica, etc. in different combinational groups of algae. Figure 3 depicts a detailed structure of the algal cell wall, whereas the characteristics of different algae are given in Table 1. Commonly used algae for biosorption are brown algae, red algae, green algae, diatoms, etc. Red algae have delicately branched thalli. Green algae have cellulose cell wall, contain chlorophyll, and store starch, as plants do, and they may be either unicellular or multicellular. Diatoms are unicellular or filamentous algae with complex cell walls that consist of pectin and a layer of silica [30].

Laminaria digitata (a brown algae) usually contain three components, cellulose (as structural support), alginic acid, and polymers (like mannuronic and guluronic acids, polysaccharides), exhibiting Sr^{2+} sorption through the cell wall functional group by following the ion-exchange mechanism [31]. Pohl and Schimmack [32] used *Laminaria digitate* for the adsorption studies of four radionuclides (^{134}Cs, ^{85}Sr, ^{226}Ra, ^{241}Am) under different pH regimes. The non-phosphorylated use of algal biomass showed very good sorption removal of ^{85}Sr and ^{226}Ra. The adsorption of phosphorylated *Laminaria digitate* could increase more at low pH but found to decline with increasing pH. The results were also compared with that of using *Laminaria japonica*, which can be depicted from the results summarized in Table 2.

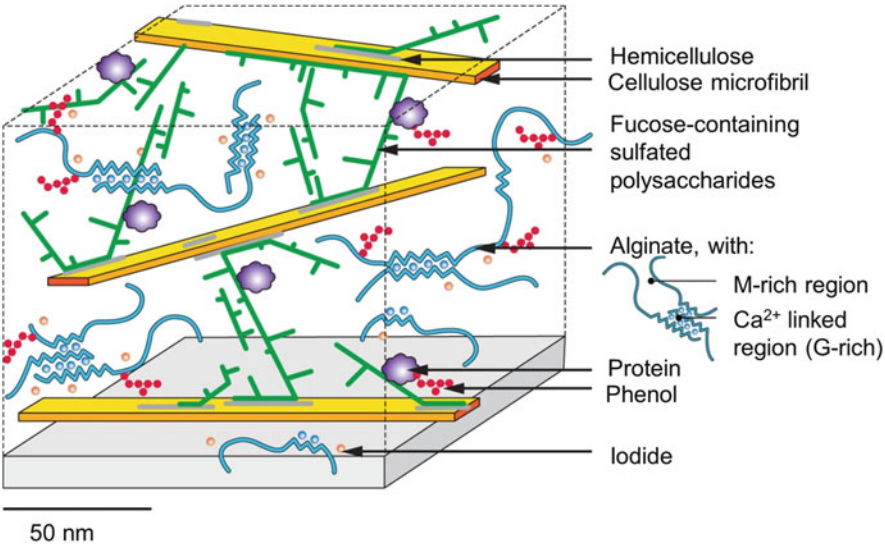

Fig. 3 Typical cell wall composition of (brown) algae (Adopted from the source: [29])

Table 1 Characteristics of various algae with their major composites

Characteristics	Brown algae	Red algae	Green algae	Diatoms	Dinoflagellates	Water molds
Phylum	Phaeophyta	Rhodophyta	Chlorophyta	Bacillariophyta	Dinoflagellata	Oomycota
Color	Brownish	Reddish	Green	Brownish	Brownish	Colorless, white
Cell wall	Cellulose and alginic acid	Cellulose	Cellulose	Pection and silica	Cellulose	Cellulose
Cell arrangements	Multicellular	Most are multicellular	Multi- and unicellular	Unicellular	Unicellular	Multicellular
Photosynthetic pigments	Chlorophyll a and c, xanthophyll	Chlorophyll a and d phycobiliproteins	Chlorophyll a and b	Chlorophyll a and c, carotene, xanthophyll	Chlorophyll a and c, carotene, xanthines	None
Storage material	Carbohydrates	Glucose polymer	Glucose polymer	Oil	Starch	None

Table 2 Adsorption of radionuclides by extracted algal materials from Phaeophyceae-phosphorylated and Phaeophyceae-non-phosphorylated biomass

Phaeophyceae-phosphorylated					Phaeophyceae-non-phosphorylated				
	^{85}Sr adsorption		^{134}Cs adsorption			^{85}Sr adsorption		^{134}Cs adsorption	
pH	μg g^{-1}	%	μg g^{-1}	%	pH	μg g^{-1}	%	μg g^{-1}	%
Laminaria digitata									
3.1	2.107	91.6	0.063	62.8	3.4	0.904	39.3	0.045	44.6
5.3	2.167	94.2	0.079	78.7	4.9	1.443	62.8	0.060	60.0
7.0	1.978	86.0	0.082	81.5	6.5	1.833	79.7	0.063	60.6
9.8	1.596	69.4	0.082	82.1	9.7	2.181	94.8	0.072	71.7
Laminaria japonica									
3.5	2.117	92.1	0.032	31.8	3.3	1.440	62.6	0.042	42.4
5.9	1.623	70.6	0.068	68.5	5.3	2.018	87.7	0.059	59.9
7.1	1.489	64.8	0.071	71.2	7.1	2.111	91.8	0.063	63.3
9.5	1.418	61.6	0.074	73.7	10.3	2.184	95.0	0.079	78.9

Scenedesmus spinosus (a green algae) typically consisting of 4–8 cells aligned in a flat plate is abundant in many natural water environments and exhibits good acceptance to the heavy metal pollution [33–35]. Liu et al. [36] observed its selectivity for Sr^{2+} and found the biosorption/bioaccumulation ratio of 9:1. The use of *Oscillatoria homogenea* (a blue-green algae) demonstrated that the change of the biosorption parameter has a key role in biosorption process of the Sr^{2+} [37]. In an important study, Rice [38] used marine planktonic algae and found that the mixed radionuclides system showed an increased radioactivity due to the uptake of Y^{90} along with Sr^{89}. Such observation emphasized that the care must be taken by considering the radioactivity of biological materials when more than one radioactive elements are used in the system, even at the minute concentration that could be adsorbed within initial 15 min of the experiment [38].

3 Biosorption by Plant/Plant-Derived Materials

Recently, plant (living/dead) derivatives have been of great interest for their ability to bind the heavy/radiotoxic metals even from the solutions of minute concentrations. The seeds of *Strychnos potatorum*, banana pith, and mustard and sunflower seeds are used for metal (including Cs^{+} and Sr^{2+}) sorption. Noteworthy consideration to the mosses in bio-monitoring surveys of radionuclide pollutants, especially after the Chernobyl incident, literature has appeared on the usage of mosses for assessing the atmospheric levels and deposition of radionuclides [39–43]. Krishna et al. [44] examined the moss as a phyto-sorbent and evaluated its potential for the removal of Cs^{+} and Sr^{2+} from low-level radioactive waste solutions. The sorption behavior indicates that the radionuclides reduced substantially to a level enabling normal discharge of the effluent, exhibiting pH-dependent sorption mechanism

albeit 48% Cs^+ and 36% Sr^{2+} could be adsorbed even at low pH ~1.2. The sorption efficiency reached 80% at solution pH ~3.0, and further increased to maximum >92% at pH ~6.0. Similar to the study by Marešová et al. [45] using the moss, *Rhytidiadelphus squarrosus*, the sorption reached to q_{max} at pH 5.0–6.0. Thereafter increasing the solution pH did not show any improvement. However within the range of initial pH from 6.0 to 10.0, a significant decrease in equilibrium pH of the supernatant was observed that infers the extent of deprotonation of carboxylic acid groups associated with the moss to act as cation exchange, as suggested by [28]. Rapid adsorption at initial stage showed the available exchangeable sites through surface-layer diffusion followed by a slower process suggesting pore diffusion mechanism.

4 Biosorption by Agro-waste

Biosorption by root tissue powders of *Amaranthus spinosus* studied by Chen [46] revealed that the sorption occurs via large pores to diffuse Sr^{2+} into the interior surfaces and gets improved after an alkaline pre-treatment. However, adsorption capacities were larger than those from the Langmuir isotherms, which might be due to the alginate that can itself adsorb positively charged ions [47]. For biosorption of Sr^{2+} from a synthetic nitrate solution, Ahmadpour et al. [48] used three different agro-wastes (almond green hull, eggplant hull, and moss) as the potential sorbents. Among all, the almond green hull demonstrated a strong affinity to uptake Sr^{2+} ions, exhibiting the q_{max} of 116.3 mg g^{-1}. A rapid biosorption process within initial 3 min of contact time follows pseudo-second-order kinetics; however, both Langmuir and Freundlich models were well-fitted to the isotherm data. A further enhancement in sorption capacity was also observed by a chemical treatment, where the amount of surface functional groups onto treated adsorbent was observed by Boehm's technique in the following order: phenolic > basic > lactonic > carboxylic. These functional groups were considered to actively participate in Sr^{2+} adsorption from the solutions. The biosorption efficiencies for untreated, NH_3/H_2O_2 treated, and HNO_3 treated were found to be with eggplant, 0, 72, and 47.6%; with moss, 78, 78, and 48.6%; and with almond green hull, 86.6, 91, and 51%, respectively.

Abdelkreem and Husein [49] used the plenty available orange peels (OP) that contain pectin (galacturonic acid), hemicelluloses, cellulose, and lignin acid bear polar functional groups (like carboxylic and phenolic acids) for biosorption studies of Sr^{2+}. The chemically modified peels after treatment with NaOH (NaOP) and KOH (KOP) exhibited better results within 1 h of sorption. The sorption capacity for Sr^{2+} removal was found to be 12.5, 54.94, and 52.36 mg g^{-1} for OP, NaOP, and KOP, respectively, with exothermic nature of the process. Imessaoudene et al. [50] studied the biosorption of Sr^{2+} by spent coffee residues and found the q_{max}, 69.01 mg g^{-1}; at pH, 7.0; temperature, 20 °C; and particles size of 200–400 μm. Instrumental spectral analysis showed that the carboxylic and amino acid groups onto the surface of coffee residues are vital to Sr^{2+} sorption. Such a result establishes

the role of –COOH group or the lone pair of electrons present in oxygen, or large number of active groups in the mucilage polysaccharide facilitates the biosorption of Sr^{2+} ions, as in the case of mucilaginous seeds of *Ocimum basilicum* [51, 52].

5 Biosorption by Bacteria

Bacteria are the most copious and adaptable group of microorganisms and able to compose the important portion of a whole living terrestrial biomass (approximately 1018 g). Bacteria own polysaccharide slime layers that promptly offer the carboxyl, amino, phosphate, and sulfate groups. Table 3 and Fig. 4 depict the selective features of bacteria and cell wall structure. The metal uptake capacity of bacteria is commonly associated with the cell wall functional groups and in the range of 0.70–568 mg g^{-1}. Metal binding on the bacterial cell wall surface is a two-stage activity: (1) in step 1, interactions between metal ions and active functional groups on the cell wall surface take place, (2) while in step 2, subsequent accumulation of metal ions follows in large concentrations. The –COOH groups of glutamic acid ($HOOC–CH(NH_2)–(CH_2)_2–COOH$) of peptidoglycan are the active sites of metal binding; however part of bacteria also infers metabolism-independent biosorption as the main mechanism, but in some cases, metabolism-dependent mechanisms are likely to augment the metal deposition on cell wall surface [55–58].

Table 3 Selected features of bacteria

Features	Bacteria
Cell type	Prokaryotic
Cell wall	Peptidoglycan
Cell membrane	Sterols absent expect in (*Mycoplasma*)
Spores	Endospores (not for reproduction), some asexual reproductive spores
Metabolism	Autotrophic, heterotrophic, aerobic , facultatively anaerobic, aerobic

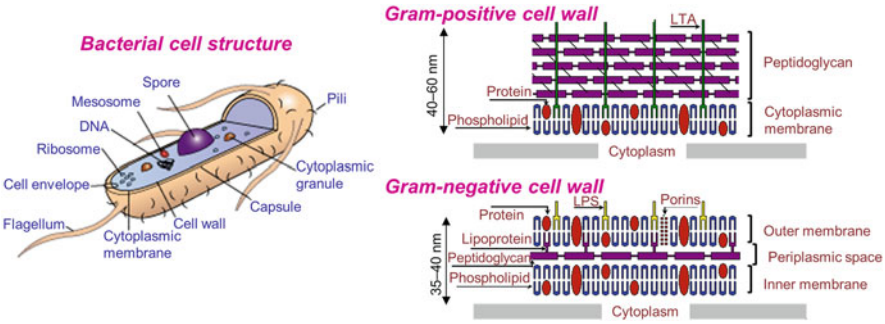

Fig. 4 Bacterial cell structure along with the cell wall structure of gram-positive and gram-negative bacteria (Adopted from the sources: [53, 54])

Bacillus cereus is a gram-positive rod-shaped, anaerobic, or facultative anaerobic, motile bacterium usually found in the soil/food particles. Glucose, galactose, N-acetylmannose, and N-acetylglucosamine compounds are the major constituents of its cell wall surface whose functional groups are identified to be hydroxyl, carboxyl, and amino groups, participating in the biosorption of Sr^{2+}. Study conducted by Long et al. [56] indicates that biosorption capacity of dead bacterial biomass gets improved with increasing pH from 3.0 to 5.0, alike to Dai et al. [59] observation of maximum Sr adsorption at pH ~4.5. A low sorption capacity at the high acidic condition corroborated to competing for proton ions with Sr^{2+} and preventing the metal's binding [23]. Nevertheless, a decline in biosorption of Sr^{2+} ions at pH $>$ 5.0 may be an effect of changing chemical speciation of strontium and activity of functional groups of the biomass used [60]. A proper rotational speed (in between 120 and 200 rpm) has also found to be influential to decrease in mass transfer resistance around the bacterial biomass to facilitate the contacts between metal ions and binding sites [56, 61, 62]. The biosorption with *Bacillus cereus* is relatively a rapid process and reaches the maximum sorption within 1 h with an uptake capacity of 40.16 mg g^{-1} Sr^{2+} while adding the biomass at a 3 g l^{-1} dosage.

Bacillus polymyxa is gram-positive, nitrogen-fixing bacteria in soil and plant roots. Their cell walls mainly composed of polymeric sugar and amino acid, peptidoglycan, etc., among which, the peptidoglycan is responsible for cellular viability, known as murine, and has a significant role in the biosorption ability [58]. Interestingly, it has been observed that the live and dead cells of *Bacillus polymyxa* are capable to uptake Sr^{2+} without competing for the Ca^{2+} ions. In the calcium-deficient media, however, Sr^{2+} may replace Ca^{2+} due to their similar physicochemical properties and takes part in some biochemical and physiological processes of living cell mass.

Micrococcus luteus is gram-positive, gram-variable, non-motile coccus that has tetrad arrangement in symmetry and saprotrophic and pigmented bacteria as well. Micrococci are the urease and catalase-positive bacteria whose key functional groups are identified as alkyl, alkenyl, alcohols, ethers, aldehydes, aromatic, and carboxylic acids, mainly participating in the biosorption process of Sr^{2+} [63]. The surface topology of Sr^{2+}-loaded and Sr^{2+}-unloaded *Micrococcus luteus* strains and surface charge were examined and found to be different from each other [64]. The matrix layers of the cell wall of loaded samples were seen to shrink and stick that can be ascribed to the robust cross-linking of Sr^{2}–C and anionic chemical groups onto the surface of cell wall. As surface charge being an essential factor to clearly describe the adsorption properties [64, 65], the zeta potential of *Micrococcus luteus* at different Sr^{2+} concentrations was examined and found to be in the range of −4.17 mV to −17.9 mV. Apparently, the zeta potentials exhibited all negative values under the varied Sr^{2+} concentrations, indicating the favorable surfaces of *Micrococcus luteus* for binding with metal cations. A declined negative charge of the surface was obtained in the concentration range of 150–450 mg ml^{-1}. It was corroborated with the protonation behavior of the bacterial surface functional groups at lower concentration of Sr^{2+} ions. A raise of surface negative charge also exhibited within the concentration range of 450–750 mg ml^{-1}. This was corroborated with the

adsorption of metal cation onto the anionic biomass surface through the columbic force of attraction after desorption [66]. The rate-controlling step in the biosorption process has found through the chemical interactions between the metal ions and sorbent's superficial functional groups [67].

Sulfate-reducing bacteria (SRB) have also been used for biosorption of Sr^{2+} from the fission waste streams (in presence and absence of Cs^{+} and Co^{2+}) [57]. The effect of initial metal concentrations of each and pH of the solution was evaluated to determine the sorption kinetics. The binary component studies were carried out to examine the competitive binding behavior of each metal in presence of another metal ion. The sorption results of single metal inferred that the SRB has the binding capacity in order of $Sr^{2+} > Cs^{+} > Co^{2+}$ with corresponding q_{max} values (in mg g^{-1}) 416.7, 238.1, and 204.1, respectively. When using the binary metal systems, Co^{2+} showed the most sensitivity to its counter ions, which resulted in a 76% lower sorption with co-exiting Cs^{+} ions. With initial concentration of 75 mg l^{-1} and pH range of 2.0–9.0, > 99.8% Sr^{2+} and Cs^{+} were adsorbed, suggesting a limited hydrolysis of both cations. Further, the SRB culture showed an improved removal capacity with higher metal concentration. The uptake of divalent cations, Sr^{2+} and Co^{2+}, exhibited a similar uptake pattern, where the uptake increased with higher metal concentration; however, Cs^{+} sorption found to progress until equilibrium could be achieved, in this case, following the uptake order of Cs < Co < Sr.

6 Biosorption by Fungi

A fungus or fungi (plural form) belong to anyone among 99,000 known species of eukaryotic organisms that include microorganisms such as yeasts, molds, and mushrooms. The structure and unity of fungus commonly depend on the mechanical strength of the cell wall that widely involves in microbial interactions to the metal/environment. It exhibits typically a complex structure that surrounds the plasma membrane and is made of an elastic configuration of the constituents given in Table 4 along with the characteristic features [30]. Typically the cell walls of fungus consist of polysaccharides (80 wt.%, usually β[1 → 3]-glucan and some of β[1 → 6]-glucan) to which an extensive collection of various proteins are anchored in the diverse manners. Nevertheless, wall composition that greatly changes between the fungal species consists of various metal-binding groups (viz., phosphate, amine, imidazole, sulfate, sulfhydryl, and hydroxyl), depending on the fungal species (the structure is shown in Fig. 5).

Table 4 Selected features of fungi

Components	Features
Fibrillar	Chitin, cellulose, β-glucan
Matricial	α-Glucan, chitosans, polyuronides, glycoproteins, lipids, inorganic salts, and pigments

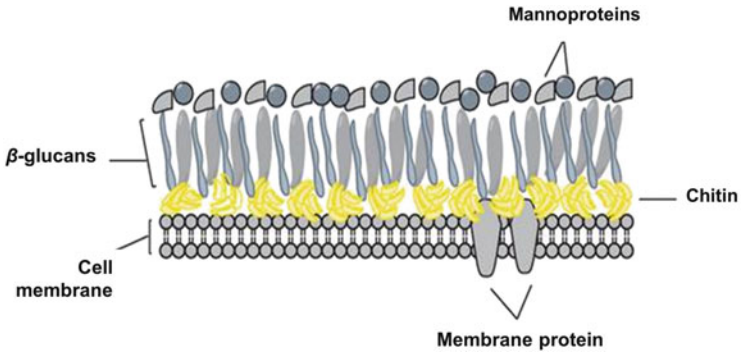

Fig. 5 Fungal cell wall structure. (Adopted from the source: [68])

The cell wall of *Aspergillus terreus* mainly consists of the amine, amides, phospholipids, glycans, and carboxylic functional groups, which participate in metal binding. Khani et al. [69] investigated the biosorption of Sr^{2+} under the parametric variations of pH, contact time, initial metal concentration, temperature, and biomass dosage. It was observed that the sorption capacity 308 mg g^{-1} was the highest at 15 °C with initial pH 9.0 and 876 mg l^{-1} Sr^{2+} concentration in the solution, which was only (q_{max}) 219 mg g^{-1} at 45 °C. The equilibrium data were found to fit well to the Langmuir model. In the multi-metal system, Chen and Wang [70] used the brewery waste biomass that yielded the sorption order $Pb^{2+} > Ag^{+} > Sr^{2+} > Cs^{+}$. The extent of metal ions binding to yeast primarily depends on the covalent index, electronegativity, and dissociation constant. It exhibited the pseudo-second-order kinetics, suggesting for the external mass transfer and intra-particle diffusion process. The sorptions following Langmuir isotherm with q_{max} per gram of sorbent are as follows: 0.413 mmol Pb^{2+}, 0.396 mmol Ag^{+}, 0.091 mmol Sr^{2+}, and 0.076 mmol Cs^{+}.

For understanding the biosorption mechanism, the metal binding takes place in mainly two steps. The first step involves a stoichiometric interaction between metal-to-reactive chemical groups in the cell wall, while second step involves an inorganic deposition of increased amounts of sorbate metals. The sorbate come across the cell wall; thereafter the metal ions get access to plasma membrane and the cell cytoplasm. In this way, metal ions first get contacted with the cell wall, the functional groups of which provide numerous active sites for binding the metal ions. Therefore, the process is regarded similar to the complex ion-exchange process using the zeolite resin beads. Furthermore, this can be regarded as the metabolically determined process if the microorganism favorably produces the compounds of metal precipitates. Otherwise, the occurrence of chemical interactions between the metal ions and cell wall can be taken as a metabolically independent process. So far a less effort has been given to examine a well-defined metal uptake; however a typical fungal-to-metal interaction in various modes is shown in Fig. 6 [69, 72, 73].

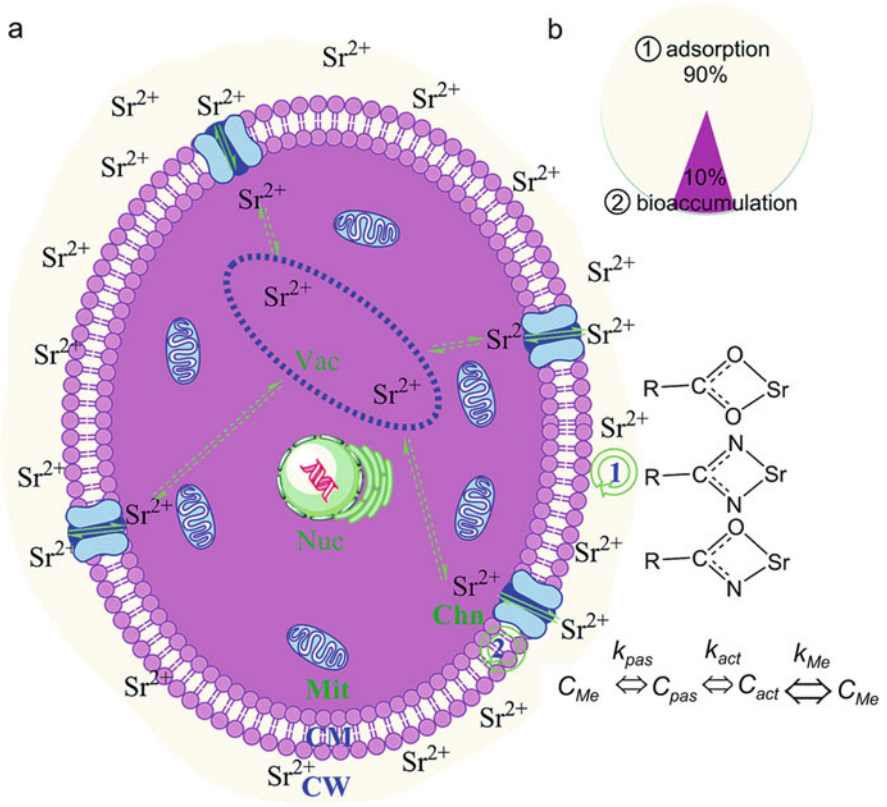

Fig. 6 Interface interactions for *Saccharomyces cerevisiae* cell biosorption of Sr^{2+} under culture conditions, (**a**) for yeast cell biosorption under culture conditions, including (1) adsorption; (2) bioaccumulation; (**b**) distribution of Sr^{2+} onto yeast cell surface and in cytoplasm. *Nuc* nucleus, *Vac* vacuole, *Mit* mitochondria, *Chn* channel protein, *CM* cell membrane, *CW cell wall*. (Adopted from the source; [71])

Recently, Qiu et al. [73] studied the effects of irradiation on biosorption capabilities of *Saccharomyces cerevisiae* for Sr^{2+} ions and established the order of influential parameters (strongest to weakest) as pH > Sr^{2+} concentration > time > temperature. The q_{max} 150 mg l^{-1} occurred at pH 7.0 and 32°C with a 30 h contact time. Liu et al. [71] found that during the sorption process, Sr^{2+} ions can be coordinated by N-atoms of the –NH– group of mannoprotein/chitin, a part of which can also be coordinated by the membrane proteins and O-atom in the –OH and –C=O groups of the chitin/glucan/mannoprotein as a mononuclear 6-(or 4-) coordinate model. Another coordination atoms included the O-atom of C=O group in asparagine and the N-atom of –NH– group and the O-atom of –C=O group in N-acetyl-glucosamine unit. It was concluded that the amino group showed a greater extent to Sr^{2+} biosorption and the carboxyl groups of some acidic amino acid residues form carboxylate with the Sr^{2+} ions. The extent of contribution in the sorption process was in the order of –NH and –OH > –COO > –COOC–.

7 Prospects and Summary

Biosorption, in fact, occurs in all bioremediation process and has the potential to be practically applied in future separation technologies, including a part of hybrid wastewater treatment. Obviously, more research would be required in this field to search for better and more selective biomasses that can be employed to multi-metal radioactive waste streams and give selective sorption results with high efficacy. Notably, many other radionuclides present in the system can adversely affect the system as observed by Rice [38]. Not only is this a recent trend on selective extractive strontium from seawater but also is a potential area for application of biosorbents. The use of biomass as a carrier of highly available microelements in livestock diet is another possible area of application, substituting microelements supplements through either biosorption or bioaccumulation.

References

1. Pathak P (2017) An assessment of strontium sorption onto bentonite buffer material in waste repository. Environ Sci Pollut Res 24:8825–8836
2. Pathak P, Sharma S (2018) Sorption isotherm, kinetics, and thermodynamics of contaminants in Indian soils. J Environ Eng 144:1–9
3. Ugajin M, Ajuria S (1985) Inorganic Ion Exchangers and Adsorbents for Chemical Processing in the Nuclear Fuel Cycle: IAEA-TEC DOC-337 IAEA, Vienna
4. Favre-Réguillon A, Dunjic B, Lemaire M, Chomel R (2001) Synthesis and evaluation of resorcinol-based ion-exchange resins for the selective removal of cesium. Solvent Extr Ion 19:181–191
5. Kore SG, Prasad V, Singh US, Yeotikar RG, Mishra A, Ali SS (2001) Removal of Ru along with Cs and Sr from the low level radioactive liquid waste of reprocessing plant by chemical treatment method. In: Indian Nuclear Society Proceeding
6. Abusafa A, Yücel H (2002) Removal of ^{137}Cs from aqueous solutions using different cationic forms of a natural zeolite: clinoptilolite. Sep Purifi Technol 28:103–116
7. Dyer A, Keir D (1984) Nuclear waste treatment by zeolites. Zeolites 4:215–217
8. Lehto J, Harjula R (1999) Selective separation of radionuclides from nuclear waste solutions with inorganic ion exchangers. Radiochim Acta 86:65–70
9. Murali MS, Mathur JN (2002) Sorption characteristics of Am (III), Sr (II) and Cs (I) on bentonite and granite. J Radioanal Nucl Chem 254:129–136
10. Samanta SK, Ramaswamy M, Misra BM (1992) Studies on cesium uptake by phenolic resins. Sep Sci Technol 27:255–267
11. Singh IJ, Sathi S, Theyyunni TK (1995) Use of molecular sieves zeolite-4A for removal of cesium and strontium from low level waste effluents of BWR origin (No. BARC--1995/E/003). Bhabha Atomic Research Centre
12. Atlas RM (1995) Bioremediation. Chem Eng News 73:32–42
13. Anjana K, Kaushik A, Kiran B, Nisha R (2007) Biosorption of Cr(VI) by immobilized biomass of two indigenous strains of cyanobacteria isolated from metal contaminated soil. J Hazard Mater 148:383–386
14. Avery SV, Codd GA, Gadd GM (1993) Biosorption of tributyltin and other organotin compounds by cyanobacteria and microalgae. Appl Microbiol Biotechnol 39:812–817

15. Garnham GW, Codd GA, Gadd GM (1993a) Accumulation of technetium by cyanobacteria. J Appl Phycol 5:307–315
16. Garnham GW, Codd GA, Gadd GM (1993b) Uptake of cobalt and caesium by microalgal- and cyanobacterial-clay mixtures. Microb Ecol 25:71–82
17. Ahemad M (2014) Remediation of metalliferous soils through the heavy metal resistant plant growth promoting bacteria: paradigms and prospects. Arab J Chem. https://doi.org/10.1016/j.arabjc.2014.11.020
18. Tsezos M (2009) Metal-microbes interactions: beyond environmental protection. Adv Mater Res 71–72:527–532
19. Volesky B (1990) Biosorption of heavy metals. CRC Press, Boca Raton
20. Volesky B (2003) Sorption and biosorption. BV Sorbex, Inc, Montreal
21. Gadd GM (1992) Metals and microorganisms: a problem of definition. FEMS Microbiol Lett 100:197–204
22. Avery SV, Tobin JM (1992) Mechanisms of strontium uptake by laboratory and brewing strains of *Saccharomyces cerevisiae*. Appl Environ Microbiol 58:3883–3889
23. Ilyas N, Ilyas S, Rahman SU, Yousaf S, Zia A, Sattar S (2018) Removal of copper from an electroplating industrial effluent using the native and modified *spirogyra*. Water Sci Technol 78:147–155
24. Wang J, Chen C (2006) Biosorption of heavy metals by *Saccharomyces cerevisiae*: a review. Biotechnol Adv 24:427–451
25. Eccles H (1999) Treatment of metal-contaminated wastes: why select a biological process? Trends Biotechnol 17:462–465
26. Greene B, Darnall DW (1990) Microbial oxygenic photoautotrophs (cyanobacteria and algae) for metal-ion binding. In: Ehrlich HL, Brierley CL (eds) Microbial mineral recovery. McGraw-Hill, Germany
27. Tsezos M, Volesky B (1981) Biosorption of uranium and thorium. Biotechnol Bioeng 23:583–604
28. González F, Romera E, Ballester A, Blázquez M, Muñoz J, García-Balboa C (2011) Algal biosorption and biosorbents. In: Kotrba P, Mackova M, Macek T (eds) Microbial biosorption of metals. Springer, Dordrecht
29. Deniaud-Bouët E, Kervarec N, Michel G, Tonon T, Kloareg B, Hervé C (2014) Chemical and enzymatic fractionation of cell walls from Fucales: insights into the structure of the extracellular matrix of brown algae. Ann Bot 114:1203–1216
30. Tortora GJ, Funke BR, Case CL (2004) Microbiology: an introduction, 12th edn. Pearson Education, Inc
31. Sheng PX, Tan LH, Chen JP, Ting YP (2005) Biosorption performance of two brown marine algae for removal of chromium and cadmium. J Disper Sci Technol 25:679–686
32. Pohl P, Schimmack W (2006) Adsorption of radionuclides (^{134}Cs, ^{85}Sr, ^{226}Ra, ^{241}Am) by extracted biomasses of cyanobacteria (*Nostoc Carneum, N. Insulare, Oscillatoria Geminata* and *Spirulina Laxissima*) and phaeophyceae (*Laminaria digitata* and *L. Japonica*; waste products from alginate production) at different pH. J Appl Phycol 18:135–143
33. Reavie ED, Jicha TM, Angradi TR, Bolgrien DW, Hill BH (2010) Algal assemblages for large river monitoring: comparison among biovolume, absolute and relative abundance metrics. Ecol Indic 10:167–177
34. Terry PA, Stone W (2002) Biosorption of cadmium and copper contaminated water by *Scenedesmus abundans*. Chemosphere 47:249–255
35. Zhang H, Hu HJ, Chao AM, Xie WF, Cen JY, Lü SH (2013) Seasonal changes of phytoplankton community structure in Jinshuitan Reservoir, Zhejiang, China. Acta Ecol Sin 33:944–956
36. Liu M, Dong F, Kang W, Sun S, Wei H, Zhang W, Liu Y (2014) Biosorption of strontium from simulated nuclear wastewater by *Scenedesmus spinosus* under culture conditions: adsorption and bioaccumulation processes and models. Int J Environ Res Public Health 11:6099–6118
37. Dabbagh R, Ghafourian H, Baghvand A, Nabi GR, Riahi H, Faghih MA (2007) Bioaccumulation and biosorption of stable strontium and ^{90}Sr by *Oscillatoria homogenea* cyanobacterium. J Radioanal Nucl Chem 272:53–59

38. Rice TR (1956) The accumulation and exchange of strontium by marine planktonic algae. Limnol Oceanogr 1:123–138
39. Aceto M, Abollino O, Conca R, Malandrino M, Mentasti E, Sarzanini C (2003) The use of mosses as environmental metal pollution indicators. Chemosphere 50:333–342
40. Berg T, Røyset O, Steinnes E (1995) Moss (*Hylocomium splendens*) used as biomonitor of atmospheric trace element deposition: estimation of uptake efficiencies. Atmos Environ 29:353–360
41. Jayaraman KS (1993) Indian tree offers nuclear waste treatment. Nature 365:779
42. Papastefanou C, Manolopoulou M, Sawidis T (1989) Lichens and mosses: biological monitors of radioactive fallout from the Chernobyl reactor accident. J Environ Radioact 9:199–207
43. Ruhling A, Tylor G (1968) An ecological approach to the lead problem. Bot Notiser 121:321–342
44. Krishna MB, Rao SV, Arunachalam J, Murali MS, Kumar S, Manchanda VK (2004) Removal of ^{137}Cs and ^{90}Sr from actual low level radioactive waste solutions using moss as a phyto-sorbent. Sep Purif Technol 38:149–161
45. Marešová J, Pipíška M, Rozložník M, Horník M, Remenárová L, Augustín J (2011) Cobalt and strontium sorption by moss biosorbent: modeling of single and binary metal systems. Desalination 266:134–141
46. Chen JP (1997) Batch and continuous adsorption of strontium by plant root tissues. Bioresour Technol 60:185–189
47. Jang LK, Lopez SL, Eastman SL, Pryfogle P (1991) Recovery of copper and cobalt by biopolymer gels. Biotechnol Bioeng 37:266–273
48. Ahmadpour A, Zabihi M, Tahmasbi M, Bastami TR (2010) Effect of adsorbents and chemical treatments on the removal of strontium from aqueous solutions. J Hazard Mater 182:552–556
49. Abdelkreem M, Husein DZ (2012) Removal of strontium from aqueous solutions by adsorption onto orange peel: Isotherms, kinetics, and thermodynamic studies. Egypt J Environ Res 1:42–61
50. Imessaoudene D, Hanini S, Bouzidi A (2013) Biosorption of strontium from aqueous solutions onto spent coffee grounds. J Radioanal Nucl Chem 298:893–902
51. Chakraborty D, Maji S, Bandyopadhyay A, Basu S (2007) Biosorption of cesium-137 and strontium-90 by mucilaginous seeds of *Ocimum basilicum*. Bioresour Technol 98:2949–2952
52. Ryding O (1992) Pericarp structure and phylogeny within Lamiaceae subfamily Nepetoideae tribe Ocimeae. Nord J Bot 12:273–298
53. Fix D (2016) General Microbiology. http://myplace.frontier.com/~dffix/medmicro/genmicr.htm
54. Creative Diagnostics. https://www.creative-diagnostics.com/Bacterial-Antigens.htm
55. Gupta VK, Nayak A, Agarwal S (2015) Bioadsorbents for remediation of heavy metals: current status and their future prospects. Environ Eng Res 20:1–18
56. Long J, Li H, Jiang D, Luo D, Chen Y, Xia J, Chen D (2017) Biosorption of strontium (II) from aqueous solutions by *Bacillus cereus* isolated from strontium hyperaccumulator *Andropogon gayanus*. Process Safety Environ 111:23–30
57. Ngwenya N, Chirwa EMN (2010) Single and binary component sorption of the fission products Sr^{2+}, Cs^{+} and Co^{2+} from aqueous solutions onto sulphate reducing bacteria. Miner Eng 23:463–470
58. Shevchuk IA, Klimenko NI (2009) Biological features of sorption of U (VII) and strontium ions by *Bacillus polymyxa* IMV 8910 cells. J Water Chem Technol 31:324–328
59. Dai Q, Zhang W, Dong F, Yulian Z, Wu X (2014) Effect of ray radiation on the biosorption of strontium ions to baker's yeast. Chem Eng J 249:226–235
60. Benson LV (2010) A tabulation of thermodynamic data for chemical reactions involving 58 elements common to radioactive waste package systems. Lawrence Berkeley National Laboratory
61. Nasseri S, Assadi MM, Sepehr MN, Rostami K, Shariat M, Nadafi K (2002) Chromium removal from tanning effluent using biomass of *Aspergillus oryzae*. Pak J Biol Sci 5:1056–1059

62. Shroff KA, Vaidya VK (2011) Kinetics and equilibrium studies on biosorption of nickel from aqueous solution by dead fungal biomass of *Mucor hiemalis*. Chem Eng J 171:1234–1245
63. Zhuang WQ, Tay JH, Maszenan AM, Krumholz LR, Tay SL (2003) Importance of Gram-positive naphthalene-degrading bacteria in oil-contaminated tropical marine sediments. Lett Appl Microbiol 36:251–257
64. Icgen B, Yilmaz F (2018) Biosorption of strontium from aqueous solutions by *Micrococcus luteus* Sr02. Geomicrobiol J 35:284–293
65. Ahmady-Asbchin S, Andres Y, Gérente C, Le Cloirec P (2008) Biosorption of Cu (II) from aqueous solution by *Fucus serratus*: surface characterization and sorption mechanisms. Bioresour Technol 99:6150–6155
66. Bernardo GRR, Rene RMJ (2009) Chromium (III) uptake by agro-waste biosorbents: chemical characterization, sorption–desorption studies, and mechanism. J Hazard Mater 170:845–854
67. Romera E, González F, Ballester A, Blázquez ML, Munoz JA (2007) Comparative study of biosorption of heavy metals using different types of algae. Bioresour Technol 98:3344–3353
68. Vega K, Kalkum M (2011) Chitin, chitinase responses, and invasive fungal infections. Int J Microbiol Article ID 920459
69. Khani MH, Pahlavanzadeh H, Alizadeh K (2012) Biosorption of strontium from aqueous solution by fungus *Aspergillus terreus*. Environ Sci Pollut R 19:2408–2418
70. Chen C, Wang J (2008) Removal of Pb^{2+}, Ag^{+}, Cs^{+} and Sr^{2+} from aqueous solution by brewery's waste biomass. J Hazard Mater 151:65–70
71. Liu M, Dong F, Zhang W, Nie X, Wei H, Sun S, Wang D (2017) Contribution of surface functional groups and interface interaction to biosorption of strontium ions by *Saccharomyces cerevisiae* under culture conditions. RSC Adv 7:50880–50888
72. Bahafid W, Joutey NT, Asri M, Sayel H, Tirry N, El Ghachtouli N (2017) Yeast biomass: an alternative for bioremediation of heavy metals. Yeast-industrial applications. InTech
73. Qiu L, Feng J, Dai Y, Chang S (2017) Biosorption of the strontium ion by irradiated *Saccharomyces cerevisiae* under culture conditions. J Environ Radioact 172:52–62

Plant Response Under Strontium and Phytoremediation

Soumya Chatterjee, Anindita Mitra, Clemens Walther, and Dharmendra K. Gupta

Contents

Abstract Strontium (Sr) is one of the plentiful elements of earth's crust. However, human activities related to nuclear reactor, nuclear weapons explosions and accidental fallouts release substantial amount of radiostrontium. Among radioisotopes, ^{90}Sr is the most important, which affects organisms, including plants, and enters into the food chain. ^{90}Sr is a β-emitter and produces ^{90}Y and ^{90}Zr through succeeding radioactive decay. Further, ^{90}Sr bear a resemblance to calcium affecting plants uptake of Ca and is extremely injurious inducing metabolic imbalances within the tissues. Sr uptake by plants is therefore a crucial matter to understand the scope of phytoremediation. Several external factors including soil properties and availability of the element at plant root zone determine the mobility and uptake of ^{90}Sr by plants. However, selected plants should qualitatively have equal efficiency of high uptake and high biomass production. Plants' native anti-stress physiological mechanisms play an important role in this issue. This chapter deals with the probable issues for

S. Chatterjee
Defence Research Laboratory, DRDO, Tezpur, Assam, India

A. Mitra
Department of Zoology, Bankura Christian College, Bankura, West Bengal, India

C. Walther · D. K. Gupta (✉)
Gottfried Wilhelm Leibniz Universität Hannover, Institut für Radioökologie und Strahlenschutz (IRS), Hannover, Germany
e-mail: guptadk1971@gmail.com; gupta@irs.uni-hannover.de

P. Pathak, D. K. Gupta (eds.), *Strontium Contamination in the Environment*,
The Handbook of Environmental Chemistry 88,
https://doi.org/10.1007/978-3-030-15314-4_5

overall phytoremediation strategies of radiostrontium to ameliorate the contaminated soil in an eco-friendly manner.

Keywords Phytoremediation · Plants · ^{90}Sr · Strontium

1 Introduction

Plants take up several essential elements from soil that help in their sustenance. Nonessential analogous elements are also present in the environment, which enter into the plant's body through the similar fashion. Strontium (symbol: Sr), the 15th abundant element of earth's crust, is one of the nonessential elements analogous to essential element calcium (Ca). Discovered (1790 AD) by Adair Crawford and William Cruickshank, Sr (atomic no. 38, in group IIa, period 5, vertically flanked by Ca and Ba) is a commonly occurring alkaline earth metal. Four stable Sr isotopes, viz.^{84}Sr, ^{86}Sr, ^{87}Sr and ^{88}Sr, and about 30 radioactive Sr isotopes (most common ^{85}Sr, ^{89}Sr and ^{90}Sr) are present in nature [1, 2]. Stable isotopes comprise more than 99.9% of natural Sr in earth's crust, with ^{88}Sr the most prevalent (~83%). Beta radiation is emitted by common radioisotopes of Sr, while ^{85}Sr emits gamma radiation. Variety of Sr natural compounds, mostly carbonate form strontianite ($SrCO_3$) and sulphate form celestite ($SrSO_4$), are being mined regularly [3]. Among radioisotopes, ^{90}Sr (radioactive half-life of 28.9 years) is the most significant, due to anthropogenic activities related to nuclear weapons explosions, nuclear reactor releases and accidental fallout like nuclear power plants of Chernobyl (1986) and Fukushima (2011) [4–6]. It is estimated that 622 PBq global fallout of radiostrontium occurred, with Chernobyl 10 PBq and Fukushima Daiichi 3.3×10^{-3}–0.14 PBq [7–9]. Being a β-radiation emitter with maximum energy of 0.54 MeV, ^{90}Sr produces ^{90}Y (yttrium) and ^{90}Zr (zirconium) through subsequent radioactive decay [10]. ^{90}Sr resembles calcium and is highly harmful as it induces metabolic imbalances, bone cancer, leukaemia and softening of bone and associated tissues [11, 12]. Although ^{90}Sr has some specific medical applications in postmenopausal osteoporosis, however, unsolicited indirect or direct exposure of this isotope causes deposition of this metal (due to low excretion rate) along with several physiological implications in human [13, 14].

2 Strontium in Environment

Plants do accumulate ^{90}Sr within their body. Several factors like soil properties, pH, agroclimatic conditions, cultivation practices and soil microbial communities influence the process of accumulation Sr in plant's body [15]. Although rocks and soils are the natural reservoir of Sr, airborne transport and deposition are also evident (Fig. 1). Depending upon meteorological conditions, especially wind and

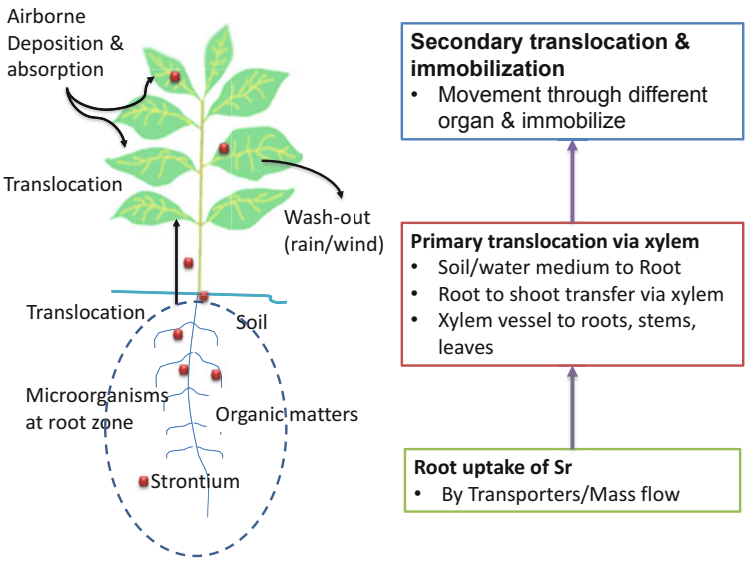

Fig. 1 Generalized scheme for strontium uptake in plants

precipitations, atmospheric deposition of Sr varies widely [16]. In sandy and humus soils, ^{90}Sr migrates downward faster, where soil particles act as reservoir of the same [17]. Following to ^{137}Cs, ^{90}Sr is likely to contribute to internal ingestion dose [18]. Concentration factor (CF = [^{90}Sr]p/[^{90}Sr]s, where [^{90}Sr]p and [^{90}Sr]s are the equilibrium-specific activities of ^{90}Sr in plant and soil), expressed in Bq kg^{-1}, can identify the migration of ^{90}Sr in the solid phase of the soil-soil solution-plant system [4, 6, 16]. Apart from the soil properties and other factors as mentioned, presence and exchangeability with calcium Ca^{2+} (macrohomologue of Sr^{2+}) play a crucial role in CF in plants [16]. Among $^{90}Sr^{2+}$–Ca^{2+} cation pairs, ^{90}Sr migration is regulated by cation-exchange capacity of the soil and presence of soil sorbents (like organozeolites) [19].

Soil-to-plant transfer (transfer factor, denoted as Fv and expressed in Bq kg^{-1} dry weight) can easily be defined as the ratio between the concentration of radionuclide in the plant and in the soil [7]. In podzolic soils, transfer factor (TF) of ^{90}Sr into rye plant was negatively correlated with P and Ca content and positively with organic content of soil [20]. Rabideau et al. [21] reported the effect of zeolite barrier on the movement of Sr. Soil moisture and temperature have significant effect on the oxidation states, speciation and geochemical formations of ^{90}Sr in soil [22]. Corcho-Alvarado et al. [23] reviewed the long-term decay kinetics with effective half-life, integrating the entire processes that possibly affect the activity and decay (including physical radioactive decay) of the radionuclides in the compartment. Similarly, in meadow soils (0–10 cm top layer) of Chernobyl NPP fallout affected areas, Lukšienė et al. [24] reported radionuclide activity and uptake by plants. ^{90}Sr in cultivable soil and in crop plants (e.g. Thatcher wheat) was reported almost 60 years back

[25–27]. Further, leakage from underground tanks used for radiological activities is also important for increase in Sr content in soil, which can be termed as "mini-radiological fallouts" [28, 29]. Freshwater ecosystems also get contaminated by atmospheric depositions, runoffs and washouts of contaminated areas. Vertical migration of ^{90}Sr was recorded around 2–4 cm year^{-1} in some water bodies at Russian-Ukrainian regions after Chernobyl accident [30]. Reports suggest that, in the same environment, the Fv values of ^{90}Sr are higher in comparison to other radionuclides including radiocaesium signifying plants' uptake preference [31, 32]. Climate can indirectly influence Sr uptake, as it affects the soil through decomposition of organic materials, which is faster in tropics than temperate regions [32].

3 Strontium Uptake by Plants

In a dynamic equilibrium, a variety of chemical species of metals exist in soil. Availability and uptake of a particular metal by plants depend on various factors like solubility, ionic potential of the metal, pH, humidity, organic content of the soil and microbial constituents at root rhizosphere [33, 34]. Phytoremediation of contaminated soil, therefore, relies on absorption of the metals through roots and afterward translocates to the aerial part of the plant. Further, root exudate secreted by plants plays a crucial role to the soil matrix for heavy metal availability and plants uptake potential [34, 35]. Manara [36] reported that extracellular carbohydrates like mucilage and callose, histidyl groups of plant cell wall, are important in regulating metals uptake into the cytoplasm. Once inside the cell, metals may enter into the xylem through apoplast for further transportation. Plants have an array of transporters in root zone, where heavy metals (HMs) transporters help in transference or exclusion of HM at plasma membrane. Inouhe et al. [37] stated that HM transporters thus support in reducing HM-induced toxicity (generation of free radicals or indirectly inducing ROS).

Interestingly, risks assessment associated with radionuclide contamination from water to aquatic organisms, including plants is difficult. As per IAEA [38], concentration ratio (CR) is defined by biota-to-water concentration of radionuclides in nonhuman organisms, which help in estimating radiation dose. However, in nature, concentration ratios of environmental radionuclides and within the organisms vary in a dynamic manner, as several spatiotemporal factors, longitudinal variation, etc. play important role [39, 40]. Whereas, Karube et al. [41] pointed out spatiotemporal basis of the ^{90}Sr uptake and accumulation in marine mussels (*Septifer virgatus*) after the Fukushima Daiichi NPP (FDNPP) accidental releases. Studies on the radiostrontium activity in the coastal areas along the Pacific coast of eastern Japan after FDNPP accident have revealed different marine fish (e.g. brown hakeling, *Physiculus maximowiczi*; rockfish, *Sebastes cheni*; fat greenling, *Hexagrammos otakii*) contamination [16, 42, 43].

In plants, radionuclide like Sr may interact first with rhizosphere (soil-root zone) or through aerial parts, where accumulation may occur over foliage via leaf cuticle

and epidermis through both active and passive transports [44, 45]. However, there is a chance of re-entry into the soil of the heavy metal when leaves or plants die and fall on the same soil. While various physico-chemical factors and water solubility of the metal compounds affect the uptake of the radionuclide in soil, however, Sr uptake in leaves has a non-specific competition with calcium during passive transport [16]. Asgari and Cornelis [46] reported that Sr is mainly deposited in leaf tissues but usually lower in seeds and fruits. Wang et al. [47] found that shoots show higher activity of ^{90}Sr accumulation and translocation as compared to roots. In a study, Willey [48] has reported that plants have more Sr in green shoots than woody parts, which might be due to more transportation activities in green parts of the plants. In earlier studies, in edible plants like wheat, rice, oats and barley, ^{90}Sr absorption activity was more in leaves and stems than fruits and kernels [26, 49]. Malek et al. [50] reported average root uptake rate of radiostrontium in *Brassica oleracea* was 240 Bq g^{-1}, while foliar absorption was 0.9 Bq g^{-1}.

Different plant parts show unalike Fv values, where shoots and stems documented higher values than for grains/seeds in plants like maize, cereals and leguminous vegetables. Fv values reflecting translocation potentiality of ^{90}Sr are reported for tree, Leaves > Branches > Fruit > Oil/Seed [32, 51], and wheat, Roots > Straw > Grain [7, 52–54]. Plants get exposed to β-radiation once they came into contact of radiostrontium. ^{90}Sr affects plants' stems and leaf shape, develops asymmetric leaf veins and inhibits growth [55]. Working with *Lepidium sativum*, Marčiulionienė et al. [56, 57] reported increase of RNA polymerase II activity during low-level exposure of Sr, while high level of exposure causes alterations of antioxidant enzyme activities, somatic mutations and chloroplast deformations. Biermans et al. [58] reported decrease in photosynthetic efficiency due to problem in PS-II. Working with *Secale cereale* seeds, Geraskin et al. [59] reported while 1.3–4.0 Gy exposure helps in faster germination, 12 Gy considerably inhibit germination.

4 Phytoremediation of Strontium

A number of researchers are working on removal of the ^{90}Sr from the soil. Among plant species like Indian mustard (*Brassica juncea*), Redroot pigweed (*Amaranthus retroflexus*) and tepary bean (*Phaseolus acutifolius*), it was reported that red root pigweed was maximum effective in accumulating ^{90}Sr from contaminated soil [60]. Competency of Caryophyllidae family of plants (agriculturally important eudicot plants like buckwheat, amaranth, beets, chards) was observed for the transfer of ^{90}Sr from soil to roots [61–63]. Eapen et al. [64], working with *Calotropis gigantea*, reported 90% radiostrontium removal within 24 h. Spanish moss (*Tillandsia usneoides*) known as a bio-indicator for ^{90}Sr, having high uptake ratio and positive correlation with concentration of the solution, showed reduction in chlorophyll content in high Sr concentration [65]. Inductively coupled plasma

(ICP)-mass spectrometry (MS) and liquid scintillation counting (LSC) are used to determine the concentration of ^{90}Sr in comestible plants [66, 67].

Van Hoeck et al. [55] reported the growth impedance effects in freshwater macrophyte *Lemna minor* due to beta-irradiation from ^{90}Sr. Variety of mushrooms can efficiently accumulate ^{90}Sr. Mushroom *Imperator rhodopurpureus* and *Boletus edulis* showed higher ^{90}Sr activity concentration at around 1.5–10 Bq kg^{-1} dry biomass [68]. Ageing effect on the transfer of ^{90}Sr to *Triticum aestivum* and *Lactuca sativa* was studied by Attar et al. [69] in respect to semiarid clayey soil in Syria. Fast growth with high biomass may be important to counter the ^{90}Sr accumulation and related effects. Among wheat, rice, oat and rye, it was found that oat is the better accumulator of ^{90}Sr; however, 99% of ^{90}Sr is accumulated in the overground non-edible parts (leaves and stems) [70, 71]. As per the existing studies, the activity concentration in a soil solution of 1 Bq L^{-1} of ^{90}Sr or ^{137}Cs corresponds to ca. 2×10^{-15} moles L^{-1}; however, the average concentrations of chemical homologues like K, Ca and Mg, respectively, in soil solution are in the order of 1 mmol L^{-1} [18]. Interestingly, organic matters present in soil moderate the preference of Ca uptake and its homologue Sr, as sorption of radiostrontium is reversibly controlled by major cations like Ca^{2+} [72]. Plant species also play a major role in uptake of Sr. Inter-varietal differences in transfer may be considered while choosing the cultivars for Sr phytoremediation. Penrose et al. [73] demonstrated that Sr accumulation is directly linked with Ca accumulation; plants that accumulate less Sr also accumulate quantities of Ca.

5 Strontium and Plant Root Zone (Rhizosphere)

Characteristically plant root-soil region (rhizosphere) is highly dissimilar from the bulk soil. Rhizosphere contains root exudates from plants that help to enrich helpful microbial population in the region by 1–4 orders of magnitude in comparison with the adjacent soil. The chemical-biological microenvironments due to root exudates specific to the plants, thus, modulate the metal availability and uptake potential. The exudates including secretions (e.g. mucilage, siderophores, allelopathic compounds, etc.), excretions (e.g. carbon dioxide, bicarbonates, protons) and diffusates (e.g. inorganic ions, organic or amino acids, water, sugars, etc.) help to harbour a specific microflora community, a unique gene pool to have improved metabolic capabilities [34, 74, 75]. As, for example, to increase the accessibility of phosphorus and potassium, plants may release H^+ and HCO_3^- at root zone to influence the pH in their immediate vicinity [18]. Similarly, ammonium (NH_4^+) mobilizes Sr on soil surface, inhibiting uptake by plants. Guillén et al. [76] reported application of common ammonium fertilizers like NPK and diammonium phosphate (DAP) may inhibit the soil-plant transfer of ^{90}Sr.

Stress due to soil contamination is also reduced by plant growth-promoting rhizobacteria (PGPR) by stimulating production of gibberellic acid, cytokinins, indole acetic acid and ethylene (plant growth regulators). For root absorption

through increased bioavailability of different metals, rhizobacteria may secrete hydrocyanic acid, antibiotics, siderophores, phosphate-solubilizing substances, 1-aminocyclopropane-1-carboxylic acid (ACC), etc. for better microbial colonization [4, 18]. Addition of rhizobacteria *Kluyvera ascorbata* SUD165/26 helped to 50–100% increase in seed germination and growth of *Brassica juncea* in a nickel-contaminated soil [77].

HM homeostasis at root cell is also controlled by diverse group of transporter proteins. These transporters or their families may be membrane bound, like CDF (cation diffusion facilitator) family, NRAMP (natural resistance-associated macrophage protein), Ca^{2+} cation antiporter (CAX), ZIP (zinc importer) families (ZRT, IRT-like protein [ZRT-zinc-regulated transporter; IRT, iron-regulated transporter]), heavy metal ATPases (HMAs) family like P1B-ATPases, copper transporter (COPT) family proteins, ATP-binding cassette (ABC) transporters, ABC transporters of the mitochondria (ATM), multidrug resistance-associated proteins (MRP), yellow stripe-like (YSL) pleiotropic drug resistance (PDR), etc. [18, 78–81]. Kramer et al. [82] reported histidine-rich ZIP family transporters are important for divalent metal ions. In root cells of *Arabidopsis thaliana*, IRT1 is responsible for transport of metals like Fe^{2+}, Zn^{2+}, Mn^{2+} and Cd^{2+} [83]. Kramer et al. [82] reported that P1B-type ATPases (HMAs family transporters) help in xylem loading of Cd and Zn and performing as an efflux pump. Vacuole level sequestration is primarily supported by AtHMA3 transporter present in the tonoplast membrane [36, 78]. Proton pumps in plants, like vacuolar proton-ATPase (V-ATPase) and vacuolar protonpyrophosphatase (V-PPase), may also involve in vacuolar sequestration [84].

6 Cellular Response of Plants Under Strontium

Plants typically accumulate numerous cations existing in their root region. Radionuclide exposures to plants lead to macromolecular damage like DNA strand breaks, lipid oxidation, or enzyme denaturation or reactive oxygen species (ROS) production through indirect radiolytic reactions [18, 79, 85]. Gupta and Sandalio [86] showed that catalase (CAT) and superoxide dismutase (SOD) and metabolites (e.g. glutathione and ascorbate) regulate the intracellular ROS performing as antioxidative defence system. Plants may circumvent (limiting the metal uptake) or endure (live in the occurrence of high internal metal concentration) to cope with toxic effects of radionuclides [87]. HM avoidance of plants involves reduction of metal concentration in flowing into the cell, biosorption to cell walls, reduced uptake and/or increased efflux [16, 18, 88]. Metal-binding ligands, such as phytochelatins (PCs) and metallothioneins (MTs), vacuolar compartmentalization, glyoxalase systems and upregulation of antioxidant defence and intracellular chelation by synthesizing organic acids, amino acids and glutathione (GSH), help to reduce the harmful effects caused by ROS [16].

Plants like *Verbascum cheiranthifolium*, *Astragalus gummifer* and *Euphorbia macroclada* were studied for potential Sr phytoremediation [89]. It was found that

shoots of these plants were capable of Sr bioaccumulation having high TLF (mean translocation factors), the quality which may be used in amelioration of Sr-contaminated soil [89]. Fellows et al. [90] reported coyote willow (*Salix exigua*) plants for efficient phytoextraction of the Sr present in the soil. Phytoremediation study examining soil microbial community-level physiological profiles (CLPPs) for *Sorghum bicolor* revealed enhanced soil-microbial diversity and activity in Sr-spiked soil with Sr content in tissues decreased in the order of leaves > roots > stems [47].

7 Conclusions

Stable strontium is plentiful in nature and it is absorbed by all plants. However, radiostrontium (^{90}Sr) is an anthropogenic product released due to fission of uranium (U) and plutonium (Pu). Atmospheric Sr used to get deposited along with precipitation, which then mixed with soil Sr. Discharge and waste disposal of Sr and its compounds has considerable impact on soil and groundwater. Plants absorb soluble Sr, which is available in their root zone. Restoration of radionuclide, like Sr-contaminated sites, using plants is a challenging task. Plants may be selected for this purpose should have both higher uptake potential and high biomass production capacity. Radionuclide once incorporated may get transferred to aerial parts of the plants by xylem-based radial translocation. The concentration within the potential plants should show significant higher level than the ambient soil concentration. However, phytoremediation of Sr from soil may be affected by several factors, including soil particle/clay/minerals properties, pH humidity of soil, humus and organic matters, plants' exudates and rhizospheric microorganism, etc. Keeping in the consideration, phytoremediation practices might be suitable for restoration of Sr radionuclide-contaminated soil when designated cultivars, those are well capable of accumulation in one hand and anti-stress physiological mechanisms on the other are used. Thus, comprehensive research on plants selection, field studies and genetic manipulation is useful to decontaminate Sr-contaminated soil in an eco-friendly manner.

Acknowledgement DKG and CW are thankful to BMBF, Germany (Funding no. 02S9276D). S.C. is thankful to Director, DRL (DRDO), Assam, India; A.N. is thankful to Principal, BCC, W.B. The authors apologize for the many colleagues who are not referenced in this work due to space limitations.

References

1. ATSDR-Agency for Toxic Substances and Disease Registry USA (2004) Toxicological profile for strontium. Agency for Toxic Substances and Disease Registry Division of Toxicology/ Toxicology Information, Atlanta. https://www.atsdr.cdc.gov/toxprofiles/tp159.pdf. Accessed 11 May 2017

2. Qi L, Qin X, Li FM, Siddique KHM, Brandl H, Xu J, Li X (2015) Uptake and distribution of stable strontium in 26 cultivars of three crop species: oats, wheat, and barley for their potential use in phytoremediation. Int J Phytoremediation 17:264–271
3. Coudert FX (2015) Strontium's scarlet sparkles. Nat Chem 7:940
4. Gupta DK, Schulz W, Steinhauser G, Walther C (2018) Radiostrontium transport in plants and phytoremediation. Environ Sci Pollut Res 25:29996–30008
5. Lipscy P, Kushida K, Incerti T (2013) The Fukushima disaster and Japan's nuclear plant vulnerability in comparative perspective. Environ Sci Technol 47:6082–6088
6. Sysoeva AA, Konopleva IV, Sanzharova NI (2005) Bioavailability of radiostrontium in soil: experimental study and modeling. J Environ Radioact 81:269–282
7. Guillén J (2018) Factors influencing the soil to plant transfer of strontium. In: Gupta DK, Walther C (eds) Behaviour of strontium in plants and the environment. Springer, Cham
8. IAEA (2015) The Fukushima Daiichi accident. Technical volume 4/5. Radiological consequences. IAEA, Vienna
9. UNSCEAR, United Nations Scientific Committee on the Effects of Atomic Radiation (2000) UNSCEAR 2000 report to the general assembly, with scientific annexes. UN, New York
10. Dubchak S (2018) Distribution of strontium in soil: interception, weathering, speciation, and translocation to plants. In: Gupta DK, Walther C (eds) Behaviour of strontium in plants and the environment. Springer, Cham
11. ATSDR-Agency for Toxic Substances and Disease Registry USA (2004) Public health statement Strontium CAS#: 7440-24-6. https://www.atsdr.cdc.gov/ToxProfiles/tp159-c1-b.pdf. Accessed 12 May 2017
12. Merz S, Shozugawa K, Steinhauser G (2016) Effective and ecological half-lives of ^{90}Sr and ^{137}Cs observed in wheat and rice in Japan. J Radioanal Nucl Chem 307:1807–1810
13. Nakano T (2016) Potential uses of stable isotope ratios of Sr, Nd, and Pb in geological materials for environmental studies. Proc Jpn Acad Ser B Phys Biol Sci 92:167–184
14. Volkle H, Murith C, Surbeck H (1989) Fallout from atmospheric bomb tests and releases from nuclear installations. Radiat Phys Chem 34:261–277
15. Yablokov AV, Nesterenko VB, Nesterenko AV (2008) Atmospheric, water, and soil contamination after Chernobyl. Radiat Prot Dosim 128:146–158
16. Gupta DK, Deb U, Walther C, Chatterjee S (2018) Strontium in the ecosystem: transfer in plants via root system. In: Gupta DK, Walther C (eds) Behaviour of strontium in plants and the environment. Springer, Cham
17. Chawla F, Steinmann P, Pfeifer HR, Froidevaux P (2010) Atmospheric deposition and migration of artificial radionuclides in Alpine soils (Val Piora, Switzerland) compared to the distribution of selected major and trace elements. Sci Total Environ 408:3292–3302
18. Gupta DK, Chatterjee S, Datta S, Voronina AV, Walther C (2016) Radionuclides: accumulation and transport in plants. Rev Environ Contam Toxicol 241:139–160
19. Maskalchuk LN, Baklaia AA, Konoplevb AV, Leontievaa TG (2014) Migration of ^{90}Sr in the solid phase of the soil–soil solution–plant systems and ways to reduce it. Radiochemistry 56:222–225
20. Claus B, Grahmann B, Hormann V, Keuneke S, Leder M, Müller H, Peters E, Rieger EM, Schmitz-Feuerhake I, Wagschal F (1990) Sr-90 transfer factors for rye in podzolic soils: dependence on soil parameters. Radiat Environ Biophys 29:241–245
21. Rabideau AJ, Van Benschoten J, Patel A, Bandilla K (2005) Performance assessment of a zeolite treatment wall for removing Sr-90 from groundwater. J Contam Hydrol 79:1–24
22. Kovacheva P, Slaveikova M, Todorov B, Djingova R (2014) Influence of temperature decrease and soil drought on the geochemical fractionation of ^{60}Co and ^{137}Cs in fluvisol and cambisol soils. Appl Geochem 50:74–81
23. Corcho-Alvarado JA, Balsiger B, Sahli H, Astner M, Byrde F, Rollin S, Holzer R, Mosimann N, Wüthrich S, Jakob A, Burger M (2016) Long-term behavior of ^{90}Sr and ^{137}Cs in the environment: case studies in Switzerland. J Environ Radioact 160:54–63

24. Lukšienė B, Puzas A, Remeikis V, Druteikienė R, Gudelis A, Gvozdaitė R, Buivydas Š, Davidonis R, Kandrotas G (2015) Spatial patterns and ratios of ^{137}Cs, ^{90}Sr, and Pu isotopes in the top layer of undisturbed meadow soils as indicators for contamination origin. Environ Monit Assess 187:268
25. Gustafson PF (1959) Ratio of Cesium-137 and Strontium-90 radioactivity in soil. Science 130:1404–1405
26. Lee CC (1959) Distribution of radioactivity in wheat plants grown in the presence of strontium-90. Science 129:1280
27. Menzel RG (1960) Transport of Strontium-90 in runoff. Science 31:499–500
28. Mahmoud NS, El-Hemamy ST (2005) On the possible leakage of ET-RR1 liquid waste tank: hydrological and migration modes studies. Sci World J 5:234–252
29. Maloshtan I, Polishchuk S, Kashparov V, Yoschenko V (2017) Assessment of radiological efficiency of countermeasures on peat-bog soils of Ukrainian Polissya. J Environ Radioact 175–176:52–59
30. Fesenko S, Fesenko J, Sanzharova NI, Karpenko E, Titov I (2011) Radionuclide transfer to freshwater biota species: review of Russian language studies. J Environ Radioact 102:8–25
31. Al Attar L, Al-Oudat M, Safia B, Ghani BA (2015) Transfer factor of ^{90}Sr and ^{137}Cs to lettuce and winter wheat at different growth stage applications. J Environ Radioact 150:104–110
32. IAEA (2010) Handbook of parameter values for the prediction of radionuclide transfer in terrestrial and freshwater environment. Technical Reports Series no. 472. IAEA, Vienna
33. Gupta DK, Chatterjee S (2014) Heavy metal remediation: transport and accumulation in plants. Nova Science, New York
34. Mitra A, Chatterjee S, Datta S, Sharma S, Veer V, Razafindrabe BHM, Walther C, Gupta DK (2014) Mechanism of metal transporters in plants. In: Gupta DK, Chatterjee S (eds) Heavy metal remediation: transport and accumulation in plants. Nova Science, New York, pp 1–28
35. Gupta DK, Chatterjee S (2017) Arsenic contamination in the environment: the issues and solutions. Springer, Cham
36. Manara A (2012) Plants and heavy metals. In: Furini A (ed) Springer briefs in molecular sciences. Springer, Heidelberg, pp 27–53
37. Inouhe M, Sakuma Y, Chatterjee S, Datta S, Jagetiya BL, Voronina AV, Walther C, Gupta DK (2015) General roles of phytochelatins and other peptides in plant defense mechanisms against oxidative stress/primary and secondary damages induced by heavy metals. In: Gupta DK, Palma JM, Corpas FJ (eds) Reactive oxygen species and oxidative damage in plants under stress. Springer, Heidelberg, pp 219–245
38. IAEA (2014) Handbook of parameter values for the prediction of radionuclide transfer to wildlife. Technical Reports Series no. 479. IAEA, Vienna
39. Batlle JVI, Beresford NA, Beaugelin-Seiller K, Bezhenar R, Brown J, Cheng JJ, Cujic M, Dragovic S, Duffa C, Fievet B, Hosseini A, Jung KT, Kamboj S, Keum DK, Kryshev A, LePoire D, Maderich V, Min BI, Perianez R, Sazykina T, Suh KS, Yu C, Wang C, Heling R (2016) Inter comparison of dynamic models for radionuclide transfer to marine biota in a Fukushima accident scenario. J Environ Radioact 153:31–50
40. Beresford NA, Wood MD, Batlle JVI, Yankovich TL, Bradshaw C, Willey N (2016) Making the most of what we have: application of extrapolation approaches in radioecological wildlife transfer models. J Environ Radioact 151:373–386
41. Karube Z, Inuzuka Y, Tanaka A, Kurishima K, Kihou N, Shibata Y (2016) Radiostrontium monitoring of bivalves from the Pacific coast of eastern Japan. Environ Sci Pollut Res 23:17095–17104
42. Fujimoto K, Miki S, Kaeriyama H, Shigenobu Y, Takagi K, Ambe D, Ono T, Watanabe T, Morinaga K, Nakata K, Morita T (2015) Use of otolith for detecting strontium-90 in fish from the harbor of Fukushima Dai-ichi Nuclear Power Plant. Environ Sci Technol 49:7294–7301
43. Konovalenko L, Bradshaw C, Andersson E, Lindqvist D, Kautsky U (2016) Evaluation of factors influencing accumulation of stable Sr and Cs in lake and coastal fish. J Environ Radioact 160:64–79

44. Fortunati P, Brambilla M, Speroni F, Carini F (2004) Foliar uptake of ^{134}Cs and ^{85}Sr in strawberry as function by leaf age. J Environ Radioact 71:187–199
45. Liu HC, Chung CH, You CF, Chiang YH (2016) Determination of $^{87}Sr/^{86}Sr$ and $\delta^{88/86}Sr$ ratios in plant materials using MC-ICP-MS. Anal Bioanal Chem 408:387–397
46. Asgari K, Cornelis WM (2015) Heavy metal accumulation in soils and grains, and health risks associated with use of treated municipal wastewater in subsurface drip irrigation. Environ Monit Assess 187:410
47. Wang X, Chen C, Wang J (2017) Phytoremediation of strontium contaminated soil by *Sorghum bicolor* (L.) Moench and soil microbial community-level physiological profiles (CLPPs). Environ Sci Pollut Res 24:7668–7678
48. Willey NJ (2014) Soil to plant transfer of radionuclides: predicting the fate of multiple radioisotopes in plants. J Environ Radioact 133:31–34
49. Ichikawa R, Eto M, Abe M (1962) Strontium-90 and Cesium-137 absorbed by rice plants in Japan, 1960. Science 135:1072
50. Malek M, Hinton T, Webb S (2002) A comparison of ^{90}Sr and ^{137}Cs uptake in plants via three pathways at two Chernobyl-contaminated sites. J Environ Radioact 58:129–141
51. Al-Oudat M, Asfary AF, Mukhalallti H, Al-Hamwi A, Kanakri S (2006) Transfer factors of ^{137}Cs and ^{90}Sr from soil to trees in arid regions. J Environ Radioact 90:78–88
52. Al Attar L, Al-Oudat M, Safia B, Ghani BA (2016) Ageing impact on the transfer factor of ^{137}Cs and ^{90}Sr to lettuce and winter wheat. J Environ Radioact 164:19–25
53. Guillén J, Baeza A, Corbacho JA, Muñoz-Muñoz JG (2015) Migration of ^{137}Cs, ^{90}Sr, and $^{239+240}Pu$ in Mediterranean forests: influence of bioavailability and association with organic acids in soil. J Environ Radioact 144:96–102
54. Sarap NB, Janković MM, Dolijanović ŽK, Kovačević DĐ, Rajačić MM, Nikolić JD, Todorović DJ (2015) Soil-to-plant transfer factor for ^{90}Sr and ^{137}Cs. J Radioanal Nucl Chem 303:2523–2527
55. Van Hoeck A, Horemans N, Van Hees M, Nauts R, Knapen D, Vandenhove H, Blust R (2015) β-radiation stress responses on growth and antioxidative defense system n plants: a study with strontium-90 in *Lemna minor*. Int J Mol Sci 16:15309–15327
56. Marčiulionienė D, Luksiene B, Kiponas D, Maksimov G, Darginaviciene J, Gaveliene V (2007) Effects of Cs-137 and Sr-90 on the plant *Lepidium sativum* L. growth peculiarities. Ekologija 53:65–70
57. Marčiulionienė D, Luksiene B, Montvydienė D, Kiponas D (2008) Estimation of ^{137}Cs and ^{90}Sr ionizing radiation impact on the plant vegetative and generative organs. http://radioecology.info/Bergen2008/proceedings.pdf. pp 1–4
58. Biermans G, Horemans N, Vanhoudt N, Vandenhove H, Saenen E, Van Hees M, Wannijn J, Batlle JV, Cuypers A (2014) An organ-based approach to dose calculation in the assessment of dose-dependent biological effects of ionising radiation in *Arabidopsis thaliana*. J Environ Radioact 133:24–30
59. Geraskin S, Dikarev V, Zyablitskaya Y, Oudalova A, Spirin Y, Alexakhin R (2003) Genetic consequences of radioactive contamination by the Chernobyl fallout to agricultural crops. J Environ Radioact 66:155–169
60. Fuhrmann M, Lasat MM, Ebbs SD, Kochian LV, Cornish J (2002) Uptake of cesium-137 and strontium-90 from contaminated soil by three plant species; application to phytoremediation. J Environ Qual 31:904–909
61. Broadley MR, Bowen HC, Cotterill HL, Hammond JP, Meacham MC, Mead A, White PJ (2003) Variation in the shoot calcium content of angiosperms. J Exp Bot 54:1431–1446
62. Broadley MR, Bowen HC, Cotterill HL, Hammond JP, Meacham MC, Mead A, White PJ (2004) Phylogenetic variation in the shoot mineral concentration of angiosperms. J Exp Bot 55:321–336
63. Willey N, Fawcett K (2006) A phylogenetic effect on strontium concentrations in angiosperms. Environ Exp Bot 57:258–269

64. Eapen S, Singh S, Thorat V, Kaushik CP, Raj K, D'Souza SF (2006) Phytoremediation of radiostrontium ((90)Sr) and radiocesium ((137)Cs) using giant milky weed (*Calotropis gigantea* R. Br.) plants. Chemosphere 65:2071–2073
65. Zheng G, Pemberton R, Li P (2016) Bioindicating potential of strontium contamination with Spanish moss *Tillandsia usneoides*. J Environ Radioact 152:23–27
66. Amano H, Sakamoto H, Shiga N, Suzuki K (2016) Method for rapid screening analysis of Sr-90 in edible plant samples collected near Fukushima, Japan. Appl Radiat Isot 112:131–135
67. Maxwell SL, Culligan BK, Noyes GW (2010) Rapid separation of actinides and radiostrontium in vegetation samples. J Radioanal Nucl Chem 286:273–282
68. Saniewski M, Zalewska T, Krasińska G, Szylke N, Wang Y, Falandysz J (2016) ^{90}Sr in King Bolete *Boletus edulis* and certain other mushrooms consumed in Europe and China. Sci Total Environ 543:287–294
69. Attar LA, Oudat MA, Safia B, Ghani BA (2016) Ageing impact on the transfer factor of ^{137}Cs and ^{90}Sr to lettuce and winter wheat. J Environ Radioact 164:19–25
70. Lin Q, Xiaoliang Q, Li F-M, Kadambot H, Siddique M, Brandl H, Xu J, Li X (2015) Uptake and distribution of stable strontium in 26 cultivars of three crop species: oats, wheat, and barley for their potential use in phytoremediation. Int J Phytoremediation 17:264–271
71. Schimmack W, Gerstmann U, Schultz W, Sommer M, Tschopp V, Zimmermann G (2007) Intra-cultivar variability of the soil-to-grain transfer of fallout ^{137}Cs and ^{90}Sr for winter wheat. J Environ Radioact 94:16–30
72. Chu Q, Watanabe T, Sha Z, Osaki M, Shinano T (2015) Interactions between Cs, Sr, and other nutrients and trace element accumulation in Amaranthus shoot in response to variety effect. J Agric Food Chem 63:2355–2363
73. Penrose B, Beresford NA, Broadley MR, Crout NMJ (2015) Inter-varietal variation in caesium and strontium uptake by plants: a meta-analysis. J Environ Radioact 139:103–117
74. Chatterjee S, Sharma S, Gupta DK (2017) Arsenic and its effect on major crop plants: stationary awareness to paradigm with special reference to rice crop. In: Gupta DK, Chatterjee S (eds) Arsenic contamination in the environment: the issues and solutions. Springer, Cham, pp 123–143
75. LeDuc DL, Terry N (2005) Phytoremediation of toxic trace elements in soil and water. J Ind Microbiol Biotechnol 32:514–520
76. Guillén J, Muñoz-Muñoz G, Baeza A, Salas A, Mocanu N (2017) Modification of the ^{137}Cs, ^{90}Sr, and ^{60}Co transfer to wheat plantlets by NH^{4+} fertilizers. Environ Sci Pollut Res 24:7383–7391
77. Burd GI, Dixon DG, Glick BR (1998) A plant growth-promoting bacterium that decreases nickel toxicity in seedlings. Appl Environ Microbiol 64:3663–3668
78. Gupta DK, Huang HG, Corpas FJ (2013) Lead tolerance in plants: strategies for phytoremediation. Environ Sci Pollut Res 20:2150–2161
79. Gupta DK, Tawussi F, Hölzer A, Hamann L, Walther C (2017) Investigation of low level ^{242}Pu contamination on nutrition disturbance and oxidative stress in *Solanum tuberosum* L. Environ Sci Pollut Res 24:16050–16061
80. Huang J, Zhang Y, Peng JS, Zhong C, Yi HY, Ow DW, Gong JM (2012) Fission yeast HMT1 lowers seed cadmium through phytochelatin-dependent vacuolar sequestration in Arabidopsis. Plant Physiol 158:1779–1788
81. Mitra A, Chatterjee S, Moogouei R, Gupta DK (2017) Arsenic accumulation in rice and probable mitigation approaches: a review. Agronomy 7:67
82. Kramer U, Talke IN, Hanikenne M (2007) Transition metal transport. FEBS Lett 581:2263–2272
83. Nishida S, Mizuno T, Obata H (2008) Involvement of histidine-rich domain of ZIP family transporter TjZNT1 in metal ion specificity. Plant Physiol Biochem 46:601–606
84. Dalcorso G, Farinati S, Furini A (2010) Regulatory networks of cadmium stress in plants. Plant Signal Behav 5:1–5

85. Gupta DK, Tawussi F, Hamann L, Walther C (2016) Moderate uranium disturbs the nutritional status and induces oxidative stress in *Pisum sativum* L. J Plant Physiol Pathol 4:1
86. Gupta DK, Sandalio LM (2012) Metal toxicity in plants: perception, signaling and remediation. Springer, Heidelberg
87. Chatterjee S, Deb U, Datta S, Walther C, Gupta DK (2017) Common explosive (TNT, RDX, HMX) and their fate in the environment: emphasizing bioremediation. Chemosphere 184:438–451
88. Gupta DK, Walther C (2014) Radionuclide contamination and remediation through plants. Springer, Heidelberg
89. Sasmaz A, Sasmaz M (2009) The phytoremediation potential for strontium of indigenous plants growing in a mining area. Environ Exp Bot 67:139–144
90. Fellows RJ, Fruchter JS, Driver CJ (2009) 100-N area Strontium-90 treatability demonstration project: food chain transfer studies for phytoremediation along the 100-N Columbia River Riparian Zone. U.S. Department of Energy (PNNL-18294), Pacific Northwest National Laboratory, Washington. http://www.pnl.gov/main/publications/external/technical_reports/PNNL-18294.pdf

Uptake, Transport, and Remediation of Strontium

Susmita Sharma

Contents

Abstract Strontium abundantly occurs in nature in the rocks and soils in the form of sulfate and carbonate minerals, i.e., celestite ($SrSO_4$) and strontianite ($SrCO_3$), in nonradioactive and nontoxic forms. However, a small amount of strontium as radioactive ^{90}Sr has been contributed to the geo-environment by the anthropogenic activities of nuclear testing and fission reactions. The contamination caused by the radioactive by-products of such activities poses major concerns due to its ease of entry into the ecosystem. The ^{90}Sr has a prolonged half-life of 28.9 years and can progressively enter into the geo-environment and also the life cycle of organisms living in close proximity to such contaminated sites. The mobility of ^{90}Sr migration in the geo-environment is often favored due to its similarity to calcium ions but can be retarded through the strong interactions with soil organic materials, clay minerals, and other oxides present in the environment. Owing to the severity of radioactive Sr contamination, this chapter thus deals with the various pathways of strontium dispersal into the geo-environment. Additionally, for the contaminated sites, studies

S. Sharma (✉)
Department of Civil Engineering, National Institute of Technology Meghalaya, Shillong, Meghalaya, India
e-mail: susmita.sharma4@nitm.ac.in

P. Pathak, D. K. Gupta (eds.), *Strontium Contamination in the Environment*,
The Handbook of Environmental Chemistry 88,
https://doi.org/10.1007/978-3-030-15314-4_6

on sorption-desorption behavior for selection of suitable remediation technology are deliberated herein. This chapter also explores the extent to which phytoremediation, an in situ modification, can be used to reclaim soils contaminated with ^{90}Sr.

Keywords Cation exchange capacity · Phytoremediation · Radioactive waste · Sorption-desorption · Strontium

1 Introduction

Radionuclides are commonly recognized by the type and energy of emitted radiation and their half-life. Depending on the half-life of a radionuclide, its existence in the geo-environment (released from routine and accidental nuclear fallout) can range from a fraction of a second to thousands of years [1]. During the process of disintegration, the radionuclide gets exposed to living beings through alleyways such as terrestrial foods, marine foods, surface water, groundwater, and inhalation exposure [2, 3]. The plants and thus take up radioactive matter with the essential nutrient from both soil and water, and consequently food products derived from such agricultural field and thus get exposed to radioactive contamination. Hence it becomes essential to quantify the transfer of radionuclides from soil to plant and animals [4–6]. This chapter thus extensively describes about one such radionuclide, strontium-90 (^{90}Sr) having half-life of 28.9 years. The chapter presents the sources of strontium occurring in natural and anthropogenic forms and the uptake and transfer characteristics of radioactive Sr in plants, ruminants, and geomaterials, viz., soil and water. Further, it elucidates different types of remediation technology available for treatment of ^{90}Sr-contaminated geomaterials.

1.1 Natural Sources of Strontium

Strontium occurs naturally in rocks and soils and consists 0.02–0.03% of the earth's crust. The minerals comprising strontium (Sr) are celestite ($SrSO_4$) and strontianite ($SrCO_3$); $SrSO_4$ and $SrCO_3$ being the only two principal ores of strontium.

Strontium subsists in forms of dry aerosols due to natural processes such as rock weathering, entrainment of Sr-contaminated dust, and resuspension of soil by wind. In the atmosphere, it exists as strontium oxide (SrO). The transfer of strontium from the atmosphere to the earth surface involves the process of wet deposition, wherein SrO reacts with moisture of the atmospheric cycle to form Sr^{2+} and $SrOH^-$ ions. Sr^{2+} has an ionic radius of 1.12 Å (refer to Fig. 1), very close to that of Ca^{2+} at 0.99 Å [7] which formulates it to act chemically as a calcium analog, surrogating for calcium in the composition of minerals [5]. In biogenic sediments, strontium occurs in aragonite (>5,000 ppm, high Sr^{2+}; ≤3,000 ppm, low Sr^{2+}) and calcite crystal (>2,000 ppm, high Sr^{2+}; ≤1,000 ppm, low Sr^{2+}) lattice, as a substitute for calcium [5]. Strontium

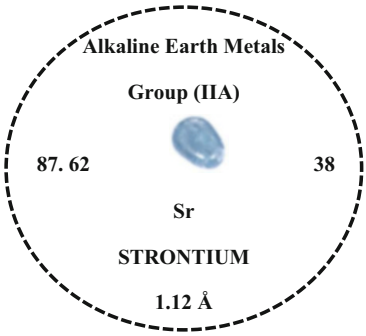

Fig. 1 Features of strontium (Sr) in periodic table

has four stable, naturally occurring isotopes which are designated as ^{84}Sr, ^{86}Sr, ^{87}Sr, and ^{88}Sr comprising about 0.55, 9.75, 6.75, and 82.75% of natural strontium. Each natural form of strontium is stable, nontoxic, and nonradioactive.

1.2 Anthropogenic Sources of Strontium

Anthropogenic (man-made) activities such as coal burning, processing of strontium compounds, and using phosphate fertilizer for land applications have been found to release strontium into the geo-environment. Report by Ondov et al. [8] stated that the atmospheric concentration of Sr around coal plant may range between 17 and 2,718 μg m^{-3}. Furr et al. [9] recounted that around 100–4,000 ppm (mg kg^{-1}) of Sr is contained in fly ash, a residual material of coal mass valorization. Similarly ~20–4,000 μg of Sr have been reported to be present in phosphate fertilizer [10]. The industrial processes, viz., (a) glassmaking; (b) ceramic making; (c) municipal landfill operations; (d) scrap metal sorting, sales, and brokerage; (e) metal melting and casting; (f) paint pigmenting; etc., and medical processes are also known to persistently contribute Sr into the environment but relatively in smaller amounts.

However, during the second half of the twentieth century, an alarming increase in the nuclear weapons' testing in all environments, viz., atmosphere, underground, and underwater, has created significant environmental impacts in terms of radionuclide migration into the environment [2, 3]. Very large amounts of release of radioactive isotope (specifically ^{90}Sr, ^{14}C, and ^{137}Cs) ~150 Mt of the atmospheric yield and ~120 Mt of underground yield between 1960–1965 in the northern hemisphere (in countries like the USA, USSR, China) and 1970–1980, respectively, were detailed in UNSCEAR 2000. Further nuclear power-plant accidents, often referred to as "nuclear fallout" like Chernobyl (1986) and Fukushima Daiichi (2011), also led to release in large amount of radionuclide (specifically ^{90}Sr, ^{137}Cs, and ^{131}I) contamination into the atmosphere. While natural Sr is stable and not hazardous to health, the radioisotopes of strontium ^{90}Sr and ^{89}Sr are dangerous component of nuclear fallout. Due to the short half-life time ~50.5 days for ^{89}Sr, this element once released into the soil environment starts decaying rapidly [1].

The concern however lies with the radionuclide ^{90}Sr, which has a long half-life of 28.8 years and are easily taken up into biological systems, owing to its analogy to calcium, an essential element for living organisms, thus generating a potential risk of deposition of ^{90}Sr in bone and causing bone diseases, deformities, and tumors [5, 6]. The exposure of ^{90}Sr induced changes in bone physiology both in humans and animals [4].

2 Exposure (External and Internal) to Radiation Caused by ^{90}Sr

The cascade decay diagram of strontium is shown in Fig. 2, wherein ^{90}Sr decays to generate unstable ^{90}Y (Yttrium-90) and later decays to stable ^{90}Zr (zirconium-90) emitting only beat radiation (one at 0.546 MeV and other at 2.28 MeV) with a short range, which can be rendered harmful if taken externally or internally by the living organism. Unlike radiocesium, which emits γ-radiation, ^{90}Sr decay involves reduced external exposure; thus toxicity of ^{90}Sr to the living organism will be most severe from inhalation or incidental ingestion of soil or dust contaminated with ^{90}Sr. The prediction on exposure of ^{90}Sr on 150 individuals consuming 2 L of water per day for 1 year is performed by USEPA, as a drinking water standard for ^{90}Sr and the ambient standard is adopted as 8-pCi L^{-1} for freshwater by the Washington State Department of Ecology. The standard applicable to aquatic organisms for protection from radiation exposure is 1.0 rad day^{-1}.

The different pathways of exposure of Sr into the atmosphere are portrayed in Fig. 3. The anthropogenic sources such as radionuclide, chemicals, pesticides, nutrients, etc. play a very vital role in the contamination of Sr for both groundwater and soil. The occurrence of Sr can also be from geogenic process, i.e., bedrock weathering and leaching. Sr, being soluble in water, it's leaching from natural or anthropogenic sources, can severely affect the quality of surface and groundwater. Sr contamination in soil is further uptaken by the plant roots and translocated in aboveground parts, depending on soil acidity, climatic conditions, and root depth. These plants with ^{90}Sr on harvesting might get assimilated in the food cycle and bioaccumulated in humans and animals. Thus the ingestion of ^{90}Sr in particular, via contaminated water and food, is a major exposure pathway for the population.

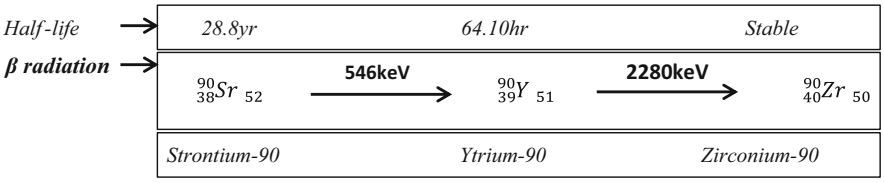

Fig. 2 Strontium in the environment from nuclear fallout – a decay diagram

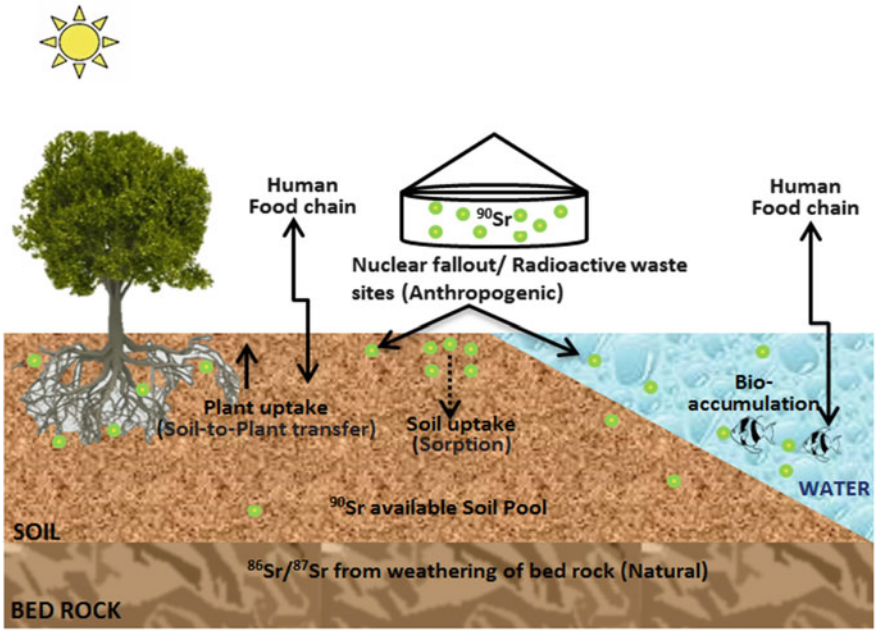

Fig. 3 Strontium exposure into atmosphere

3 Strontium Exchange Characteristics

3.1 Strontium Uptake/Transfer Characteristics in Plants and Dietary Products

Radioactive strontium, ^{90}Sr possessing a half-life of 28.9 years persists in the environment for a long time and progressively enters the food chain. The absorption of a radionuclide onto the plant components depends on plant type as well as the nature of the elements. Studies on behavioral/growth patterns of plants have revealed that plant species have selective ability to absorb or resist certain elements present in the soil. The radiological impact of Sr released to the terrestrial environment (plant, animal, and human) is usually predicted by a mathematical model referred to as "transfer factor or transfer coefficient" [11–15]. Transfer factor (TF) is defined as the baseline background level information about natural radionuclides corresponding to the radiological impact of radionuclides released to the environment [16, 17]. The equilibrium coefficient of transfer for activity, TF_P from soil to plant 0–10 cm for grass and 0–20 cm for all other crops, including trees, is usually expressed as

$$TF_P = \frac{\text{Concentration of Sr in plant, Bq kg}^{-1}\text{dry crop mass}}{\text{Concentration of Sr in soil, Bq kg}^{-1}\text{dry soil mass in upper 20 cm}} \quad (1)$$

The transfer of Sr from soil to plant follows the same trend as its nutrient analog Ca under homogeneous soil condition [16]. Veresoglou et al. [13] reported that uptake parameters of Ca-accumulating plants provide good estimates for Sr. Jolly et al. [11] opined that different TF_P values for Sr ranged between 0.051 and 0.433 for different edible plant species (viz., spinach, *Amaranthus*, brinjal, tomato, radish, bean, cauliflower, carrot). Studies reported by Zhuang et al. [15] and Jolly et al. [11] revealed that leafy vegetables are found to show a higher transfer factor for moderate concentration of Sr ranging between 7.23 mg kg^{-1} and 61.65 mg kg^{-1}. A similar observation was recorded by Velasco et al. [18]; they revealed that major contribution of TF_P was observed for around 30% leafy vegetables, followed by grasses, root crops, and leguminous vegetables, under both tropical and subtropical ecosystems. IAEA [19] acknowledged TF_P values in the increasing order for leaves > branches > fruit > oil/seed. However, Sarap et al. [12] acquired TF_P values within different parts of the wheat plant. This study further revealed TF_P values in the increasing order, roots > straw > grain. Thus it can be opined that different plant species function differently in the uptake of ^{90}Sr from soil. Figure 4 demonstrated studies conducted at 3 km west from accident site (most contaminated with ^{90}Sr) at Ukraine which revealed that with ^{90}Sr concentration in the soil as high as 40.12 Bq kg^{-1}, the transfer factor is restricted to 1.2. This case study demonstrated that the TF_P values for both soil and root range between 0.01 and 12 ([14, 17, 24, 25]).

IAEA 2010 further categorized TF_P values for ^{90}Sr in case of tropical environments (maximum recorded as 3.4) and for subtropical environments (maximum recorded as 0.63), depending on 140 and 209 entries, respectively, thus corroborating that plant accumulation of Sr may not be consistent throughout and is highly affected by changes in climate condition [19, 26] in addition to plant species.

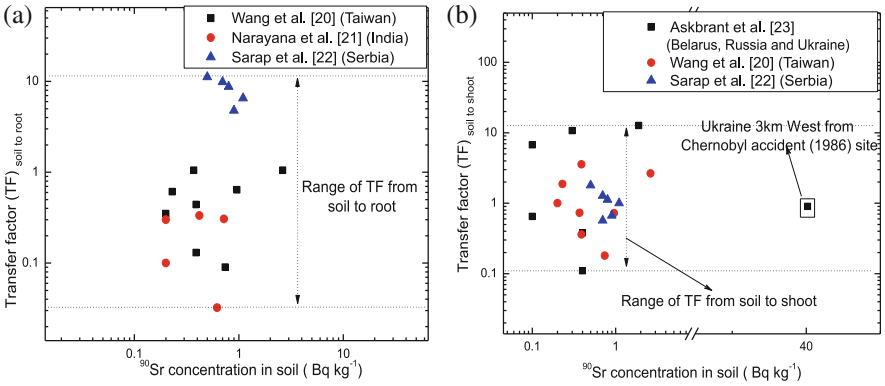

Fig. 4 Extent of transfer (**a**) from soil to root and (**b**) soil to shoot [20–23]

Additionally, the occurrence of organic content in the soil might influence the nutrients dynamics of the soil, thereby changing its cation exchange capacity (CEC) and pH. The change of these properties might influence the kinetics of the sorption of Sr within the root zone, thereby affecting the rate of movement of Sr through soil. Hence, the concentration of Sr in the soil cannot be the only factor controlling its uptake by plants [27]. Thus for a better understanding of the mechanism of soil-to-plant transfer of Sr, soil solid-liquid distribution of Sr (discussed in Sect. 3.2) in addition to the uptake mechanism at the plant root becomes imperative [16, 28].

The transfer coefficient of a radionuclide in case of animal-derived food products (milk, meat, etc.) was first proposed by Ward and Johnson [29]. It is quantified as a ratio between the ^{90}Sr activity concentrations in the food products and that of daily dietary radionuclide intake referred as "feed" [29, 30]. The equilibrium coefficient of transfer for activity from feed to milk, TF_m, and from feed to meat, $TF_{me,}$ is usually expressed as

$$TF_m = \frac{\text{Concentration of Sr in milk, Bq L}^{-1}}{\text{Daily intake of Sr, Bq d}^{-1}} \tag{2}$$

$$TF_{me} = \frac{\text{Concentration of Sr in meat, Bq kg}^{-1}}{\text{Daily intake of Sr, Bq d}^{-1}} \tag{3}$$

Table 1 gives the activity of ^{90}Sr on consumable food items [19, 26, 31–34]. The table summarizes the transfer values for the prediction of ^{90}Sr transfer available for direct intake by the human being. Such transfer coefficient must be within a constant range to be worked out for incorporation into predictive food chain models [35, 36]. The range of transfer coefficient for ^{90}Sr to milk under homeostatic control conditions milk of cow, goat, and sheep are recorded as 0.001–0.003, 0.006–0.039, and 0.04, respectively [26, 31, 32].

Since strontium and calcium generally follow similar metabolic pathways, the response of strontium is strongly influenced by that of calcium in the case of ruminants. Thus to determine the transfer coefficient of Sr (originating from milk) with that of Ca (originating from skeletal sorption), another mathematical model observed ratio (OR) was proposed by Howard et al. [32].

$$OR = \frac{\text{Concentration of Sr in milk, Bq L}^{-1} / \left[\text{Daily intake of Sr, Bq d}^{-1}\right]}{\text{Concentration of Ca in milk, g L}^{-1} / \left[\text{Daily intake of Ca, g d}^{-1}\right]} \tag{4}$$

Sirotkin [37] and Howard et al. [32] have reported that for ^{90}Sr, the transfer to milk can be reduced by 40–60%, increasing the dietary calcium intake (providing the supplementary dosage of 100–200 g day^{-1}) in case of the ruminants.

Sr is not known to possess any biological role and not regarded as an essential element; however, owing to the amount or dosage of existence in the geo-

Table 1 Specific activity or transfer factor of ^{90}Sr on food products

Element	TF_m (d L^{-1})	Standard deviation (SD)	Min (d L^{-1})	Max (d L^{-1})	No of obs. for experiment	References
Cow milk	1.5×10^{-3}	8.1×10^{-4}	3.4×10^{-4}	4.3×10^{-3}	154	Coughtrey [31], IAEA [26], Howard et al. [32, 33], Calmon et al. [34] and IAEA [19]
Goat milk	2.1×10^{-2}	2.0×10^{-2}	5.8×10^{-3}	8.1×10^{-2}	21	
Sheep milk	3.0×10^{-2}	1.2×10^{-2}	1.3×10^{-2}	4.0×10^{-2}	4	
Cow meat	2.1×10^{-3}	2.2×10^{-3}	2.0×10^{-4}	9.2×10^{-3}	35	
Sheep meat	1.7×10^{-3}	7.5×10^{-4}	3.0×10^{-4}	4.0×10^{-3}	25	
Pig meat	3.6×10^{-3}	2.7×10^{-3}	5.0×10^{-4}	8.0×10^{-3}	12	
Duck meat	2.3×10^{-2}	1.2×10^{-2}	7.0×10^{-3}	4.1×10^{-2}	7	
Egg	8.8×10^{-1}	1.5	2.5×10^{-1}	4.8	9	
Mushroom	$5–6 \times 10^{-3}$	–	–	–	–	
Bilberry	7.1×10^{-3}	–	3×10^{-3}	12.2×10^{-3}	–	
Wild strawberry	9.2×10^{-2}	–	6.2×10^{-3}	12.2×10^{-2}	–	

Text mentioned in italics has units in d kg^{-1} and represents TF_{me} values
For d L^{-1} and d kg^{-1}, refer to Eqs. (2) and (3)
– Data not available

environment, it can have both beneficial and deleterious effects in plant and living beings. Sr analogs calcium (Ca) both in its physical and chemical properties and accordingly binds tightly to Ca-sensing receptors and therefore can be accidentally assimilated into the teeth, bones, and seashells in place of calcium [38, 39].

3.2 *Strontium Uptake/Transfer Characteristics in Geomaterials, viz., Soil and Water*

Soil, a complex mixture of a 3-phase system comprising of solid particles (mineral grains, rock fragments) with water and air in the voids between the particles, can be contaminated with ^{90}Sr deposition either from (1) leaching of naturally occurring minerals present in the rock, (2) discharge of waste to land or water, or (3) nuclear fallout or test as illustrated in Fig. 3. The absorption of ^{90}Sr in soil primarily depends on soil characteristics (influencing sorption), organic matter content, rate, and amount of rainfall (influencing desorption). The range of soil solid particles (containing a variable amount of crystalline clay minerals, noncrystalline clay minerals, non-clay minerals, and organic matter) may vary from submicron diameter <2 μm mostly colloids to gravels of diameter 75 mm [40, 41]. Mineralogy of these particles is the prime factor controlling their physical and chemical properties and associated fate and transfer of contaminants in the environment [42]. Pathak et al. [43] and Pathak [44] evaluated that clay with montmorillonite having higher SSA and CEC values of 621 $m^2\ g^{-1}$ and 105.05 meq 100 g^{-1}, respectively, exhibited higher sorption ability of Sr compared with clay containing kaolinite of passive mineralogy. The pathway for faster dispersion of ^{90}Sr in soils is highly dependent on both the soil and contaminant characteristics and the matrix. In addition to size and mineralogy, soil-Sr uptake depends on cation exchange capacity (CEC), organic content (OC) of particles, as well as the ionic strength (IS), liquid-soil solid ratio (L/S), pH of the contaminant fluid [41, 43–47], and matrix characteristics, viz., ion-exchange and fixation mechanisms, leachability, uptake by plants, etc.

Typically partition/distribution coefficient K_d (which demonstrates the sorption characteristics of a radionuclide onto a soil) is employed to model the migration of Sr in the soil and groundwater environments [43, 48]:

$$K_d = \frac{C_I - C_E}{C_E} \times \frac{L}{S} \tag{5}$$

where C_I and C_E are initial and final concentrations of contaminant (in mg L^{-1}) in solution after equilibrium time [25, 42, 48, 49].

The retention of contaminant (sorption) on to the surfaces of the soil solids presides via adsorption, surface precipitation, and polymerization [43, 46, 48]; on the other hand, the behavior of Sr in the aqueous system is governed by sorption process [50]. At alkaline pH 6–8, Sr^{2+} is often readily adsorbed to sediments,

potentially retarding its migration in the environment [42, 43]. Batch sorption studies have reported that below the point of zero charge (PZC) of the soil, i.e., at low pH, the less adsorption of Sr takes place, as compared to the adsorption values above PZC, at higher pH [51, 52]. Experimental studies on competitive adsorption of ^{90}Sr with varying ionic compositions of Ca, Mg, and Na on soil sediments of pure clay phases revealed that Sr adsorption onto the Ca-saturated clay predominantly follows the ion-exchange mechanism [51]. In both inorganic and organic sediments, Sr occurs primarily in outer sphere sorption complexes along with its effective competitors Ca and Mg for adsorption sites [53, 54] of other cations. Similar observations were also predicted by Krouglov et al. [55]; they opined that Sr adsorption mechanism in soil is mainly an ion-exchange reaction and adsorbed Sr could not exist in the fixation fraction. Sr adsorption is observed to be reversible and mainly controlled by cation exchange and shows highest mobility in the soil-water system [43, 44]. Further in addition to clay minerals and organic content/matter, effective absorbents like hydrous metal oxides and primary aluminosilicates [56] affect Sr adsorption by modifying the properties of the regular exchange sites, viz., addition of OC causes a decreases in the distribution coefficient of ^{90}Sr, whereas chemical removal of OC usually leads to an increase in Sr adsorption associated with the clay layers. Ivashkevich and Bondar [57] have found that for soil of OC 0.95–4.64, 44–81% of Sr could be extracted in 2 days and 94% within 5 days under an environment of 1 m KCL, whereas for peat soil having OC $<$ 15, 11–48% of Sr could be extracted in 2–4 days. In inorganic fractions, CEC increases with clay content [58], whereas in the organic fractions, a high CEC originates from existence of specific carbon functional groups [59] carboxylic, phenolic, and enolic. Further, various ligands available in protein groups would complex Sr, thus providing the binding sites necessary for high adsorption. Hence, speciation of Sr is another important factor affecting the availability of Sr for uptake. Again, a large proportion of proteins in organic sediments has been found to originate from the microbial decay of organic matter, and presence of aromatic carbons may be related to Sr desorption from organic substrates. Thus the uptake/transfer of ^{90}Sr sorption by soils is prejudiced by soil characteristics. Thus transport, bioavailability, and fate of ^{90}Sr in the environment are guided by its sorption-desorption processes at interfaces between soil particles and solution. The restriction of movement of ^{90}Sr from the source of contamination can be regulated by resorting to different conventional and contemporary technologies as elucidated in Table 2.

4 Techniques for Remediation

The remediation of radionuclide-contaminated sites (both solid and liquid media sites) has become increasingly important due to its associated radiation hazard. Apart from the site characteristics (soil geochemistry, soil properties), radionuclide concentration (pCi g^{-1}, Bq L^{-1}), half-life of the radionuclide, type of radionuclide

Table 2 Technologies for preventing geomaterial radionuclide contamination

Sl No	Media	Technology	Approach	Process undertaken	Type of waste	Salient feature	Costs
1.	Solid	Containment	Conventional	In situ (capping, vertical barrier), ex situ (encapsulation)	All classes of radioactive waste including Sr	Conventional approach (viz., capping, encapsulation, or solidification/stabilization techniques) does not remove or remediate contaminated media but prevent radionuclide migration. Such techniques can be usually applicable to small areas but often require high capital inputs and are labor and energy intensive. However the major shortcoming associated with such techniques is that the bio-flora and bio-fauna (soil biodynamics) of the site is disturbed/hampered after remediation	4-acre capped site – $10,000 (yearly) [60] 2.4 acre landfill – $53,733 (yearly) [61]
2.		Solidification/ stabilization		In situ or ex situ (cement S/S, chemical S/S)			$150–$512 per cubic yard [62] depending on shallow/deep applications
3.	Solid and liquid	Physical separation	Conventional (physicochemical)	In situ (dry soil separation), ex situ (dry soil separation, soil washing, membrane processes)	Not applicable for Sr	Physicochemical approach which includes chemical processing of the soil to immobilize the metals, ion exchange (95 to 99% removal), precipitation, or flocculation followed by sedimentation is substantially challenging and not likely cost-effective [63, 64]. Some of these listed processes	25 ton per h soil – 3 to $5 million [60]
4.	Liquid	Chemical separation		In situ (permeable reactive barrier), ex situ (ion exchange)	All classes of radioactive waste including Sr		$1,000 per cubic yard [61]

(continued)

Table 2 (continued)

Sl No	Media	Technology	Approach	Process undertaken	Type of waste	Salient feature	Costs
						require pretreatment of the contaminated media and have an adverse effect on soil biological activity and soil structural changes after treatment	
5.	Solid	Vitrification	–	–	Not applicable for Sr	–	$300 to $650 per ton [61]
6.	Liquid	Attenuation	–	In situ (monitored natural attenuation)	Applicable for Sr	Depends on natural processes to attenuate radionuclide and thus requires a long-term monitoring (may be years depending on half-life of the target contaminant)	–
7.	Solid and liquid	Biological treatment	Contemporary	In situ (phytoremediation)	All classes of radioactive waste including Sr	A green remediation technology but limited to shallow depth but very effective for removal (88.7%) of Sr within 24 weeks, in soils For liquid 95% removal of Sr within 10 days Major advantage is the flora and fauna of the site which is not significantly altered after completion of the remediation process	$10,000 to $25,000 per acre [65]

The table mostly focuses on removal technology of strontium from solid (viz., soil, tailings, sediments) to liquid (viz., groundwater and surface water, wastewater, and leachate) medium based on EPA (2007)

(alpha, beta, or gamma emitters), and the selection of a technology for remediation are governed by other factors as the following:

a. Treatment cost economics.
b. The technological effectiveness depends on the previous data available from field studies.
c. Risks associated with the exposure of humans and the environment or proximity of the waste to populations.
d. Availability of resources, i.e., remediation/decontamination process, is selected on the basis of site-specific considerations.
e. Availability, handling, and complexity associated with the level of personal protective equipment required for the decontamination process.
f. Post-remediation(monitoring) activities.

USEPA [60, 62] has identified seven categories of technologies for preventing radionuclide (applicable for low-level, mixed, and commercial radioactive waste) contamination/migration. Table 2 elaborates the key limitations of each of the technologies specifically used for remediation of Sr-contaminated geomaterials (solid, viz., soil, tailings, sediments, and liquid, viz., groundwater and surface water, wastewater, leachate). As identified in Table 2, the financial and technical implication associated with the technologies has made soil remediation an intricate task. The conventional approaches utilized to achieve the goal of remediation have limitations related to skilled labor, high cost, permanent chances in soil micro-macro fauna, and soil geochemistry. In this context, eco-friendly, solar-driven techniques like phytoremediation are adopted as an effective remediation approach worldwide. The term phytoremediation originated from the Ancient Greek word phyto meaning "plant" and the Latin word remedium meaning "restoring balance" [66]. Thus, phytoremediation is a green remediation technology which involves effective use of plants for in situ removal, detoxification, or immobilization of the contaminants present in soil, water, or sediments, by virtue of plants' natural activities and processes [63, 64, 67]. Raskin et al. [63] have also referred to it as botanical bioremediation; which can be applied to remediated both organic and inorganic pollutants present in the soil, water, or air.

Phytoremediation includes different categories of remediation techniques through different parts of the plant body such as the following:

a. *Phytoextraction*: involves the use of plants to remove contaminants from soil/sediments and helps in getting accumulated in the harvestable parts, i.e., roots, stem, and leaves, which can be removed to dispose of or burnt to recover metals.
b. *Phytofiltration:* involves the roots of plants to encapsulate contaminants from soil/wastewater/groundwater. The uses of plant species such as algae, hydrilla, water lens, and pondweed are effectively recorded to reduce the extent of contamination.

c. *Phytostabilization*: in phytostabilization, the plant roots absorb the pollutants from the soil and keep them in the rhizosphere, thus reducing the mobility and bioavailability of the pollution and preventing them from leaching.
d. *Phytovolatilization:* involves the use of plants to volatilize pollutants from their foliage and the transformation of the products into volatile compounds by plant uptaking into its tissues and organs.
e. *Phytodegradation:* plants and associated microorganisms in the plant roots degrade organic pollutants through the process of mineralization [67].

The schematic sketch of phytoremediation for Sr migration and plant uptake in solid medium, i.e., soil (and also applicable to liquid medium), is presented in Fig. 5. It shows the different mechanisms of remediation in each part (from root/shoot/leaves) of the plant. For metal contaminants or radionuclide "like ^{90}Sr," plants showed the potential for uptake and recovery of contaminants into above-ground biomass (*phytoextraction*), filtering metals from water onto root systems (*rhizofiltration*), or stabilizing and evapotranspirating hefty quantities of water (*phytostabilization*). For organic contaminants as well, plants have established that they can contain high concentrations of organic contaminants without displaying toxic effects. The toxic chemicals are converted quickly to less toxic metabolites (*phytofiltration*) [68] or degraded in the rhizosphere (*phytodegradation*). The rhizosphere (soil surrounding the root system) typically is rich in microflora (viz., bacteria, pathogenic fungi, oomycetes, viruses, nematodes, root-feeding arthropods, and other microorganisms) by 1–4 orders of magnitude compared to its adjacent bulk soil. Substances released from plant root system (called root exudates) in drops or small quantities of carbohydrates, organic acids, and vitamins aid to degrade ^{90}Sr [66]. However, this ability to accumulate ^{90}Sr varies significantly with varying plant species (single plant species also have confirmed the ability to involve in two or more categories of phytoremediation), as the mechanism of

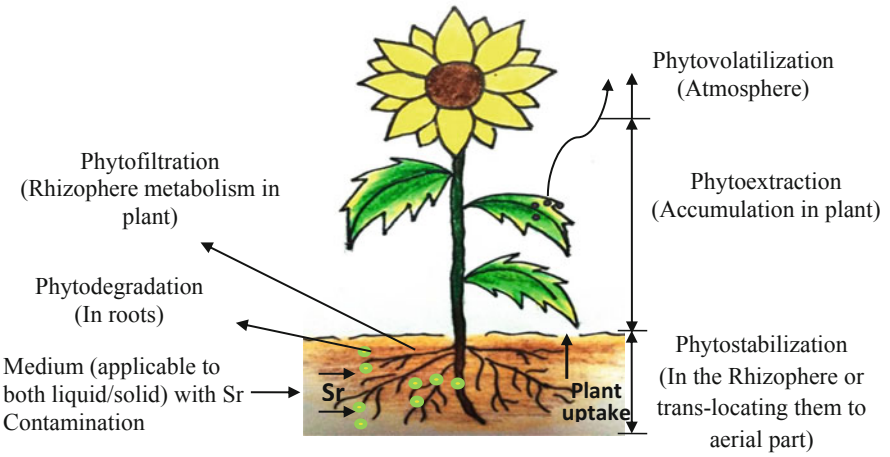

Fig. 5 Schematic sketch showing the unique features and mechanism of phytoremediation

ion uptake in each species is based on their genetic and physiological characteristics. Sasmaz and Sasmaz [24] have utilized three plant species for studying the uptake of ^{90}Sr on shoots, roots corresponding to the soil. They recorded an uptake of 153, 243, and 453 mg kg^{-1} for *Euphorbia macroclada* (EU); 149, 106, and 398 mg kg^{-1} for *Verbascum cheiranthifolium* (VR); and 278, 223, and 469 mg kg^{-1} for *Astragalus gummifer* (AS) with transfer factors varying between 1.18 and 2.08. Li et al. [17] employed *Parthenocissus quinquefolia* and cultured an uptake of 3.92 mg kg^{-1} of ^{90}Sr in the shoots. *Sorghum bicolor (L.) Moench* with a TF of 1.29 recorded an uptake of 193.9, 68.9, and 400 mg kg^{-1} on shoots, roots corresponding to ^{90}Sr content in soil [14].

Depending on the cost-benefit analysis using environmental economics also, it has been observed that phytoremediation techniques have added benefits: (1) energy recovery from rapid growing plants and plants with high biomass, (2) recovery of metals from harvesting and combustion of the plant yield, (3) minimization of risk of migration of contamination, and (4) increasing fertility of soil. With all the advantages of phytoremediation techniques, for high specific activity radionuclide like ^{90}Sr, application of the same is still a challenge due to the presence of very low molar concentration of radionuclide in soil ($\sim 10^{-12}$ mol kg^{-1}) and higher concentration of naturally present stable element, Ca, in soil [69]. Sorption of Sr on bentonite is reported to have decreased in the order of $Ca^{2+} > Mg^{2+} > K^{+} > Na^{2+}$, due to the presence of complementary cations [70]. Similarly, the prospect of phytoextraction of ^{90}Sr gets minimized if sorption of ^{90}Sr takes places in the interspaces of soil clay minerals, which is confirmed to be highly specific and irreversible occurrence [69]. Similar studies for ^{137}Cs reported that soil clay minerals immobilize the migration of ^{137}Cs through the geo-environment, thus significantly reducing the extent of bioavailability for plant uptake. However, availability of passive mineralogy, viz., non-clay minerals, is reported to have assisted in higher uptake of both ^{90}Sr and ^{137}Cs in plants [69, 71].

4.1 Selection of Plant Species

As discussed in the previous section, different plant species show a different pattern of uptake of the contaminant from a soil/liquid medium [72]. The survival strategy as identified by Baker and Walker [73] stated that plant cannot refrain itself from metal uptake but can restrict it and accumulate in the plant tissues at varying degrees. Depending on the strategies adopted by the plants for growth and survival on metal-contaminated medium, Baker and Walker [73] have categorized plants into three groups, namely, *metal excluders*, *indicators and accumulators*, *or hyperaccumulators.* The accumulators and excluders are the extremes of physiological, cellular, and biochemical response of plants surviving on metal-contaminated medium [74–76]. Plant excluders limit the level of contamination translocation within shoot and roots, thereby maintaining lower concentration in shoots as compared to its roots, whereas plant accumulators (hyperaccumulators) concentrate the contaminant in aboveground tissues to a high concentration than that existing

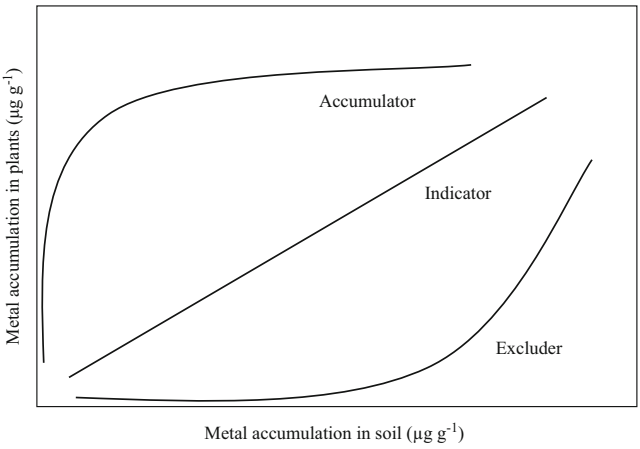

Fig. 6 Pattern of contaminant uptake by of aerial parts

in the soil. Thus hyperaccumulators are widely used in phytoremediation. The pattern of specific contaminant uptake for all the three categories of plant species is shown in Fig. 6.

Determination of hyperaccumulator and excluder plant species is based on strict criteria.

For a plant to be classified as hyperaccumulator [72, 77], the following mathematical model is utilized as shown below:

$$\frac{\text{Amount of contamination in shoot}}{\text{Amount of contamination in root}} > 1 \tag{6}$$

$$\frac{\text{Amount of contamination in shoot}}{\text{Amount of contamination in soil}} > 1 \tag{7}$$

whereas for a plant to be classified as excluders ideally [78, 79], the subsequent mathematical model is employed:

$$\frac{\text{Amount of contamination in shoot}}{\text{Amount of contamination in root}} < 1 \tag{8}$$

For a plant to be classified as an indicator, levels of heavy metals in the tissues are similar to those in the surrounding contaminated environment [73, 79]. Hyperaccumulator (with 37.4–78.1% radionuclide absorbing rate) can modify the uptake of the contaminant in plant shoot than in plant root. Kalacska et al. [80] employed hyperaccumulator like sunflower and *Cannabis* for absorbing >95% of cesium and strontium in a span of 30 days. However, as pointed out in Sect. 3.1, transfer factor (TF_p) becomes an essential preliminary information for identification of the plant species, which can be a trigger to modify its removal capabilities by resorting to different breeding techniques.

5 Conclusions

Radioactive strontium, ^{90}Sr, exposure in the environment is mainly due to man-initiated nuclear chain reaction. Though the quantity of ^{90}Sr in the environment is much lower than that of stable strontium, due to the long half-life of 28.9 years, ^{90}Sr can reside in the environment for around three decades; thus routine radiation monitoring in environmental samples, viz., soil, water, air, and plants, is necessary. ^{90}Sr is responsible for long-term internal and external radiation hazard via food chain due to ingestion of foodstuff cultivated on contaminated agricultural field and bioaccumulation in aquatic organisms. The accumulation of ^{90}Sr to surface water and groundwater has been recognized to be leaching of contaminant-coated soil and rocks. The uptake of ^{90}Sr into plants from soil and water is strongly influenced by the chemical characteristics of contaminated medium-plant zone. The transfer factors demonstrated that accumulation of ^{90}Sr is primarily on the edible leafy parts of the plant body, and in case of animal milk, the uptake of ^{90}Sr can be reduced significantly by increasing the dietary calcium intake of the ruminants. For soil, the mobility of ^{90}Sr is retarded by the strong interaction with clay mineralogy, soil organic materials, CEC of the soil solids, and pH of the pore fluid. Studies also revealed that ^{90}Sr in contaminated sediments remains primarily weak in bound surface complexes; thus with the increase in groundwater ionic strength, substantial remobilization of ^{90}Sr might be expected. Further, for environmental management of ^{90}Sr, the technique of application of plant species proved to be beneficial. In addition to plant species selection, the potential of a plant to be used in phytoremediation has been demonstrated to be dependent on the (a) concentration of a target element of the contaminated site, (b) speciation and pH of contamination, (c) plant age (the younger the plant, the more the uptake), and (d) ecology around plant shoot to root. Additionally, phytoremediation can be utilized as one of suitable and recognized treatment methods for treating a wide range of anthropogenic pollutions in addition to ^{90}Sr depending on applicability, economic feasibility, and efficiency of the method.

References

1. NISA (Nuclear and Industrial Safety Agency) (2011) About the evaluation of the state of reactor core of No. 1, 2 and 3 concerning the accident of the Tokyo Electric Power, Fukushima Daiichi Nuclear Power Plant
2. Kamei-Ishikawa N, Ito A, Umita T (2013) Fate of stable strontium in the sewage treatment process as an analog for radiostrontium released by nuclear accidents. J Hazard Mater 260:420–424
3. Ramirez-Guinart O, Vidal M, Rigol A (2016) Univariate and multivariate analysis to elucidate the soil properties governing americium sorption in soils. Geoderma 269:19–26
4. Musilli S, Nicolas N, El Ali Z, Orellana-Moreno P, Grand C, Tack K, Kerdine-Römer S, Bertho JM (2017) DNA damage induced by Strontium-90 exposure at low concentrations in mesenchymal stromal cells: the functional consequences. Sci Rep 7:41580

5. UNSCEAR (United Nations Scientific Committee on the Effects of Atomic Radiation) (1982) Ionizing radiation: sources and biological effects. UNIPUB No. E.82.IX.8, 06300P, New York
6. UNSCEAR (United Nations Scientific Committee on the Effects of Atomic Radiation) (2000) Sources and effects of effects ionizing radiation: UNIPUB No. E.82.IX.8, 06300P, New York
7. Faure G, Powell JL (1972) Strontium isotope geology. Springer, Berlin
8. Ondov JM, Choquette CE, Zoller WH, Gordon GE, Blermann AH, Hef RE (1989) Atmospheric behavior of trace elements on particles emitted from a coal-fired power plant. Atmos Environ 23:2193–2204
9. Furr AK, Parkinson TF, Hinrichs RA, Van Campen DR, Bache CA, Gutenmann WH, St John Jr LE, Pakkala IS, Lisk DJ (1977) National survey of elements and radioactivity in fly ashes: absorption of elements by cabbage grown in fly-ash soil mixtures. Environ Sci Technol 11:1194–1201
10. Raven KP, Loeppert RH (1997) Heavy metal in the environment; trace element composition of fertilizers and soil amendments. J Environ Qual 26:551–557
11. Jolly YN, Islam A, Akbar S (2013) Transfer of metals from soil to vegetables and possible health risk assessment. Springer-Plus 2:385–393
12. Sarap NB, Janković MM, Dolijanović ŽK, Kovačević DĐ, Rajačić MM, Nikolić JD, Todorović DJ (2015) Soil-to-plant transfer factor for ^{90}Sr and ^{137}Cs. J Radioanal Nucl Chem 303:2523–2527
13. Veresoglou DS, Tsialtas T, Barbayiannis N, Zalidis GC (1995) Caesium and strontium uptake by two pasture plant species grown in organic and inorganic soils. Agric Ecosyst Environ 56:37–42
14. Wang X, Chen C, Wang J (2017) Phytoremediation of strontium contaminated soil by *Sorghum bicolor* (L.) Moench and soil microbial community-level physiological profiles (CLPPs). Environ Sci Pollut Res Int 24:7668–7678
15. Zhuang P, McBride MB, Xia H, Li N, Li Z (2009) Health risk from heavy metals via consumption of food crops in the vicinity of Dabaoshan mine, South China. Sci Total Environ 407:1551–1561
16. Casadesus J, Sauras-Yera T, Vallejo VR (2008) Predicting soil-to-plant transfer of radionuclides with a mechanistic model (BioRUR). J Environ Radioact 99:864–871
17. Li GY, Hu N, Ding DX, Zheng JF, Liu YL, Wang YD, Nie XQ (2011) Screening of plant species for phytoremediation of uranium, thorium, barium, nickel, strontium and lead contaminated soils from a uranium mill tailings repository in South China. Bull Environ Contam Toxicol 86:646–652
18. Velasco H, Ayub JJ, Sansone U (2009) Influence of crop types and soil properties on radionuclide soil-to-plant transfer factors in tropical and subtropical environments. J Environ Radioact 100:733–738
19. IAEA (International Atomic Energy Agency) (2010) Handbook of parameter values for the prediction of radionuclide transfer in terrestrial and freshwater environment. Technical reports series no. 472, Vienna
20. Wang CJ, Wang JJ, Chiu CY, Lai SY, Lin YM (2000) Transfer factors of 90Sr from soil to the sweet potato collected in Taiwan. J Environ Radioact 47:15–27
21. Narayana Y, Somashekarappa HM, Karunakara N, Avadhani DN, Mahesh HM, Siddappa K (2000) Prominent artificial radionuclide activity in the environment of coastal Karnataka on the southwest coast of India. J Radiol Prot 20:295–313
22. Sarap NB, Jankoviać MM, Pantelić GK (2014) Validation of radiochemical method for the determination of 90Sr in environmental samples. Water Air Soil Pollut 225:1–12
23. Askbrant S, Melin J, Sandalls J, Rauret G, Vallejo R, Hinton T, Cremers A, Vandecastelle C, Lewyckyj N, Ivanov YA, Firsakova SK, Arkhipov NP, Alexakhin R (1998) Mobility of radionuclides in undisturbed and cultivated soils in Ukraine, Belarus and Russia six years after the Chernobyl fallout. J Environ Radioact 31:287–312
24. Sasmaz A, Sasmaz M (2009) The phytoremediation potential for strontium of indigenous plants growing in a mining area. Environ Exp Bot 67:139–144

25. Wang XS (2011) Batch sorption of lead (II) from aqueous solutions using natural kaolinite. Int J Environ Waste Manag 8:258–272
26. IAEA (International Atomic Energy Agency) (1994) Handbook of transfer parameter values for the prediction of radionuclide transfer in temperate environments. Technical reports series no. 364, IAEA, Vienna
27. Robison WL, Conrado CL, Hamilton TF, Stoker AC (2000) The effect of carbonate soil on transport and dose estimates for long-lived radionuclides at a U.S. Pacific Test Site. J Radioanal Nucl Chem 24:459–465
28. Lembrechts JF, Van Ginkel JH, Desmet G (1990) Comparative study on the uptake of ^{85}Sr from nutrient solutions and potted soils by lettuce. Plant Soil 125:63–69
29. Ward GM, Johnson JE (1965) The caesium-137 content of beef from dairy and feed lot cattle. Health Phys 11:95–100
30. Ward GM, Johnson JE (1986) Validity of the term transfer coefficient. Health Phys 50:411–414
31. Coughtrey PJ (1990) Radioactivity transfer to animal products (EUR 12608 EN). Commission of the European Communities, Luxembourg 22(3)
32. Howard BJ, Beresford NA, Mayes RW, Hansen HS, Crout NMJ, Hove K (1997) The use of dietary calcium intake of dairy ruminants to predict the transfer coefficient of radiostrontium to milk. Radiat Environ Biophys 36:39–43
33. Howard BJ, Beresford NA, Barnett CL, Fesenko S (2009) Radionuclide transfer to animal products: revised recommended transfer coefficient values. J Environ Radioact 100:263–273
34. Calmon P, Thiry Y, Zibold G, Rantavaara A, Fesenko S (2009) Transfer parameter values in temperate forest ecosystems: a review. J Environ Radioact 100:757–766
35. Brown J, Simmonds JR (1995) Farmland: a dynamic model for the transfer of radionuclides through terrestrial food chains. National Radiological Protection Board (NRPB-R273), International Nuclear Information System 26(24)
36. Russell RS (1966) Radioactive strontium in food chains: general review. In: Russell RS (ed) Radioactivity and human diet. Pergamon Press, Oxford, pp 173–186
37. Sirotkin AN (1978) Sr-90 excretion in milk of cows with different levels of calcium concentration and sources of calcium in ration. Agric Biol 13:234–237
38. O'Hara MJ, Burge SR, Grate JW (2009) Automated radioanalytical system for the determination of Sr-90 in environmental water samples by Y-90 Cherenkov radiation counting. Anal Chem 81:1228–1237
39. Pors NS (2004) The biological role of strontium. Bone 35:583–588
40. Pathak P, Sharma S (2018) Sorption isotherms, kinetics, and thermodynamics of contaminants in Indian soils. J Environ Health Sci Eng 144:04018109
41. Sharma S, Meenu PS, Latha RA, Shashank BS, Singh DN (2016) Characterization of sediments from the sewage disposal lagoons for sustainable development. Adv Civil Eng Mater 5:1–23
42. Choi S, O'Day PA, Rivera NA, Mueller KT, Vairavamurthy MA, Seraphin S, Chorover J (2006) Strontium speciation during reaction of kaolinite with simulated tank-waste leachate: bulk and microfocused EXAFS analysis. Environ Sci Technol 40:2608–2614
43. Pathak P, Singh DN, Pandit GG, Rakesh RR (2014) Determination of distribution coefficient: a critical review. Int J Environ Waste Manag 14:27–64
44. Pathak P (2017) An assessment of strontium sorption onto bentonite buffer material in waste repository. Environ Sci Polut Res 24:8825–8836
45. Guimaraes V, Azenha M, Rocha F, Silva F, Bobos I (2015) Influence of pH, concentration and ionic strength during batch and flow-through continuous stirred reactor experiments of Sr^{2+}-adsorption onto montmorillonite. J Radioanal Nucl Chem 303:2243–2255
46. Naidu R, Bolan NS, Kookana RS, Tiller KG (1994) Ionic strength and pH effects on the sorption of the cadmium and the surface charge of soils. Eur J Soil Sci 45:419–429
47. Naidu AD, Rao BH, Shanthakumar S, Singh DN (2010) Determination of distribution coefficient of geomaterials and immobilizing agents. Can Geotech J 47:1139–1148
48. Bell J, Bates TH (1988) Distribution coefficient of radionuclides between soils and ground water and their dependence on various test parameter. Sci Total Environ 69:297–317

49. Celis R, Real M, Hermosin MC, Cornejo J (2005) Sorption and leaching behavior of polar aromatic acids in agricultural soils by batch and column leaching tests. Eur J Soil Sci 56:287–297
50. Sellafield (2008) Land quality programme groundwater monitoring annual report. Sellafield. http://www.sellafieldsites.com/land/pages/groundwater_monitoring.html
51. Marinin DV, Brown GN (2000) Studies of sorbent/ion-exchange materials for the removal of radioactive strontium from liquid radioactive waste and high hardness ground waters. Waste Manag 20:545–553
52. Sposito G (1989) The chemistry of soils. Oxford University Press, New York
53. Ahmad SHSS (1995) Competitive adsorption of ^{90}Sr on soil sediments, pure clay phases and feldspar minerals. Appl Radiat Isot 46:287–292
54. Wallace SH, Shaw S, Morris K, Small JS, Fuller AJ, Burke IT (2012) Effect of groundwater pH and ionic strength on strontium sorption in aquifer sediments: implications for 90Sr mobility at contaminated nuclear sites. Appl Geochem 27:1482–1491
55. Krouglov SV, Kurinov AD, Alexakhin RM (1998) Chemical fraction of ^{90}Sr, ^{106}Ru, ^{137}Cs and ^{144}Cs in Chernobyl-contaminated soils: an evolution in the course of time. J Environ Radioact 38:59–76
56. Brady NC (1990) The nature and properties of soils. Macmillan Publishing Company, New York
57. Ivashkevich LS, Bondar YI (2006) Effect of basic chemical characteristics of soils on mobility of radionuclides in them. Radiochemistry 50:98–102
58. Helling CS, Chesters G, Corey RB (1964) Contribution of organic matter and clay to soil cation-exchange capacity as affected by the pH of the saturating solution. Soil Sci 28:517–520
59. Broadbent FE, Bradford GR (1952) Cation-exchange groupings in the soil organic fraction. Soil Sci 74:447–458
60. US EPA (United Nations Environmental Protection Agency) (1998) Innovative site remediation technology, design & application. EPA/542/B-97/006, Liquid Extraction Technologies
61. FRTR (Federal Remediation Technologies Roundtable) (2004) Technology cost and performance, cap at DOE's. Lawrence Livermore National Laboratory, Landfill
62. US EPA (United Nations Environmental Protection Agency) (1995) Contaminants and remedial options at selected metal contaminated sites. EPA/540/R-95/512
63. Raskin I, Smith RD, Salt DE (1997) Phytoremediation of metals: using plants to remove pollutants from the environment. Curr Opin Biotechnol 8:221–226
64. McGrath SP, Zhao FJ, Lombi E (2001) Plant and rhizosphere process involved in phytoremediation of metal-contaminated soils. Plant Soil 232:207–214
65. Schnoor JL (2002) Phytoremediation of soil and groundwater. Technology evaluation report TE-02-01, Prepared for the Ground-Water Remediation Technologies Analysis Center
66. Cunningham SD, Anderson TA, Schwab PA, Hsu FC (1996) Phytoremediation of soils contaminated with organic pollutants. Adv Agron 56:55–114
67. Garbisu C, Alkorta I (2001) Phytoextraction: a cost effective plant-based technology for the removal of metals from the environment. Bioresour Technol 77:229–236
68. Schnoor JL (1997) Phytoremediation-technology evaluation report. The University of Iowa Department of Civil and Environmental Engineering and Center for Global and Regional Environmental Research Iowa City, Iowa for Ground-Water Remediation Technologies Analysis Center, Pittsburgh
69. Fuhrmann M, Lasat MM, Ebbs SD, Kochian LV, Cornish J (2002) Plant and environment interactions uptake of Cesium-137 and Strontium-90 from contaminated soil by three plant species; application to phytoremediation. J Environ Qual 31:904–909
70. Khan SA, Riaz-ur-Rehman, Khan MA (1995) Sorption of strontium on bentonite. Waste Manag 15:641–650
71. Lasat MM, Fuhrmann M, Ebbs S, Cornish J, Kochian L (1998) Phytoremediation of a radiocesium-contaminated soil: evaluation of cesium-137 bioaccumulation in the shoots of three plant species. J Environ Qual 27:165–169

72. Rotkittikhun R, Kruatrachue M, Chaiyarat R, Ngernsansaruay C, Pokethitiyook P, Paijitprapaporn A, Baker AJM (2006) Uptake and accumulation of lead by plants from the Bo Ngam lead mine area in Thailand. Environ Pollut 144:681–688
73. Baker AJM, Walker PL (1990) Ecophysiology of metal uptake by tolerant plants: heavy metal tolerance in plants. In: Shaw AJ (ed) Evolutionary aspects. CRC Press, Boca Raton, pp 155–177
74. Ernst WHO (1975) Physiology of heavy metal resistance in plants, vol 2. In: Proceeding of international conference on heavy metals in the environment. Toronto, Canada, pp 121–213
75. Ernst WHO, Verkleij JAC, Schat H (1992) Metal tolerance in plants. Acta Bota Neerland 41:229–248
76. Turner RG (1969) Heavy metal tolerance in plants. In: Rorison IH (ed) Ecological aspects of the mineral nutrition of plants. British ecological society symposium, vol 9. Blackwell Scientific Publications, Hoboken, pp 399–410
77. Harrison RM, Chirgawi MB (1989) The assessment of air and soil as contributors of some trace metals to vegetable plants: use of a filtered air growth cabinet. Sci Total Environ 83:13–34
78. Boularbah A, Schwartz C, Bitton G, Aboudrar W, Ouhammou A, Morel JL (2006) Heavy metal contamination from mining sites in South Morocco: assessment of metal accumulation and toxicity in plants. Chemosphere 63:811–817
79. Mganga N, Manoko MLK, Rulangaranga ZK (2011) Classification of plants according to their heavy metal content around North Mara gold mine, Tanzania: implication for phytoremediation. Tanz J Sci 37:109–119
80. Kalacska M, Arroyo-Mora P, Snirer E, Parent R (2011) A review of cannabis properties and experiments for its biological control. World wide weed: global trends in Cannabis cultivation and its control. Ashgate Publishing, Aldershot, pp 215–224

Spatial Distribution of ^{90}Sr in the Ecosystems of Polesye State Radiation-Ecological Reserve

Sergey A. Kalinichenko, Aleksander N. Nikitin, Ihar A. Cheshyk, and Olga A. Shurankova

Contents

Abstract In this chapter, activity concentration of ^{90}Sr in the soil and plants from different types of ecosystems in the Belarussian sector of the exclusion zone of Chernobyl NPP after three decades of accident is shown. Lateral migration of ^{90}Sr and variability of its activity in the topsoil in different forest types are discussed here. Influence of soil properties and peculiarities of species in plant communities on the accumulation of the radioisotope in the main compartments of ecosystems is presented. The obtained results may be actuals for designing of mathematical landscape models intended for the forecast of space-time redistribution of radioisotopes after emergency emissions. The authors proved that soil litter is an integral indicator of affinity the living parts of an ecosystem regarding the radioisotope.

Keywords Contamination · Horizontal distribution · Soil · Strontium-90

S. A. Kalinichenko
Department of Radiation and Ecological Monitoring, State Environmental Research Institution, Polesye State Radiation-Ecological Reserve, Khoiniki, Belarus

A. N. Nikitin (✉) · I. A. Cheshyk · O. A. Shurankova
Laboratory of Radioecology, State Scientific Institution, Institute of Radiobiology of the National Academy of Sciences of Belarus, Gomel, Belarus
e-mail: nikitinale@gmail.com

P. Pathak, D. K. Gupta (eds.), *Strontium Contamination in the Environment*,
The Handbook of Environmental Chemistry 88,
https://doi.org/10.1007/978-3-030-15314-4_7

1 Introduction

Now, the radioecological situation in the exclusion zone of the Chernobyl NPP is primarily determined not by the levels and the amounts of radioactive isotopes deposed with aerosols and fuel particles at the acute stage of the accident but by weather, climate, and landscape conditions that control the biotic and abiotic migration of radioisotopes. The formation of spatial contamination of the soil surface in the most contaminated part of the zone of the Chernobyl accident is a dynamic process that can significantly change the situation after many decades from the moment of radioactive fallout. Such changes depend on biological and non-biological factors: weather, landscape differentiation, succession in plants communities, anthropogenic impact, bioturbation [1–4].

Until recently, spatial and temporal patterns of landscape differentiation of man-made radioisotopes have not been sufficiently studied both because of methodological difficulties and because of their variability at different scale levels. According to the Russian researcher [4], the study of the landscape differentiation of man-made radioisotopes remains relevant for the organization of radiation monitoring and planning of rehabilitation measures in contaminated areas. Landscape analysis and assessment of the distribution of radioisotopes are essential elements of the radiation safety system aimed to improving the radioecological situation. The type and degree of development of forest canopy are important factors for this kind of investigation. The specificity of the redistribution of radioisotopes will vary significantly, depending on the type of the soil top organogenic layer, where both the fast decaying litter of deciduous forest and the thick multilayered litter of pine forest can act as a dead organic material. The spatial redistribution of radioisotopes on the surface of the areas lacking forest canopy (meadows, former arable areas, drylands) has other peculiarities.

There is a high degree of heterogeneity of radioactive substances exploded from the reactor, radioisotope composition and physicochemical forms, their migration in environment media, and spatial distribution in the contaminated area [2]. This is specific characteristic of the post-accidental situation on the territories with high density of radioisotopes deposition. In the initial period after the accident, soil contamination with radioisotopes in the exclusion zone is characterized by high levels of the coefficient of variation (CV=60% and higher) [3]. The values of *CV* should be much lower now according to many researchers [1, 5, 6].

The distribution of radioisotope stocks between different components of ecosystems in the conditions of the exclusion zone formed after the Chernobyl accident has its peculiarities. One of the most potent factors is the forest-growing conditions that influence the accumulation of radioisotopes in the biota compartments, in the forest litter, and the mineral part of the soil. Significant differences are typical for forest ecosystems and meadow ecosystems, where the behaviour of elements of mineral nutrition and radioactive isotopes can have sharp differences. The processes of biogenic migration and the accumulation of organic matter in each case also occur

in different ways. The species composition, landscape conditions, and geochemical cycles occurring in ecosystems play a significant role here. All these factors significantly influence the spatial distribution of radioisotopes, their vertical and lateral migration.

Studies on the spatial migration of radioisotopes were carried out by some scientific teams, both in Belarus and abroad. According to [7], dissolved in soil water radioisotopes move along the alluvial layer in summer and along the edges of frozen soil in the winter in conjugated landscapes of forest ecosystems. Thus, the content of radioisotopes in the top parts of the alluvial landscapes decreases and they accumulate in geochemical barriers. These processes affect the accumulation and redistribution of radioisotopes by compartments of the whole ecosystem. Similar data were obtained by other scientists [1–4, 8–13]. These studies are inseparably linked with the activity of the whole ecosystems, as a single system, where a change in one compartment can lead to a change in the life activity of the whole community, down to its succession shift.

The distribution of radioisotopes by ecosystem compartments is undoubtedly a matter of scientific interest, allowing to establish the patterns of ecosystem transformation in the zone of radioactive contamination and to pinpoint the most vulnerable links subject to the most significant radiation press. Ideal, in this case, would be the creation of some dynamic balance model, which allows predicting the direction of the biocenotic processes taking into account the radiation factor. To carry out such tasks in full-scale conditions is quite tricky, although attempts are being made by various researchers. However, each new factor introduced into the system only increases the error, up to uncertainty. Our investigations touch on only some aspects that can later help in solving data relevant from a scientific and practical point of view.

The purpose of the research was assessing horizontal heterogeneity of soil contamination with ^{90}Sr 30 years after its deposition due to accident on Chernobyl NPP and revealing the main factors impact on the distribution of ecosystems contamination.

The objectives were:

- To investigate heterogeneity of soil contamination with ^{90}Sr on sampling plots 100 × 100 m in different types of ecosystems
- To research the distribution of ^{90}Sr in main compartments of the ecosystems in comparison with ^{137}Cs and ^{241}Am
- To reveal the main factors that impact on peculiarities of ^{90}Sr spatial distribution in ecosystems in the long-term period of the consequences of Chernobyl accident

2 Materials and Methods

The investigations were carried out in the Belarusian sector of the Chernobyl Exclusion Zone on the territory of the Polesye State Radiation-Ecological Reserve (PSRER). We studied the features of the horizontal distribution of ^{90}Sr in the soil of

ecosystems with different forest-growing conditions in the years 2011–2015. The investigations were carried out on the territory of a hydromorphic mixed deciduous forest (birch forest), the former farmland with an automorphic type of soil (former farmland), and in a pine forest with a low level of soil water (pine forest). All three experimental plots are located in the 10–15 km distance from the ChNPP close to the research station "Masany". To determine the range of variation of the radioisotope content in the soil, the Pearson's coefficient of variation (CV) was determined:

$$\mathrm{CV} = 100\% \cdot S_x/x,$$

where S_x is the standard deviation in the sample and x is the arithmetic mean of the sum of partial or group averages.

The soil-to-plant (soil-to-litter) aggregated transfer factors (T_{ag}) were determined by:

$$T_{\mathrm{ag}} = A_{\mathrm{b}}/A_{\mathrm{s20}},$$

where A_{b} is the activity concentration of the radioisotope in the biological sample or litter, Bq/kg, and A_{s20} surface contamination density of soil by the radioisotope for the upper 20 cm soil layer, kBq/m^2.

The size of the primary sampling plots was 100 × 100 m. Method of nested squares was used for studying the spatial heterogeneity of radioactive fallout. Mixed soil samples were sampled within small sites with size 10 × 10 m situated within the primary sampling plots. Standard sampler with a diameter of 4 cm and a depth of 20 cm was used for sampling soil. At the same time, measurements of the dose rate of gamma radiation (MD) at the height of 1 m and 3–4 cm from the soil surface were carried out using a dosimeter-radiometer MKS(EL)-1117A. An investigation of the ^{90}Sr in the litter horizon on experimental sites was carried out using the method of intersecting transects.

Transfer factors of ^{90}Sr were determined at the same sites for dominant plant species. Thus, transfer of the radioisotope in the grasses and foliage of birch was estimated for the former farmland; needles or leaves, as well as under-canopy-dominant plants, were investigated in the forest ecosystems.

Soil sampling was carried out at the time of dry weather conditions in the spring period before the starting of grasses growth. Mixed soil samples, consisting of five cores, as well as litter layer, grasses, needles, and leaves, were packed in polyethylene bags, logged, and transferred for laboratory processing.

The samples of the litter and plants were dried at a temperature of 20–25°C under laboratory conditions. Species identification was made at this time. At the end of the sample preparation, they were homogenized and placed in the containers for the measurements of the radioisotope activity concentration. Activity concentration of ^{90}Sr, ^{137}Cs, and ^{241}Am was performed in the Laboratory of Spectrometry and Radiochemistry of PSRER using standard methods.

Statistical processing of the results was carried out using standard biometric methods using packages Pandas, NumPy, SciPy, and Matplotlib (Python).

2.1 Description of Experimental Objects

Birch (*Betula pendula* Roth) was dominant in the mixed deciduous forest (sampling plot "birch forest") situated in the Radinskoye forest area. *Alnus glutinosa* (L.) Gaertn., *Frangula alnus* (Mill.), and *Quercus robur* (L.) also grow here. The soil is a hydromorphic type. The under-canopy layer was populated with *Elytrigia repens* (L.) Nevski, *Calamagrostis arundinacea* (L.) Roth, *Carex sylvatica* (Huds.), and *Deschampsia cespitosa* (L.) Beauv. The soil is sod-podzolic, with an average density of 0.70 g/cm^3, which indicates a significant proportion of the organic part. In the central part of the site, there was a fringe (open place) stretched from west to east. This type of ecosystem is typical and widespread for the territory of the PSRER and in the Belarusian Polesye in general.

The average height of the sample plot above sea level is 112.3 m. Geographical coordinates of the corner points of the plot are presented in Table 1.

The next sampling plot locates on the lands of the former farmland. The soil is sod-podzolic with an average density of 1.47 g/cm^3. The processes of natural regeneration are beginning, and single plants of pine undergrowth are found in the southern part of the site, closer to the Ukrainian border. There are several surviving plants of fruit trees and raspberries along the southern boundary of the plot. This type of ecosystem is typical and widespread for the territory of the reserve and in the Belarusian Polesye in general. The average height of the sample plot above sea level is 112.3 m.

The plant composition on this sample plot is very diverse; among many other species, we found representatives of *Poaceae*, *Fabaceae*, *Polygonaceae*, *Asteraceae*, *Ranunculaceae*, and other plant families. The dominant species of herbaceous plants are *Elytrigia repens* (L.) *Nevski*, *Bromopsis inermis* (Leys.) *Holub*, *Agrostis canina* L., *Rumex acetosa* L., *Melandrium album* (Mill.) *Garcke.*,

Table 1 Coordinates of the corners of sampling plots

Sampling plot	SW[a]	NW	NE	SE
Birch forest	51°30.638′ N	51°30.691′ N	51°30.668′ N	51°30.619′ N
	30°01.460′ E	30°01.497′ E	30°01.576′ E	30°01.548′ E
Former farmland	51°30′20.8″ N	51°30′23.9″ N	51°30′22.8″ N	51°30′19.6″ N
	30°01′21.0″ E	30°01′22.7″ E	30°01′27.8″ E	30°01′26.0″ E
Pine forest	51.514480° N	51.515177° N	51.514378° N	51.513814° N
	30.017025° E	30.018157° E	30.018892° E	30.017631° E

[a]SW, NW, NE, and SE are southwest, northwest, northeast, and southeast corners of sampling plot correspondingly

Equisetum arvense L., *Viola arvensis* Murr., *Ranunculus acris* L., and *Veronica chamaedrys* L.

Third sampling plot is situated in a pine forest (*Pinus sylvestris* L.) with an automorphic type of soil and low groundwater level. The soil is sod-podzolic with an average density of 1.62 g/cm^3. The south-western part of the site has a slight increase in altitude – the height difference is 11 m. The western corner of the plot is a slope of a ravine, where groundwaters protrude to the surface and oak seedlings growing in the under-canopy layer. This type of ecosystem is typical and widespread for the territory of the PSRER and in the Belarusian Polesye in general. The average height of the sample plot above sea level is 156.5 m.

The plant composition of the ecosystem is characteristic for the *Pinetum pleurozium* association. *Pleurozium Schreberi* Brid. and *Hypogymnia physodes* (L.) Nyl. dominated in the under-canopy plants' tier. There are rare *Viola arvensis* Murr., *Asarum europaeum* L., *Lupinus polyphyllus* Lindl., *Poa nemoralis* L., and *Corynephorus canescens* L. P. Beauv growth here. There is undergrowth consisted of *Betula pendula* Roth and *Quercus robur* L. at the south-western boundary of the plot.

3 Lateral Migration ^{90}Sr in the Surface Layer of Soil

The condensation-fuel type of radioactive precipitation is typical for radioisotope contamination for investigated experimental plots, as well as for the entire 30 km zone of the Chernobyl NPP. The behaviour of radioisotopes represented by the condensation component of deposition is similar to the behaviour of radioisotopes of global deposition. The radiological significance of highly reactive fuel particles largely depends on the density of their deposition, dispersity, and degree of physical and chemical stability of the matrix (degradation) in real soil-climatic conditions. However, in both cases, the process of lateral redistribution of radioisotopes in the microrelief will occur in different ways. It is due both to the differences in biogenic migration and to the physicochemical properties of the elements themselves. The changes in both of these properties are determined by many factors, among which we consider the most determinant, both for the initial period of deposition and for the remote period of time: the type of forest canopy or its absence and the water regime of the top layers of the soil. The factors will later reveal differences in the processes of spatial migration and the formation of heterogeneity in the distribution of radioisotopes in various ecosystems.

The analysis of measurements shows the ^{90}Sr content in soil has a maximum level in the plot "birch forest" equal to 3,908.3 kBq/m^2. Horizontal redistribution of ^{90}Sr in the upper 20 cm layer of soil had not a significant heterogeneity. However, areas with a higher activity of ^{90}Sr are mostly localized, and levels of their contamination have a more significant difference compared to the average value (Fig. 1).

The coefficient of variation of soil surface contamination by ^{90}Sr for the sampling plot "birch forest" was 48.3%, which characterizes its more local character of spatial

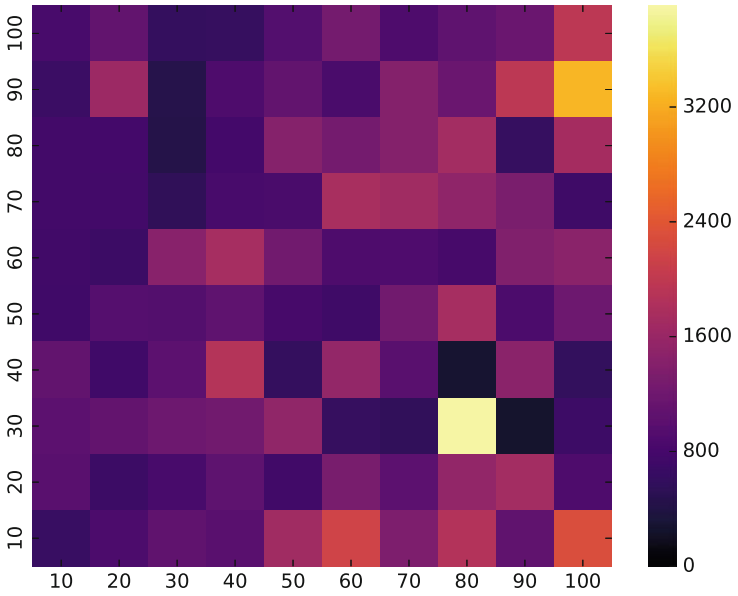

Fig. 1 Lateral distribution of ^{90}Sr in the birch forest (kBq/m^2)

distribution. As can be seen from the projection of the pollution density with ^{90}Sr on the sampling plot, the sites with the highest levels of the radioisotope activity immediately adjoin the area where its content is 15 times lower. This circumstance is most likely due to the presence of this radioisotope as part of the fuel particle matrix in the near zone of the Chernobyl accident. According to Ukrainian researchers, 95 $\pm$ 5% of ^{90}Sr in the near zone of the Chernobyl accident initially was in the fuel component of the Chernobyl radioactive fallout [9].

The nature of the fluctuations in the content of ^{90}Sr on the territory of the experimental plot is also influenced by the processes of initial precipitation of aerosols onto the surface with subsequent redistribution of radioisotopes. It is natural to assume that at the initial period of the accident the maximum precipitation was characteristic for the soil surface areas that were not covered by the forest. However, this does not mean a static scenario for further changes in the radioecological situation, when the most significant influence is exerted exclusively by physical decay. In many cases, the heterogeneity of the microrelief, the type and properties of the soil, the activity of living organisms, and lateral migration can significantly alter the radiation situation. In this connection, there is a high probability that in the remote period of the accident the hydromorphic sites of the areas covered with woody vegetation may contain the most substantial content of the man-made radioisotopes, which does not manifest itself in any way, until the water regime changes.

The analysis of measurements shows the ^{90}Sr content in soil has a maximum level in the plot “former farmland” equal to 4,550.9 kBq/m^2. The nature of the ^{90}Sr

distribution in this sampling plot mainly relates to the processes of the initial deposition of aerosols onto the surface, followed by the redistribution of radioactivity involving biota and weather-climatic factors.

At the time of radioactive fallout, this site was typical farmland with a minimal number of plant species right up to monoculture. This circumstance makes it possible to consider this site as an example of the influence of natural succession processes on the lateral redistribution of radioisotopes during the time elapsed since the accident, in contrast to the areas covered by forest. The heterogeneity of the microrelief and the water regime, in this case, have no a significant effect on the change in the radiation situation since the altitude differences are insignificant and levelled by the burrowing activity of ungulates and other animals.

There is a tendency for a stronger correlation of ^{90}Sr content with ^{137}Cs in the soil of former farmland. Sampling points with high and low soil contamination densities with the radioisotopes are often coinciding (Fig. 2). The variation coefficient of ^{90}Sr activity on the "former farmland" sampling plot is 36.0%. The difference between the minimum and maximum soil contamination density with ^{90}Sr in this site was 6.5 times.

The analysis of measurements shows the ^{90}Sr content in soil has a maximum level in the plot "pine forest" equal to 2,109.9 kBq/m^2. There were no significant successional processes since the moment of radioactive fallout. Therefore, the lateral redistribution of induced radioisotopes during the time since the accident was influenced only by natural fluctuations, changes due to age development of forest ecosystem, weather and climatic conditions, and digging activity of animals.

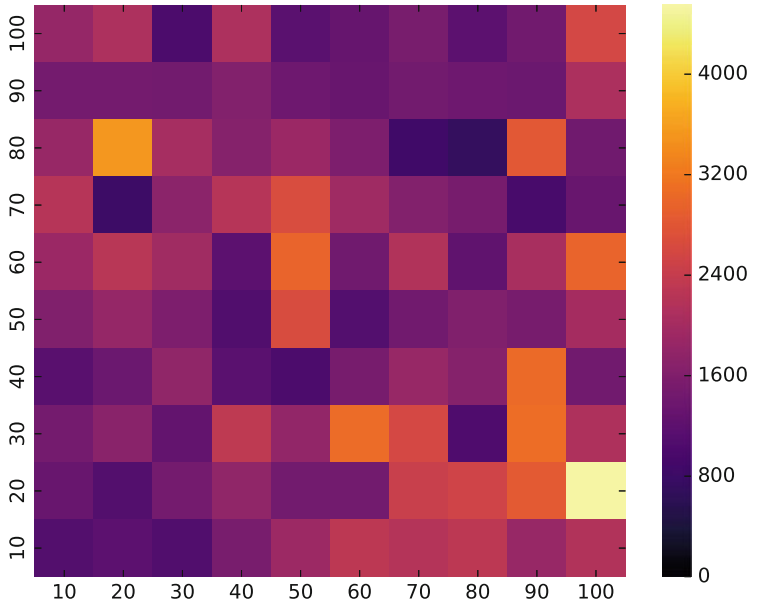

Fig. 2 Lateral distribution of ^{90}Sr on the former farmland (kBq/m^2)

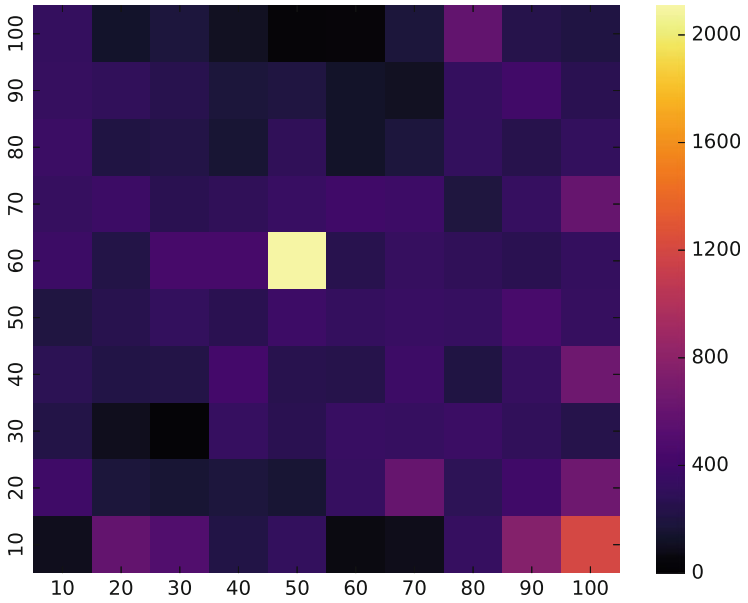

Fig. 3 Lateral distribution of ^{90}Sr in the pine forest (kBq/m^2)

Lateral redistribution of ^{90}Sr in the soil of pine forest was not as unambiguous as in the other cases studied by us. However, there is a significant discreteness of soil contamination density in the pine forest (Fig. 3).

The relatively insignificant total content of ^{90}Sr in the upper 20 cm layer of soil in the sampling plot attracts attention, taking into account the general radioecological situation of this area. This circumstance can be explained by the accumulation of a significant part of the radioisotope in a coniferous litter.

A coefficient of variation of ^{90}Sr activity in the pine forest was 75.2%, which differ significantly from other investigated sites. Perhaps, despite the same origin and very similar processes of lateral migration of radioisotopes in other ecosystems, the pine forests have some peculiarities associated with their structural organization. The difference between the minimum and maximum soil contamination density with ^{90}Sr in this site was 6.5 times.

We had calculated the parameters of probability distribution, the surface contamination density of soil on the experimental plots, and its compliance with normal probability distribution (Table 2). Calculation of confidence intervals in most cases showed a slight deviation from the mean values with a significance level for such studies ($P \leq 0.05$), which indicates the high reliability of the observations. The variance and the standard deviation are acceptable for the given conditions.

An analysis of the nature of the variation showed that ^{90}Sr in the forest ecosystems is more subjected to the variability of the radioisotope activity in the upper layer of the soil compared to other radioisotopes (Fig. 4). The most significant coefficient of variation confirms it. The least levels of variation of the radioisotope activity in

Table 2 Statistical parameters of the ^{90}Sr contamination density at the experimental site, kBq/m^2

x	lim		σ	σ^2	As	Ex	t_{As}	t_{Ex}	Conf. int.[a]	CV, %
	x_{min}	x_{max}								
Birch forest										
1,141.7	274.1	3,908.3	551.0	303,609.8	1.99	6.89	8.23	14.41	108.0	48.3
Former farmland										
1,778.8	698.9	4,550.9	640.9	410,698.0	1.28	2.67	5.29	5.59	125.61	36.0
Pine forest										
321.8	18.4	2,109.9	242.1	58,616.4	4.60	30.41	19.04	63.62	47.45	75.2

[a]The level of confidence is equal to 0.05

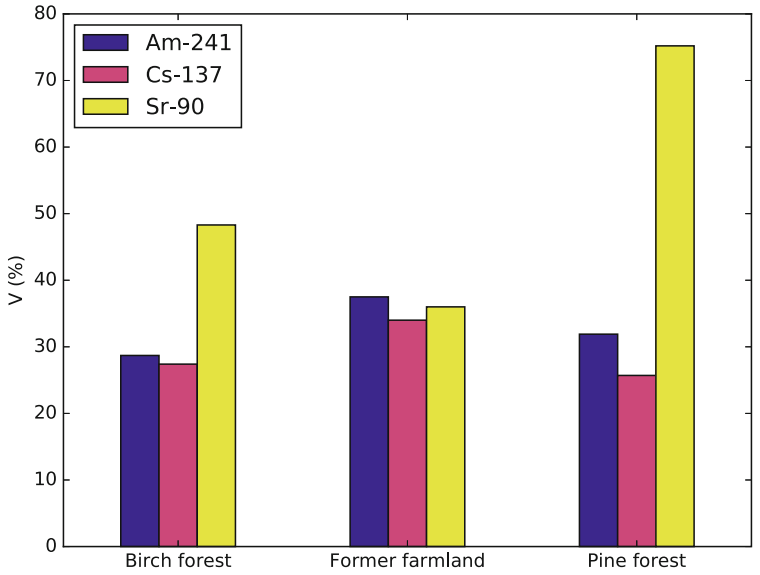

Fig. 4 Variability of ^{137}Cs, ^{90}Sr, and ^{241}Am activity in the upper soil layer at sampling plots (%)

the upper soil layer were in the former farmland, which mainly depends on the structure of the plant community here and absence of the developed tree canopy.

The obtained results indicate, on the one hand, higher mobility of ^{90}Sr in the soils of the exclusion zone, in comparison with other radioisotopes of Chernobyl origin, and, on the other hand, the ability of the biotic compartments in the studied ecosystems to use this chemical element in the metabolic processes to a greater extent than other man-made radioisotopes.

However, these variation characteristics do not contain information about the distribution law of the entire set of obtained data. Consequently, the analysis of variation series with the verification of the null hypothesis was carried out (Fig. 5).

During the calculation of the parameters of the variation series, the asymmetry and kurtosis parameters were estimated. At $N = 100$, as in our studies, the errors of these estimates are $S_{As} = 0.24$ and $S_{Ex} = 0.48$. The results showed that the distribution deviates greatly from the normal distribution. It should be noted that many other researchers confirm this situation [1, 4, 14, 15] and talk about the so-called log-normal distribution in the study of Chernobyl fallout.

In the study of the spatial distribution ^{90}Sr, the right-hand (positive) asymmetry of the variation histogram and its discreteness with increasing values of the contamination density are noticeable in all cases. The samples with the highest activity have increased discreteness and asymmetry, which confirms the possible presence of radioisotopes in the hot particles at this site. Since the number of hot particles decreases with distance from the epicentre of the accident, it is natural, taking into account the results obtained, a regular decrease in the correlation coefficients and variations will be observed. If we assume the conditions for a uniform distribution of

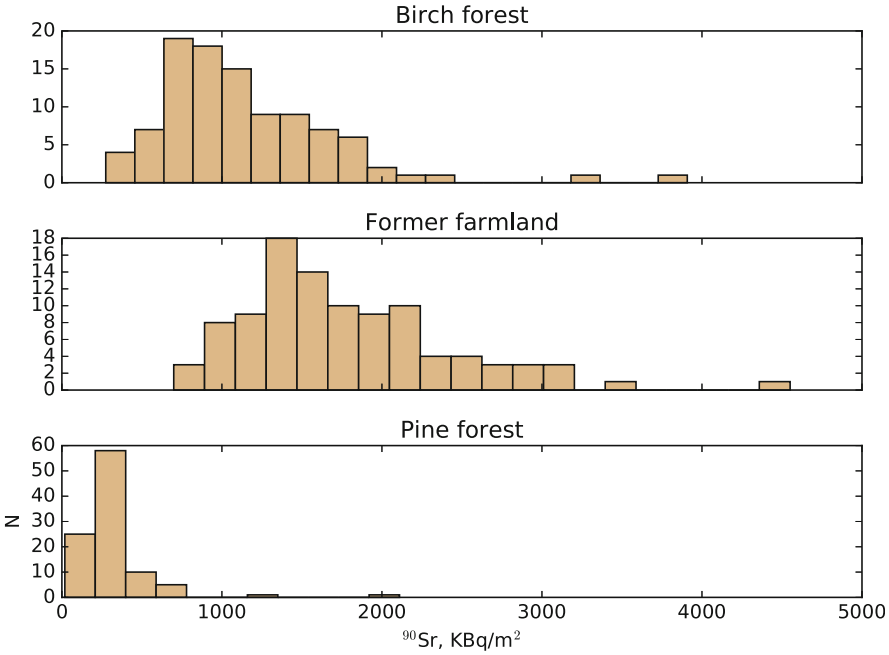

Fig. 5 Probability distribution histograms of ^{90}Sr in the upper 20 cm layer of the soil surface on the sampling plots (kBq/m^2)

fuel particles in the soil, then, other things being equal, such a decrease will be directly proportional.

Based on the statistical analysis, we can conclude that, for ^{90}Sr, the situation seems to be more complicated than for other radioisotopes of the Chernobyl release, which is associated with its gradual release from the matrix of fuel particles and the increase in the number of mobile forms. These processes are currently continuing. At the same time, it is also necessary to take into account the specifics of radioactive contamination of the ecosystems surface (the type of deposition, radioisotope composition, etc.). Being in the soil in specific forms and possessing different physicochemical properties, each radioisotope will react to different degrees on the impact of environmental factors.

The investigated parameters of variation reflect the processes of radioisotopes spatial transformation taking into account the specific properties of the selected landscape. Another word, they have specific peculiarities in each type of ecosystems. Variability of the radionuclides content in the soil depends on many factors. Therefore, the presented picture of the reduction in the coefficient of variation is conditionally permissible. Only long-term monitoring observations at a stationary landfill will help to more accurately predict changes in the coefficient of variation and the rate of its decline. It also allows establishing the most significant factors in this process. Multifractality of the spatial distribution of the radioisotope activity

concentration in soil does not effect on the degree of variation, since it is equally manifested at different scale levels, preserving the same statistical patterns.

The statistical analysis indicates a high coefficient of variation (75.2%) for the ^{90}Sr on the sampling plot located in the pine forest; it is more characteristic for fresh radioactive fallouts, which is most likely related to the structural organization of the pine forest ecosystem. Coefficients of variation for other investigated plots are characteristic for the long-term period of the accident and are confirmed by studies of Russian and Ukrainian scientists [2–4, 9, 10].

Since all the studied traits must obey the standard distribution law regardless of the level of organization of living matter, according to the postulates of biological statistics, then over time the radioisotope migration parameters in the system under investigation will reach such values at which all dynamic components will be balanced output on its quasi-stable state. Naturally, these processes will occur with different intensities for each radioisotope, which is related to its physical properties, quantity, properties of the soil itself and water regime, and, of course, the power of the living part.

In general, it is necessary to emphasize that the features of the behaviour of the ^{90}Sr described above are characteristic precisely for those conditions in which they were studied. In other conditions, the processes of lateral migration can proceed differently. Thus, for example, the heterogeneity of the radioisotope contamination density increases with increasing soil hydromorphism. Structural oscillations of the microrelief play an essential role in the horizontal distribution of radioisotopes, its convex forms are demolition zones, and concave forms are zones of accumulation of radioactivity.

4 Distribution of ^{90}Sr Between the Compartments of Various Ecosystems in the Exclusion Zone of the Chernobyl Accident

Further study of radioisotope transfer parameters in plant biomass made it possible to clarify the possibility of the influence of various ecosystem compartments on the formation of radioecological conditions. Taking into account the possible high T_{ag} and significant biomass of some compartments of a certain level of an ecosystem, we can assume their significant influence on redistribution of the radioisotopes.

The initial factor determining the intensity of radioisotope fluxes between individual compartments in the ecosystems, naturally, is the density of soil contamination and the physicochemical features of the radioactive elements in it. Further the role of biotic and abiotic factors in the redistribution of radioisotopes in ecosystem parts will significantly increase. Consequently, with the passage of time that has elapsed since the entry of radioisotopes into the ecosystems, significant changes may occur in their accumulation by separate structural parts of the community.

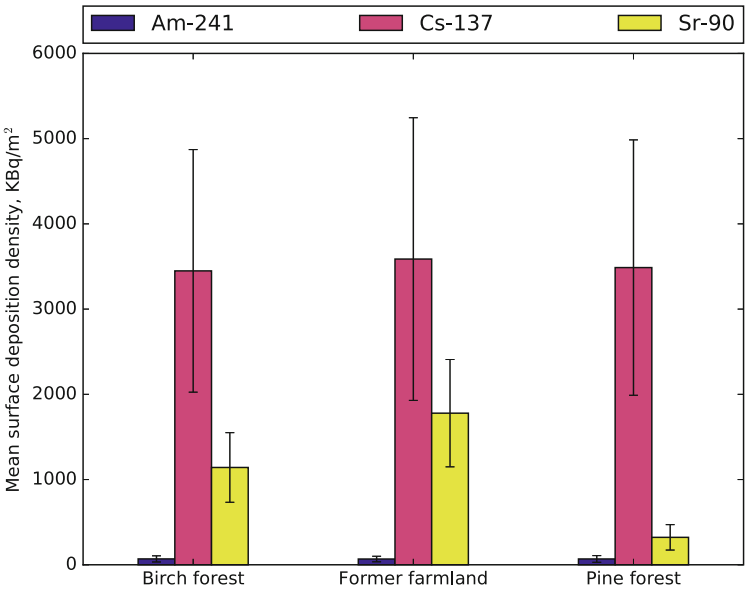

Fig. 6 Density of soil contamination with radioisotopes (kBq/m^2)

The nature of the distribution of radioisotopes in the surface layer of soil on the investigated objects is described above. It should be noted that the soil contamination density with ^{90}Sr significantly decreases with distance from the epicentre of the accident (Fig. 6).

Such a decrease in the soil surface contamination density is most likely due to the intensity of the initial radioactive fallout, although it is impossible to discount the further redistribution of radioisotopes in the compartments of the ecosystems. The accumulation of the radioisotopes by various compartments in the ecosystems could dramatically depend both on various soil properties factors (the mechanical composition of the soils, the degree of moistening, etc.) and on the specific features of the structural parts themselves. The activity of the radioactive isotope in the soil, apparently, does not play such a significant role. It is more important to create conditions that can make the radioisotope more accessible to biota.

The results of our investigations show that the distribution of ^{90}Sr on the compartments of pine and birch forests is identical despite the more significant levels of its content in the soil of the birch forest (in 11 times) (Fig. 7). The higher level of ^{137}Cs activity in comparison with ^{90}Sr is characteristic for practically all the studied compartments of the ecosystem with the exception for the assimilation organs of woody plants, where the activity of ^{90}Sr is 2–3 times more. Some differences are also in the somewhat more significant accumulation of strontium by the lower grassy tier of the pine forest, represented in this case by different types of moss, compared with that for the deciduous forest, where the grass layer mainly consists of cereals.

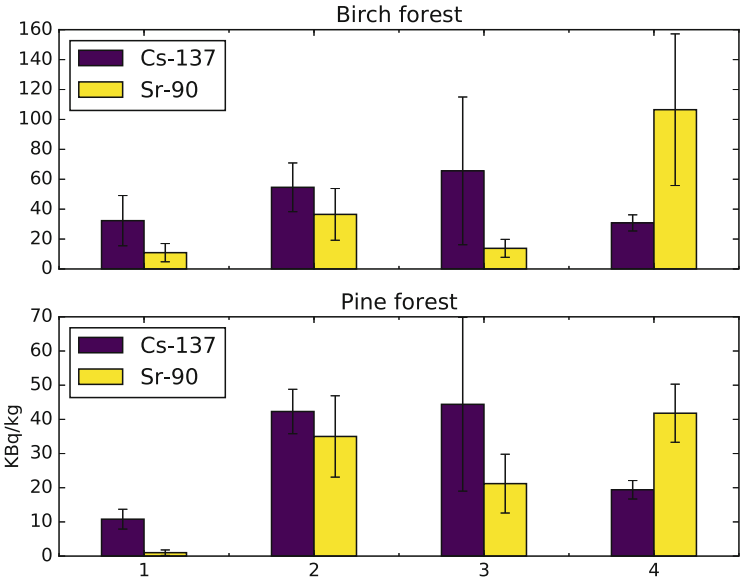

Fig. 7 Activity concentration of ^{137}Cs and ^{90}Sr in the compartments of birch and pine forests (kBq/kg). 1, soil; 2, litter; 3, under-canopy plants; 4, leaves of birch

A slightly different picture of the distribution of radioisotopes in the compartments of the ecosystem observed for the former farmland (Fig. 8). Accumulation of ^{90}Sr, in this case, is more intensive not only for foliage but also for meadow motley grass, which naturally reflects on the content of this radioisotope in the litter layer, which is formed mainly from the dead organic remains of the grass layer. It is noted a considerable discrepancy between levels of radioisotope content in the compartments of the former farmland and forest ecosystems. Despite the rather high content of ^{90}Sr in the soil of the former farmland, it is usually lower for other compartments. The only exception is the high content of ^{90}Sr in the fallow motley grass.

Apparently, this feature is due to the absence of the tree layer, which is an influential redistribution factor that changes the physical and chemical properties of the soil and other compartments of the ecosystem, and the vegetation of the fallow meadow, which in its current conditions has its threshold in the accumulation of radioisotopes, is not able to absorb significant amounts of ^{90}Sr from the soil. Woody plants have some differences in the accumulation of radioisotopes from annual herbaceous plants, possessing a cumulative type of accumulation [1]. It means that the processes of accumulation and release of radioisotopes in woody vegetation occur much more slowly than in herbaceous plants.

Comparative analysis of the distribution of the content of ^{137}Cs, ^{90}Sr, and ^{241}Am in soil and litter in the three studied plots showed a significant decrease of the fraction of ^{137}Cs in the litter layer in all cases (Fig. 9). In this case, the fraction of ^{90}Sr in the litter increases, which indicates its higher mobility and ability to be better

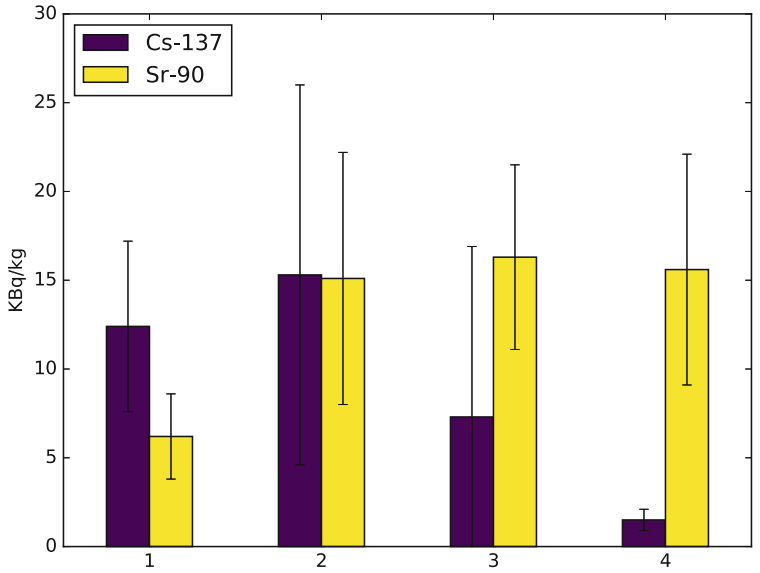

Fig. 8 Contents of ^{137}Cs and ^{90}Sr in the compartments of the former farmland (kBq/kg). 1, soil; 2, litter; 3, plants; 4, leaves of birch regrowth

absorbed by plants and, accordingly, accumulate in the litter. The mobility of ^{90}Sr in soils is currently increasing, but the mobility of ^{137}Cs is decreasing, which is reflected in the transfer of radioisotopes to the plants. ^{241}Am also retains its positions only on former farmland, where a thick layer of meadow grasses has the advantage in the absence of a tree layer in the absorption of the radioisotope. In general, the productivity of photosynthesis plays a prominent role in the cycle of mineral nutrients and radioisotopes also, which is related to the activity of root systems and the stock of soil organic matter. Soil organic matter changes the mobility of radioisotopes in the soil and has strong interrelation with the type of plant communities and their biological productivity. Yakushev [16] emphasized the significant role of vegetation in the entropy of radioisotopes of natural-plant complexes; ecosystems are arranged by increasing the mobility of radioisotopes in the soil: dry pine forest < mossy pine forest < meadow < marsh. At the same time, there is a direct relationship between the density of soil contamination in the ecosystem with radioisotopes and the specific activity of all constituent parts of the community.

It has long been known from the forest radioecology that foliage and needles of trees, consisting of meristematically active living tissues, possess the highest activity concentration of the radioisotopes, and the least concentrating ability belongs to wood [1, 16]. The data obtained in our work indicate that now ^{90}Sr is most actively accumulated by foliage and needles, reaching maximum values in them, in comparison with other parts of phytocoenosis.

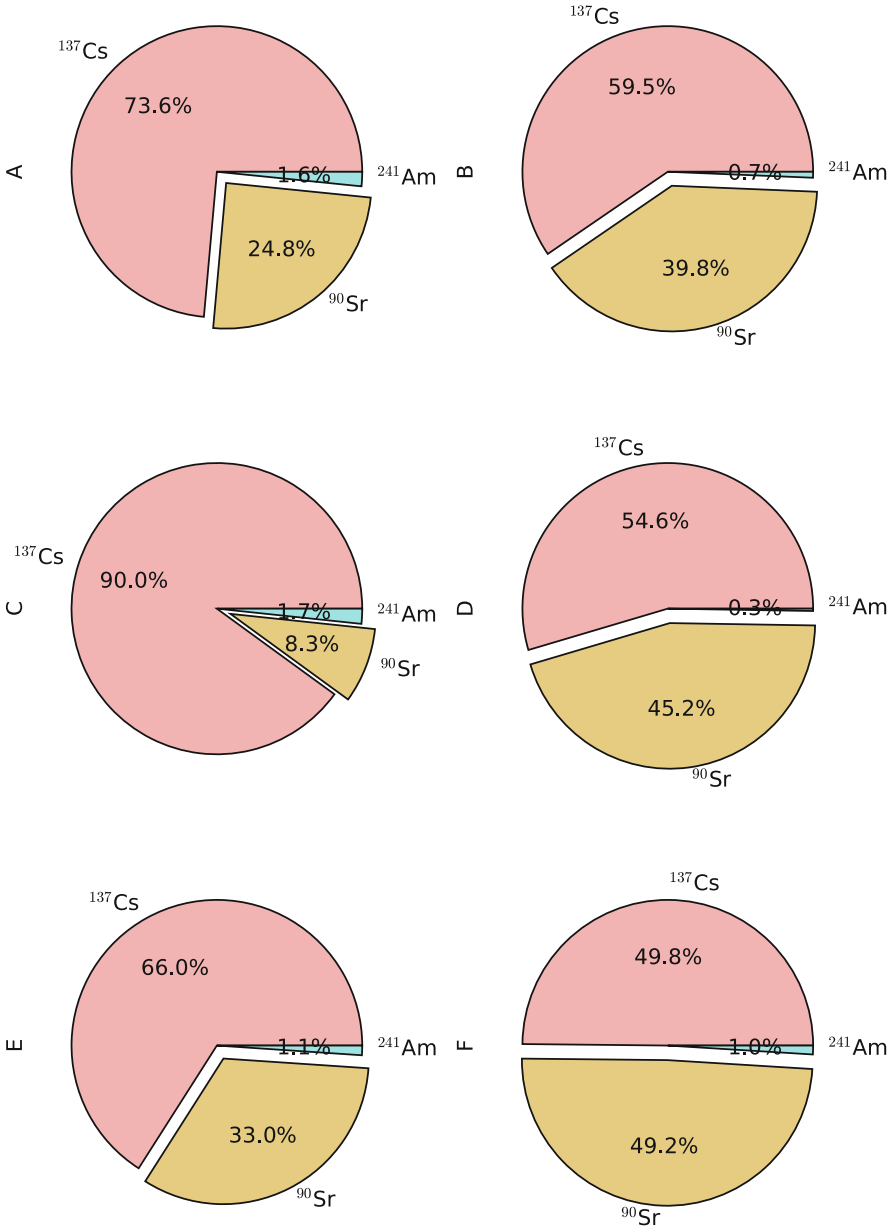

Fig. 9 Distribution of radioisotopes in the soil and litter compartments of studied ecosystems (%). (**a**) Birch forest, soil; (**b**) birch forest, litter; (**c**) pine forest, soil; (**d**) pine forest, litter; (**e**) former farmland, soil; (**f**) former farmland, litter

In general, considering the peculiarities of the structure and biology of plants, the redistribution of radioisotopes between the compartments of the ecosystems takes place unevenly. As noted above, lignified organs and tissues, which play only a

conducive role, accumulate radioisotopes to a lesser extent. The compartments that actively accumulated radioisotopes, as a rule, have a fast metabolism. Thus, the lowest tier of phytocoenosis, represented by mosses and lichens, has the highest specific activity, followed by herbaceous plants, shrubs, and under-canopy woody plants, and the lowest specific radioactivity is characteristic for the upper tree layer. Consequently, the under-canopy, mainly herbaceous, plants takes a more active part in the cycle of the radioisotopes in natural plant complexes [14, 15].

The distribution of radioisotopes in the compartments of ecosystems can occur in different ways depending on many factors, including soil-landscape-geochemical, microclimatic, biological features, etc. At the same time, the litter is an integrating compartment that reflects the affinity of the entire biocenosis for the accumulation of specific radioisotopes. According to the data, the ratio is levelled in the litter of sampling plots and approaches to 50–60% for ^{137}Cs, 40–50% for ^{90}Sr, and 0.3–1.3% for ^{241}Am irrespective of the fraction of radioisotopes in the soil.

The most objective picture of the redistribution of radioisotopes in the compartments of phytocoenoses, as well as the places of their intensive transformation, allows us to represent the values of T_{ag} of them from the soil. In this matter, our investigations clarify and supplement the already known regularities obtained in conditions after the Chernobyl accident. However, this makes it possible to emphasize the factors contributing to the spatial migration of radioisotopes in the remote period after the catastrophe for various natural and plant complexes. So, despite the powerful biomass and high density of herbs of the meadow community, their absorptive capacity was lower, in comparison with forest ecosystems. Leaves of 10–15 years birch trees also accumulate less of the radioisotope (Table 3).

It should be noted that the density of soil contamination by ^{90}Sr at the former farmland was higher in comparison with the forest ecosystems. The regularities speak in favour of a more significant influence of soil properties and forest-growing conditions as well as species peculiarities on the accumulation of radioisotopes by the compartments of the ecosystems, as suggested above.

There is an overwhelming dependence on forest areas. The highest T_{ag} ^{137}Cs for motley grass and foliage has a phytocoenosis of deciduous forest, but the transfer of ^{90}Sr is higher for the compartments of pine forest.

A high level of T_{ag} fluctuation did not allow revealing an essential dependence of change of accumulation of radioisotopes by structural parts of ecosystems during the period of vegetation. This circumstance is natural, especially for ecosystems of accumulative type, which include forest biotopes of temperate latitudes, where these processes proceed slowly, stretching for years.

Table 3 Aggregated transfer factors of the radioisotopes at sampling plots (Bq/kg)/(kBq/m^2)

	Herbaceous vegetation		Foliage/needles	
Sampling plot	^{137}Cs	^{90}Sr	^{137}Cs	^{90}Sr
Birch forest	19.0	12.1	8.9	93.2
Pine forest	12.7	65.9	5.6	130.0
Former farmland	2.0	9.1	0.4	8.7

Thus, the conducted studies confirm the significant influence of soil properties, forest growth conditions, and species peculiarities on the accumulation of radioisotopes in the compartments of ecosystems. These factors significantly level the values of surface contamination. It is established that the litter from the dead biomass is an integrating element reflecting the affinity of the entire investigated biosystem for the accumulation of individual radioisotopes. The data show that irrespective of the fraction of radioisotopes in the soil, this ratio is levelled in the litter of sampling plots and approaches to 50–60% for ^{137}Cs, 40–50% for ^{90}Sr, and 0.3–1.3% for ^{241}Am. An analysis of the aggregated transfer factors shows that the absorption capacity to the radioisotopes was lower for grassy vegetation in the former farmland compared with the under-canopy herbaceous plants in the forest ecosystems. The highest T_{ag} ^{137}Cs for motley grass and foliage has a phytocoenosis of deciduous forest, but the transfer of ^{90}Sr is higher for the compartments of pine forest.

5 Conclusions

The analysis of the influence of the considered landscape factors on the spatial distribution of ^{90}Sr and the estimation of the variability of its content in the soil is the basis for studying the processes of lateral and vertical migration. The obtained results may be important for designing of numeric landscape models intended for the forecast of spatial-temporal redistribution of radioisotopes after emergency emissions. Radioisotopes can play a role of labels in the investigation of landscape heterogeneity and for identifying hierarchical structures which characterize intensity of landscape formation. The study of the spatial distribution of radioactive isotopes is an essential step in the development of radiation situation forecasts. The study of the migration of radioisotopes considering the spatio-temporal structure of landscapes of the exclusion zone of Chernobyl NPP at different scale levels can serve for spatial assessment of radioecological situations and is the basis for the radiological expertise of contaminated territories.

It should be noted that the existing differences in the variation of the lateral distribution of radioisotope activity in the soil of ecosystems in the near zone of the Chernobyl accident not only depend on their properties and timespan but also on the landscape structural organization of ecosystems, changes in hydrological and weather-climatic conditions, and activity of animals.

References

1. Ipatiev VA (1999) Forest People Chernobyl. Forest ecosystems after the Chernobyl accident: the state, the forecast, the reaction of the population, ways of rehabilitation. Forest Institute of NAS of Belarus, Gomel, Belarus

2. Ivanov YA, Lewyckyj N, Levchuk SE, Prister BS, Firsakova SK, Arkhipov NP, Arkhipov AN, Sandallsg J, Askbrant S (1997) Migration of ^{137}Cs and ^{90}Sr from Chernobyl fallout in Ukrainian, Belarussian and Russian soils. J Environ Radioact 35:1–21
3. Linnik VG (1996) Landscape-geographical research in connection with the Chernobyl accident. Proceeding of Moscow State University, Ser. 5, Geography, pp 348–344
4. Linnik VG (2008) Landscape differentiation of technogenic radioisotopes: geoinformation systems and models. Dissertation, Moscow State University, Moscow, Russia
5. Aleksakhin RM (1982) Nuclear energy and the biosphere. Energoizdat, Moscow, Russia
6. Warner F, Harrison RM (1993) Radioecology after Chernobyl: biogeochemical pathways of artificial radionuclides. Wiley, Chichester
7. Tyuryukanova EB (1974) Radiogeochemistry of soils of the polessyes in Russian plain (the example of the Meshchera lowland). Nauka, Moscow
8. Aleksakhin RM, Naryshkin MA (1977) Migration of radioisotopes in forest biogeocenoses. Nauka, Moscow, Russia
9. Kashparov VA, Lundin SM, Khomutinin YV, Kaminsky SP, Levtchuk SE, Protsak VP, Kadygrib AM, Zvarich SI, Yoschenko VI, Tschiersch J (2001) Soil contamination with ^{90}Sr in the near zone of the Chernobyl accident. J Environ Radioact 56:285–298
10. Linnik VG, Khitrov LM, Korobova EM (1991) Principles of landscape geochemical and radioecological mapping of territories contaminated with radioisotopes as a result of the Chernobyl accident (RADLAN project). Vernadsky Institute, Moscow
11. Naryshkin MA, Aleksakhin RM, Molchanov AA (1975) Patterns of distribution of radioactive fission products of global fallout in the forests of the North European part of the USSR. Russ J Forest Sci 4:104–106
12. Pavlotskaya FI (1973) State and forms of radioisotopes in the global deposition. Atomizdat, Moscow
13. Tikhomirov FA, Aleksakhin RM (1973) Effect of ionizing radiation on forest biogeocenoses. In: Klechkovskii VM (ed) Radioecology. Wiley, New York, pp 197–224
14. Bulavik IM (1990) Contamination of the main elements of forest biocenosis with Cesium-137. In: Radiobiological and radioecological aspects of the consequences of the Chernobyl accident, vol 1, Moscow, Russia.
15. Parfenov VI, Yakushev BI (1995) Radioactive contamination of vegetation of Belarus connecting with Chernobyl accident. Nauka i technika, Minsk
16. Yakushev BI (1991) Entropy and migration of radioisotopes in the soil-plant system. In: Abstracts of the conference problems of elimination of consequences of the Chernobyl disaster, Obninsk, Russia, p 45

Spatial Distribution of ^{90}Sr from Different Sources in Soils of the Ural Region, Russia

Ludmila N. Mikhailovskaya and Vera N. Pozolotina

Contents

Abstract The presence of some enterprises of the nuclear fuel cycle (NFC) in the Ural region has caused the formation of a radioactive contamination on large territories that exceeds the level of global fallouts typical for the middle latitudes of the Northern Hemisphere. Currently, additional sources of man-made radionuclides in the Urals are (1) the operating NFC enterprises, the largest of which are "Mayak" Production Association and Beloyarsk Nuclear Power Plant (permissible emissions), and (2) contaminated zones that are sources of secondary pollution of the environment. The activity of PA "Mayak" created the most problematic areas: the Techa River, which was polluted with liquid radioactive wastes, and the East Ural Radioactive Trace (EURT), which was the result of the Kyshtym accident of 1957. These local zones possessed very high levels of radionuclides, including ^{90}Sr. The inventory of ^{90}Sr reached 70,000 kBq/m^2 in the EURT head part. Prolonged input of global fallout and gas-aerosol emissions from the NFC enterprises and transport of

L. N. Mikhailovskaya (✉)
Laboratory of Common Radioecology, Institute of Plant and Animal Ecology, Ural Branch of Russian Academy of Sciences, Yekaterinburg, Russia
e-mail: mila_mikhaylovska@mail.ru

V. N. Pozolotina
Laboratory of Population Radiobiology, Institute of Plant and Animal Ecology, Ural Branch of Russian Academy of Sciences, Yekaterinburg, Russia

P. Pathak, D. K. Gupta (eds.), *Strontium Contamination in the Environment*,
The Handbook of Environmental Chemistry 88,
https://doi.org/10.1007/978-3-030-15314-4_8

radionuclides from contaminated areas supported during a long time stable global (1.3 Bq/m^2) and regional (1.6–3.0 Bq/m^2) levels of ^{90}Sr in the Urals. Migration of ^{90}Sr within geochemical conjugations depends on the sources of intake (gas-aerosol emission or liquid discharges) of the radionuclide into the environment. The depth of vertical migration and the character of the distribution of the radionuclide depend on the regime of moistening and the type of soils.

Keywords ^{90}Sr · East Ural Radioactive Trace · Production association "Mayak" · Soils · Techa River · Urals, Beloyarsk NPP

1 Introduction

Contamination in Ural region with radioactive waste is characterized by high heterogeneity. The worldwide fallout from nuclear weapons testing in the Northern Hemisphere made the most contribution of the ^{90}Sr to regional pollution. The value of global fallout in the middle latitudes is currently estimated as 1.3 kBq/m^2 [1, 2]. In fact, the ^{90}Sr content in the Ural soil varies in the range of 1.2–3.5 kBq/m^2 [3–5]. Exceeding the background level is due to the function of enterprises of the nuclear fuel cycle (NFC), the largest of which are "Mayak" Production Association (PA "Mayak") and Beloyarsk Nuclear Power Plant (BNPP) (Fig. 1). Currently, all enterprises are operating in normal mode. Regulated discharges of radionuclides into

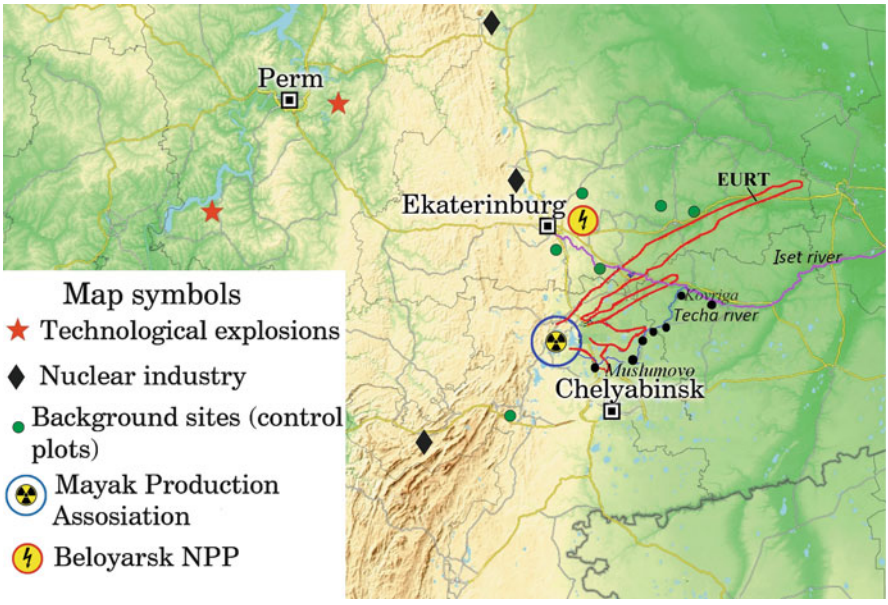

Fig. 1 Sources of ^{90}Sr in the Middle and Southern Urals

the environment are made, but they do not exceed the permissible levels adopted in the Russian Federation [6].

Several technogenic accidents formed local zones with very high content of radionuclides, in particular ^{90}Sr. In 1949–1956 PA "Mayak" dumped in the Techa River liquid radioactive waste. The main causes of discharges were the lack of reliable technologies for processing and storing radioactive waste, as well as a lack of understanding of the possible consequences of radioactive contamination. In total, during this period, 76 million m^3 of waste was discharged with a total activity of beta emitters of 100 PBq; the share of ^{90}Sr was more than 10% [7, 8].

In 1957, East Ural Radioactive Trace (EURT) was formed as a result of accident at the PA Mayak (named the Kyshtym accident). The ^{90}Sr prevailed among long-lived radionuclides in emergency fallouts. The EURT area was subjected to secondary pollution in 1967 due to the wind transfer of radioactive bottom sediments from Lake Karachay (technological reservoir of PA Mayak). In this case, the main pollutant was ^{137}Cs [9, 10]. The total inventory of ^{90}Sr at the EURT zone including the Karachay incident is estimated now as 572 TBq [11, 12]. At present the local zones (EURT, Techa River) are secondary sources of radioactive contamination of adjacent territories [2].

Additional sources of radionuclides are considered the storage of radioactive waste and nuclear explosions carried out in different years for peaceful purposes (Fig. 1), although their contribution to the overall pollution in the Ural region is insignificant, because the pollutions are locally and incomparably small compared with the above sources. The aim of this research was to investigate spatial distribution of ^{90}Sr in different origins of soils at Ural region.

2 Material and Methods

The research was conducted in 2003–2016 in the Middle and Southern Urals (Sverdlovsk and Chelyabinsk regions). According to geobotanical zoning, the territory of the Middle Urals belongs to the taiga region of the Ural plain mountainous country, the southern one – to the Trans-Ural forest-steppe. The climate is continental; the amount of precipitation is 350–500 mm per year. In this territory, according to Roshydromet's data, winds prevail in the northwestern, western, and southwestern directions. In the northern part of the studied territory, burozems, rzhavozems, soddy podburs, and soddy-podzolic soils predominate; in the south there are various subtypes of forest gray soils, chernozems, and meadow soils [4, 12]. We used our own results on the content of ^{90}Sr in soils of different places of Urals as well as data from literature sources [2, 13, 14].

Principles and methods of landscape-geochemical studies were used to estimate the geochemical migration of ^{90}Sr. We took into account the radionuclide entry pathways and the landscape-geographical features of the locations. The reference sites were chosen at different distances from the main sources of pollution, under conditions of homogeneous relief and similar types of soils and vegetation. In the

coastal zones of lakes and rivers, we surveyed geochemical conjugations, which included plakors (watershed territories), slopes, and foots of slopes. Within each site of 100 m^2, three soil sections were laid, placing them at the corners of the triangle with a side of 10 m. Samples of the soil were taken by layers with a thickness of 5–10 cm, taking into account the sample area to a depth of 50 cm.

The contribution of ^{90}Sr from two accidents (In Kyshtym, 1957 and in Karachay, 1967) was assessed using radionuclide ratios and the density of soil contamination at the reference sites. The $^{90}Sr/^{137}Cs$ ratio in the fallout from the Kyshtym accident was 71.0 and from the Karachay incident – 0.3 [9, 15].

All samples were dried, triturated, and passed through a sieve (cell diameter was 1 mm). The samples were then incinerated at 450°C. All analytical methods were performed in accredited laboratories of the Institute of Plant and Animal Ecology (accreditation certificate CAPK RU.0001.441492). The content of ^{90}Sr was determined using radiochemical methods [16]. The procedures were based on radionuclide leaching by 6N HCl solutions from prepared preliminary samples. Precipitation of ^{90}Sr occurred in the oxalate form, separating the ^{90}Sr that remained in balance with the ^{90}Y daughter product of decay. The measurement of ^{90}Y was performed with the use of a UMF-2000 alpha-beta radiometer (Russia), whose detection precision was 0.2 Bq. All results for the samples were calculated on an air-dry weight basis. We used Student's *t*-test to assess the significance of differences.

3 The Main Sources of ^{90}Sr Pollution in the Urals

The level of radioactive contamination in the Ural region was set up and is being maintained at present from several sources: (1) global radioactive fallout from the atmosphere, (2) standardized gas-aerosol emissions and liquid discharges from NFC enterprises, (3) Kyshtym accident and discharges to the Techa River from the PA "Mayak," (4) technological explosions, and (5) secondary sources that contaminate the environment as a result of migration processes, the most important of them are the territory of the EURT, open reservoirs of radioactive waste, and Techa River floodplain. The map (Fig. 1) shows the most significant sources of ^{90}Sr inflow to the environment. In this article, we consider in detail the influence of the largest of them – BNPP and PA "Mayak."

3.1 Beloyarsk NPP

Beloyarsk NPP has been operating in an accident-free mode since 1964. Now in operation there are two power units with fast neutron reactors of industrial power level BN-600 and BN-800 (Fig. 2). Since 1966 the Institute of Reactor Materials (IRM) was located near the BNPP. This Institute has a research reactor with a power of 15 MW. Noble gases are dominated in gas-aerosol emissions of both enterprises;

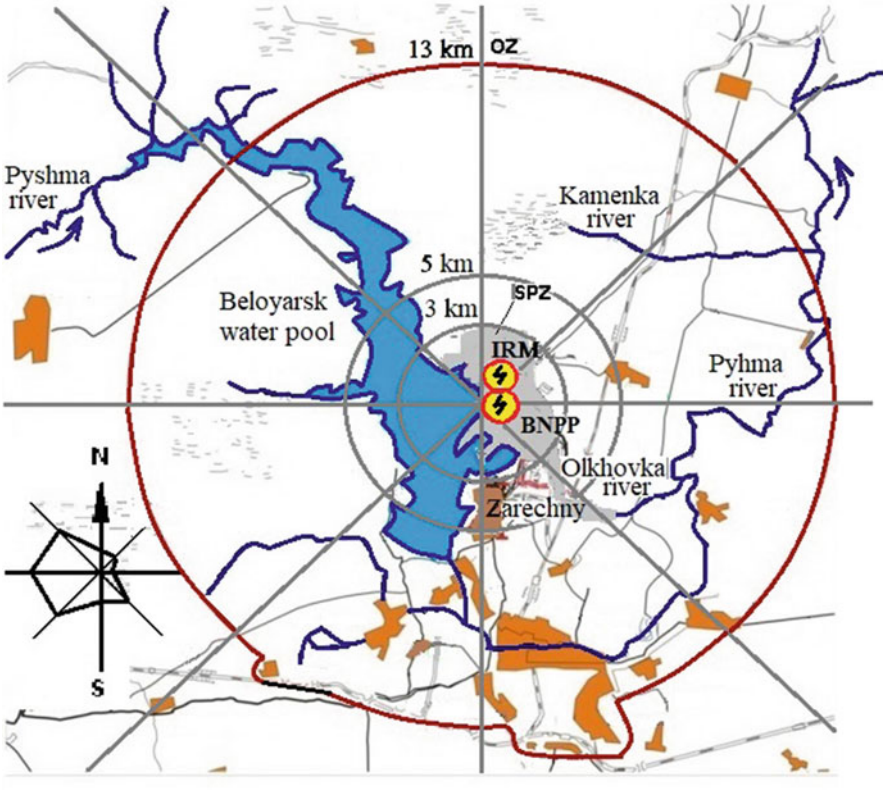

Fig. 2 Map scheme of the observed zone of BNPP and IRM. *SPZ* sanitary protection zone, *OZ* observable zone

the ^{137}Cs and ^{90}Sr are also present. It is impossible to divide the contribution of these two sources to radioactive contamination of the adjacent territory. Therefore, the data presented below should be considered as a result of the combined effect of BNPP and IRM [2].

Investigation of the impact zone of these enterprises (30 km), including the Zarechny City, revealed a variation in the ^{90}Sr contamination density (0–10 cm soil layer) from 0.4 to 2.4 kBq/m^2. An analysis of the spatial distribution showed that the level of contamination does not depend on the azimuthal direction (Table 1).

The differences are, as a rule, insignificant (t_{st}, $p > 0.05$). In general, soil contamination levels by ^{90}Sr in the impact zone of BNPP and IRM belonged to the background range typical for the Ural region [4].

Approximately the same level of soil contamination by ^{90}Sr was revealed in the impact zone of the BNPP 35 years ago [17]. During this period, the ^{90}Sr content should be reduced by a factor of 2 due to processes of radioactive decay. Evidently, preserving soil contamination level for a long period of time is due to additional

Table 1 Density of soil contamination (0–10 cm layer) by ^{90}Sr within 15 km impact zone of BNPP and IRM (kBq/m^2)

Distance from BNPP in km	Azimuthal sector							
	N-W		N-E		S-E		S-W	
	M±SD	Min-max	M±SD	Min-max	M±SD	Min-max	M±SD	Min-max
0–3	1.2±0.3	1.0–1.6	1.7±0.4	1.5–1.9	1.8±0.5	1.2–2.4	1.0±0.2	0.4–1.3
3–15	1.1±0.3	0.6–2.0	1.3±0.1	1.2–1.3	1.3±0.2	1.2–1.4	1.5±0.4	1.3–1.7

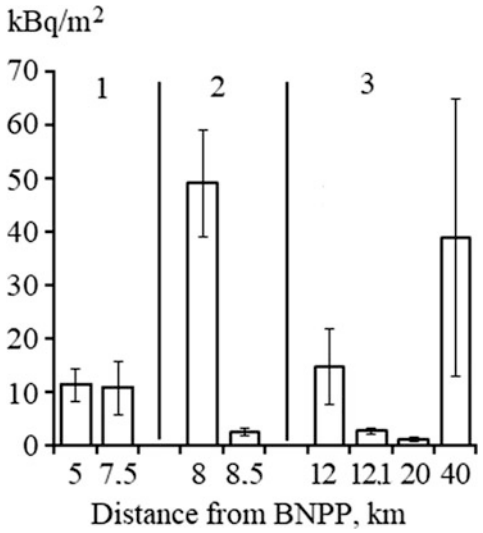

Fig. 3 Inventory of ^{90}Sr in flooded floodplain soils from the discharge of liquid wastes of BNPP. 1, Ol'khovskoye swamp; 2, Ol'khovka River; 3, Pyshma River

entrance of ^{90}Sr from the atmosphere. In addition to BNPP and INR, various sources took part in the formation of this contamination: gas-aerosol emissions of PA "Mayak," global radioactive fallout, and the possible transfer of ^{90}Sr from the territory of the EURT.

During the whole period of operation of the BNPP, the low-radioactive unbalanced water is discharged into the Ol'khovskoye swamp, which is connected with the river system: Ol'khovka-Pyshma-Tura-Tobol-Irtysh-Ob. The Ol'khovskoye swamp turned into a natural repository of radioactive waste and a source of environmental pollution [14, 18]. The densities of soil contamination by ^{90}Sr in the swamp and floodplains of the Ol'khovka-Pyshma rivers vary from 1 to 50 kBq/m^2 (Fig. 3). The distance from the source of pollution does not affect the inventory of ^{90}Sr in floodplain soils. The uneven distribution of radionuclides along the Pyshma

Table 2 The content of ^{90}Sr in soils of geochemical conjugation, kBq/m^2

Site	Element of relief	Distance from swamp, in m	Elementary geochemical landscape	0–5 cm layer		0–50 cm
				Bq/kg	kBq/m^2	kBq/m^2
Non-flood	Watershed	500	Eluvial	7.9±0.3	0.3±0.1	2.4±0.9
	Slope	35	Trans-eluvial	16±5	0.8±0.3	2.1±1.5
Flooded	Swamp shore	15	Trans-accumulative	250±35	2.2±0.3	10.6±2.2
	Swamp	0	Trans-accumulative	156±38	0.5±0.2	30.6±10.8
	The bank of the Ol'khovka River	500	Trans-accumulative	161±32	2.3±0.7	49.0±12.0

River is caused by the relief of the floodplain and the hydrological regime of the river. This fact was also revealed in other studies [19].

The width of floodplain soils in the shore zone of the swamp and Ol'khovka River is 10–20 m. We have investigated a geochemical profile (about 1,000 m long) that began at the top of a coastal slope, passed through a swamp, and ended in the floodplain of the Ol'khovka River. The evaluation has included the ^{90}Sr content of upper 0–5 cm soil layer and the density of contamination of 0–50 cm soil layer (Table 2). In general, pollution increases along the flow vector and reaches a maximum in trans-accumulative landscapes. The values of contamination on the watershed and on the slope are comparable to regional background level [3–5]. The soil contamination levels of ^{90}Sr increase by about an order of magnitude in the flooded sites.

Comparison of the current results with the data obtained 30–40 years ago [17] allows us to conclude that the contamination of non-flooded soils by ^{90}Sr does not changed. The inventory of ^{90}Sr in the flooded soils has decreased, and this is due to self-cleaning processes. However, at present, contaminated sites still serve as a source of secondary pollution of the river system [14, 18].

3.2 PA "Mayak"

PA "Mayak" was Russia's first enterprise for the production of weapons-grade plutonium. At present, PA "Mayak" is engaged in the production of radioactive isotopes for scientific and medical purposes, as well as the processing and storage of radioactive waste.

3.2.1 Discharges into the Techa River

In the initial period of the enterprise's operation (1949–1952), liquid radioactive wastes were discharged into the Techa River, and from there they entered to the open hydrographic network. A total of 76 million m^3 of waste with a total radioactivity of 10^{17} Bq was discharged; the contribution of ^{90}Sr in the isotope mixture was approximately estimated as 12%. Detailed studies of the river system Techa-Iset-Tobol-Irtysh-Ob were carried out during the period 1993–2005 [7, 20–23].

We investigated the floodplains of the Techa and Iset rivers, choosing sites with homogeneous relief and with similar types of soils and vegetation. They were located at different distances from the source of pollution, near the villages Muslumovo (78 km), Brodokalmak (107 km), Lobanovo (158 km), Anchugovo (169 km), Shutikha (206 km), and Zatechenskoe (237 km); in addition, the sites were chosen on the Iset River: the village of Krasnoisetskoe (250 km from the source of contamination) and the village of Kovriga (277 km). Alluvial-layered and sod-meadow soils predominate in the floodplain. Samples of soils were taken at a distance of 5–15 m from the water's edge.

Pollution of floodplain soils by ^{90}Sr was heterogeneous. The maximum content of ^{90}Sr was 1,600 kBq/m^2 in the riparian and 900 kBq/m^2 in the central floodplain of the Techa River. The density of ^{90}Sr contamination of floodplain soils decreases by one to three orders of magnitude with increasing distance from the source. This pattern is well approximated by a power function (Fig. 4). The minimum values are noted in the riparian (40 kBq/m^2) and central floodplains (25 kBq/m^2) at the distance of 277 km. These values exceed by an order of magnitude the contamination levels of the Iset River floodplain above the confluence of the Techa River (riparian,

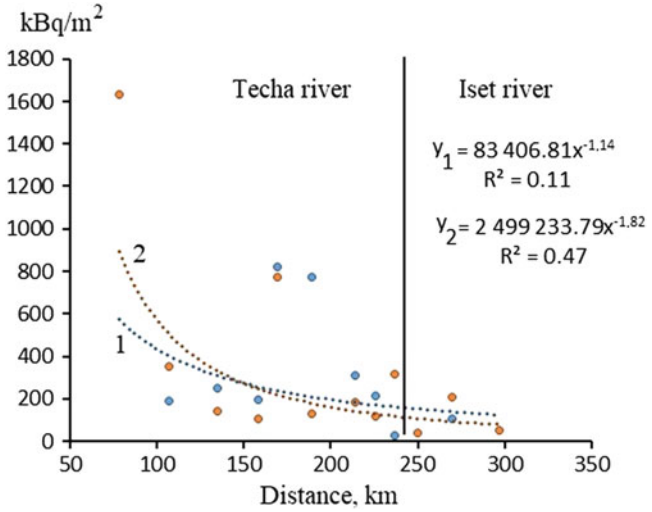

Fig. 4 Density of soil contamination by ^{90}Sr in the floodplains of the Techa and Iset rivers. 1, the central floodplain; 2, the riverine

3.8 kBq/m^2; central part, 4.2 kBq/m^2). Assessments based on empirical data and special mathematical models have shown that the ^{90}Sr inventory in the soils of the floodplains of the Techa and Iset rivers amounted to 75 TBq [14].

The mobile radionuclide – ^{90}Sr – can migrate predominantly in water-soluble forms [24–27]. For the years that have passed since the beginning of the Techa River pollution, the discharges have formed a radioactive trace of ^{90}Sr in the Ob-Irtysh river system. It is assumed that about 1% of the total discharges have entered to the Kara Sea [20].

3.2.2 Kyshtym Accident (1957) and East Urals Radioactive Trace

The explosive nature of the Kyshtym accident defined the spatial distribution of ^{90}Sr on the territory of the EURT. An impact zone with a maximum soil contamination by ^{90}Sr was formed in the vicinity of the epicenter of the accident; around it was formed a halo (buffer zone). The ^{90}Sr inventories within the central axis of the head part of the EURT are 253–316 TBq, at the western periphery 2.2–2.4 TBq, and at the eastern periphery 7.5–9.2 TBq [28]. The content of ^{90}Sr in trace soils decreases with increasing distance from the epicenter in accordance with the exponential dependence [12, 29, 30]. The same character of the ^{90}Sr distribution is observed at the

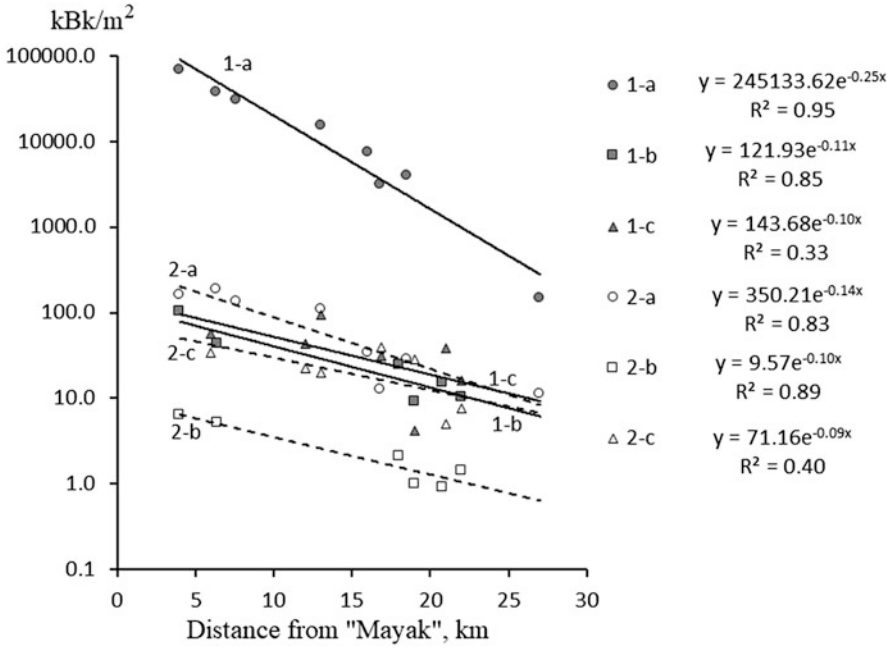

Fig. 5 Distribution of ^{90}Sr in the soils of the EURT head part. Sources of pollution: 1, Kyshtym accident in 1957; 2, Karachay incident in 1967. Part of the trace: a, axis of EURT; b, western periphery; c, eastern periphery

western periphery of the EURT (Fig. 5). The reliability of the approximation is 83–95%. A similar regularity was not found on the eastern periphery due to the high heterogeneity of the soil contamination by ^{90}Sr. The intensive air transport of radioactive aerosols was observed in the first years after the accident in the direction of prevailing winds (east, southeast, and northeast), and in the sequel this process was decreased [31]. The decrease of the ^{90}Sr transfer by wind is associated with its migration deep into the soil and with the retention on the surface of vegetation and litter [32].

Estimation of the contribution of different sources of ^{90}Sr showed that 91.8–99.8% of the total content came into the soils of central axis as a result of the Kyshtym accident. In the western periphery, the contribution of the Kyshtym accident was reduced to 75–92.5% and in the eastern periphery to 20.1–91.3%. The Karachay incident added to the ^{90}Sr contamination of different parts of the EURT on average 0.2–7.0%, 4.9–10.5%, and 8.5–43.3%, respectively.

The regular ^{90}Sr emissions of PA "Mayak" were amount about 1.5 kBq/m^2; it is similar to global fallout [9, 15]. Thus, the allowable emissions of the PA "Mayak" in the contamination of the EURT territory by ^{90}Sr are very small in comparison with emergency fallout (0.002–1.0%), and their contribution does not exceed 1.8–16.7% in the adjacent territories.

Spatial trends were not detected outside the EURT zone and the observed BNPP zone [14, 18]. We compared the contamination of automorphic soils by ^{90}Sr received from different sources (Table 3). The maximum content of ^{90}Sr reaches 70,000 kBq/m^2 in the soils of the head part of the EURT. In the zones of influences of PA "Mayak" and BNPP (on distance 50 and 30 km correspondently), the content of ^{90}Sr is two to four orders of magnitude lower than in the EURT territory and 2.6–6.0 times higher than the level of global fallout. High variability of the soil contamination is due to both the unevenness of atmospheric fallout and the numerous factors that influence the redistribution of the radionuclide. It is impossible to unequivocally assess the contributions of regional and global fallout. The data indicate that sites with raised ^{90}Sr content in soils, as well as territories contaminated only with ^{90}Sr global fallout, take place within the Ural region.

At present, all sources of atmospheric deposition are relevant, but their contribution to soil contamination by ^{90}Sr is very small. The highest level was found only in

Table 3 Current levels of ^{90}Sr in atmospheric fallout and density of soil contamination within the Ural region

Site	Inventory of ^{90}Sr in 0–50 cm layer, kBq/m^2	Atmospheric fallout, Bq/m^2 per year [2, 33] mean (min-max)
Head part of EURT	9–70,000	48.4(21–170)
100 km zone of PA "Mayak"	0.5–3.5	4.9 (2.2–19.5)
30 km zone of BNPP	0.4–4.8	0.94 (0.52–1.92)
Background of Ural region (control plots)	0.8–3.5	1.6 (1.56–1.71)
Global background	1.3 [2]	<0.3

Table 4 Concentrations of ^{90}Sr in components of terrestrial ecosystems within the EURT central axis

Component	^{90}Sr, kBq/kg	
	Air-dry matter	Ash
Aboveground mass of plants: woody	9–209	324–10,460
Grassy	4–590	63–15,690
Litter	4–914	15–6,950
Soils, 0–5 cm	4–400	–

the observed territory of PA Mayak; it is caused by the wind transfer of the radionuclide from the EURT zone and reservoirs of radioactive waste storage [2]. A significant contribution of ^{90}Sr can be found only at the sites with soil contamination level <10 kBq/m^2. In other territories supplementary ^{90}Sr was found only in vegetation and litter, but not in soils [29]. The increased migration of ^{90}Sr was observed during the fires that occur annually in the EURT zone. They lead to the formation of large amount of ash with a concentration of ^{90}Sr by one to two orders of magnitude higher than in air-dry matter (Table 4). The high volatility of ash particles causes an increase in their wind transfer along the direction of the prevailing winds [34].

It is important that in the Ural region, the content of ^{90}Sr in the soils of the control areas (conditionally background sites) has been maintained at approximately the same level for many years. Approximately 30 years ago, the level of global fallout in the mid-latitudes of the Northern Hemisphere was 1.5 kBq/m^2 [9, 35, 36]; currently it is estimated at 1.3 kBq/m^2 [1, 2]. In the Southern and Middle Urals, in 1985–1990 the background level of soil contamination by ^{90}Sr was determined as 0.8–3.5 kBq/m^2 [9, 37]; now it is estimated as 1.6–3.0 kBq/m^2 [4, 14].

4 Migration of ^{90}Sr Within Geochemical Conjugations

We have investigated the barrier functions of hydromorphic soils in geochemical conjugations at the shores of lakes and rivers polluted with radioactive materials from different sources [38–40]. Table 5 shows the ^{90}Sr inventory in the soils of shores of several lakes. Soils of eluvial and trans-eluvial elements of the landscape (for each lake) were contaminated by ^{90}Sr approximately equally. The runoff processes did not have a significant effect on the redistribution of this radionuclide in the shores of lakes located both in the EURT zone and outside it. The levels of soil contamination rose with increasing distance from the water's edge (Berdenish Lake, EURT). This phenomenon is associated with the processes of self-purification of subaquatic soils in the shore zones. The same ^{90}Sr distribution was found in other lakes in the Urals [14, 18, 39, 40].

A similar level of soil contamination by ^{90}Sr within eluvial and trans-eluvial elements of the landscape was also observed on riverbanks (Table 6). The content of

Table 5 ^{90}Sr inventories in the soils of geochemical conjugations (coastal zone of the EURT lakes)

Zone	Coordinates	Site	Elementary landscape	Distance from bank of lake, m	kBq/m^2
Impact EURT	55°48′ N, 60°51′ E	Southeastern bank of Berdenish Lake	Trans-accumulative	1	270±50
			Trans-accumulative	4	2,300±630
			Trans-eluvial	20	16,700±3,540
			Eluvial	150	11,833±3,570
Buffer EURT	56°21′ N, 61°33′ E	Northern bank of Sungul' Lake	Trans-eluvial	10	22.7±9.3
			Eluvial	200	13.0±5.0
Background	56°49′ N, 61°54′ E	Western bank of Kurtuguz Lake	Trans-eluvial	10	0.8±0.2
			Eluvial	100	1.1±0.3

Table 6 The ^{90}Sr inventories in floodplains of rivers contaminated from different sources, kBq/m^2

Elementary landscape	Distance from bank, m	Gas-aerosol emissions		Liquid discharges	
		PA "Mayak" zone, Karabolka River	BNPP zone, Kamenka River	PA "Mayak" zone, Techa River	BNPP zone, Ol'khovka River
Trans-accumulative (foot of the slope)	1–3	160±20	2.8±1.0	128.6±30.2	49.0±12.0
Trans-eluvial (slope)	10–20	110±50	3.1±0.3	17.0±5.2	2.9±1.9
Eluvial (watershed)	100–500	200±50	1.7±0.5	12.2±3.6	2.4±1.1

^{90}Sr varies slightly in the soils of trans-accumulative sections of riparian zones of the Karabolka and Kamenka rivers contaminated with atmospheric fallouts.

A different situation develops in the floodplains of rivers contaminated by discharges of radioactive waste. ^{90}Sr inventories were an order of magnitude higher in the floodplain of the Techa and Ol'khovka rivers in comparison with the soils of the watershed and the coastal slope. Floodplains are the geochemical barriers on which ^{90}Sr accumulates as a result of sorption by soil particles from contaminated river waters and can for a long time be a source of secondary pollution of the environment [38].

Comparison of the data allows us to conclude that the distribution of ^{90}Sr in the geochemical conjugations of the shore zones of the rivers and lakes depends on the source of radionuclide intake. The runoff processes make insignificant contribution to the migration of ^{90}Sr in the landscapes connected through a runoff. Migration processes in the shore zones of rivers and lakes can balance the runoff or substantially exceed it.

Table 7 The ^{90}Sr inventory in 0–20 cm layer of automorphic and hydromorphic soils, % of the total content in the soil profile

	Density of contamination, %			
	Automorphic soil		Hydromorphic soil	
Site, distance from source of contamination	Min-max	M	Min-max	M
Center axis of EURT, 4–20 km	72.1–95.6	86.0	81.2–88.5	84.8
Floodplain of the Techa River, 70–300 km	85.7–92.8	88.5	17.4–54.0	40.4
Observed zone of BNPP, 13 km	72.5–100.0	95.0	17.2–65.6	44.4
Outside of any contaminated zones	93.5–100.0	99.3	8.9–68.9	38.6

5 Vertical Distribution of ^{90}Sr in Soil Profiles

For 60 years since the accident, the ^{90}Sr migrated deep into the soil profile. The depth of migration depended mainly on the soil moisture regime (Table 7). The upper 0–20 cm layers of the EURT automorphic soils contain 86% of ^{90}Sr. The values reach 95.0–99.3% in the zone of influence of BNPP and beyond. Other researchers [13] also found the accumulation of the main amount of ^{90}Sr in the 0–20 cm soil layer as in the EURT zone and beyond.

The inventories of ^{90}Sr are much lower in hydromorphic soils (Table 7). The maximum content of ^{90}Sr was found in the upper 0–20 cm layer of hydromorphic soils of EURT, which were located in the shore zone of lakes and were characterized by a small thickness (25–30 cm). In other sites, in river floodplains, the thickness of the soils reached 60 cm. More than 50% of the total radionuclide content migrated beyond the 0–20 cm layer of these soils. Apparently, the morphology of soils also affects the scale of vertical migration of ^{90}Sr.

The vertical distribution of ^{90}Sr in automorphic soils does not depend on the source of contamination (Fig. 6). The influence of soil characteristics (chernozem or sod-podzolic soil) was also insignificant. For example, the maximum of ^{90}Sr was expressed more sharply in sod-podzolic soils than in chernozem.

The vertical distribution of ^{90}Sr in soil profiles strongly depends on the water regime [41]. So on the dry sites (watershed, slope), where pollution was formed mainly due to the atmospheric fallout, the maximum of ^{90}Sr was revealed at a depth of 5–15 cm (Fig. 7). At a depth of 30 cm, very small amounts are noted. In the flooded soils of the Ol'khovka floodplain, the content of ^{90}Sr increases downward along the soil profile and reaches a maximum at a depth of 30 cm. The minimum amounts of ^{90}Sr are found even at a depth of 80 cm.

6 Conclusions

1. The activities of NFC enterprises in the Urals led to increased radioactive contamination of the territory. Densities of contamination in floodplain soils of Techa River by ^{90}Sr in the residential area vary from 20 to 1,600 kBq/m^2; the

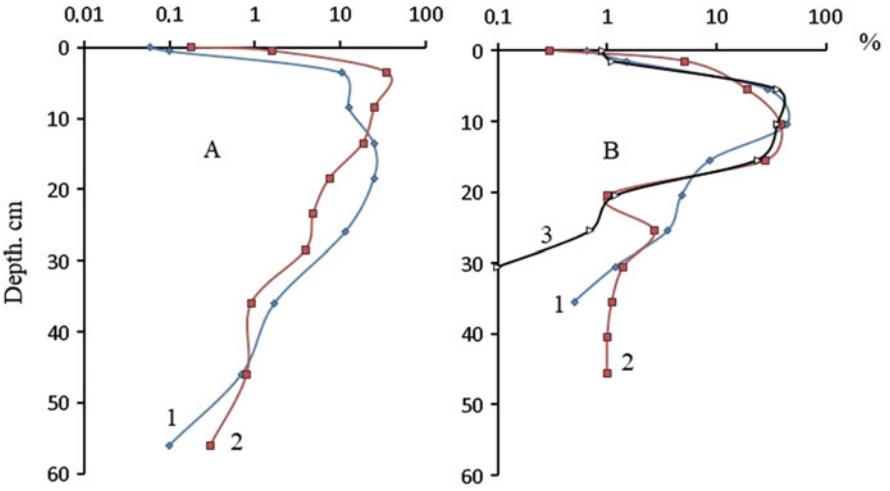

Fig. 6 The vertical distribution of ^{90}Sr in chernozem (**a**) and in sod-podzolic soil (**b**) contaminated from various sources. 1, central axis of the EURT; 2, eastern periphery of the EURT; 3, observed zone of BNPP

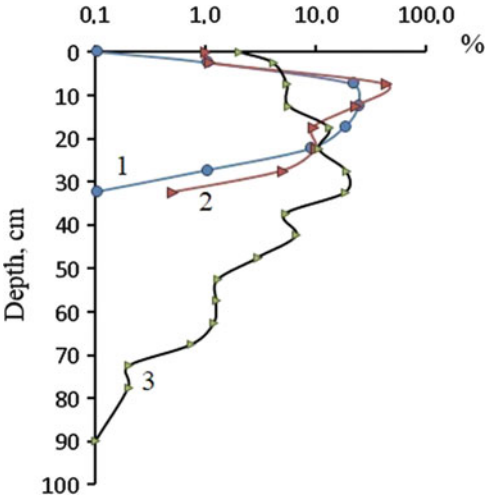

Fig. 7 The vertical distribution of ^{90}Sr in the soils in geochemical conjugations in the zone of influence of the BNPP liquid discharges. 1, watershed, brown forest soil; 2, slope, soddy-meadow soil; 3, foot of the slope, alluvial peat-gley soil

values are one to three orders of magnitude higher than the background level. Migration of the radionuclide downstream led to contamination of the river system: Iset-Tobol-Irtysh-Ob.

2. The density of soil contamination by ^{90}Sr in the EURT zone reaches 70,000 kBq/m^2. The radionuclide content decreases with distance from the epicenter of the Kyshtym accident in accordance with the exponential function. The central axis of the EURT was contaminated mainly (91.8–99.8%) as a result of the Kyshtym accident. Contamination of the eastern periphery was also due to wind transfer of the radionuclide from the shores of the Karachay Lake; the contribution reaches 70% in some sites.
3. The soil contamination by ^{90}Sr in the zone of influence of gas-aerosol emissions of BNPP and IRM remains unchanged for 35 years. The values differ insignificantly from the background levels of ^{90}Sr in the soils of the Middle and Southern Urals. Liquid discharges of BNPP caused increased concentrations of ^{90}Sr in the Ol'khovskoye swamp and in the floodplain soils of the Ol'khovka and Pyshma rivers. The maximum pollution does not exceed 50 kBq/m^2.
4. The chronic gas-aerosol emissions from NFC enterprises and global fallouts have maintained a stable background level of ^{90}Sr for many years, both global (1.3 Bq/m^2) and regional (1.6–3.0 Bq/m^2) origins. All background sites were located within 100 km zones of influence of PA "Mayak" and BNPP. There are no significant differences in the content of ^{90}Sr between these sites, so it can be assumed that the data in the range 1.3–3.5 kBq/m^2 are the background for the Middle and Southern Urals.
5. Migration of ^{90}Sr within geochemical conjugations depends on the sources of intake (gas-aerosol emission or liquid discharges) of the radionuclide into the environment. The depth of vertical migration and the character of the distribution of the radionuclide in soil profile depend on the regime of moistening and the type of soils.

Acknowledgments This study was performed within the frameworks of state contract with the Institute of Plant and Animal Ecology, Ural Branch, Russian Academy of Sciences.

References

1. Izrael YA (2013) Atlas of the East Ural and Karachay Radioactive Trace including forecast up to 2047. "Infosphere" Foundation, IGCE Rosgidromet and RAS, Moscow, Russia
2. Shershakov VM, Bulgakov VG, Kryshev II, Vakulovsky SV, Katkova MN, Kim VM, Kryshev AI (2017) Radiation situation in the territory of Russia and neighboring countries in 2016 yearbook. Roshydromet, Moscow, Russia
3. Mikhailovskaya LN, Molchanova IV, Nifontova MG (2015) Global fallout radionuclides in plants of terrestrial ecosystems of the Ural region. Russ J Ecol 46:7–13
4. Molchanova IV, Kaygorodova SY, Mikhailovskaya LN, Gaberstein TY, Hlystov IA (2016) Composition, property and level of radionuclide contamination of the soil cover within 15 km zone of the Beloyarsk Nuclear Power Plant. J Siber Fed Univer Biol, pp 321–337

5. Trapeznikova VN, Korzhavin AV, Trapeznikov AV, Plataev AP (2017) The results of the long-term monitoring of the cross-border air transport of the artificial radionuclides to the territory of the Sverdlovsk region from the nuclear fuel cycle facilities located in the Chelyabinsk region. Medico-Biol Socio-Psychol Probl Saf 1:84–93
6. NRB-99/2009 Norms of Radiation Safety (2009) Sanitary-epidemiological rules and regulations (SanPiN 2.6.1.2523-09): approved and entered into force on 01.09.2009. Federal Center for Hygiene and Epidemiology of Rospotrebnadzor, Moscow, Russia
7. Aarkrog A, Trapeznikov AV, Molchanova IV, Pozolotina VN, Polikarpov GG, Dahlgaard H, Nielsen SP (2000) Environmental modelling of radioactive contamination of floodplains and sorlakes along the Techa and Iset rivers. J Environ Radioact 49:243–257
8. (1991) Conclusions of the Commission to assess the of ecological situation in the area of the production association "Mayak" Nuclear Power Ministry of the USSR, organized by order of the Presidium of the USSR No 1140-501 on 12/06/1990. Radiobiologiya 31:436–452
9. Aarkrog A, Dahlgaard H, Nielsen SP, Trapeznikov AV, Molchanova IV, Pozolotina VN, Karavaeva EN, Yushkov PI, Polikarpov GG (1997) Radioactive inventories from the Kyshtym and Karachay accidents: estimates based on soil samples collected in the South Urals (1990-1995). Sci Total Environ 201:137–154
10. Nikipelov BV, Romanov GN, Buldakov LA, Babaev NS, Kholina YB, Mikerin EI (1989) A radiation accident in the Southern Urals in 1957. Sov Atom Energy 67:569–576
11. Molchanova IV, Pozolotina VN, Karavaeva EN, Mikhaylovskaya LN, Antonova EV, Antonov KL (2009) Radioactive inventories within the East-Ural radioactive state reserve on the Southern-Urals. Radioprotection 44:747–757
12. Pozolotina VN, Molchanova IV, Mikhaylovskaya LN, Antonova EV, Karavaeva EN (2012) The current state of terrestrial ecosystems in the Eastern Ural Radioactive Trace. In: Guillen FJ (ed) Radionuclides: sources, properties and hazards. Nova Science Publication, New York, pp 1–22
13. Tarasov OV, Fedorova OV, Tananaev IG, Sergienko VI (2016) Forms of state and the migration of radionuclides in the soil of the East Ural Radioactive Trace. Bull Far East Branch Russ Acad Sci 1:47–52
14. Trapeznikov AV, Molchanova IV, Karavaeva EN, Trapeznikova VN (2007) The migration of radionuclides in freshwater and terrestrial ecosystems. Year Book, Ekaterinburg. Russia
15. Mikhaylovskaya LN, Molchanova IV, Karavaeva EN, Pozolotina VN, Tarasov OV (2011) Radioecological investigation of the soil cover of Eastern Urals State radioactive reserve and neighboring areas. Radiats Biol Radioecol 51:476–482
16. Tsvetaeva NE, Filin VM, Ivanova LA, Revnov VN, Rodionov EP, Rudaya LY, Suslin IA, Shapiro KY (1984) Use of monoisooctylmethylphosphonic acid and its trivalent iron salt in determining radionuclides in effluents. Sov Atom Energy 57:548–552
17. Kulikov NV, Molchanova IV, Karavaeva EN (1990) Radioecology of soil and vegetation cover. Sverdlovsk. Russia
18. Molchanova IV, Karavaeva EN, Mikhailovskaya LN (2013) Radioecological research on ecosystems of Beloyarsk NPP on the Ural. LAP LAMBERT Academic Publishing, Riga
19. Utkin VI, Chebotina MY, Evstigneev AV, Ekidin AA, Rybakov EN, Trapeznikov AV, Shchapov VA, Yurkov AK (2000) Radioactive disasters of the Ural. Ural Branch of the Russian Academy of Sciences, Year Book, Ekaterinburg, Russia
20. Trapeznikov AV, Pozolotina VN, Chebotina MY, Chukanov VN, Trapeznikova VN, Kulikov NV, Nielsen SP, Aarkrog A (1993) A radioactive contamination of the Techa River, the Urals. Health Phys 65:481–488
21. Trapeznikov A, Aarkrog A, Pozolotina V, Nielsen SP, Polikarpov G, Molchanova I, Karavaeva E, Yushkov P, Trapeznikova V, Kulikov N (1994) Radioactive pollution of the Ob river system from urals nuclear enterprise 'MAJAK'. J Environ Radioact 25:85–98
22. Trapeznikov AV, Pozolotina VN, Molchanova IV, Yushkov P, Trapeznikova VN, Karavaeva EN, MYa C, Aarkrog A, Dahlgaard H, Nielsen SP, Chen Q (2000) Radioecological investigation of the Techa-Iset' river system. Russ J Ecol 31:224–232

23. Trapeznikov AV, Molchanova IV, Karavaeva EN, Mikhailovskaya LN, Nikolkin VN, Trapeznikova VN, Korzhavin AV, Peremyslova LM, Popova IY, Vorobyova MI, Kostyuchenko VA (2007) The results of long-term radioecological research Techa river. Rad Safet Issue 3:36–49
24. Mikhailovskaya LN, Molchanova IV, Pozolotina VN, Karavaeva EN (2002) Experimental assessment of the water migration of radionuclides in floodplain soils of the Techa river. Eurasian Soil Sci 35:1003–1006
25. Mokrov YG (1996) A semiempirical model of the transport of strontium-90 with the waters of the river Techa. Vopr Radiats Bezopas 1:20–27
26. Molchanova IV, Karavaeva EN, Mikhailovskaya LN (2009) The results of long-term radioecological monitoring of Natural Ecosystems in the area of liquid waste discharges from the Beloyarsk NPP. Vopr Radiats Bezopas 4:20–26
27. Molchanova IV, Pozolotina VN, Antonova EV, Mikhaylovskaya LN (2011) The impacts of permanent irradiation on the terrestrial ecosystems of the Eastern-Ural Radioactive Trace. Radioprotection 46:567–572
28. Molchanova I, Mikhailovskaya L, Antonov K, Pozolotina V, Antonova E (2014) Current assessment of integrated content of long-lived radionuclides in soils of the head part of the East Ural Radioactive Trace. J Environ Radioact 138:238–248
29. Mikhailovskaya LN, Pozolotina VN, Antonova EV (2018) Accumulation of ^{90}Sr by plants of different taxonomic groups from the soils at the East Ural Radioactive Trace. In: Gupta DK, Walther C (eds) Behavior of strontium in plants and the environment. Springer, Cham, pp 61–73
30. Molchanova IV, Mikhailovskaya LN, Pozolotina VN, Antonova EV (2014) Man-made radionuclides and their accumulation by plants of different taxonomic groups from the soils of the Eastern Ural Radioactive Trace. Radiats Biol Radioecol 54:77–84
31. Chukanov VN, Bazhenov AV, Varaksin AN, Volobuev PV, Zhukovsky MV, Izyumov MV, Kazantsev VS, Katsnelson BA, Korobitsyn BA, Kuligin AP, Gjkpbr EB, Privalova LI (1996) The East Ural Radioactive Trace (Sverdlovsk Oblast). Yekaterinburg: UB RAN
32. Bakurov AS, Shein GP, Aksyonov GM, Rovny SI (2007) Experience of overcoming the consequences of technogenic disasters and the development of nuclear technologies: material of the scientific and practical conference marking the 50th anniversary of the PA MAYAK disaster. Chelyabinsk, pp 8–25
33. Shershakov VM, Bulgakov VG, Kryshev II, Vakulovsky SV, Katkova MN, Kim VM, Kryshev AI (2016) Radiation situation in the territory of Russia and neighboring countries in 2015 yearbook. Roshydromet, Moscow, Russia
34. Sadchikov VI, Bondar YI, Zabrotski VN, Kalinin VN, Brown JE, Dowdall M (2018) Radionuclides in soil in the areas of forest on the territory of the Exclusion zone in the Republic of Belarus. Radiats Biol Radioecol 58:183–194
35. Makhon'ko KP (1990) Radiation situation in the territory of the USSA in 1989. Yearbook. NPO Tayfun, Obninsk, Russia
36. UNSCEAR United Nations Scientific Committee on the Effects of Atomic Radiations (1996) Sources and effects of ionizing radiation. Report to the General Assembly, with Scientific Annexes. New York. http://www.unscear.org/unscear/en/publications/1996.html
37. Molchanova IV, Karavaeva EN (1985) Distribution of ^{90} Sr and ^{137} Cs in the geochemically-conjoint landscape areas. Sov J Ecol 1:69–72
38. Molchanova IV, Karavaeva EN, Mikhailovskaya LN, Pozolotina VN, Lobanova LV (2003) The role of floodplain soils as a barrier to radionuclide migration: an example of the Techa-Iset river system. Russ J Ecol 34:236–241
39. Pozolotina VN, Molchanova IV, Karavaeva EN, Mikhailovskaya LN, Antonova EV (2008) The current state of terrestrial ecosystems at the East Ural Radioactive Trace area: contamination levels and biological effects. Goschitsky Press, Ekaterinburg

40. Pozolotina VN, Molchanova IV, Karavaeva EN, Mikhaylovskaya LN, Antonova EV (2010) Radionuclides in terrestrial ecosystems of the zone of Kyshtym accident in the Urals. J Environ Radioact 101:438–442
41. Perevolotskaya TV, Bulavik IM, Perevolotsky AN (2009) On the effect of partial flooding on ^{137}Cs and ^{90}Sr in forest biogeocenosis. Radiats Biol Radioecol 49:291–301

^{90}Sr in the Components of Pine Forests of Belarusian Part of Chernobyl NPP Exclusion Zone

Maksim Kudzin, Viachaslau Zabrotski, Dzmitry Garbaruk, and Anatoliy Uhlianets

Contents

Abstract The significant part of the territory (43.3%) of State nature conservation research institution "Polessye State Radiation Ecological Reserve" is occupied by the pine stands. The forest litter in case of mossy, heath, bilberry types of pine forest remained to be the accumulator of large part of ^{90}Sr retaining from 26 to 38% of its inventory. The common peculiarity of distribution of ^{90}Sr through mineral part of soil profile in pine stands was its accumulation by upper 0–5 cm under litter layer with following decreasing in dipper layers. The part of ^{90}Sr absorbed by mineral soil layer varied from 21 to 36% of its inventory in pine forests. The ability of tree organs and tissues of pine plantations to accumulate ^{90}Sr was decreasing in the following order: bark > roots > wood on the automorphic (well drained) soils and roots > bark > wood on the semihydromorphic soils. The transfer of ^{90}Sr to the wood of understory vegetation was decreased in the order: oak > Persian berry > mountain ash. For the leaves, the same row was mountain ash > Persian

M. Kudzin · V. Zabrotski (✉) · D. Garbaruk · A. Uhlianets
Polessye State Radiation Ecological Reserve, Khoiniki, Gomel, Belarus
e-mail: vzabrotski@tut.by

P. Pathak, D. K. Gupta (eds.), *Strontium Contamination in the Environment*,
The Handbook of Environmental Chemistry 88,
https://doi.org/10.1007/978-3-030-15314-4_9

berry > oak. Each species of understory vegetation was characterized by its own specificity of ^{90}Sr absorption by the organs and tissues. The content of ^{90}Sr in species of alive soil cover in pine forests was decreasing in the following order: adderspit > dicranum moss > Schreber's big red stem moss. Their aboveground phytomass accumulated more ^{90}Sr than roots. The experimental data described in the paper were received in the period 2014–2017.

Keywords β-Radiometry · Chernobyl radioactive contamination · Dose rate · Pine forest · Strontium-90 · Transfer factor

1 Introduction

The peculiarity of Chernobyl accident consists in releasing into environment the high quantity of the radionuclides in the form of particles of the irradiated nuclear fuel (fuel particles) [1]. About 30% of ^{137}Cs, 73% of ^{90}Sr, and 97% of Pu fallen on the territory of Belarus were deposited on the territory of Polessye State Radiation Ecological Reserve [2, 3] mainly as fuel particles. Due to weathering, the fuel particles began to dissolve with following transfer of ^{90}Sr into moveable form available to vegetation. There are numerous experimental evidences that content of ^{90}Sr in woods of exclusion zone exceeds that of ^{137}Cs in tenth times [4, 5]. ^{137}Cs and ^{90}Sr are regarded as the most dangerous radionuclides due to their relatively high half-life periods and mobility in environment. The radiotoxicity of ^{90}Sr is higher than that of ^{137}Cs [6]. At the same time, the quantity of studies devoted to its behavior in environment is substantially less [7]. Such situation is explained by difficulties of its registration in environmental samples because of absence of any gamma-emission lines in its decay scheme [8]. The accident at Fukushima Daiichi attaches additional impulse to radioecological studies, in particular of radioactively contaminated forest [9]. Nevertheless, the quantity of experimental data devoted to study of ^{90}Sr behavior in the environment is still insufficient. The purpose of current work was to present more experimental data about behavior of ^{90}Sr in forest ecosystems after Chernobyl accident.

2 Brief Description of Pine Forests of Belarusian Part of Chernobyl Exclusion Zone

Pine forests dominate in the sylva-covered territory of Belarusian part of ChNPP exclusion zone. They occupy 523 km^2 or 43.3% of all afforested territory. The upland pineries prevail; they occupy 99.8% of square of pine formation and are usually used for fuelwood production. Pines' mean age is approximately 50 years. More than half (55%) pineries do not have any admixtures of other species and are pure stands. Forty-five percent of pine forests fall on mixed stands. In 90% of

mixed pineries, the admixture is birch, in 4.1% aspen, in 3.1% black alder, and in 2.8% oak. Sometimes the representatives of other local and alien wood species occur (eight species to the middle of 2018), and their total percentage is 0.2%. The mean inventories of the timber (wood production) in upland pineries come to 18, 500 m^3 km^{-2}.

The pine is undemanding to the soil fertility and able to live in conditions of various soil humidities. On that reason, its plantings occur in very different soil conditions. The following classification of the soils according to their fertility is accepted in Belarus: poor, relatively poor, comparatively rich, and rich. The main territories occupied by pine forests (85%) are related to poor conditions. 14.2% of pineries are growing on relatively poor soils, and only 0.8% relates to comparatively rich soils. The distribution of the territory occupied by pine forests depending on soil wetting type is the following: 86.5%, automorphic (well drained); 12.8%, semihydromorphic; and 0.7%, hydromorphic (swamped).

Forest type is the main classification unit being used in Belarus for description of forest ecosystems. The term "forest type" relates to the forests with homogeneous forest growing conditions, with corresponding species composition and other vegetation. The name of the wood species dominating in the forest (edificator) is used to designate the forest type. The same is true for the plant (indicator) characterizing the soil cover, undergrowth, and wood story [10]. Since it is practically important for the forest management, the analysis of radiation situation and evaluation of radionuclide accumulation by wood plants is bound to forest type [11–15].

The mossy, heath, and bilberry pineries dominate in typological structure of upland pine forests of exclusion zone. They occupy 51.8, 22.0, and 12.8% of total square of upland pineries (subformation) accordingly. They are growing on poor sandy soils widely distributed in exclusion zone. The planting of 41–60 years is the main (42.0%) in their age structure. The percentage of young growth (up to 40 years) is two times less (19.8%) as well as for stands of 61–80 years (19.5%). Only 7.2% of the territory occupied by pine forests falls on planting older than 81 years.

The total inventory of trunk wood in upland pine forests of exclusion zone amounts 9.7 million cubic meters including 8.6 million cubic meters or 88.7% of total inventory of subformation falling on pine. Its main part (89.9%) concentrates in mossy (57.7%), heath (17.1%), and bilberry (15.1%) pineries.

According to Belarusian classification [16], the heath pineries occupy raised relief elements with poor sod-podzol sandy dryish (characterizing little (if any) humidity) or fresh soils. Their stands are characterized by III or (more seldom) II growth class. Common heather (*Calluna vulgaris* (L.) Hull) serves as the plant indicator of forest type. The mossy pineries cover plain sites with sod-podzol fresh sandy soils. Their productivity corresponds to II (I) growth class. Plant indicator of forest type – moss. The soils of both last-named forest types are characterized by automorphic (well drained) humidification type. The bilberry pineries are located at the foot of the slopes passing to the swamps, lows, and valleys. Their soils are sod-podzol, gleyey, sandy, and sometimes sandy loam with semihydromorphic humidification type. Due to more rich and moistened soils, the productivity of bilberry pineries is evaluated as I sometimes II growth class. Their plant indicator is common bilberry (*Vaccinium myrtillus* L.).

ChNPP exclusion zone is situated in southeast of Belarusian Polessye which territory is characterized by weakly expressed relief and relatively close groundwater level. At these conditions, the heath and mossy pineries are often characterized by close soil hydrological conditions [17] that should be taken into account in evaluation of radionuclide accumulation by tissues and organs of pine stands.

3 Object and Methods of Research

3.1 Object of Research

The objects of research were the components (wood, bark, roots) of pine plantings of the most widespread forest types in exclusion zone of ChNPP – heath pinery (*Pinetum callunosum*), mossy pinery (*Pinetum pleurociosum*), and bilberry pinery (*Pinetum myrtillosum*), according to Belarusian classification [16].

The heath pineries (Table 1) were represented by five plantings aged 41–73 years both natural and man-made origin, III and II growth classes. There was no admixture of other species in stand composition. The man-made stands were thicker than natural. Their undergrowth was incomplete and contained mainly Persian berry (*Frangula alnus* Mill.) and mountain ash (*Sorbus aucuparia* L.). Heather (*Calluna vulgaris* (L.) Hull), adderspit (*Pteridium aquilinum* L.), Schreber's big red stem moss (*Pleurozium schreberi* Brid.), and dicranum moss (*Dicranum polysetum* Sw.) dominated in living soil cover. The plantations of heath pineries usually occupied the raised relief elements with poor sandy fresh or dryish soils. There was a 16.5-fold difference in density contamination of the plantings by ^{90}Sr – from 36.7 to 605.1 kBq m^{-2} (Table 1).

The mossy pineries (six plantings) aged from 49 to 75 years presumably of man-made origin were characterized mainly by I (sometimes II) productivity class. Their thickness of stand was close to that of heath pine forests. The undergrowth was thick and included Persian berry (*Frangula alnus* Mill.), mountain ash (*Sorbus aucuparia* L.), and English oak (*Quercus robur* L.). The inventory of trunk wood in mossy pineries was higher than that of heath pine stands. Schreber's big red stem moss (*Pleurozium schreberi* Brid.), dicranum moss (*Dicranum polysetum* Sw.), and common bilberry (*Vaccinium myrtillus* L.) were extended in living soil cover. As concerns the relief, the mossy pineries were situated below heath pineries and occupied flat lands. The density contamination of such plantations varied from 63.3 to 249.8 kBq m^{-2} (Table 1).

There were three plantations of bilberry pine forests of natural origin aged 61–64 years and I–Ia productivity classes. Up to 10% of silver birch (*Betula pendula* Roth.) and white birch (*Betula pubescens*) could be occurred in the stands. Aspen (*Populus tremula* L.) could be found very seldom. The main constituent of young growth was English oak (*Quercus robur* L.); Persian berry (*Frangula alnus* Mill.) and mountain ash (*Sorbus aucuparia* L.) were the main constituents in undergrowth. The living soil cover included common bilberry (*Vaccinium myrtillus* L.), adderspit

Table 1 Forestry-radiological characteristic of the pine stands in the sample areas

Composition[a]	Forest type	Age, year	Productivity class	Tree density, number, km^{-2}	Mean		Wood production, m^3 km^{-2}	^{90}Sr contamination density, kBq m^{-2}
					D[b], cm	H[c], m		
10P	Heath	73	II	59,600	28.5	21.3	39,000	68.9
10P	Heath	64	II	83,200	25.2	23.4	44,000	137.7
10P	Heath	73	III	74,000	24.0	17.8	30,000	36.7
10P	Heath	41	III	291,000	13.4	11.9	22,000	605.1
10P	Heath	50	III	229,000	14.8	15.0	30,000	129.9
10P	Mossy	52	I	138,400	21.9	20.2	53,000	63.3
10P	Mossy	57	I	134,000	21.7	19.9	47,000	87.5
10P	Mossy	71	I	82,400	27.3	24.9	54,000	158.3
10P	Mossy	54	I	230,000	18.2	16.9	45,000	48.8
10P	Mossy	49	II	231,000	16.0	15.4	36,000	26.4
10P	Mossy	75	I	56,000	26.5	33.6	58,000	249.8
9P1B	Bilberry	64	Ia	61,000	32.9	25.7	45,000	121.5
9P1B	Bilberry	61	Ia	54,000	32.5	25.6	49,000	169.1
9P1B + A	Bilberry	64	I	43,000	32.7	23.1	33,000	24.1

[a]*P* pine, *B* birch, *A* aspen
[b]*D* diameter of the trunk
[c]*H* tree's height

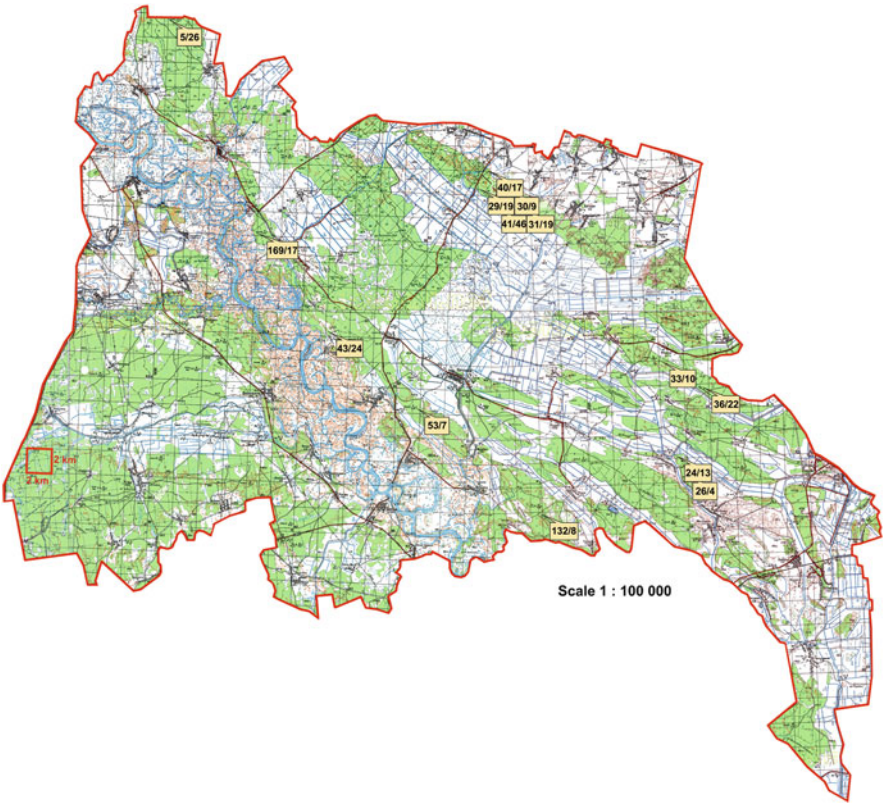

Fig. 1 The locations of the sample areas

(*Pteridium aquilinum* (L.) Kuhn ex Decken), blue moor grass (*Molinia caerulea* (L.) Moench), Schreber's big red stem moss (*Pleurozium schreberi* Brid.), and dicranum moss (*Dicranum polysetum* Sw.). The plantations were growing on bottom parts of gentle slopes adjusting the swamps. The density contamination of soil by ^{90}Sr in that forest type was substantially lower (24.1–169.1 kBq m^{-2}), than in heath and mossy pineries (Table 1). The locations of the sample areas are demonstrated in Fig. 1.

3.2 Methods of Research

In each type of the forest, three sample areas (further "SA") were arranged. Preliminarily the gamma-radiation dose rate (further "DR") was measured at the height of 1 m in each sample area to be sure that the level of radioactive contamination of the SA is similar. If difference in values of dose rates was higher than 10%, another place for sample area was chosen with more uniform characteristics of radioactive contamination.

In accordance with adopted normative documents in and around radiation examination and monitoring of forest resources [18–20], the dimensions of the sample area corresponded 50 × 50 m.

Samples of soil with alive soil cover and forest litter were taken in nine points (in the angles and along the diagonals of the sample area) not closer than 1 m from the tree's trunks. The standard sampler with diameter 4 cm and height 20 cm was used.

Dose rate was measured in the points of soil sampling at the heights of 3–4 cm and 1 m above soil surface. The dose rate at the height of 3–4 cm was measured for the rejection of the unrepresentative points (with uncharacteristic local contamination). If the value of dose rate measured at the height 3–4 cm differed from the DR measured at the height of 1 m more than two times, this place was regarded as uncharacteristic, and soil was sampled in another point.

The sampling forest litter and soil were exempted in undisturbed places between tree's crones not less than 1–1.5 m from the trunk (or stump) avoiding glades, openings, and depressions. The mandatory checking of dose rate value was simultaneously fulfilled at the height of 3–4 cm and 1 m.

To determine the content of ^{90}Sr along the soil profile, the following fourfold (quadruplicated) samples were taken:

Forest litter using pattern (template) 20 × 20 cm from three layers: tree waste (Ol), enzymatic (Of), and humified (Oh)

Soil in 5 cm layers on the depth of 40 cm with the use of sampler 20 × 20 cm.

To determine the content of ^{90}Sr in organs and tissues of the plants, the following samples were taken:

Roots and phytomass of the vegetation of a live soil cover

Roots, wood, and leaves of the vegetation of undergrowth and young growth

Roots, bark, and wood of the vegetation of trees of main story.

The samples of the wood without bark were taken in the sample area at the height 1.3 m from 20 to 30 growing trees of I–II classes of growth and development according to the Kraft (Craft) classification. The age-specific wood borer was used (the borer reached the center of the trunk). One core sample was taken from each tree. The quantity of the trees, from which the core samples were taken, depended on the values of the tree's trunk diameters: 20 samples were enough if the diameters were more than 35 cm; 25 samples were taken if the tree diameters changed from 25 to 35 cm; and 30 samples were taken if the tree diameters were less than 25 cm.

The trees for the sampling of the bark were chosen from the growing trees of I–II classes of growth and development according to the Kraft classification. Bark samples were taken from seven to ten growing trees from the height 1.3 m. The cylindrical borer with diameter 40 mm was used to take the bark with bast (inner bark). If the bast remained on the trunk after the withdrawal of the borer from the tree, it was separated using knife and added to the bark sample.

The quadruplicated root samples were taken simultaneously with soil through the digging procedures. The sampling of roots, wood, and leaves of the vegetation of understory as well as roots and phytomass of the vegetation of a live soil cover was exercised evenly through all sample areas in quantity enough for the representative

sample. The samples selected were packed into the doubled plastic bags providing the presence of the sample's passport. After transportation they were dried on the air until air-dried condition. Soil was thoroughly mixed; stones, roots, and other inclusions were removed. The samples of the forest litter, wood, roots, bark, leaves, grassy plants, and mosses were cut into pieces of 2–3 cm in dimensions using scissors and pruners. Then they were mixed again until uniform distribution of the matter of the sample was reached.

The dose rate measurements were performed using AT6130 Radiation Monitor. The content of ^{90}Sr in soil samples was determined using MKS AT1315 gamma-beta-spectrometer [31]. The intrinsic relative error of the spectrometer during activity measurement according to producer data equals 20% (Atomtex). During the measurement of the parallel samples characterizing the same component of pine forest, the relative standard uncertainty of the mean as a rule was substantially increased under the influence of wide range of different factors and very often exceeded the value of 100%. All measurements were performed by the staff of laboratory of spectrometry and radiochemistry which is accredited according to the requirements ISO/IEC 17025 since 2005. Since 2011, the laboratory regularly participates in worldwide proficiency tests organized by IAEA on the determination of natural and artificial radionuclides in different environmental objects. The laboratory does it to receive the proof of reliability of its analytical data. Transfer factors of ^{90}Sr in tissues and organs of plants (T_{ag}) were calculated to be used as characteristics of their ability to accumulate the ^{90}Sr regardless of density contamination of the soil. T_{ag} was calculated as activity concentration in plant compartments (Bq kg^{-1} dry weight) divided by density of contamination of the soil (Bq m^{-2}).

4 Distribution of ^{90}Sr Between Horizons of Forest Litter and Soil of Dominating Types of Pineries

The ability of the forest litter to accumulate radionuclides depends on its thickness, composition and structure, availability of mossy cover, percentage of the conifers in the plantations, and availability of deciduous undergrowth species, bushes, and semifrutex. Accumulation of radionuclides by forest litter is decreasing in rising of deciduous species percentage and in change of the soil wetting type from automorphic to hydromorphic [3].

The thick layer of forest litter is usually forming in pine plantations. Due to slow mineralization of coniferous mossy tree waste (from 4 to 6 years) [21], only little part of radionuclides is capable to migrate into humic-eluvial horizon.

The specificity of radioecological research as well as genesis and structure of pine forests makes it necessary to differ the examination of the vertical distribution of the radionuclides in organogenic horizon (forest litter) from that in mineral layer. The change of radionuclide percentage in a certain layer with time could be used as

an indicator of radionuclide redistribution through the vertical profile. According to the results of our research, the distribution of ^{90}Sr between forest litter and soil depended on forest type. The ^{90}Sr content in the forest litter was as much as up to 32.0% for the mossy pinery, up to 60.2% in heath pinery, and up to 53.2% in bilberry pinery (Fig. 2). The difference in ^{90}Sr inventory in Ol layer reached two times and depending on forest type changed from 8.0% in bilberry and 10.1% in mossy up to 4.5% in heath pinery (from its inventory in soil profile) (Fig. 2).

The differences in ^{90}Sr inventory for Of layer were less substantial. In enzymatic layer it varied on an average from 5.2% in bilberry and 5.7% in mossy types of forest to 8.5% in heath one. The largest quantity of ^{90}Sr was concentrated in humified (Oh) layer of the forest litter, and its inventory changed depending on forest type in the range of three and more times from 16.2% in mossy type to 40.2% in bilberry and 47.2 in heath ones (Fig. 2). Mention should be made about inhomogeneous distribution of ^{90}Sr through the forest litter layers and absence of any regularity in its migration through their horizons.

Conclusion could be made that the redistribution of ^{90}Sr inventory between the layers of forest litter depended on its inflow in soil surface with tree waste, soil-ecological conditions, and speed of organic matter degradation and composition of plantation. On that reason the velocities of ^{90}Sr migration for various layers of forest litter were different, but total feature was the maximum of its content in lower

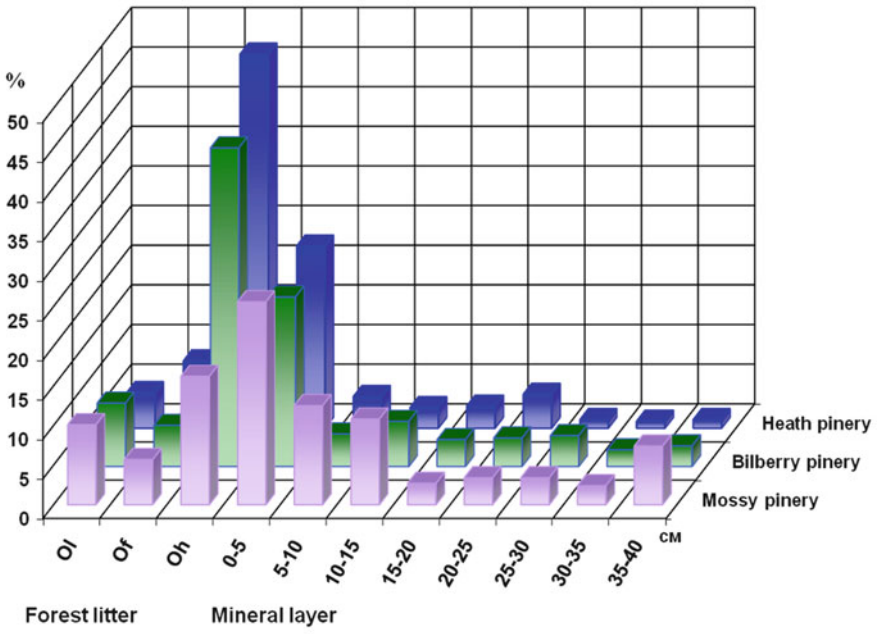

Fig. 2 Distribution of ^{90}Sr in litter and mineral layer of mossy, heath, and bilberry types of pine forest of the reserve

Oh layer. The minimal ^{90}Sr inventory in the observable forest types occurred for Ol and Of layers, but the value of its content was not stable. The main part of ^{90}Sr inventory was accumulated in Oh layer of the forest litter. The same results are reported both by up-to-date researches [3, 22] and in studies fulfilled before Chernobyl accident [23]. The variations of ^{90}Sr content in Oh layer according to the results of our research were quite substantial. Nevertheless, the conclusion could be made that the humified layer kept on to be the main accumulator of ^{90}Sr in soil profile; that is one more proof of high ability of organogenic horizon to fix ^{90}Sr.

The inhomogeneous distribution of the radionuclides is usual for the mineral part of soil profile. The specificity of their distribution in forest soils directly under the litter depends on large quantity of factors: dynamics of the accumulation and decomposition of organic residues, thickness and structure of forest litter, regime of soil humidification, its fertility and acidity, grain size and mineralogical composition, plantation age, its species composition and type of forest growing, digging activity of animals, vital functions of the soil fauna, mushrooms, capillary effects, diffusion, climatic and weather conditions, and chemical features of the radionuclides themselves [3, 21, 24–26].

Overall, regularity in distribution of ^{90}Sr through mineral part of soil profile for all observable types of pine forests of Polessye reserve at present time was its accumulation by upper 0–5 cm layer (immediately after forest litter). In pine forests regardless of forest type, the similar percentages of ^{90}Sr were accumulated in that layer. In heath forest type, 23.0% of ^{90}Sr fell on that layer, in bilberry 21.4%, and in mossy 25.6%. Sharp decrease of ^{90}Sr content (in 2–4 times) occurred in 5–10 cm layer. For the next layers, the differences were not so remarkable and amounted 2.7–3.4%. The characteristic feature of ^{90}Sr migration in soil profile was its irregular decreasing and distribution between layers. For layers of 25–30 cm and 35–40 cm, its quantity was higher than that for super stratum; in case of mossy type of pinery, that difference was three times more (Fig. 2). This is due to chemical nature of ^{90}Sr as well as due to geochemical features of Polessye region in which ^{90}Sr can develop its ability to migrate with water flow [27]. On that reason, ^{90}Sr together with water flow penetrates into deep horizons of the soil.

The data received pointed out that the main part of ^{90}Sr in upland pine forests of the Polessye reserve was accumulated by mineral part of the soil. Only in bilberry pinery, more than one half of ^{90}Sr inventory (53.2%) was concentrated in forest litter. Distribution of ^{90}Sr between forest litter layers pointed out that the main part of radionuclide has moved to the underlayers. Thereby, the main backup of ^{90}Sr in upland pine forests of the Polessye reserve at the time of sample taking and their following analysis (2014–2017) was the underlayers of forest litter and upper layer (0–5 cm) of mineral soil horizon. On that reason, the further ^{90}Sr intake into mineral part of the soil and then into forest plants could be regarded as quite possible.

5 Accumulation of ^{90}Sr by Phytomass of Pine Forests

5.1 Accumulation of ^{90}Sr by Wood of Pine Forests

The pine is characterized by lower levels of accumulation of ^{90}Sr in comparison with other indigenous forest-forming species of Chernobyl exclusion zone [3]. The range of variation of activity concentration of ^{90}Sr in pine tissues and organs was substantially wider (Table 2) than that of ^{137}Cs [28]. Difference between the minimal and the maximal activity concentration of ^{90}Sr in pine wood was as high as 292 times, for bark 358 times and for roots 214. The same figures for automorphic (well-drained) soils were 55, 52, and 59 and for semihydromorphic soils 6, 10, and 15 times. The difference between the minimal and the maximal content of ^{90}Sr was decreasing in the row: heath (pinery) > mossy > bilberry. In the same row, the soil humidity was increasing at simultaneous decreasing of ^{90}Sr accumulation by wood, bark, and pine roots.

Accumulation of radionuclides is affected by many factors; the most important of them are biological peculiarities of the species, conditions of forest growing, speciation of settled radionuclides and their properties, and density contamination of the soil [3, 22]. Forest type, its age, and other elements of the plantations are also very important [3, 11, 12, 22].

It is known that increasing of soil radioactive contamination comes to higher content of ^{90}Sr in pine wood [3, 12]. The ^{90}Sr density contamination for every forest type varied in wide range; their mean values were close for mossy and bilberry forests and were two times higher for heath pine forest (Fig. 3). The same forest type was characterized by largest dispersion of activity concentration of ^{90}Sr in tissues and organs of pine (Table 2).

The influence of density contamination on ^{90}Sr accumulation by pine tissues and organs was confirmed by data of correlation analysis (Fig. 4). Higher correlation between density contamination and ^{90}Sr content in pine tissues and organs was registered for pine wood and roots, and less correlation was registered in case of bark. For more uniform conditions (only automorphic soils), the degree of correlation was higher. There is still more correlation between arithmetic means of ^{90}Sr activity concentration in pine components (Table 2) with mean values of density contamination (Fig. 3): wood, 0.988; bark, 0.987; and roots, 0.993.

The ratio of the maximal to the minimal ^{90}Sr T_{ag} into pine wood for all investigated plantations equaled 25. For bark and roots, the same ratio equaled 65 and 9 correspondingly. In case of automorphic soils, their values – 23, 39, and 8 – were many times higher than that for semihydromorphic soils, 1.2, 1.4, and 2.1. The mean ^{90}Sr T_{ag} values into pine components of heath and mossy pineries (automorphic soils) were close to each other, but there was a tendency of their decreasing from heath to mossy forest. They were decreased sharply in bilberry pinery (semihydromorphic soils). There was substantial difference between ^{90}Sr T_{ag} values into components of pine growing on automorphic and semihydromorphic soils (Table 2).

Table 2 Accumulation of ^{90}Sr (activity concentration, kBq kg^{-1} and ^{90}Sr T_{ag}, 10^{-3} m^2 kg^{-1}) by the organs and tissues of pine growing in different types of pine forest

Pine forest type	N[a]	Tissue/organ	Arithmetic mean		Standard deviation		Minimum		Maximum	
			kBq kg^{-1}	T_{ag}	kBq kg^{-1}	T_{ag}	kBq kg^{-1}	T_{ag}	kBq kg^{-1}	T_{ag}
Heath	5	Wood	5.3	20.9	7.5	21.4	0.3	5.5	17.5	55.2
	5	Bark	17.7	88.3	22.3	130.7	0.8	12.4	42.9	318.3
	5	Roots	14.8	52.1	23.9	31.5	1.1	28.0	57.1	94.4
Mossy	6	Wood	1.1	13.0	1.2	16.4	0.2	2.4	3.1	45.9
	6	Bark	3.7	55.5	3.4	58.8	0.8	8.1	8.9	140.9
	6	Roots	3.7	44.4	3.7	37.6	1.0	12.3	10.7	101.2
Bilberry	3	Wood	0.2	2.4	0.2	0.3	0.1	2.2	0.4	2.7
	3	Bark	0.7	6.2	0.5	1.1	0.1	4.9	1.2	6.9
	3	Roots	1.9	15.8	1.9	6.9	0.3	11.2	4.0	23.7

[a]*N* quantity of the samples analyzed

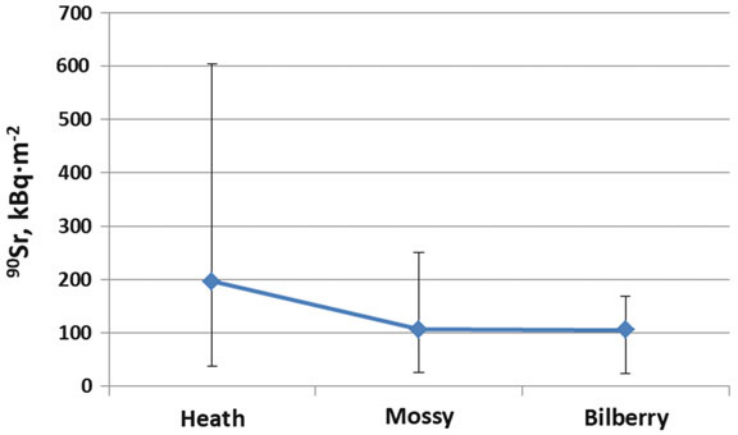

Fig. 3 Range of density contamination of sample areas by ^{90}Sr (kBq m^{-2}) for different types of pine forest

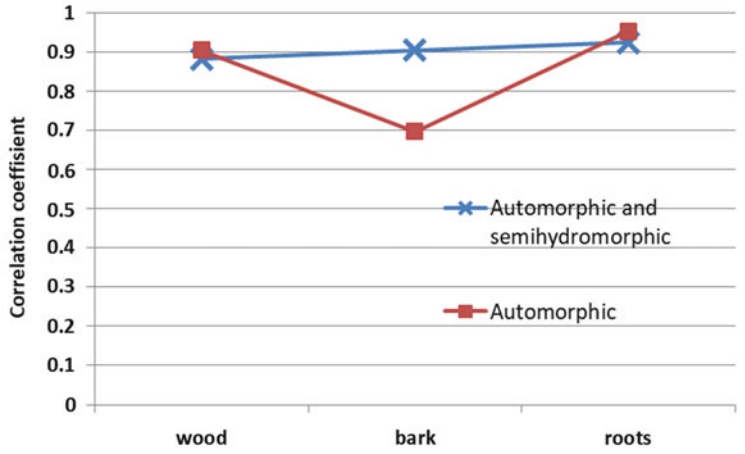

Fig. 4 Correlation of density contamination of plantation by ^{90}Sr with activity concentration of ^{90}Sr in tissues and organs of pine growing on different types of soil

It should be noted that in moving through the row "heath pinery–mossy pinery–bilberry pinery" – that is, in direction of humidification rising – the uptake of ^{90}Sr by components of pine (activity concentration and transfer factor) was decreased (Table 2).

Difference between mean values of ^{90}Sr T_{ag} into these organs and tissues for associated forest types was insignificant, but at the same time, it was significant for soils of different humidification types (Table 3).

Table 3 Significance of difference ($t_{calc.}$) between ^{90}Sr T_{ag} into pine components depending on conditions of forest growing

Forest or humidification type	$t_{calc.}$			t_{crit}
	Wood	Bark	Roots	
Heath/mossy	0.826	0.562	0.524	2.262
Mossy/bilberry	1.582	2.054	1.805	2.365
Automorphic/semihydromorphic	2.570	2.264	2.960	2.228

Table 4 The dynamics of ^{90}Sr T_{ag} into pine wood and bark according to the literature data

Forest type	Time (year, range)						
	1993 [13]	1996–2001 [3]		2001–2006 [11]		2012 [14]	
	Wood	Wood	Bark	Wood	Bark	Wood	Bark
Heath	7.1–38.5	39.1 ± 5.9	142 ± 25	8.3–12.8	33.4–41.6	–	–
Mossy				7.4–8.6	26.4–33.5	16.5	62.1
Bilberry				2.1	7.1–7.3	4.1	14.5

The similar results are presented by other authors. The decreasing of ^{90}Sr T_{ag} into pine wood and bark in pine forests of associated landscapes of exclusion zone occurs in the row of pineries: lichen > mossy > bilberry [14]. Statistically significant decreasing of the same factor is registered for the row of pine forests: heath > mossy > bilberry [11]. According to paper [12], the lower ^{90}Sr accumulation by pine components in semihydromorphic soils in comparison with automorphic ones is provided by the presence of exchangeable calcium (chemical analog of ^{90}Sr) in humid soils. As concerns automorphic soils, ^{90}Sr T_{ag} into pine wood and bark is several times higher than ^{137}Cs T_{ag} into the same components.

Differentiation of ^{90}Sr T_{ag} into pine wood and bark in some extent was determined by type of soil humidification. In case of automorphic soils (heath and mossy pine forests), that transfer factor was decreased into the row bark > roots > wood. There was another row for the same factor in bilberry pinery on semihydromorphic soils – roots > bark > wood.

The analysis of dynamics of ^{90}Sr T_{ag} into pine components in exclusion zone of ChNPP was fulfilled by the review of literature data (Table 4).

According to our data for the period 2014–2017 (Table 2), the mean values of ^{90}Sr T_{ag} into pine wood ($n = 14$) corresponded $13.6 \pm 4.6 \times 10^{-3}$ m^2 kg^{-1}, into bark $57 \pm 23 \times 10^{-3}$ m^2 kg^{-1}, and into roots $41 \pm 9 \times 10^{-3}$ m^2 kg^{-1}.

It was difficult to make any concrete conclusions concerning the tendency of changing of ^{90}Sr T_{ag} values with time on the base of the data shown in Table 4. For the relatively short time intervals, the alterations of ^{90}Sr T_{ag} into these pine tissues are not significant because of the constant level of its bioavailability [29]. According Zabrotski [5], the mean annual values of ^{90}Sr T_{ag} into pine wood growing in Chernobyl exclusion zone were permanently increased and only from 2012 reached the plateau about 19–22 $\times 10^{-3}$ m^2 kg^{-1}. One of possible explanations of

that is the predominant ^{90}Sr deposition in Chernobyl zone mainly in the matrix of fuel particles [30]. Due to their weathering, ^{90}Sr come to the soil solution in moveable form which is only weakly absorbed by soil components but is easily extracted by pine and accumulated by their tissues and organs. That leads to continuous increase of ^{90}Sr T_{ag}; that process is described by exponential function [22]. Stopping of increment of the factors and relative stabilization in time [5] could be explained by ending the fuel particle weathering [11] and depletion of the source of moveable ^{90}Sr.

Such factor as remoteness of the stands from the initial source of radioactive release is important for their contamination because of changing of radionuclide speciation with distance. More close to ChNPP, where fuel components of the radioactive release dominates, ^{90}Sr T_{ag} into pine wood is substantially higher than in more remote territories [3, 13, 22]. According to the data 2005–2006, the mean values of ^{90}Sr T_{ag} into wood and bark of pine in heath and mossy pineries of southern part of exclusion zone (mainly 30-km zone) were only little higher than that of northern part, in bilberry pinery – even close. So the absence of reliable territorial differences for the transfer factors of ^{90}Sr into pine tissues could be explained by termination of the fuel particle weathering [11].

According to our data (Table 5), for the automorphic soils, ratio of activity concentrations of ^{90}Sr in wood (bark and roots) of pine in 30-km zone to that at farther distances from ChNPP composed 13.4 (16.2, 8.6) times. The difference in ^{90}Sr T_{ag} values was less (3.8, 9.1, 3.6) but significant (Table 6). Depending on distance from the place to source of radioactivity, the tissues and organs accumulated ^{90}Sr differently. In 30 km zone, the accumulation increased in the row wood < roots < bark, but at the periphery of the reserve, the same row was wood < bark < roots.

All elements of the forest phytocenosis are usually taking part in redistribution of the radionuclides in its interior. For the radionuclide deposition in the components of wood species, the forestry characteristics of the stand could be very important. Such indicators of ^{90}Sr accumulation as activity concentration and its transfer factor were used to test their correlation with some forestry characteristics. The negative

Table 5 Contamination of pine components by ^{90}Sr on automorphic soils depending on distance from the source of the release

Distance away from source	Activity concentration, kBq kg^{-1}			T_{ag}, 10^{-3} m^2 kg^{-1}		
	Wood	Bark	Roots	Wood	Bark	Roots
Up to 30 km, $N = 5$	6.0	20.6	17.0	29.9	137.0	78.9
Farther than 30 km, $N = 6$	0.5	1.3	1.9	5.5	15.0	22.1

Table 6 Significance of difference ($t_{calc.}$) between contamination of pine components by ^{90}Sr inside and outside the 30 km zone

$t_{calc.}$ for ^{90}Sr activity concentration			$t_{calc.}$ for ^{90}Sr T_{ag}			$t_{crit.}$
Wood	Bark	Roots	Wood	Bark	Roots	
1.81	2.19	1.48	2.62	2.49	5.34	2.26

Table 7 Coefficients of correlation between ^{90}Sr accumulation indicators and some forestry parameters

Indicator	Tissues and organs	Age	Tree density	Wood production
Activity concentration	Wood	−0.584	0.676	−0.565
	Bark	−0.601	0.708	−0.580
	Roots	−0.533	0.595	−0.527
Transfer factor	Wood	−0.481	0.710	−0.384
	Bark	−0.504	0.678	−0.399
	Roots	−0.598	0.857	−0.515

moderate correlations were found between last-named indicators and age of wood species, a little weaker – with wood production – and a little stronger positive association, with tree density (Table 7).

The negative strong correlations between ^{90}Sr content in pine components and age of stands are established in paper [22]. In most cases that correlations with high degree of significance are approximated by exponential equations [22]. That negative correlations are understandable because ^{90}Sr uptake with time is decreasing – younger plants need more mineral matter and appropriately take more ^{90}Sr [3].

Correlation of ^{90}Sr accumulation with thickness of stands was stronger (Table 7). Perevolotski [3] discusses the influence of the silvicultural parameter on ^{90}Sr uptake by the pine. He suggests that higher saturation of the soil by suction roots occurs in thicker stands. On the score of root competition for mineral substances, ^{90}Sr extraction from the soil is more complete.

5.2 *Accumulation of ^{90}Sr by Vegetation of Understory and Young Growth of Pine Stand*

The representative residents of the undergrowth in heath, mossy, and bilberry pineries of Belarusian Polessye are Persian berry, mountain ash, and oak (the oak in bilberry type of the forest is regarded as young growth at that) [17]. The main component of the undergrowth in heath pinery is Persian berry (64–89% of the plants); in mossy pineries, Persian berry (54–55%) or oak (46%); in undergrowth of bilberry pineries, Persian berry (49–96%); and in young growth, oak (11–85%). The mountain ash in little amounts is always presented in all forest types.

The species peculiarity of ^{90}Sr accumulation by organs and tissues of the plants is characteristic for the undergrowth and young growth; the peculiarity depends on forest type at that. It should be noted that species peculiarity of the radionuclide uptaking by the plants is more important than forest growing conditions and density contamination of the soil [15].

According to our data (Table 8), there were no substantial differences in the undergrowth and young growth contamination by ^{90}Sr for the different forest types. ^{90}Sr T_{ag} values into Persian berry and mountain ash wood and roots in heath pinery were a little higher in comparison with mossy and bilberry pineries. ^{90}Sr T_{ag} values into leaves of the same species in bilberry pinery were relatively increased. The oak differed from others by enhanced ^{90}Sr T_{ag} values into wood in mossy pinery and into leaves in bilberry pinery. For automorphic soils all mentioned species were characterized by raised mean ^{90}Sr transfer factors into wood and roots and by lowered ones into leaves in comparison with semihydromorphic soils. Some increasing in accumulation of ^{90}Sr by wood and roots of undergrowth and young growth was registered in more dry soils of heath forests. By contrast, ^{90}Sr T_{ag} into leaves were increasing with rising of soil humidity.

Table 8 ^{90}Sr transfer factors into organs and tissues of undergrowth and young growth of heath, mossy, and bilberry pine forests, 10^{-3} m^2 kg^{-1}

Species	Tissues and organs	*N*	Arithmetic mean	Standard deviation	Minimum	Maximum
Heath pinery						
Persian berry (*Frangula alnus* mill.)	Wood	2	62.5	51.3	26.2	98.7
	Roots	2	83.1	81.5	25.5	140.7
	Leaves	2	47.1	20.7	32.4	61.7
Mountain ash (*Sorbus aucuparia* L.)	Wood	1	42.1	–	–	–
	Roots	1	65.7	–	–	–
	Leaves	1	58.7	–	–	–
Mossy pinery						
Persian berry (*Frangula alnus* Mill.)	Wood	3	45.2	4.9	41.9	50.9
	Roots	3	44.7	5.4	39.7	50.5
	Leaves	3	46.5	27.2	21.2	75.2
Mountain ash (*Sorbus aucuparia* L.)	Wood	2	39.9	0.2	39.8	40.1
	Roots	2	55.0	3.3	52.7	57.3
	Leaves	2	48.7	20.4	34.3	63.1
English oak (*Quercus robur* L.)	Wood	2	53.7	20.2	39.4	68.0
	Roots	2	45.7	15.8	34.5	56.8
	Leaves	2	12.3	2.7	10.4	14.2
Bilberry pinery						
Persian berry (*Frangula alnus* mill.)	Wood	3	46.7	3.6	42.7	49.5
	Roots	3	47.4	17.5	28.7	63.3
	Leaves	3	62.4	34.3	42.5	102.0
Mountain ash (*Sorbus aucuparia* L.)	Wood	3	31.7	6.9	26.4	39.5
	Roots	3	44.1	10.6	32.7	53.6
	Leaves	3	77.2	37.3	44.1	117.8
English oak (*Quercus robur* L.)	Wood	2	43.1	18.4	30.2	56.0
	Roots	2	47.5	19.8	33.5	61.5
	Leaves	2	28.5	0.9	27.9	29.1

The rows of ^{90}Sr T_{ag} values for organs and tissues of Persian berry and mountain ash in heath and mossy pineries (on automorphic soils) were close but differed for soils of different humidification types. The same rows for English oak were close for both soil types (Table 9). This is why the significance of difference of ^{90}Sr transfer factors not only between species but also between their components for soils of different types of humidification was supposed.

^{90}Sr accumulation by different components for various species was examined. ^{90}Sr T_{ag} into wood was decreasing in the row oak > Persian berry > mountain ash; for the leaves the similar row was mountain ash > Persian berry > oak. For all forest types, the wood of mountain ash accumulated ^{90}Sr less than other species. One more peculiarity of mountain ash consisted in the largest, as compared with other species, ^{90}Sr accumulation by leaves. ^{90}Sr on both types of soil humidification was accumulated by oak wood larger than in case of other species. This was not the case for leaves which accumulate ^{90}Sr less than other species. Persian berry occupied the intermediate position. Any general regularity of distribution of ^{90}Sr in roots of undergrowth species was not revealed (Table 10).

According to the data of Parfenov et al. [15] in 1987, ^{90}Sr content in leaves of mountain ash was higher than that of Persian berry. During 5 years (until 1992), it was increased by an order of magnitude for Persian berry and two orders of magnitude for mountain ash [15]. Therefore, it may be concluded that over a period of 30 years, the leaves of mountain ash accumulate ^{90}Sr more intensively than that of Persian berry.

Table 9 The rows of ^{90}Sr T_{ag} in organs and tissues of some species of undergrowth and young growth of different forest types

Forest type	Persian berry	Mountain ash	English oak
Heath	Roots > wood > leaves	Roots > leaves > wood	–
Mossy	Roots ≈ wood ≈ leaves	Roots > leaves > wood	Wood > roots > leaves
Bilberry	Leaves > roots ≈ wood	Leaves > roots > wood	Wood ≈ roots > leaves

Table 10 The rows of ^{90}Sr transfer factors into components of undergrowth and young growth species of different forest types

Forest type	Wood	Roots	Leaves
Heath	Persian berry > mountain ash	Persian berry > mountain ash	Mountain ash > Persian berry
Mossy	Oak > Persian berry > mountain ash	Mountain ash > Persian berry ≈ oak	Mountain ash ≈ Persian berry > oak
Bilberry	Oak ≈ Persian berry > mountain ash	Oak ≈ Persian berry ≈ mountain ash	Mountain ash > Persian berry > oak

5.3 Accumulation of ^{90}Sr by Alive Soil Cover

Schreber's big red stem moss is one of the most widely distributed species of alive soil cover of the pine forests of exclusion zone. According to our data, it dominated in mossy pinery (65–80% of the projective cover) and in heath pinery (15–90%) and was often found in bilberry pinery (5–60%). Dicranum moss covered 15–25% of the territory of mossy pinery and 5–25% of the heath one and in little amounts (up to 1%) was presented in bilberry pineries. Common bilberry was widely distributed in bilberry pinery (30–90%) and also was found in mossy pinery. Common heather was the species indicator of heath pinery. Adderspit attended in heath pineries (up to 20%) and bilberry ones (up to 25–75%). Blue moor grass was not uncommon in bilberry pineries (20–45%).

The conditions of forest growth, biological features of the plants themselves, and in some degree soil density contaminations determine the contamination level of plants of alive soil cover. During the first 8 years after Chernobyl accident, the plants of mossy pinery formed the following row of decreasing of their ability to accumulate ^{90}Sr, moss > fern > cowberries, and in bilberry pinery, moss > fern > Ericaceae > cowberries. According to the data of Parfenov et al. [15], the decreasing of ^{90}Sr activity concentration as well as its concentration ratio took place for the Schreber's big red stem moss in mossy pinery since 1987–1988 up to 1992–1993. On the contrary, the same indicators for the adderspit, common bilberry, and common heather at the same time and the same forest type were increased. In bilberry pinery the values of these parameters were decreased to 1992 for all species apart from adderspit.

According to the data received, ^{90}Sr T_{ag} into components of the plants of alive soil cover differed each other depending on forest type (Table 11). Adderspit demonstrated the maximal ability to accumulate ^{90}Sr in its above-soil part in heath pinery. There was a little decrease of ^{90}Sr transfer factor in the row: dicranum moss > common heather > Schreber's big red stem moss. Also a little difference in ^{90}Sr T_{ag} values into phytomass was registered in mossy pinery for the following plant row, dicranum moss ≥ Schreber's big red stem moss ≥ common bilberry, and in bilberry pinery, adderspit > common bilberry ≈ dicranum moss ≥ Schreber's big red stem moss ≥ blue moor grass. It could be interested to know that ^{90}Sr transfer factors into plant roots were lower than that into aboveground phytomass. In heath pinery the roots of adderspit usually accumulated ^{90}Sr as much as the roots of common heather. In bilberry pinery the row of decrease of ^{90}Sr accumulation by roots looked like adderspit ≈ common bilberry > blue moor grass.

The lowering of ^{90}Sr transfer factors for aboveground phytomass in the following row of alive soil cover species – adderspit > dicranum moss > Schreber's big red stem moss – was general for all forest types. There was no difference for the heath and mossy pineries in the values of ^{90}Sr transfer factors into phytomass of dicranum moss and Schreber's big red stem moss. At the same time, the common

Table 11 ^{90}Sr transfer factors into components of alive soil cover of heath, mossy, and bilberry pineries, 10^{-3} m^2 kg^{-1}

Species	Tissues and organs	*N*	Arithmetic mean	Standard deviation	Minimum	Maximum
Heath pinery						
Common heather (*Calluna vulgaris* L.)	Phytomass	3	27.2	15.7	7.2	39.7
	Roots	3	13.9	14.9	1.8	30.6
Adder-spit (*Pteridium aquilinum* L.)	Phytomass	2	40.2	5.1	36.6	43.8
	Roots	2	12.6	5.5	8.7	16.5
Dicranum moss (*Dicranum polysetum* Sw.)	Phytomass	5	31.0	33.7	4.4	85.5
Schreber's big red stem moss (*Pleurozium schreberi* Brid.)	Phytomass	5	25.3	33.5	1.5	82.7
Mossy pinery						
Common bilberry (*Vaccinium myrtillus* L.)	Phytomass	2	20.4	3.5	17.9	22.9
	Roots	2	5.8	4.8	2.4	9.2
Dicranum moss (*Dicranum polysetum* Sw.)	Phytomass	6	27.3	23.3	5.3	64.4
Schreber's big red stem moss (*Pleurozium schreberi* Brid.)	Phytomass	6	23.5	21.2	4.4	59.1
Bilberry pinery						
Common bilberry (*Vaccinium myrtillus* L.)	Phytomass	3	10.3	0.7	9.7	11.1
	Roots	3	8.2	2.7	6.0	11.2
Adder-spit (*Pteridium aquilinum* L.)	Phytomass	2	26.4	4.2	23.4	29.4
	Roots	2	11.6	0.4	11.3	11.9
Blue moor grass (*Molinia caerulea* L.)	Phytomass	3	3.0	1.4	1.9	4.5
	Roots	3	2.6	1.4	1.3	4.1
Dicranum moss (*Dicranum polysetum* Sw.)	Phytomass	3	8.6	4.2	6.0	13.4
Schreber's big red stem moss (*Pleurozium schreberi* Brid.)	Phytomass	3	5.6	0.7	5.0	6.3

bilberry, adderspit, and both species of moss more intensively accumulated ^{90}Sr on automorphic soils (heath and mossy forest types) in comparison with semihydromorphic ones.

Mean values of ^{90}Sr T_{ag} into adderspit and common bilberry roots both on automorphic and semihydromorphic soils were close.

5.4 Accumulation of ^{90}Sr by Pine Ecosystems

After 30 years from Chernobyl accident, the most part of ^{90}Sr inventory in pine ecosystems remained in forest litter and mineral part of soil (Fig. 5). In automorphic soils, the percentage of that radionuclide in soils was substantially higher than that in semihydromorphic ones.

The percentage of ^{90}Sr in stand components in bilberry pineries was substantially higher at the expense of increasing of phytomass stocks on semihydromorphic soils. In phytocenosis the main reserves of ^{90}Sr were accumulated in stands. The stock of ^{90}Sr in undergrowth, young growth, and alive soil cover was insignificant in comparison with other ecosystem elements.

The distributions of ^{90}Sr between pine structural components were close for heath and mossy pineries. Substantially more differences were characterized for pine forests situated near automorphic and semihydromorphic soils. Substantial stocks of ^{90}Sr in bilberry pineries were accumulated by tree roots.

6 Conclusions

The mossy, heath, and bilberry pineries growing on poor sandy soils dominate in typological structure of upland pine forests of Chernobyl exclusion zone. Their stands are situated on various relief elements and differ on degree of soil humidification. The soils of heath and mossy pineries are characterized as automorphic humidification type, the soils of bilberry pine forests – as semihydromorphic one.

Over a period of 30 years after the radioactive depositions, ^{90}Sr transfer factors from soil to pine wood in exclusion zone were increasing, but since 2012, their growth rates began to go down.

The ^{90}Sr accumulation in the wood, roots, and bark was closely connected with density contamination of the soil. The activity concentration of the radionuclide in organs and tissues was increased with its raising.

The factor of soil humidification had substantial influence on intensity of accumulation of ^{90}Sr by pine components. The soil humidification was increasing in the next row of pine forest types, heath $>$ mossy $>$ bilberry, as well as from automorphic to semihydromorphic soils. The changes of ^{90}Sr accumulation by tree components in the same row were opposite – the ^{90}Sr absorption fell in rising of water content in soil.

^{90}Sr accumulation was increased in the row wood $<$ roots $<$ bark on automorphic soils; on semihydromorphic soils, the similar row looked like wood $<$ bark $<$ roots.

On automorphic soils of 30 km zone, the soil contamination and ^{90}Sr content in pine components were substantially higher than outside its territory. Inside the zone the upgrowth of activity concentration and ^{90}Sr transfer factors occurred in the row wood $<$ roots $<$ bark while outside the zone in the row wood $<$ bark $<$ roots.

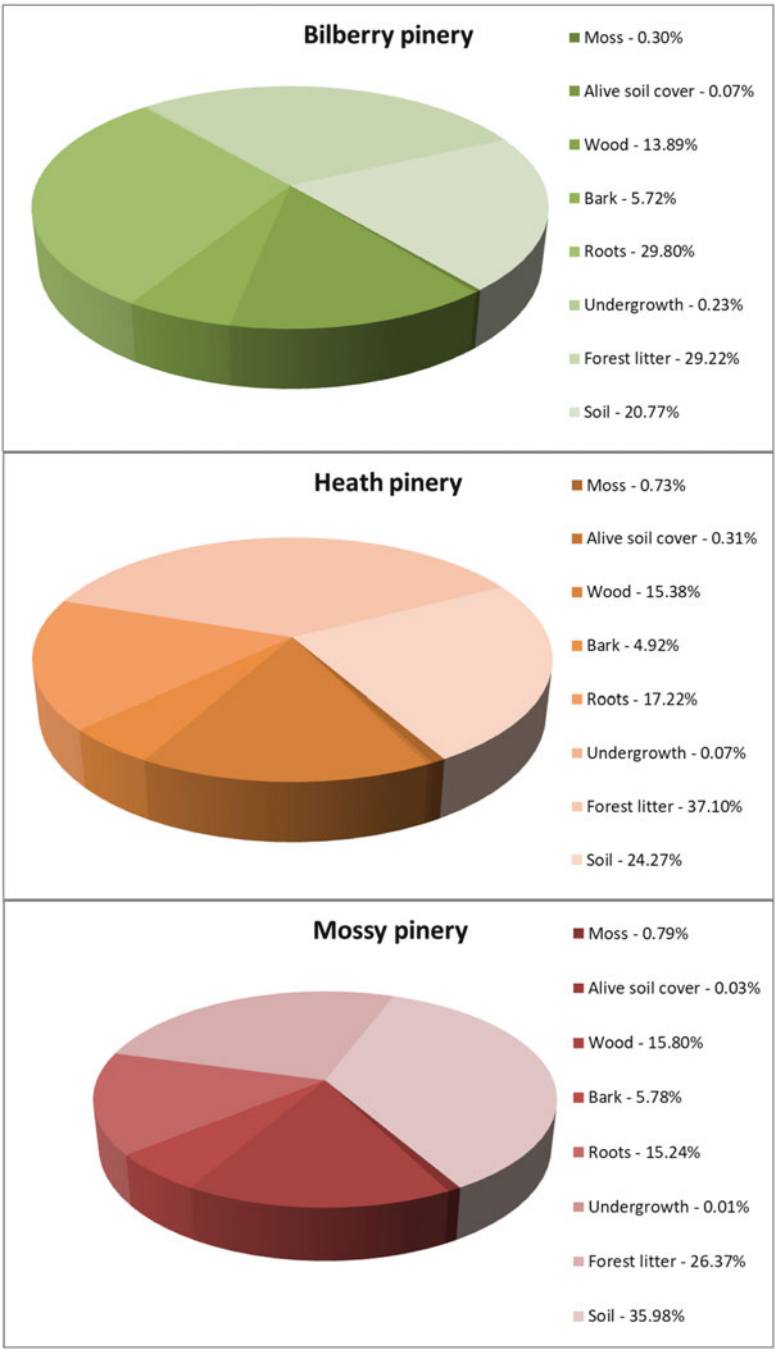

Fig. 5 ^{90}Sr distribution between components of ecosystems of different types of pine forests

^{90}Sr accumulation in wood, bark, and roots was decreased with age as well as with increase of body wood stocks and with decrease of the stand thickness.

The ability of organs and tissues of different species to accumulate ^{90}Sr determined its absorption by plants of undergrowth and young growth.

The storage of ^{90}Sr in components of undergrowth and young growth depended on soil moisture and changed a little from one forest type to another. The tendency of lowering of ^{90}Sr content in components of undergrowth and young growth was registered with rise of humidity.

Distributions of the components of undergrowth and young growth on ^{90}Sr transfer factor magnitudes differed for soils of different types of watering. The general tendency of ^{90}Sr T_{ag} rising from wood to roots was traced. The leaves of different species had their own absorption specificity without any general tendency.

Because of specificity of ^{90}Sr absorption, its transfer factors into components of plants of alive soil cover varied substantially depending on forest types. The majority of the species more intensively accumulated that radionuclide by the aboveground phytomass on the automorphic soils (heath and mossy types of forest) in comparison with semihydromorphic soils. The overall feature for all forest types was the lowering of ^{90}Sr T_{ag} into aboveground phytomass in the following row – adderspit > dicranum moss > Schreber's big red stem moss. Values of ^{90}Sr T_{ag} into plant roots were less than that into their aboveground parts.

In regard to phytomass of the pine forests, the main quantities of ^{90}Sr were concentrated in the stands. Their distribution between pine components on automorphic soils was the same for heath and mossy pineries. The great difference occurred between ^{90}Sr accumulation by phytomass of pine trees growing on automorphic and semihydromorphic soils. Substantial amounts of ^{90}Sr in bilberry pinery were accumulated by roots.

References

1. UNSCEAR (2008) Sources and effects of ionizing radiation 2008. In: United Nations scientific committee on the effects of atomic radiation UNSCEAR 2008, report to the general assembly with scientific annexes, vol 2. Annex D. Health effects due to radiation from the Chernobyl accident. United Nations, New York
2. Germenchuk MG (2007) Chernobyl accident and radioactive contamination of Belarus. In: Shevchuk BE (ed) 20 years after Chernobyl accident: consequences in Belarus and their overcoming. National Report, Minsk, pp 6–12. (in Russian)
3. Perevolotski AN (2006) Distribution of ^{137}Cs and ^{90}Sr in forest ecosystems. Institute of Radiology, Homel, p 255. (in Russian)
4. Kashparov VA, Ahamdach N, Zvarich SI, Yoschenko VI, Maloshtan IM (2004) Kinetics of dissolution of Chernobyl fuel particles in soil in natural conditions. J Environ Radioact 72:335–353
5. Zabrotski V (2018) Contamination of firewood taken from the Exclusion Zone of the Chernobyl NPP by ^{90}Sr according to data from 2005–2016. In: Gupta DK, Walther C (eds) Behaviour of strontium in plants and the environment. Springer, Cham, pp 109–124

6. ICRP (2012) Compendium of dose coefficients based on ICRP publication 60. ICRP publication 119. Annals of the ICRP 41 (Suppl)
7. Beresford NA, Fesenko S, Konoplev A, Skuterud L, Smith JT (2016) Thirty years after the Chernobyl accident: what lessons have we learnt? J Environ Radioact 157:77–89
8. Guillen J (2018) Factors influencing the soil to plant transfer of strontium. In: Gupta DK, Walther C (eds) Behaviour of strontium in plants and the environment. Springer, Cham, pp 19–31
9. Mahara Y, Ohta T, Ogawa H, Kumata A (2014) Atmospheric direct uptake and long-term fate of radiocesium in trees after the Fukushima nuclear accident. Sci Rep 4:7121
10. Encyclopedia of forestry (2006) Vol 2. M. VNIILM, pp 416. (in Russian)
11. Bulavik IM, Bogachenko DS (2013) Peculiarities of accumulation of ^{137}Cs and ^{90}Sr by wood and bark of Scotch pine in different forest types in Polessye State Radiation Ecological Reserve. Problems of forestry and silviculture, vol 73. Institute of Forest National Academy of Sciences of Belarus, Homel, pp 378–387. (in Russian)
12. Ipat'ev VA, Baginsky VF, Bulavik IM, Baginsky V, Goncharenko G, Dvornik A (1999) Forest and Chernobyl: forest ecosystems after Chernobyl NPP accident: 1986–1994. J Environ Radioact 42:9–38
13. Ipat'ev VA, Baginsky VF, Bulavik IM, Baginsky V, Goncharenko G, Dvornik A (1999) Forest, Human, Chernobyl. Forest ecosystems after Chernobyl accident: state, prognosis, reaction of population, ways of rehabilitation. Institute of Forest National Academy of Sciences of Belarus, Homel, p 452. (in Russian)
14. Matusov GD, BUlko NI, Mashkov IA, Shabaleva MA (2013) Dynamics of migration and accumulation of ^{137}Cs and ^{90}Sr in pine plantations of associated landscapes of exclusion zone of Chernobyl NPP. In: Bondar Y (ed) Ecosystems and radiation: aspects of existence and development. Collected scientific articles devoted to 25th anniversary of Polessye State Radiation Ecological Reserve. Institute of Radiology, Minsk, pp 265–277. (in Russian)
15. Parfenov VI, Yakushev BI, Martinovich BS (1995) Radioactive contamination of vegetation of Belarus. Navukaitehnika, Minsk, p 578. (in Russian)
16. Yurkevich ID (1980) Selection of forest types in forest management operations. Navuka i tehnika, Minsk, p 120. (in Russian)
17. Lovchiy NF (2012) Cadastre of types of pine forest of Belarusian Poles'e. In: Parfenov VI (ed) Belaruskaya navuka, Minsk, pp 221. (in Russian)
18. Bogdevich IM (2006) Large-scale agrochemical and radiological examination of the soil of agricultural lands of Belarus. In: Bogdevich IM (ed) Methodological guidance. Institute of Soil Science and Agrochemistry of National Academy of Sciences of Belarus, Minsk, p 64. (in Russian)
19. TKP 240-2010 (2010) Radiation control. Examination of the forest lands. The order of fulfillment. TKP 240-2010 (02080). Ministry of Forest Economy of Belarus, Minsk. (in Russian)
20. TKP 498-2013 (2013) Radiation monitoring of forest resources. Making of constant observation point. The order of fulfillment. TKP 498-2013 (02080). Ministry of Forest Economy of Belarus, Minsk. (in Russian)
21. Krasnov VP, Orlov OO, Buzun VA, Landin VP, Shelest ZM (2007) Applied forest radioecology. Polissia, Zhytomyr, pp 680. (in Russian)
22. Shcheglov AI (2000) Biogeochemistry of anthropogenic radionuclides in forest ecosystems: according to materials of 10-years researches in Chernobyl zone. Nauka, Moskva, p 268. (in Russian)
23. Tyuryukanova EB (1974) Radio geochemistry of soils of Russian plain woodlands. Nauka, Mascow, p 156. (in Russian)
24. Averin VS (2007) Radioecological consequences of Chernobyl accident. In: Shevchuk BE (ed) 20 years after Chernobyl accident: consequences in Belarus and their overcoming. National Report, Minsk, pp 13–35. (in Russian)

25. Markina ZN, Glazun IN (2005) Distribution of ^{137}Cs through soil profile in forest ecosystems of Bryansk region. In: Ipat'ev VA (ed) Problems of forestry and silviculture, vol 63. Institute of Forest National Academy of Sciences of Belarus, Homel, pp 487–489. (in Russian)
26. Perevolotskaya TV (2008) Distribution of ^{137}Cs and ^{90}Sr in forest ecosystems in conditions of impoundment. In: Radiation and ecosystems: proceedings international science conference, Homel, pp 71–74. (in Russian)
27. Kopeikin VA (1995) Geochemical consequences of Chernobyl catastrophe. In: Problems of Chernobyl exclusion zone. Scientific-technical collected articles, vol 2. Kiev. Naukova dumka, pp 128–137. (in Russian)
28. Kudzin M, Zabrotski V, Harbaruk D (2016) Distribution of ^{137}Cs between the components of pine forest of Chernobyl NPP exclusion zone. In: Gupta DK, Walther C (eds) Impact of cesium on plants and the environment. Springer, Cham, pp 149–169
29. Perevolotski AN, Perevolotskaya TV (2010) Analysis of long-stage dynamics of ^{137}Cs and ^{90}Sr accumulation by wood and bark of Scotch pine in different conditions of forest growing. Problems of forestry and silviculture, vol 70. Institute of Forest National Academy of Sciences of Belarus, Homel, pp 467–478. (in Russian)
30. Ivanov YA, Kashparov VA, Lazarev NM (1996) Physicochemical forms of ChNPP fallout and long stage dynamics of radionuclide behavior in agroecosystem components. In: Materials of IV international science technical conference "Outcome of 8-years work on liquidation of consequences of the accident on Chernobyl NPP". Chernobyl, vol 1, pp 256–269. (in Russian)
31. Atomtex Gamma beta radiation spectrometer AT1315. http://atomtex.com/en/at1315-gamma-beta-spectrometer. Accessed July 2018

Removal of Strontium by Physicochemical Adsorptions and Ion Exchange Methods

Nevin Koshy and Pankaj Pathak

Contents

Abstract Strontium, a relatively abundant alkaline element in the earth's crust, occurs in four stable isotopes, ^{84}Sr, ^{86}Sr, ^{87}Sr and ^{88}Sr. The separation of soluble Sr^{2+} ion from water, mainly seawater, can be achieved through one or a combination of methods such as adsorption, chemical precipitation, ion exchange, membrane technology and solvent extraction, amongst which adsorption and membrane processes are popular solutions. The regeneration of spent adsorbents along with Sr recovery is the inherent advantage of the adsorption process. Natural adsorbents such

N. Koshy (✉)
Department of Civil Engineering, Indian Institute of Technology Jammu, Jammu and Kashmir, India
e-mail: nevin.koshy@iitjammu.ac.in

P. Pathak
Department of Environmental Science & Engineering, Marwadi University, Rajkot, Gujarat, India

P. Pathak, D. K. Gupta (eds.), *Strontium Contamination in the Environment*,
The Handbook of Environmental Chemistry 88,
https://doi.org/10.1007/978-3-030-15314-4_10

as alginate microspheres, attapulgite, bentonite, dolomite, goethite, hematite and natural zeolites and inorganic ion-exchange materials, viz. activated carbon, antimony oxide, artificial zeolites, carbon and titanate nanotubes, gel and macroporous resins, titanium oxide and synthetic birnessite, have been used for immobilization of Sr. Industrial wastes (coal fly ash and industrial sludges) and agricultural byproducts (almond green hull, eggplant hull, moss and waste rice straw) are also potential Sr adsorbents. The adsorption process is greatly influenced by pH, initial concentration of contaminant, temperature and textural characteristics of the adsorbents. Membranes from polymeric and ceramic materials have also been used for Sr attenuation, and hybrid membrane technologies using multiple membranes have been found to be effective.

Keywords Adsorption · Heavy metal removal · Ion exchange · Isotherms · Strontium removal

1 Introduction

Strontium (Sr) is a relatively abundant alkaline earth metal on the earth's crust, mainly present as a divalent cation Sr^{2+} or as different complexes depending on the environmental conditions [1]. It is highly mobile in surface water, groundwater and sediments, and its isotope ratios such as $^{87}Sr/^{86}Sr$ and $^{88}Sr/^{86}Sr$ are commonly used as biogeochemical and hydrogeological traces [2]. Strontium is a calcium analogue and bioaccumulates in the hydroxyapatite of bones and teeth [3]. The Fukushima Daiichi nuclear reactor disaster caused by the earthquake and tsunami in March 11, 2011, led to the spillage of radioactive nuclides ^{90}Sr and ^{137}Cs into the sea which have half-lives of 28.9 and 30.17 years, respectively [4–6]. Large amounts of low-level radioactive wastes are also being produced from nuclear power plants and nuclear laboratories [7]. Potential leaks from waste repositories and nuclear disasters can be immobilized only to a limited extent using backfill clay materials [3]. Furthermore, radioactive ^{90}Sr fallouts from weapon tests can result in chronic environmental contamination, thus requiring their quick, efficient and economical immobilization, especially from large waterbodies like seawater [8].

Adsorption, chemical precipitation, coagulation/sedimentation, membrane filtration, sand filtration, solvent extraction and biological methods are some of the remediation methods for Sr contamination [4, 9]. Of these, adsorption is one of the most common methods employed for large-scale attenuation and/or extraction of hazardous elements [4, 5, 10]. Using adsorption also reduces the use of organic solvents, thus making the attenuation process simple and safer [10]. In some cases, a combination of physical and chemical sorption and/or ion exchange takes place simultaneously [11, 12]. Materials with high cation exchange capacity (CEC) such as zeolites and hydroxyapatite have also been used for the removal of cations through ion-exchange mechanism [13–15]. In hydroxyapatite, the Ca^{2+} sites are preferentially exchanged with the larger Sr^{2+} cations [13]. Figure 1 shows the morphological alterations in the sheets of bentonite clay particles after Sr sorption at pH 1 and 8.5.

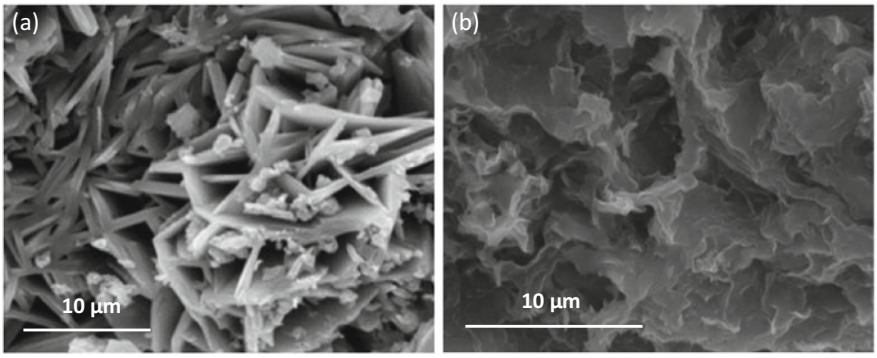

Fig. 1 Bentonite clay particles after Sr sorption (0.1M $SrCl_2$) at (**a**) pH 1 and (**b**) pH 8.5 (with permission from the publisher [16])

2 Natural and Synthetic Adsorbents and Ion Exchangers

Adsorbents used for Sr removal can be natural, such as soils, clays and biosorbents, or synthetically prepared, such as acrylic acid-grafted polypropylene and synthetic hydroxyapatite [13, 17]. The valorization of agricultural and industrial wastes for adsorption may be economical, environmentally friendly and/or sustainable [14, 18]. With this in view, Kubota et al. [19] have collected seawater containing ^{85}Sr, the only nuclide emitting gamma rays, near Matsushita beach, Fukushima, Japan, and used activated carbon, bentonite and zeolite to remove the radioactive Cs, I and Sr from the water. Table 1 shows the maximum adsorption capacities of various Sr adsorbents and their operating conditions.

2.1 Natural Adsorbents

The study of soils and clays are important in the context of geological repositories for radioactive waste disposal since geological formations are economical and may be able to retard the isotope migration and subsequent leaching into the groundwater in case of possible leakage [11]. Soils [26, 27], clays [28] and clay minerals such as smectites, bentonite/montmorillonite [6, 29], kaolinite [30] and attapulgite [5] have been successfully used for Sr removal. Although negligible Sr sorption is expected at pH < 4 due to protonation of the sorption sites, the organic matter present in soil can behave as a sorbent [31]. Rocks may offer isolation of radioactive wastes for very long periods ($\sim 10^5$ years) and are potential backfill materials for high-level waste repositories [11]. Marble rock powder, an alkaline sorbent, containing calcite and small amounts of quartz with specific surface area ~63 $m^2\ g^{-1}$ and total pore volume ~0.03 $cm^3\ g^{-1}$, showed low Sr uptake of 2.1 mg g^{-1} [11]. Porous minerals (e.g. zeolites) and clay minerals such as attapulgite (hydrated magnesium aluminium

Table 1 Sorption characteristics of natural and synthetic Sr adsorbents

Adsorbent	SSA ($m^2\ g^{-1}$)	q_m (mg g^{-1})	Temperature (°C)	pH	t_e (h)	Dosage (g L^{-1})	References
Acrylic acid-grafted polypropylene	0.01	60.97	25	7.5	1		Lee et al. [17]
Activated carbon	1,200	44.42	20	4	8	–	Chegrouche et al. [20]
Alginate/zeolite A	64.6	96.15	–	–	–	1.13	Vipin et al. [21]
Alginate/carbon nanotube/zeolite A	82.4	107.5	–	–	–	1.13	Vipin et al. [21]
Alginate/humic acid/Fe-aminoclay	8.7	45.65	25	7	24	2	Choe et al. [22]
Almond green hull	–	116.3	25	7	–	6	Ahmadpour et al. [18]
Ammonium molybdophosphate-polyacrylonitrile	32.69	16.17	20	5	24	33.33	Park et al. [7]
Attapulgite	198	7.98	–	–	0.5	–	Kilincarslan Kaygun et al. [5]
Carbon nanotubes-chitosan	–	205.1	–	–	–	–	Li et al. [9]
Clinoptilolite	–	9.8	20	5	24	5	Smičiklas et al. [23]
Graphene oxide	–	140	25	6	–	0.5	Amer et al. [24]
Graphene oxide-EDTA	–	158	25	6	–	0.5	Amer et al. [24]
$K_2Ti_4O_9$	2.53	104	25	7.5	1		Lee et al. [17]
Marble	63.02	2.1	25	9	1.5	20	Hamed et al. [11]
Rice straw biochar	71.53	175.95	35	7	2		Jang et al. [25]
Soil	–	4.46	25	4	24	33.33	Chiang et al. [26]

q_m maximum adsorption capacity, t_e adsorption equilibrium time, – not reported

silicate) with high surface area and/or cation exchange capacity are potential ion exchangers which can exchange their native innocuous cations such as Na^+ and Mg^{2+} for the heavy metals and radioactive cations [5, 14]. Boyer et al. [1] showed that wetland sediments could attenuate Sr through strong and almost irreversible adsorption. Wetland substrates such as moss could retain Sr for long periods, while bone charcoal and clinoptilolite (a natural zeolite) were not recommended due to considerable Sr leaching.

Zeolite refers to a group of porous aluminosilicate minerals known for their high cation exchange capacities, CEC and extensive pore structures [32, 33]. It has a large network of pores and channels which act as ion-exchange sites for the removal of heavy metals and other cations in aqueous media [21, 34]. Compared to untreated natural clinoptilolite, Serbian clinoptilolite (>90% purity) showed moderate Sr adsorption capacity of 9.8 mg g^{-1} [23]. On the other hand, Kubota et al. [19] have reported that though bentonite and zeolite were effective for Cs and Sr removal from river water, they were ineffective for Sr removal from seawater. Table 2 lists radioactive contaminant sources (actual and simulated) treated using different adsorbents.

Plant-related sorbents are often cheaper and easily available for large-scale wastewater treatment. Almond green hull, an agricultural crop residue which accounts for 0.25–0.6 wt% of the almond fruit, has an Sr uptake capacity of 116.3 mg g^{-1} [18]. Out of biochars prepared from rice straw, paprika plant and mushroom substrate (particle size ranging from 300 to 710 μm), the alginate-encapsulated rice straw-based biochar with a microporous structure (specific surface area, SSA 71.53 m^2 g^{-1}) showed the best Sr adsorption of 175.95 mg g^{-1} [25].

Alginate, a natural polymer derived mainly from brown algae, is a potential adsorbent due to its biodegradable and biocompatible characteristcs [22]. However, excessive swelling of certain alginate adsorbents like hydrogel-type alginate beads due to ion concentration and subsequent poor mechanical strength make them impractical for seawater treatment [4]. An alginate-zeolite composite foam has higher mechanical stability in seawater and improved Sr sorption [4]. Goethite (α-FeOOH) is a naturally occurring and thermodynamically stable iron mineral. Iron oxides and iron oxy-hydroxides commonly occur as corrosion products from

Table 2 Contaminant sources and adsorbents used for Sr removal

Contaminant source	Adsorbent	References
Low-level waste	Ammonium molybdophosphate-polyacrylonitrile	Park et al. [7]
Low-level waste	Zeolite 4A	Fang et al. [10]
Nuclear waste	Di-2-ethyl hexyl phosphoric acid	Kocherginsky et al. [35]
High-level waste	MIL-101-SO_3H	Aguila et al. [36]
Radioactive seawater	Sodium nonatitanate, zeolite A	Merceille et al. [37]
Radioactive seawater	Activated carbon, bentonite, zeolite	Kubota et al. [19]

the oxidation of the high-level waste steel container surface and are excellent metal cation sorbents [3].

Column studies are essential for proper deployment of adsorbents for large-scale Sr contamination treatment. Rice straw-based biochar (SSA 71.53 $m^2\ g^{-1}$) was reported to have a maximum Sr sorption capacity of 173.67 mg g^{-1} at a flow rate of 0.5 ml min^{-1} and bed thickness of 6 cm [25]. A hydroxyapatite column showed about 80% Sr^{2+} removal efficiency with negligible leaching [15].

In the case of natural adsorbents, the selection and pretreatment processes of the materials are vital to obtain maximum sorption. Washing with distilled water, drying at 105°C and grinding/sieving to a specific size limit or size range are the common physical treatment methods [23]. Ahmadpour et al. [18] used almond green hull with particle sizes less than 88 μm, while Chiang et al. [26] and Wallace et al. [31] dried and sieved soils to less than 2 mm. Chemical pretreatment is used for separating the soluble organic compounds and for improving the chelating efficiency. Almond green hull was treated with 2 vol% of both ammonia and hydrogen peroxide [18], while soils were treated with 30% hydrogen peroxide and heated to remove organic matter [26].

2.2 *Synthetic Adsorbents*

Apart from naturally occurring zeolites (e.g. clinoptilolite), synthetic ones can be prepared from pure alumina and silica sources as well as from industrial byproducts such as fly ash and coal gangue [32, 38]. Synthetic zeolites may perform better than their natural counterparts due to better crystal structure and/or lack of impurities [10]. Zeolites show greater adsorption efficiencies in alkaline environment [10], while their crystal structures may break down in highly acidic conditions [14].

Cement-based materials behave very differently compared to natural adsorbents like soils and clay minerals [12]. Based on the mineral composition, their alkaline pore solution is conducive for sorption of Sr^{2+} and Cs^+. In hardened cement paste, calcium silicate hydrates (C-S-H) are the main adsorbents, and the sorption process is considered as an ion-exchange mechanism between the native cations (Na^+ and K^+) and the contaminant cations at the negatively charged sites or acidic silanol (Si-OH) sites (Cs^+, Sr^{2+}) [39]. Hyperalkaline (pH 13.5), K-rich young cement water enhances the Sr sorption potential of sediments through mineralogical alterations [40].

Synthetic hydroxyapatite with SSA 158 $m^2\ g^{-1}$ showed a maximum removal capacity of 218 mg g^{-1} [13]. Graphene oxide and EDTA functionalized graphene oxide possess good stability due to their negative surface charge [24].

3 Parametric Effects, Reaction Kinetics and Isotherms

The physical, chemical and mineralogical characteristics of the adsorbents as well as the operating conditions affect the sorption process. Higher specific surface area (SSA) can enhance adsorption due to the availability of more adsorption sites as observed in the case of adsorbents such as hydroxyapatite (SSA 158 $m^2\ g^{-1}$) [13] and rice straw biochar (SSA 71.53 $m^2\ g^{-1}$) [25]. The surface area can be improved through grinding [5, 41] and sieving [31] the raw materials. Incidentally, synthetic adsorbents such as acrylic acid-grafted polypropylene [17], alginate/humic acid/Fe-aminoclay [22] and potassium titanate oxide [17] with very low surface area also show high adsorption capacity due to their chemical structural modifications.

An essential parameter for the economical design of water treatment process is the equilibrium time (t_e) for adsorption [11]. Initially, the adsorption process is faster, and the rate slows down near t_e due to slower diffusion into the interior adsorption sites. The equilibrium time varies from few minutes to several hours depending on the adsorbent characteristics, its dosage and initial contaminant concentration. For low-level radioactive waste treatment, t_e for synthetic zeolite A was 45 min, while natural zeolite took 180 min [10]. It was found that 24 h is optimum for Sr removal from high-level nuclear waste using a metal organic framework, MIL-101-SO_3H, at an adsorbent dosage of 4 g L^{-1} [36]. At higher initial contaminant concentrations, the ratio of Sr ions to the available sorption sites will be higher, and the binding sites are saturated faster [18]. Furthermore, high sorption efficiency and easily available sorption sites reduce the equilibrium time required [18].

3.1 Influence of pH

Changes in pH to either acidic or alkaline environment can adversely affect the mineralogy and the release of exchangeable cations leading to a reduction in concentrations of fixation sites and change in competitive adsorption behaviour of the cations [6, 11, 31]. Table 3 shows the favourable pH range of few adsorbents used for strontium removal. In general, a neutral pH is ideal for Sr immobilization, while some materials such as clinoptilolite and wetland sediments are effective adsorbents over a wide range of acidic and alkaline conditions. Marble with an inherent alkalinity (pH 8.5) showed a sharp increase in Sr uptake capacity with pH ranging from 3 to 7 [11]. At lower pH values, H^+ ions compete with strontium ions for adsorption sites, and their removal is inhibited at low pH [16]. A Taiwanese soil (pH 4.6) was reported to have a maximum Sr adsorption capacity of 4.46 mg g^{-1} at pH 4 [26]. At pH ranging from 5 to 11, Sr^{2+} is present in its free form, and variations in pH within this range do not appear to have a significant effect on Sr removal [1]. Above pH 13, strontium ions form $Sr(OH)^+$ species resulting in very low removal efficiency [25]. In cement or concrete, the high pH (>12) of the pore fluids prevents significant migration of Sr [40]. For chitosan surface-modified carbon

Table 3 Favourable pH range for strontium removal

Adsorbent	Favourable pH	References
Acrylic acid-grafted polypropylene	5–8	Lee et al. [17]
Alginate/humic acid/Fe-aminoclay	7	Choe et al. [22]
Attapulgite	4–8	Kilincarslan Kaygun et al. [5]
Carbon nanotubes-chitosan	6–9	Li et al. [9]
Clinoptilolite	2–10	Smičiklas et al. [23]
Goethite	6–8	Nie et al. [3]
Graphene oxide-EDTA	6	Amer et al. [24]
$K_2Ti_4O_9$	7–8	Lee et al. [17]
Marble	3–7	Hamed et al. [11]
Sediments	6–8	Wallace et al. [31]
Wetland sediments	5–11	Boyer et al. [1]

nanotubes, the Sr^{2+} uptake was effective over a wide range of pH (1–9) although there was a slight increase from pH 6 [9]. High values of pH (e.g. pH >7 for marble and >10 for natural clinoptilolite) can result in significant increase in Sr removal due to adsorption of hydrolytic species and/or surface precipitation [11, 23].

3.2 Temperature and Thermodynamics

For most of the adsorbents, higher temperatures are favourable for Sr adsorption process which increases the rate of adsorbate molecular/ionic diffusion in the internal pores of the adsorbent and across the external boundary layer [11, 18]. For rice straw biochar beads, an increase in temperature from 15 to 35°C resulted in an increase in adsorption capacity from 22.24 to 32.44 mg g^{-1} [25]. On the contrary, for alginate-humic acid-Fe-aminoclay hydrogel, reactions at lower temperature (25°C) showed better adsorption capacity as compared to that at higher temperature (35°C) [22]. For EDTA functionalized graphene oxide, 40°C has been reported to be the ideal temperature for Sr^{2+} removal [24]. Incidentally, almond green hull is a natural adsorbent and was reported to be temperature independent [18].

Sr adsorption is either exothermic as in the case of attapulgite and modified alginate [5, 22] or endothermic (indicated by the positive enthalpy change) and spontaneous reactions (i.e. enthalpy change <40 kJ mol^{-1}) in adsorbents like activated carbon, attapulgite and marble, which is indicative of physical process [5, 20, 25].

3.3 Reaction Kinetics

Sr adsorption on most of the natural adsorbents, e.g. almond green hull, bentonite, biochar and marble [11, 16, 18, 25], and synthetic ones such as acrylic acid-grafted

polypropylene, alginate/humic acid/Fe-aminoclay hydrogel chitosan-chelated carbon nanotubes, graphene oxide, $K_2Ti_4O_9$ and zeolite-alginate composite [4, 9, 17, 22] followed pseudo-second-order kinetics indicating that chemical adsorption is the rate-limiting step [11, 42]. For soils near a Taiwanese nuclear facility, it was found that the rate-limiting step was diffusion-controlled processes [26]. Activated carbon followed pseudo-first-order kinetics whose rate constant increased with increase in particle size, pH and temperature [20].

3.4 Isotherms

Langmuir isotherm, which is typical of monolayer adsorption, has been reported to best fit most Sr adsorbents, while few synthetic materials such as alginate-humic acid-Fe-aminoclay [22], alginate-zeolite [4], carbon nanotubes with chitosan [9] and $K_2Ti_4O_9$ [17] satisfied the Freundlich model, indicating multilayer adsorption. Some adsorbents (e.g. almond green hull and chitosan-chelated carbon nanotubes) were reported to fit both Langmuir and Freundlich isotherms [9, 18]. However, Dubinin–Radushkevich (D–R) isotherm fitted the Sr adsorption on natural attapulgite [5].

3.5 Competitive Adsorption

In most cases, the untreated water (seawater, in particular) would have salts, surfactants and/or innocuous cations such as Al^{3+}, Ca^{2+}, Mg^{2+}, K^+ and Na^+ which can lead to a competitive adsorption process [7, 19]. Radioactive cations, Co^{2+} and Cs^+, as well as cationic and anionic surfactants present in low-level waste adversely affect the adsorption of Sr^{2+} [7]. Alginate-based hydrogel showed Sr^{2+} selectivity of two and three times that of Ca^{2+} and Mg^{2+}, respectively [22]. For biochar adsorbents, Al^{3+}, Mg^{2+} and K^+ show negligible influence on Sr adsorption, while higher concentrations of Ca^{2+} and Na^+ are detrimental to Sr adsorption [25]. The adsorption capacity of potassium titanate oxide ($K_2Ti_4O_9$) was unaffected by K and Na ions, while it decreased in the presence of Ca and Mg ions [17]. In the case of acrylic acid-grafted polypropylene fabric, the Sr adsorption greatly reduced in the presence of Na, K, Ca and Mg cations [17]. The ion selectivity series was $Mg^{2+} > K^+ > Na^+ > Ca^{2+}$ for chitosan surface-modified carbon nanotubes although the Sr^{2+} affinity was high [9]. The presence of EDTA hindered Sr adsorption (5.5% decrease) on natural clinoptilolite due to the formation of large sized complexes with positively charged surface groups [23]. A positive interaction exists between the radionuclides Se and Sr at pH range of 6–8; Se^{4+} promotes Sr^{2+} adsorption on goethite by a factor of 5 [3].

3.6 Regeneration of Spent Adsorbents

The desorption and degree of reusability of the spent adsorbents influence the economical viability of the process apart from making it sustainable through resource recovery [43, 44]. The regeneration of used adsorbents can be achieved through acid washing [31]. 0.5 N HCl for $K_2Ti_4O_9$ and acrylic acid-grafted polypropylene [17] and 1M HNO_3 in the case of nickel hexacyanoferrate-sericite beads [45] help to recover the radioactive cations. On the other hand, desorption test on hydroxyapatite using 0.1M $CaCl_2$ showed negligible leaching [15]. Alginate microspheres showed incomplete regeneration after 2–3 cycles of adsorption and washing with up to 1M $CaCl_2$ [43]. For radioactive waste treatment, washing vermiculite with 0.3M KCl was observed to be ineffective, while the coexistence of a zeolite (mordenite and Linde-type A) greatly improved the regeneration, and the two adsorbents could be separated by wet sieving [46].

4 Membrane Technology

Membrane technology is effective for water treatment applications such as desalination and removal of hazardous and toxic contaminants. The membrane is a thin selective barrier separating two streams from each other and acts as a distinct thin interface that regulates the infiltration of ionic species in contact with it. It can either be homogeneous, i.e. uniform in composition and structure, or heterogeneous, i.e. having holes or pores of finite dimensions [47]. In membrane technology, permeate is the flow through a membrane, and the rejected flow is called the retentate. Further, membranes are either employed for concentration or separation of solutes from a solution. Hence, depending upon the desired objective, both permeate and concentrate can be separated effectively. Additionally, different driving forces, viz. pressure, chemical, electrochemical, thermal, vapour pressure and concentration gradients, are associated with the membrane processes. Amongst all, pressure-driven membrane process is more economical and generally used in removal of heavier ions from the water flow. The membrane is formed in different pore sizes, viz. micro-, ultra- and nanofiltration along with reverse osmosis based on the desired removal of solutes [48]. Separation of solute and permeates is done on the basis of molecular size through sieving effects of pressure membranes. However, Judd [49] has shown molecular size and charges with ions play an important role in pressure-driven membrane separation. The materials commonly used to make membranes are summarized in Table 4.

The present study is focused on strontium separation from the waste stream where polymeric membrane can be effectively used to separate or concentrate the metal ions from the wastewater [51]. Different types of membranes based on their structure and pore size are shown in Fig. 2.

Table 4 Materials used in membrane process (after [48–50])

S. No.	Materials	Chemicals	Advantages	Disadvantages
1.	Polymeric materials	Polyamide, cellulose acetate, polymer sulphone	It is organic in nature, cost effective	Lesser efficiency than ceramic materials due to hydrophobicity and leads to high fouling
2.	Ceramic materials	Aluminium oxide, zirconium oxide, titanium oxide, zinc oxide, silicon oxide	Inorganic in nature, higher mechanical strength and permeating flux, chemical and thermal stability	Very expensive, surface poisoning

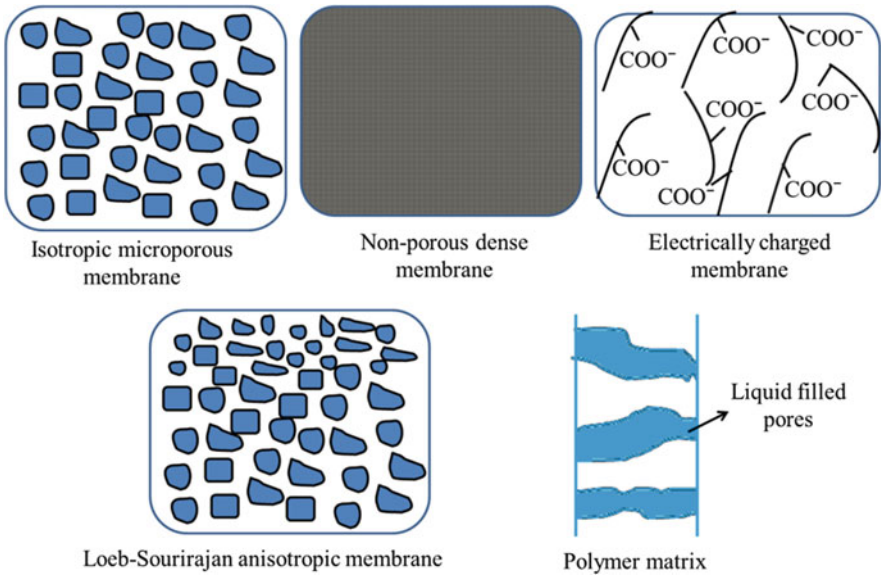

Fig. 2 Different types of membranes used in filter to remove ions (with permission from the publisher [47])

The size of isotropic microporous membrane ranges from 0.01 to 10 μm which is quite bigger than the atomic size of strontium, i.e. 255 pm [47]. On the other hand, non-porous membranes possess dense film and pass liquid through the driving force of a pressure, concentration or electrical gradient. This membrane is more favourable for gases and liquid where similar type of concentration gradient is involved in the membrane. The electrically charged membrane is dense microporous and having positive and negative charged ions in the pores.

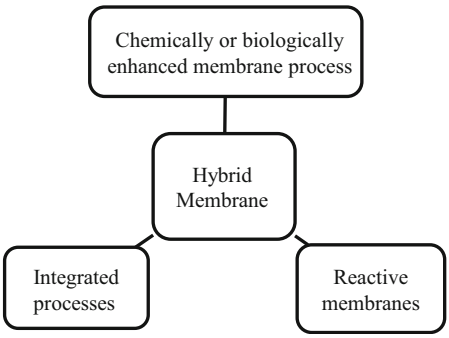

Fig. 3 Different types of hybrid membrane processes

4.1 Hybrid Membranes

Hybrid membrane is a combination of two membranes which perform better as compared to individual membrane processes [52]. Since two decades, the application of hybrid membrane technology has gained attention in water treatment because of its ability in quality improvement of the product and in minimization of environmental and energy loads to any system [53]. Based on the required target, there are different types of hybrid membranes as shown in Fig. 3.

The hybrid system can improve the performance of treatment technologies with higher removal efficiency, an increased amount of treated water, a lower fouling tendency, etc. [53, 54]. Moreover, conventional membrane process, i.e. nanofiltration and reverse osmosis, can employ a hybrid or integrated membrane system (IMS) as an advanced pretreatment method for removal of Sr [54]. The 'integrated membrane process' is used when water purification techniques are employed one after another. On the other hand, hybrid membrane process is a combination of treatment techniques and can surpass the limitations of conventional processes [55]. It reduces the membrane fouling effectively and improves the performance of membrane used. Divakaran et al. [56] have done parametric studies for removal of Sr using hybrid membrane where 98% Sr was removed by maintain feed pH 8 from nuclear waste solution. For example, a pretreatment in preceding to the membrane process is one type of a hybrid process that can increase the flux of the membrane unit to make the process more efficient [52]. However, the biggest limitation with membrane process is its complicated system design henceforth its investment costs can increase.

4.2 Graphene Oxide-Based Membranes

Graphene oxide (GO) is an emerging nanomaterials and is being used in the fabrication of separation membrane for ionic and molecular sieving. The structure of GO is shown in the Fig. 4. The two-dimensional single-atomic-thick honeycomb

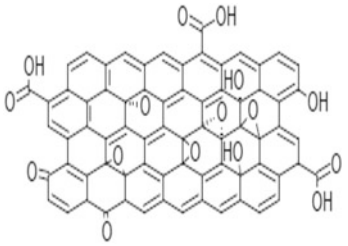

Fig. 4 Structure mode of graphene oxide (with permission from the publisher [57])

Table 5 Characteristics and applications of graphene oxide

Properties	Membrane fabrication method	Application	References
Young's modulus 5.08 GPa Elastic modulus 10–32 GPa Tensile strength 46–70.7 MPa Water flux 1,869 L m^{-2} h^{-1}; Elongation 1.29%	Vacuum filtration, drop-casting, pressurized ultrafiltration, spin casting, dip coating	Ion dialysis separation, oil/water separation, gas separation, water purification, metal removal	Zhao et al. [59], Jia et al. [60], Cotet et al. [61] and Ma et al. [58]

lattice structures make the GO suitable for several applications, viz. solar cell, biosensor, water purification, and salt and metal removal [58]. Table 5 lists the characteristics and applications of GO.

GO possesses high mechanical strength, surface area, chemical inertness and frictionless surface with good flexibility [58]. It can be used for the removal of metals and other impurity ions from water/wastewater. Shannon et al. [62] have reported that a single-layer nanoporous graphene membrane is better than RO membranes for water permeability and rejection of salts. Ma et al. [58] reported that permeation of alkali metal ions and alkali-earth metal ion, Sr(II), is higher as compared to rare earth metal ions, viz. Y, La and Sm, and actinide metal ions, viz. U and Th. Therefore, GO membranes are extremely used to separate ions from the wastewater.

4.3 Vacuum Membrane Distillation

Membrane distillation is thermally driven separation technique where separation occurs due to phase change for non-volatile solute. In this technique, the aqueous solution is separated at certain variance of temperatures using a hydrophobic microporous polymer membrane where feed and permeates get separated by changing

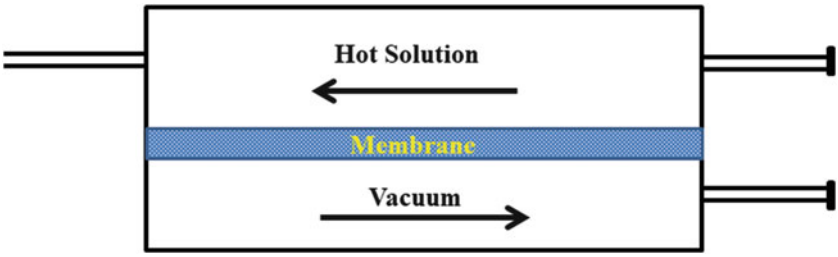

Fig. 5 A schematic diagram of vacuum membrane distillation (VMD)

water pressure as shown in Fig. 5. There are four different types of membrane: (1) direct contact membrane distillation (DCMD), (2) air gap membrane distillation (AGMD), (3) sweeping gas membrane distillation (SGMD) and (4) vacuum membrane distillation (VMD).

Amongst all, the VMD seems to be a potential membrane as it permits higher partial pressure gradients; therefore, it exhibits high permeate flux and less conductive heat loss. In the VMD configuration, a pump is used to create a vacuum in the permeate membrane side, and further condensation takes place outside the membrane module. The heat lost by conduction is negligible [63], and membrane is cost-competitive, capable to work at lower temperature 50–60°C [64].

In addition, when VMD is integrated with reverse osmosis (RO) process, then high concentrated brine water can be converted in fresh water. It has been reported that ~90% water recovery can be done when VMD is coupled with RO plant [63, 65]. However, 100% water recovery has been noticed when VMD is associated with nanofiltration [66]. On the other hand, utilization of renewable energy resources that is solar energy can also be one of the best integrated VMD. In this process, solar collector will act as heat source where 0.1 μm pore size membrane would be there in VMD and it can distillate underground water. Consequently, it can accomplish high permeate flux, i.e. 32.19 kg m^{-2} h^{-1}, where the daily water flux was in the order of 173.5 kg m^{-2} [63].

5 Challenges and Future Scope

Most adsorption studies concentrate on simulated contaminant sources using single or binary contaminant solutions. Wastewater contains various types of contaminants which may behave differently in the presence of other innocuous ions commonly present in water or seawater such as Na^+, K^+, Ca^{2+}, Mg^{2+}, etc. For practical reasons, competitive sorption studies need to be conducted for understanding the actual potential of various adsorbent materials. Furthermore, studies using actual contaminant sources or those closely simulating the actual conditions would be better useful for contaminant attenuation. Although the regeneration of the spent adsorbents is vital for economic feasibility, very few studies address this aspect in recent

adsorption studies. Leaching characteristics are also important to determine the long-term effectiveness of the adsorbents to attenuate Sr and alleviate the contaminated waterbodies and wastewater. Limited research exists on the immobilization of Sr in low-level wastes which contain radioisotopes, dissolved solids, electrolytes, surfactants and suspended solids. In spite of the vital importance of column studies for large-scale adsorption application, in the recent past, there is a dearth of reported research on the same. Pressure-driven membrane technology, viz. reverse osmosis, microfiltration, ultrafiltration and nanofiltration, has already demonstrated their potential for removal of radioactive contaminants. Amongst all, nanofiltration can separate mono and divalent ions effectively. However, this technology has not been commercialized in a broader spectrum due to high cost. In this context, hybrid membrane may be ideal due to its higher efficiency and can also minimize the drawback of individual membranes. Moreover, it is economic for removal of radioactive contaminants like Sr, and hence, there is the need to explore more possibilities for different combinations of hybrid membranes.

References

1. Boyer A, Ning P, Killey D, Klukas M, Rowan D, Simpson AJ, Passeport E (2018) Strontium adsorption and desorption in wetlands: role of organic matter functional groups and environmental implications. Water Res 133:27–36
2. Andrews MG, Jacobson AD (2017) The radiogenic and stable Sr isotope geochemistry of basalt weathering in Iceland: role of hydrothermal calcite and implications for long-term climate regulation. Geochim Cosmochim Acta 215:247–262
3. Nie Z, Finck N, Heberling F, Pruessmann T, Liu C, Lützenkirchen J (2017) Adsorption of selenium and strontium on goethite: EXAFS study and surface complexation modeling of the ternary systems. Environ Sci Technol 51:3751–3758
4. Hong HJ, Kim BG, Ryu J, Park IS, Chung KS, Lee SM, Lee JB, Jeong HS, Kim H, Ryu T (2018) Preparation of highly stable zeolite-alginate foam composite for strontium(^{90}Sr) removal from seawater and evaluation of Sr adsorption performance. J Environ Manag 205:192–200
5. Kilincarslan Kaygun A, Eral M, Akyil Erenturk S (2017) Removal of cesium and strontium using natural attapulgite: evaluation of adsorption isotherm and thermodynamic data. J Radioanal Nucl Chem 311:1459–1464
6. Siroux B, Beaucaire C, Tabarant M, Benedetti MF, Reiller PE (2017) Adsorption of strontium and caesium onto an Na-MX80 bentonite: experiments and building of a coherent thermodynamic modelling. Appl Geochem 87:167–175
7. Park Y, Lee YC, Shin WS, Choi SJ (2010) Removal of cobalt, strontium and cesium from radioactive laundry wastewater by ammonium molybdophosphate-polyacrylonitrile (AMP-PAN). Chem Eng J 162:685–695
8. Li YC, Min XB, Ke Y, Chai LY, Shi MQ, Tang CJ, Wang QW, Liang YJ, Lei J, Liu DG (2018) Utilization of red mud and Pb/Zn smelter waste for the synthesis of a red mud-based cementitious material. J Hazard Mater 344:343–349
9. Li T, He F, Dai YD (2016) Prussian blue analog caged in chitosan surface-decorated carbon nanotubes for removal cesium and strontium. J Radioanal Nucl Chem 310:1139–1145
10. Fang XH, Fang F, Lu CH, Zheng L (2017) Removal of Cs^{+}, Sr^{2+}, and Co^{2+} ions from the mixture of organics and suspended solids aqueous solutions by zeolites. Nucl Eng Technol 49:556–561

11. Hamed MM, Aly MI, Nayl AA (2016) Kinetics and thermodynamics studies of cobalt, strontium and caesium sorption on marble from aqueous solution. Chem Ecol 32:68–87
12. Li K, Pang X (2014) Sorption of radionuclides by cement-based barrier materials. Cem Concr Res 65:52–57
13. Janusz W, Skwarek E (2016) Study of sorption processes of strontium on the synthetic hydroxyapatite. Adsorption 22:697–706
14. Koshy N, Singh DN (2016) Fly ash zeolites for water treatment applications. J Environ Chem Eng 4:1460–1472
15. Nishiyama Y, Hanafusa T, Yamashita J, Yamamoto Y, Ono T (2016) Adsorption and removal of strontium in aqueous solution by synthetic hydroxyapatite. J Radioanal Nucl Chem 307:1279–1285
16. Pathak P (2017) An assessment of strontium sorption onto bentonite buffer material in waste repository. Environ Sci Pollut Res 24:8825–8836
17. Lee T, Na CK, Park H (2018) Adsorption characteristics of strontium onto $K_2Ti_4O_9$ and PP-g-AA nonwoven fabric. Environ Eng Res 23:330–338
18. Ahmadpour A, Zabihi M, Tahmasbi M, Bastami TR (2010) Effect of adsorbents and chemical treatments on the removal of strontium from aqueous solutions. J Hazard Mater 182:552–556
19. Kubota T, Fukutani S, Ohta T, Mahara Y (2013) Removal of radioactive cesium, strontium, and iodine from natural waters using bentonite, zeolite, and activated carbon. J Radioanal Nucl Chem 296:981–984
20. Chegrouche S, Mellah A, Barkat M (2009) Removal of strontium from aqueous solutions by adsorption onto activated carbon: kinetic and thermodynamic studies. Desalination 235:306–318
21. Vipin AK, Ling S, Fugetsu B (2016) Removal of Cs^+ and Sr^{2+} from water using MWCNT reinforced zeolite-A beads. Microporous Mesoporous Mater 224:84–88
22. Choe SR, Haldorai Y, Jang SC, Rethinasabapathy M, Lee YC, Han YK, Jun YS, Roh C, Huh YS (2018) Fabrication of alginate/humic acid/Fe-aminoclay hydrogel composed of a grafted-network for the efficient removal of strontium ions from aqueous solution. Environ Technol Innov 9:285–293
23. Smičiklas I, Dimović S, Plećaš I (2007) Removal of Cs^{1+}, Sr^{2+} and Co^{2+} from aqueous solutions by adsorption on natural clinoptilolite. Appl Clay Sci 35:139–144
24. Amer H, Moustafa WM, Farghali AA, El Rouby WMA, Khalil WF (2017) Efficient removal of Cobalt(II) and Strontium(II) metals from water using ethylene diamine tetra-acetic acid functionalized graphene oxide. Z Anorg Allg Chem 643:1776–1784
25. Jang J, Mirana W, Divine SD, Nawaz M, Shahzad A, Woo SH, Lee DS (2018) Rice straw-based biochar beads for the removal of radioactive strontium from aqueous solution. Sci Total Environ 615:698–707
26. Chiang PN, Wang MK, Huang PM, Wang JJ, Chiu CY (2010) Cesium and strontium sorption by selected tropical and subtropical soils around nuclear facilities. J Environ Radioact 101:472–481
27. Powell BA, Miller T, Kaplan DI (2015) On the influence of ionic strength on radium and strontium sorption to Sandy loam soils. J South Carolina Acad Sci 13:4
28. Abdel-Karim AAM, Zaki AA, Elwan W, El-Naggar MR, Gouda MM (2016) Experimental and modeling investigations of cesium and strontium adsorption onto clay of radioactive waste disposal. Appl Clay Sci 132-133:391–401
29. Başçetin E, Atun G (2010) Adsorptive removal of strontium by binary mineral mixtures of montmorillonite and zeolite. J Chem Eng Data 55:783–788
30. Ning Z, Ishiguro M, Koopal LK, Sato T, Kashiwagi JI (2017) Strontium adsorption and penetration in kaolinite at low Sr2+ concentration. Soil Sci Plant Nutr 63:14–17
31. Wallace SH, Shaw S, Morris K, Small JS, Fuller AJ, Burke IT (2012) Effect of groundwater pH and ionic strength on strontium sorption in aquifer sediments: implications for 90 Sr mobility at contaminated nuclear sites. Appl Geochem 27:1482–1491

32. Koshy N, Jha B, Kadali S, Singh DN (2015) Synthesis and characterization of Ca and Na zeolites (non-pozzolanic materials) obtained from fly-ash–$Ca(OH)_2$ interaction. Mater Perform Charact 4:MPC20140053
33. Koshy N, Singh DN, Jha B, Kadali S, Patil J (2015) Characterization of Na and Ca zeolites synthesized by various hydrothermal treatments of fly ash. Adv Civil Eng Mater 4:131–143
34. Koshy N, Singh DN (2016) Textural alterations in coal fly ash due to alkali activation. J Mater Civ Eng 28:04016126
35. Kocherginsky NM, Zhang YK, Stucki JW (2002) D2EHPA based strontium removal from strongly alkaline nuclear waste. Desalination 144:267–272
36. Aguila B, Banerjee D, Nie Z, Shin Y, Ma S, Thallapally PK (2016) Selective removal of cesium and strontium using porous frameworks from high level nuclear waste. Chem Commun 52:5940–5942
37. Merceille A, Weinzaepfel E, Barré Y, Grandjean A (2012) The sorption behaviour of synthetic sodium nonatitanate and zeolite A for removing radioactive strontium from aqueous wastes. Sep Purif Technol 96:81–88
38. Jha B, Koshy N, Singh DN (2014) Establishing two-stage interaction between fly ash and NaOH by X-ray and infrared analyses. Front Environ Sci Eng 9:216–221
39. Hong SY, Glasser FP (2002) Alkali sorption by C-S-H and C-A-S-H gels: part II. Role of alumina. Cem Concr Res 32:1101–1111
40. Wallace SH, Shaw S, Morris K, Small JS, Burke IT (2013) Alteration of sediments by hyperalkaline k-rich cement leachate: implications for strontium adsorption and incorporation. Environ Sci Technol 47:3694–3700
41. Václavíková M, Vitale K, Gallios GP, Ivanicová L (2010) Water treatment technologies for the removal of high-toxicity pollutants, vol 49. Springer, Cham
42. Pathak P, Sharma S (2018) Sorption isotherms, kinetics, and thermodynamics of contaminants in Indian soils. J Environ Eng 24:04018109
43. Hong HJ, Ryu J, Park IS, Ryu T, Chung KS, Kim BG (2016) Investigation of the strontium (Sr(II)) adsorption of an alginate microsphere as a low-cost adsorbent for removal and recovery from seawater. J Environ Manag 165:263–270
44. Ryu J, Kim S, Hong HJ, Hong J, Kim M, Ryu T, Park IS, Chung KS, Jang JS, Kim BG (2016) Strontium ion (Sr^{2+}) separation from seawater by hydrothermally structured titanate nanotubes: removal vs. recovery. Chem Eng J 304:503–510
45. Jeon C (2016) Removal of cesium ions from aqueous solutions using immobilized nickel hexacyanoferrate-sericite beads in the batch and continuous processes. J Ind Eng Chem 40:93–98
46. Munthali MW, Johan E, Aono H, Matsue N (2015) Cs^+ and Sr^{2+} adsorption selectivity of zeolites in relation to radioactive decontamination. J Asian Ceramic Soc 3:245–250
47. Baker RW (2004) Membrane technology and application. Wiley, Hoboken
48. Ahmed F, Lalia BS, Kochkodan V, Hilal N, Hashaikeh R (2016) Electrically conductive polymeric membranes for fouling prevention and detection: a review. Desalination 391:1–15
49. Judd S (2010) The MBR book: principles and applications of membrane bioreactors for water and wastewater treatment. Elsevier, Amsterdam
50. Gallucci F, Basile A, Hai FI (2011) Introduction – a review of membrane reactors. In: Basil A, Gallucci F (eds) Membranes for membrane reactors: preparation, optimization and selection. Wiley, Hoboken, pp 1–61
51. Weerasekara NA, Choo KH, Choi SJ (2013) Metal oxide enhanced microfiltration for the selective removal of Co and Sr ions from nuclear laundry wastewater. J Memb Sci 447:87–95
52. Ang WL, Mohammad AW, Hilal N, Leo CP (2015) A review on the applicability of integrated/hybrid membrane processes in water treatment and desalination plants. Desalination 363:2–18
53. Drioli E, Curcio E, di Profio G, Macedonio F, Criscuoli A (2006) Integrating membrane contactors technology and pressure-driven membrane operations for seawater desalination: energy, exergy and costs analysis. Chem Eng Res Des 84:209–220

54. Chu Z, Liu J, Han C (2015) Removal of strontium ions from aqueous solution using hybrid membranes: kinetics and thermodynamics. Chin J Chem Eng 23:1620–1626
55. Ding S, Yang Y, Li C, Huang H, Hou LA (2016) The effects of organic fouling on the removal of radionuclides by reverse osmosis membranes. Water Res 95:174–184
56. Divakaran S, Ponraju D, Varughese S, Swaminathan T (2018) Parametric studies for strontium separation and volume reduction of a simulated nuclear waste solution. Sep Sci Technol 53:1732–1740
57. Obata S, Saiki K, Taniguchi T, Ihara T, Kitamura Y, Matsumoto Y (2015) Graphene oxide: a fertile nanosheet for various applications. J Phys Soc Jpn 84:121012
58. Ma J, Ping D, Dong X (2017) Recent developments of graphene oxide-based membranes: a review. Membranes 7:52
59. Zhao X, Su Y, Liu Y, Li Y, Jiang Z (2016) Free-standing graphene oxide-palygorskite nanohybrid membrane for oil/water separation. ACS Appl Mater Interfaces 8:8247–8256
60. Jia Z, Wang Y, Shi W, Wang J (2016) Diamines cross-linked graphene oxide free-standing membranes for ion dialysis separation. J Membr Sci 520:139–144
61. Cotet LC, Magyari K, Todea M, Dudescu MC, Danciu V, Baia L (2017) Versatile self-assembled graphene oxide membranes obtained under ambient conditions by using a water-ethanol suspension. J Mater Chem A 5:2132–2142
62. Shannon M, Bohn PW, Elimelech M, Georgiadis JG, Mariñas BJ, Mayes AM (2008) Science and technology for water purification in the coming decades. Nature 452:301–310
63. Abu-Zeid MAER, Zhang Y, Dong H, Zhang L, Chen HL, Hou L (2015) A comprehensive review of vacuum membrane distillation technique. Desalination 356:1–14
64. Jia F, Li J, Wang J, Sun Y (2017) Removal of strontium ions from simulated radioactive wastewater by vacuum membrane distillation. Ann Nucl Energy 103:363–368
65. Mericq JP, Laborie S, Cabassud C (2010) Vacuum membrane distillation of seawater reverse osmosis brines. Water Resour 44:5260–5273
66. Drioli E, Criscuoli A, Curcio E (2002) Integrated membrane operations for seawater desalination. Desalination 147:77–81

Use of Sorption Method for Strontium Removal

Anna Vladimirovna Voronina, Vladimir Sergeevich Semenishchev, and Dharmendra K. Gupta

Contents

Abstract Stable isotopes of strontium are common components of natural waters, soils, and soil solutions, whereas radioactive isotopes such as Sr-90 are components of liquid radioactive waste and pollutants of the environment. Sorption method is used for decreasing toxicity of drinking waters when elevated concentrations of stable isotopes are present as well as for deactivation of aqueous media containing radioactive isotopes of strontium. The chapter discusses natural and artificial sorbents for strontium sorption from various aqueous solutions. Mechanisms of strontium sorption by various types of sorbents and factors affecting strontium sorption

A. V. Voronina (✉) · V. S. Semenishchev
Radiochemistry and Applied Ecology Department, Ural Federal University, Physical Technology Institute, Ekaterinburg, Russia
e-mail: av.voronina@mail.ru

D. K. Gupta
Gottfried Wilhelm Leibniz Universität Hannover, Institut für Radioökologie und Strahlenschutz (IRS), Hannover, Germany

P. Pathak, D. K. Gupta (eds.), *Strontium Contamination in the Environment*, The Handbook of Environmental Chemistry 88,
https://doi.org/10.1007/978-3-030-15314-4_11

are described. The effect of concentrations of cations and anions in a solution on sorption and redistribution of strontium between liquid and solid phase is shown.

Keywords Natural water decontamination · Sorbents for strontium · Strontium in the environment

1 Contamination of Natural Waters and Soils by Strontium

1.1 Contamination by Stable Strontium

Stable strontium is a natural component of natural waters, soils, and soil solutions. Content of strontium varies depending on geochemical characteristics of a region being conditioned by the presence of strontium-containing minerals. Natural waters contact with the minerals resulting in strontium leaching. Thus, strontium may appear in underground and surface waters including drinking water sources. Concentration of strontium in soils is conditioned by participation of strontium-containing minerals in processes of soil formation. The use of fertilizers containing strontium is another source of appearance in soils and natural waters [1].

Increased content of strontium ions in natural waters being used for drinking purposes may result in ingrowth of strontium concentration in human organisms and therefore health diseases. Strontium is a physicochemical analogue of calcium [2] and is an alkaline earth metal; thus, it can replace calcium in the bone and in tooth. Typical toxic effect of strontium is so-called strontium rachitis or Urov disease (according to the Urov river in the East Transbaikalia) resulting in deformation of joints and fragility of bones in children [3]. It should be mentioned that strontium rachitis appears mainly in children in cases of combination of a high strontium intake and other negative factors such as deficiency of calcium and vitamin D, malnutrition, and violation of the ratio of trace elements. In Russia, the maximal acceptable level of strontium in drinking water is 7 mg L^{-1} [4]; the same level of 7 mg L^{-1} is accepted in Canada [5]. In the USA, the maximum contaminant level of strontium is not accepted, but drinking water equivalent level is 20 mg L^{-1} [6]. In the European Union, strontium is not included to the mandatory parameters of drinking water quality [7].

Concentration of strontium in natural water varies from 2.3 to 62.7 mg L^{-1} [8]. These significant variations of strontium concentrations in ground and underground waters are conditioned by different concentrations of strontium in soils and rocks. Concentration of strontium in freshwaters varies from 10^{-5} to several mg L^{-1} [9]; in seawater, strontium concentration depends on salinity and varies from 7 to 50 mg L^{-1} [10]. Underground water of Salekhard city (Russia) contains nearly 1 mg L^{-1} of strontium [11]; tap water of Yekaterinburg city (Russia) contains 10^{-4} mg L^{-1} [12].

Contamination of natural water by stable strontium may be observed in locations of strontium ore deposits. For example, the problem of contamination of surface and

underground waters by Sr^{2+} appeared as a result of developing strontium salt deposit in Kungur subregion of the Perm region (Russia). Mazuevskoe deposit contains strontium as celestite, strontium-containing calcite, and aragonite-strontianite. The total square of the deposit is 20 km^2; concentration of strontium oxide in the ore varies from 1.1 to 31.3%. An increased content of strontium ions is observed in natural waters of this region [13].

The problem of drinking water decontamination from stable strontium became especially actual after wide involving artesian waters as a source of drinking water; concentration of stable strontium may exceed the maximal acceptable level by a factor of 5–20. Increased concentrations of strontium are observed in middle waters of the Moscow Artesian Basin. It is located on the territory of Moscow, Smolensk, Tula, Kaluga, Kalinin, Yaroslavl, Vladimir regions, and Mordovia [3]. Elevated concentrations of strontium were found in wells of Archangelsk and Voronezh regions, Nizhny Novgorod city, and some other towns [14]. Deposits of fresh underground waters in Archangelsk region are belonging to Northern Dvina Artesian Basin. Abnormally high concentrations of strontium up to 50 mg L^{-1} and even more are observed in the lower reach of Mezen River, near Mezen city [15]. Public tap water of the Mezen city is supplied from 18 wells; concentrations of strontium exceed the maximal acceptable level in five of these well.

Typical concentrations of strontium in uncontaminated soils vary from 0.01 to 0.28% [16]. A special genesis of soils may result in a significant increase of strontium content. In the USA, the maximal content of strontium is observed in light desert soils (70–2,000 mg kg^{-1}) and soils on volcanic rocks, granites, and gneisses (50–1,000 mg kg^{-1}) [17]. An increased strontium concentration of 544 mg kg^{-1} was found in humus-carbonate soil of Krasnodar region, Russia, whereas in brown mountain forest soils, the strontium concentration is only 111 mg kg^{-1} [18]. Alluvial-marsh soils being located along the Karelian coast of the White Sea contain up to 900 mg kg^{-1} of strontium [19]. Elevated concentrations of strontium are also observed in soils of Khibiny Tundra, the Amur and central Kamchatka, some regions of Northern Kazakhstan, Tajikistan, as well as the Tejen oasis of Turkmenistan [20].

Speciation of strontium in soils (water-soluble, exchangeable, and acid-soluble) and its mobility depend on the conditions of a soil formation as well as physico-chemical characteristics of a soil and type of its use. The percentage of water-soluble forms of strontium increases as a result of agricultural use of a soil. In the plow horizon of sod-podzolic soil, the concentration of water-soluble strontium form is two times higher than in the humus-accumulative horizon of the virgin soil [21].

Concentration of strontium in inorganic fertilizers is not regulated. Phosphoric fertilizers contain usually from 25 to 500 mg kg^{-1} of strontium [22]. The use of strontium-containing fertilizers and ameliorators results in an increase of both total content of strontium and exchangeable forms of strontium in soils [1, 23].

1.2 Contamination by Radioactive Strontium

Radioactive isotopes of strontium are released into the environment as a result of nuclear weapon tests, daily work of enterprises of the nuclear fuel cycle, operation of nuclear power plants, industrial use, and radiation accidents. Daily work of radiochemical enterprises results in the formation of liquid radioactive waste (LRW) containing Sr-90 among other long-lived beta-emitting radionuclides. Radionuclides penetrate into the environment due to outlet of LRW to water basins as well as migration of radionuclides from deposition places and technological water bodies through surface and underground waters. Some major nuclear accidents that released Sr-90 and other radioactive elements into the environment were the Techa River accidental releases in the 1950s in the Soviet Union, the 1986 nuclear reactor accident at Chernobyl (now Ukraine, former USSR), and the 2011 accident at the Fukushima nuclear plant in Japan. The most significant contamination of the environment by Sr-90 occurred because of radiation accidents and nuclear weapon tests. According to the assessment of Myasoedov [24], nuclear weapon tests resulted in the release of 604 PBq of Sr-90, whereas 6.9 PBq and 5.4 PBq were released as a result of spent nuclear fuel reprocessing and Kyshtym disaster (September 29, 1957), respectively. Other sources of Sr-90 release to the environment are rather less significant. Being a pure beta emitter, Sr-90 is very dangerous in case of uptake by an organism and internal irradiation. Consumption of contaminated water and food is the main source of radiostrontium intake to a human's body. The inhalation path is of less importance. Radionuclides of strontium are bone-seeking radionuclides; they are selectively accumulated in bone tissue resulting in long-term irradiation of bones and marrow.

Voronina et al. [25] presented a detailed analysis of contamination of natural waters by Sr-90 and maximal allowable levels of Sr-90 in drinking water being accepted in various countries. The most significant contamination of natural water by Sr-90 can be found in areas of serious radiation accidents as well as at former nuclear testing sites. Activity concentration of Sr-90 in these waters may reach 10^4–10^5 Bq L^{-1}. Decontamination of natural waters with various chemical compositions and liquid radioactive waste treatment with concentration and immobilization of strontium are necessary for radiation safety.

2 Methods of Strontium Removal from Various Aqueous Media

Thermal, sedimentation, sorption, extraction, and membrane methods are used for strontium removal from aqueous media [26]. Choice of the method depends on chemical composition of a contaminated solution and the state of strontium in the solution. Strontium presents in aqueous solutions mainly as Sr^{2+}; however, it can also form complex compounds and colloidal species. Sorption method is the main

method used for decontamination of natural waters; nevertheless, sedimentation and membrane methods are also acceptable in certain cases. All five methods are widely used for LRW treatment depending on the type and chemical composition of LRW. In natural waters and soil solutions, Ca^{2+} ions present together with Sr^{2+} providing a negative competitive effect in processes of strontium removal. Therefore, selective methods of strontium concentration are required for decontamination of natural waters. Thus, sorption method based on the use of selective natural and synthetic sorbents is the most promising for strontium removal from natural waters with various chemical compositions.

2.1 Thermal Method

The thermal method is based on removal of a volatile dissolvent (water) from contaminated water or liquid waste with further condensation of the decontaminated dissolvent and concentration of stable or radioactive contaminants in the residue. The thermal method requires a high-energy consumption that is a significant disadvantage. Therefore, distillation is not economically reasonable for decontamination of water from stable strontium [3].

Thermal distillation is considered as the main method for the treatment of strontium-containing LRW from nuclear power plants and spent nuclear fuel reprocessing. Evaporation can be successfully used for treating any quantities of LRW containing any stable and radioactive components. This method provides a high decontamination factor of condensate, $D = 10^4$–10^6. The value of decontamination factor depends on the number of evaporation stages, construction of evaporator, area of evaporating surface, intensity of boiling, as well as chemical and radionuclide composition of radioactive waste. Distillation allows decontamination of condensate from radionuclides in ionic, molecular, and colloidal forms. It is possible to treat LRW with any salt content providing maximal concentration of salts; it also does not result in an increase of salt weight due to the absence of reagents used. These are the significant advantages of the thermal method. After distillation, the vat residue should be solidified and buried, whereas the condensate can be reused after dosimetric control.

2.2 Sedimentation Method

Among sedimentation methods of strontium removal, there are coagulation with iron and aluminum salts, carbonate coagulation, phosphate coagulation, and some other. The idea of the method is addition of chemical reagents (coagulants) to water contaminated by strontium in order to coprecipitate microamounts of strontium with the precipitate of the coagulant. It is the simplest method that does not require complex and expensive equipment. $Al_2(SO_4)_3$, $Fe_2(SO_4)_3 \cdot 7H_2O$, $FeCl_3$ and

$FeSO_4 \cdot 7H_2O$ are commonly used as coagulants. If concentration of stable strontium in water is high enough for exceeding the solubility product (K_{sp}), then it is possible to precipitate strontium as carbonate: K_{sp} ($SrCO_3$) = 1.1×10^{-10} [27]. It is also possible to perform coprecipitation of strontium with calcium carbonate, K_{sp} ($CaCO_3$) = 3.8×10^{-9}, or calcium phosphate, K_{sp} ($Ca_3(PO_4)_2$) = 2.0×10^{-29} [27].

Effectiveness of coagulation strongly depends on anionic composition of water. Optimal conditions for coagulation can be found by varying quantity of reagents and pH of the water. It is important to consider the fact that water (especially contaminated natural water) usually contains micro-concentration of radioactive strontium; therefore, *the isotopic dilution method* is used to improve coprecipitation of radiostrontium. For example, stable strontium is added to wastewater in order to precipitate ^{90}Sr. The coprecipitation is performed in coagulators; then the precipitate is filtered using a sand filter. The precipitation methods provide relatively low decontamination factors up to 100.

Coprecipitation of strontium with individual and mixed hydroxides of some metals was studied by Plotnikov et al. [28]. Coprecipitation was studied in 0.25 mol L^{-1} $NaNO_3$ solutions at the temperature of 20°C; time of coprecipitation was 30 min. It is shown that strontium coprecipitation with tetravalent metal hydroxides depends on pH of the solution. Based on the results given in this publication, we have calculated distribution coefficients of strontium at pH 8; these values are 10^5, 10^4, and 10^3 mL g^{-1} for titanium, tin (IV), and zirconium hydroxides, respectively. These hydroxides show the highest selectivity for strontium in weakly base media. The values of distribution coefficients of strontium exceed 10^5 mL g^{-1} at pH 11–12 indicating that this method is very promising for strontium separation from alkaline aqueous solutions.

Alexeev and Gladkova [3] suggested a method for stable strontium removal from water based on electrochemical impact on water resulting in strontium precipitation as carbonate. The method allows decreasing strontium concentration in water from 50 mg L^{-1} to 2…5 mg L^{-1}.

2.3 Sorption Method

Sorption method is one of the most often used techniques for water decontamination in which a pollutant (heavy metals, radionuclides, etc.) is separated from a solution by a ready solid phase (sorbent). Sorption can be realized in dynamic or static conditions. Sorption in dynamics means that the solution is passed through a sorbent's layer; therefore, it is suitable to organize the process as filtration through a sorption filter or column. Sorption in statics is a temporal contact of the phases at mixing with their further separation.

Among the main characteristics allowing assessment of the effectiveness of sorption process, there are degree of sorption, distribution coefficient, separation factor, and decontamination factor.

Degree of sorption (S) is a dimensionless parameter indicating the share of the component being consumed by a sorbent. S is calculated in accordance with (1):

$$S = \frac{C_0 - C}{C_0} \tag{1}$$

where C_0 and C are the initial and final concentrations of the component.

Distribution coefficient (K_d) is calculated according to the Eq. (2):

$$K_d = \frac{S}{1 - S} \cdot \frac{V}{m} \tag{2}$$

where V is the volume of a solution, mL; m is a sorbent weight, g; and S is sorption degree.

In case of sorption use for decontamination of a solution rather than a valuable component separation, the sorption process is characterized by *decontamination factor* (D_f). It shows the relative decrease of concentration of a component after one decontamination step. The dimensionless value of decontamination factor is calculated in accordance with the Eq. (3):

$$D_f = 1/(1 - S) \tag{3}$$

Natural waters always contain several components, whereas in certain cases it is necessary to remove only one component. Selectivity of sorption of a component over other components is characterized by *separation factor* (D) being calculated in accordance with the Eq. (4):

$$D_{(x,y)} = K_{d,x}/K_{d,y} \tag{4}$$

where $K_{d,x}$ and $K_{d,y}$ are distribution coefficients of the separated components x and y, respectively.

Various types of sorbents can be used for strontium removal from natural waters, soil solutions, and liquid radioactive waste. Natural inorganic sorbents or modified sorbents based on them are often used for decontamination of natural aqueous systems. Both natural and synthetic inorganic sorbents are used for treating wastewater and LRW. Raw and chemically modified natural sorbents are eco-friendly and chemically stable; they can be disposed in a soil or a water body for a long period without further removal. In this option, the sorbent works as a sorption matrix for immobilization of radiostrontium preventing its migration in the environment and transfer to food chains. In case of decontamination of drinking water or LRW treatment, sorbents can be used as filters and sorption columns of various sizes. In this case, the sorption process will be organized in dynamic conditions.

The most promising filters for decontamination of drinking water with the sorbent load of 1–1.5 kg allow strontium removal from up to 4,000 L of drinking water [25]. The most effective filters for strontium removal from drinking water contain

titanium hydroxide based on natural clinoptilolite TH-CL (2,000 L resource and the decontamination factor of 1,000÷10), ISM-S sorbent (4,000 L resource and the decontamination factor of 162÷17), and IPF-MP + TH-CL sorbents (4,000 L resource and the decontamination factor of 1,000÷10) [25].

A "barrier" sorption filter is developed for strontium removal from LRW containing seawater. A sorption-reagent filtering material based on $BaSiO_3$ is used in this sorption filter. During the period of 2000–2016, more than 5,000 m^3 of LRW was treated using this device [29].

The Astrakhan Oil and Gas Company uses natural marl from Astrakhan region possessing high sorption capacity for strontium in the system for strontium removal from contaminated water [30].

A sorption filter loaded with the clinoptilolite from Holinskoye deposit (Russia) was tested for decontamination of drinking water from stable strontium. The lab filter had the diameter of 16 mm, height of the bed layer was 55 cm, and the sorbent volume was $V = 1 \times 10^{-4}$ m^3. The filter allowed for decontamination of 260 bed volumes of an underground water containing 32 mg L^{-1} of strontium providing the strontium concentrations in decontaminated water not more than the maximal acceptable limit [14].

2.4 Membrane Method

In contrast to other methods, membrane decontamination performs separation on molecular level and does not result in the formation of a new phase. Reverse osmosis, electrodialysis, and ultrafiltration are interesting for strontium removal from water solutions. Separation of salt from water is the main task of decontamination in this method. This separation occurs due to selective transfer of ions (electrodialysis) or water (reverse osmosis) due to electric potential or different pressure respectively. Membrane methods are not selective and make large volumes of concentrates that should be treated additionally.

In electrodialysis, transport of ions through a membrane is performed due to direct current. Desalted filtrate is the product of electrodialysis. The method does not allow separating pollutants presenting in colloidal forms. It provides only separation of ionic forms, predominately weakly hydrolyzed alkaline, and alkaline earth elements. Hydrolysis of an ion decreases significantly its separation. For example, the degrees of separation of radionuclides by electrodialysis are nearly 99% for ^{137}Cs and ^{90}Sr, 95% for hydrolyzed fission products (HFP), and only 70% for ^{106}Ru. Thus, the effectiveness of decontamination decreases in the following series:

$$^{137}Cs > {}^{90}Sr > HFP > {}^{106}Ru$$

200–400 mg L^{-1} is the lowest limit of salt content of solutions which treatment by electrodialysis is reasonable. Lower salinity results in a dramatic decrease of

electrical conduction of the solution. The upper limit of salt content depends on economic reasons since the electrical power being consumed in the process is proportional to the quantity of separated ions.

Osmosis is based on separation of solutions with different concentrations through a semipermeable membrane. If the pore size of the membrane is small enough, water can pass through the membrane, whereas dissolved matter cannot. Water diffuses from a diluted solution to more concentrated one in order to make concentrations equal. This results in an increase of volume and pressure in the cell with more concentrated solution up to the value depending on the initial difference of concentrations; this additional pressure is called osmotic pressure. For realization of the *reverse osmosis*, i.e., filtration of water from concentrated solution to diluted one, the pressure more than osmotic pressure is exerted to the concentrated solution. Thus, the concentrate becomes more concentrated. Reverse osmosis requires using the finest microporous membranes.

As a rule, reverse osmosis is used for treatment of solutions containing 0.5–5 g L^{-1}. Ion exchange is reasonable for solutions with lower salt content, whereas evaporation is suitable in more concentrated solutions because in these cases working pressure is too high and decontamination becomes worse.

Ultrafiltration uses membranes with wider pores than reverse osmosis; both water and salts pass through the membrane, whereas colloids and suspended particles remain on the membrane. This method is rarely used as an independent method for water decontamination. It is reasonable to combine ultrafiltration with chemical precipitation or to use it as a preliminary step before reverse osmosis or ion exchange.

2.5 Extraction Method

Extraction is based on distribution of a component between two immiscible liquids. As compared with sorbents, organic extractants provide higher capacity, rather faster kinetics, and excellent selectivity. However, the distribution coefficients are lower: typically, K_d values are 10^3–10^6 for sorbents and 1–10 for organic extractants. Organic extractants possess a limited solubility in water; therefore, liquid-liquid extraction is not suitable for decontamination of drinking water because of toxicity of the vast majority of extractants. In addition, extraction is usually performed in acidic media. Thus, the main applications of extraction systems for strontium are LRW treatment and separation of strontium in analytical methods [31].

Strontium presents in acidic solutions as Sr^{2+}; therefore, it can be extracted by cation exchange extractants. For example, SREX process of separation of valuable radionuclides from high-active raffinates of PUREX process is based on joint extraction of Sr, Am, Cm, and lanthanides by bis-2-ethyl-hexyl phosphoric acid (HDEHP) with further elution of individual components. In this technology, diluted sulfuric acid is used for strontium elution due to the formation of strontium sulfate in molecular form.

Among other extraction systems selective for strontium, there are mixtures based on dicarbollylcobaltate [32–34] and crown ethers [35, 36]. Extractants based on 4,4′(5′)-bis-tert-butyl cyclohexyl-18-crown-6 show exclusively high selectivity for strontium and lead (II) in 1–10 HNO_3 solutions due to proximity of the cavity of the crown ether and ionic radii of Sr^{2+} and Pb^{2+} [37]. For more comfortable and easy use, the organic extractants are produced as extraction chromatographic resins [36, 38] and supported liquid membranes [39].

3 Sorbents for Strontium Removal from Aqueous Media

3.1 Raw and Modified Natural Sorbents

Natural sorbents are used for decontamination of natural waters from strontium for a long time [40–42]. It is economically reasonable to treat large volumes of contaminated water using these sorbents due to their low cost and availability. Distribution coefficients of strontium differ for the same minerals from different deposits depending on the degree of Si^{4+} ion replacement by Al^{3+}, Fe^{3+}, and Mg^{2+} ions in the crystal lattice of the silicate mineral as well as on content of Na^{+}, K^{+}, Ca^{2+}, and Mg^{2+} ions locating in the tetrahedral caves of the silica tetrahedrons for compensation of redundant negative charge. Elevated distribution coefficients of strontium are typical for vermiculite, clinoptilolite, and bentonite. Table 1 shows the main sorption characteristics (distribution coefficients and static exchange capacities) of natural sorbents and modified sorbents based on them with respect to strontium. The distribution coefficients of strontium on natural aluminosilicates vary within 10–10^4 mL g^{-1}. The natural aluminosilicates possess relatively low selectivity for strontium over other ions. In the presence of calcium, sorption of strontium dramatically decreases for all studied types of the sorbents. This significant competitive effect of calcium can be explained by the proximity of the hydrated Sr^{2+} and Ca^{2+} ion radii, 0.5 nm and 0.6 nm, respectively [57].

Methods of chemical modification of the natural sorbents are developed to increase their selectivity and static exchange capacity for strontium and decrease reversibility of sorption. Methods of acidic and alkaline activation of the minerals are known. Treatment of the aluminosilicates by salt solutions results in the formation of different ionic forms of the minerals, such as Na-form, Ca-form, Mg-form, etc. Sparingly soluble compounds possessing selectivity for strontium can precipitate on the surface and in the porous space of the minerals. However, the increase of selectivity for strontium due to chemical modification is not so significant; the distribution coefficient can increase not more than by the factor of 5–10.

Among the sorbents possessing high capacity for strontium, there are titanium hydroxide based on clinoptilolite (TH-CL) with the static exchange capacity of 550 mg g^{-1} [44] and nickel-potassium ferrocyanide based on clinoptilolite (NPF-CL) with the capacity of 415 mg g^{-1} [46]. For the comparison, the static exchange capacity of the natural clinoptilolite is only 63 mg g^{-1}.

Table 1 Distribution coefficients (K_d) and static exchange capacities (SEC) of natural sorbents and modified sorbents based on them with respect to strontium

Natural sorbent	Deposit	Modification	Composition of treated water, pH	K_d, mL g^{-1} SEC	References
Clinoptilolite	Dzegvi (Georgia)	Untreated	0.1 Mol L^{-1} $NaNO_3$	3.4×10^2	[43]
			1.0 Mol L^{-1} $NaNO_3$	50	
			0.01 Mol L^{-1} $Ca(NO_3)_2$	30	
		Na(Ca)-form	0.1 Mol L^{-1} $NaNO_3$	1.3×10^3	
			1.0 Mol L^{-1} $NaNO_3$	75	
			0.01 Mol L^{-1} $Ca(NO_3)_2$	5.2×10^2	
		Titanium hydroxide based on clinoptilolite (TH-CL)	Drinking (tap) water pH 7.2 ± 0.1	3.5×10^3 SEC = 550 mg g^{-1}	[44]
		Titanium phosphate based on clinoptilolite	Drinking (tap) water pH 7.2 ± 0.1	4.7×10^3	[45]
	Shivertooyskoe (Russia)	Untreated	Drinking (tap) water pH 7.2 ± 0.1	2.5×10^3 SEC = 63 mg g^{-1}	[46]
		Nickel-potassium ferrocyanide based on clinoptilolite	Drinking (tap) water pH 7.2 ± 0.1	7.9×10^3 SEC = 415 mg g^{-1}	
		Untreated	Drinking (tap) water	5.8×10^2	[47]
		Untreated	$CaCl_2$ with the concentration of 0.02 mg-eqv L^{-1}, pH 6.0	310	[48]
	–	Na-form	0.1 Mol L^{-1} HNO_3	5.9×10^2	[49]
			Na:Ca:Mg:Cl = 1:5:5:25, total salt content 0.8 g L^{-1}	1.1×10^3	
		Zirconium chromate based on clinoptilolite	0.1 Mol L^{-1} HNO_3	3.3×10^2	
			Na:Ca:Mg:Cl = 1:5:5:25, total salt content 0.8 g L^{-1}	2.4×10^3	
		Antimony (V) ferrocyanide based on clinoptilolite	0.1 Mol L^{-1} HNO_3	5.3×10^2	
			Na:Ca:Mg:Cl = 1:5:5:25, total salt content 0.8 g L^{-1}	2.6×10^3	

(continued)

Table 1 (continued)

Natural sorbent	Deposit	Modification	Composition of treated water, pH	K_d, mL g^{-1} SEC	References
		Antimony and silicone copolymer	0.1 Mol L^{-1} HNO_3	2.4×10^4	
			Na:Ca:Mg:Cl = 1:5:5:25, total salt content 0.8 g L^{-1}	2.4×10^4	
Vermiculite	Vermiculite Poland, Ltd. (city Elk, Poland)	Activation by hot nitric or hydrochloric acid	Acidified distilled water at pH 3.0 with noncarrier-added Sr-85	2×10^3 (calculated according to experimental data of the article)	[50]
	Rosvermiculite (Russia)	–	Simulated underground water (mg L^{-1}): Ca^{2+} 94.0, Mg^{2+} 21.6, Na^+ 45.4, $\sum CO_3^{2-} + HCO_3^-$ 465.4, SO_4^{2-} 30.0 and Cl^- 10.0; pH 7.3–7.5	2.0×10^4	[51]
Apatite	Hibinskoye (Russia)	–		36	
Shungite	Zazhoginskoye (Russia)	–		7	
Zeolite	Kondopozhskoye (Russia)	–		6.2×10^3	
Dolomite	Volkovysk (Belarus)	Treatment by H_3PO_4	0.01–5 g L^{-1} $Sr(NO_3)_2$ solution	$(4.7–5.4) \times 10^3$	[52]
Calcite	Ruba (Belarus)	Treatment by H_3PO_4	0.01–5 g L^{-1} $Sr(NO_3)_2$ solution	$(5–9) \times 10^2$	
Bentonite	Taganskoye (Kazakhstan)	Untreated	Solutions with pH 7.2–8.0	2.2×10^3	[53]
		Na-form		2.9×10^3	
		Mg-form		2.1×10^3	
		Ca-form		5.1×10^3	
	Jelšový potok (Slovakia)	Dried for 2–3 h at 105°C	1×10^{-5} M $Sr(NO_3)_2$	9.8×10^3	[54]
			5×10^{-2} M $Sr(NO_3)_2$	10	
	Lieskovec (Slovakia)	Dried for 2–3 h at 105°C	1×10^{-5} M $Sr(NO_3)_2$	4.1×10^3	
			5×10^{-2} M $Sr(NO_3)_2$	7	
	Kopernica (Slovakia)	Dried for 2–3 h at 105°C	1×10^{-5} M $Sr(NO_3)_2$	6.9×10^3	
			5×10^{-2} M $Sr(NO_3)_2$	11	

Montmorillonite clay	Belgorod region (Russia)	Untreated	Drinking (tap) water Salinity 540 mg L^{-1}, pH 7.1	3.3×10^2 (48 h of sorption)	[47]
		Concentrated	Drinking (tap) water Salinity 540 mg L^{-1}, pH 7.1	3.8×10^2 (48 h of sorption)	
		Na-form	Drinking (tap) water Salinity 540 mg L^{-1}, pH 7.1	2.1×10^2 (48 h of sorption)	
		Mg-form	Drinking (tap) water Salinity 540 mg L^{-1}, pH 7.1	1.8×10^2 (48 h of sorption)	
	Alfa Aesar (Korea)	MT was ground and mixed with solid form of NaOH at different weight ratios. The mixture was heated to 300°C for 1 h under a flow of nitrogen	$SrCl_2$ solution with the concentration of 24 mg L^{-1}	1.4×10^4–8.1×10^4 (48 h of sorption)	[55]
White alluvial clay	Moldarskoye (Kazakhstan)	Dried at 115°C	Water from Beloyarskoye pond,	6.1×10^2 (6 days of sorption)	[56]
			Salinity 265 ± 15 mg L^{-1}, pH 8.5 ± 0.2	2.8×10^3 (300 days of sorption)	
			Drinking (tap) water	7.6×10^2 (6 days of sorption)	
			Salinity 115 ± 5 mg L^{-1}, pH = 6.5 ± 0.2	2.9×10^3 (300 days of sorption)	
Glauconite	Karinskoye (Russia)	Quartz-glauconite concentrate dried at 115°C	Water from Beloyarskoye pond	2.1×10^2 (6 days of sorption)	[56]
			Salinity 265 ± 15 mg L^{-1}, pH 8.5 ± 0.2	2.8×10^3 (300 days of sorption)	
			Drinking (tap) water	1.5×10^2 (6 days of sorption)	
			Salinity 115 ± 5 mg L^{-1}, pH = 6.5 ± 0.2	1.7×10^3 (300 days of sorption)	
		Untreated	Drinking (tap) water, pH = 7.8 ± 0.1	79 (7 days of sorption). SEC = 21 mg g^{-1}	[46]
		Nickel-potassium ferrocyanide based on quartz-glauconite concentrate	Drinking (tap) water, pH = 7.8 ± 0.1	1.3×10^2 (7 days of sorption). SEC = 36 mg g^{-1}	

3.2 Synthetic Sorbents for Strontium

Synthetic sorbents such as synthetic zeolites, polyvalent metal hydroxides (Fe, Ti, Mn), phosphates (Fe, Ti, Zr), titanosilicates, etc. are developed for strontium separation from water solutions. In aqueous solutions, manganese varies its oxidation state in a wide range of +2 to +7 and shows a tendency to the formation of many different oxides including schistose, tunnel, and frame structures. Some of these compounds show selective reversible sorption of Sr^{2+}. Leontieva [58] described a structural modification of manganese (III, IV) oxides resulting in synthesis of sorbents selective for strontium. The study of sorption properties of iron, manganese, titanium, aluminum, and silicone oxides with respect to ^{90}Sr was performed by Kuznetsova and Generalova [59]. A new approach to the problem of strontium removal is using a sorption-reagent systems (SRS) based on amorphous $BaSiO_3$. The SRS (amorphous $BaSiO_3$ in a solution containing SO_4^{2-} ions) have found the practical application for decontamination of seawater from radiostrontium [29]. Table 2 presents distribution coefficients of strontium for some synthetic sorbents. Many sorbents are characterized by very similar distribution coefficients for strontium within 10^3–10^4 mL g^{-1}. It is interesting to compare distribution coefficients for strontium in the presence of high calcium concentrations in a solution. Seawater and $CaCl_2$ are the examples of these media. The SRS based on amorphous $BaSiO_3$ showed the highest selectivity for strontium over calcium: distribution coefficient of strontium in seawater is as high as 6.4×10^3 mL g^{-1} [29]. The $K_{2x}Mn_xSn_{3-x}S6$ sorbent has distribution coefficient of strontium of 1.83×10^4 mL g^{-1} in solutions with a less calcium concentration of 11.14 mg L^{-1} [67].

A mixed nickel-potassium ferrocyanide based on hydrated titanium dioxide T-5 possesses a high selectivity for strontium that is realized under limited conditions. It does not adsorb calcium from $CaCl_2$ solutions with the calcium concentration of 0.05–110 g L^{-1} at pH 5–6; however, distribution coefficient of strontium in these conditions is 5.0×10^2 mL g^{-1} independently on calcium concentration [70].

Magnesium hydrophosphate is another one synthetic sorbent with a high static exchange capacity for strontium. The value of capacity of magnesium hydrophosphate for Sr^{2+} ions reaches 280 mg g^{-1} that exceeds the corresponding values for calcium phosphates by an order of magnitude [52].

4 Mechanisms of Strontium Sorption from Aqueous Media

Sorbents can be separated by dissolved components from solutions due to either physical interaction (molecular adsorption) or chemical interaction between sorbent and the component such as chemical connection of atom or molecule and ion exchange. There are four main mechanisms of interaction between a sorbent and a sorbate [26]:

Table 2 Distribution coefficients (K_d) and static exchange capacities (SEC) of synthetic sorbents with respect to strontium

Sorbent	Producer (developer)	Composition of treated water, pH	K_d, mL g^{-1} SEC	References
Zirconium phosphate T-3A	Termoxid (Russia)	0.1 Mol L^{-1} $NaNO_3$	40	[60]
		0.01 Mol L^{-1} Ca $(NO_3)_2$	75	
Synthetic zeolite NaA	TC 2163-003-15285215-2006	0.1 Mol L^{-1} $NaNO_3$	2.5×10^4	
		0.01 Mol L^{-1} Ca $(NO_3)_2$	106	
Synthetic zeolite NaX	–	0.1 Mol L^{-1} $NaNO_3$	7.9×10^3	
		0.01 Mol L^{-1} Ca $(NO_3)_2$	345	
Synthetic Chabazite KG-13	–	0.1 Mol L^{-1} $NaNO_3$	2.5×10^5	
		0.01 Mol L^{-1} Ca $(NO_3)_2$	250	
Granulated sodium-birnessite		Seawater	$0.8–1.2 \times 10^2$	[61]
Sodium titanate Sr-treat	Finland		2.0×10^5	[62]
Sodium titanosilicate TiSi-Na	ISPE NAS (Ukraine)	Seawater	5.2×10^2	[63]
Titanosilicate AM-4		0.001 Mol L^{-1} NaCl	5.2×10^4	[64, 65]
		0.5 Mol L^{-1} NaCl	5.2×10^3	
		2.0 Mol L^{-1} NaCl	2.2×10^3	
Sorption material based on amorphous barium silicate $BaSiO_3$ SRS-Sr	Institute of Chemistry RAS, Vladivostok (Russia)	Seawater	6.4×10^3	[48]
		Seawater	6.0×10^4; V/m = 100 mL g^{-1} 6.0×10^3; V/m = 100 mL g^{-1}	[29]
Synthetic ivanukite	Center of Nanomaterials Science RAS (Russia)	Seawater	61	[48]
		0.02 mg-eq. L^{-1} $CaCl_2$ solution at pH 6.0	8.6×10^3	
Schistose titanosilicate SL3	Center of Nanomaterials Science RAS (Russia)	Seawater	29	
Modified manganese dioxide (MMD)	IPCE RAS, Moscow (Russia)	Seawater	5.9×10^2	
		0.02 mg-eq. L^{-1} $CaCl_2$ solution at pH 6.0	1.4×10^3	

(continued)

Table 2 (continued)

Sorbent	Producer (developer)	Composition of treated water, pH	K_d, mL g^{-1} SEC	References
Mesoporous manganese oxide OMS-2	Institute of General and Inorganic Chemistry of the national Academy of Sciences of Belarus	1–1,000 mg L^{-1} $Sr(NO_3)_2$. 0.1 Mol L^{-1} NaCl 0.05 Mol L^{-1} $CaCl_2$ pH 5.7 ± 0.2 (all solutions)	For the best samples: (1.15–1.95) × 10^4; SEC = 100–160 mg g^{-1} (9.15–20.78) × 10^4; SEC = 20–30 mg g^{-1} (2.3–3.5) × 10^2; SEC = 25–30 mg g^{-1}	[66]
Manganese oxide ISM-S	Perm National Research Polytechnic University (Russia)	0.01 Mol L^{-1} $CaCl_2$	1.1 × 10^3	
Manganese oxide ISMA-3	Perm National Research Polytechnic University (Russia)	0.01 Mol L^{-1} $CaCl_2$	5.0 × 10^2	
KMS-1 $K_{2x}Mn_xSn_{3-x}S_6$ (x = 0.5–0.95)	Northwestern University (Evanston, USA)	Distilled water	1.58 × 10^5	[67]
		Solution containing (mg L^{-1}): 3.70 of Mg^{2+}, 11.14 of Ca^{2+}, 9.17 of Cs^+, 25.96 of Na^+, and 4.60 of Sr^{2+}	1.83 × 10^4	
		0.1 M Sr^{2+} + Na^+ solution	4.5 × 10^5	[68]
Hydrated titanium dioxide T-5	Termoxid (Russia)	0.1 Mol L^{-1} $NaNO_3$	49	[60]
		0.01 Mol L^{-1} $Ca(NO_3)_2$	9	
		Drinking (tap) water, pH 7.8 ± 0.1; strontium concentrations were from 10^{-5} to 10^2 mg L^{-1}	6.3 × 10^2. SEC = 114 mg g^{-1}	[69]
		Solution based on tap water, pH > 8	1.5 × 10^4	
		0.05–2 g L^{-1} $CaCl_2$ solution, pH 7÷8	5.0 × 10^2	[70]
		2–110 g L^{-1} $CaCl_2$ solution, pH = 7÷8	500–25 (linear decrease with the increase of calcium concentration)	

(continued)

Table 2 (continued)

Sorbent	Producer (developer)	Composition of treated water, pH	K_d, mL g^{-1} SEC	References
		0.05–110 g L^{-1} $CaCl_2$ solution, pH 5÷6	No strontium sorption	
Mixed nickel-potassium ferro-cyanide based on hydrated titanium dioxide (NPF-HTD)	Ural Federal University (Russia)	0.05–2 g L^{-1} $CaCl_2$ solution, pH 7÷8	3.2×10^2	[70]
		2–110 g L^{-1} $CaCl_2$ solution, pH = 7÷8	316–50 (linear decrease with the increase of calcium concentration)	
		0.05–110 g L^{-1} $CaCl_2$ solution, pH 5÷6	5.0×10^2	
		Drinking (tap) water, pH 7.8 ± 0.1; strontium concentrations were from 10^{-5} to 10^2 mg L^{-1}	1.0×10^3. SEC = 143 mg g^{-1}	[69]
		Solution based on tap water, pH > 8	1.5×10^4	
Magnetic CuHCNPAN nano composite (copper hexacyanoferrate based on polyacrylonitrile)	Nuclear Science and Technology Research Institute (Iran)	Strontium nitrate solutions at concentrations of 100–1,000 ppm	SEC up to 80 mg g^{-1}	[71]
Calcium hydrophosphate (CHP) $CaHPO_4$	Institute of General and Inorganic Chemistry of the national Academy of Sciences of Belarus	0.01–5 g L^{-1} $Sr(NO_3)_2$ solution	$0.1 \div 0.7 \times 10^3$ SEC = 10.9 mg g^{-1}	[52]
Calcium phosphate dihydrate (CPD) $Ca_3(PO4)_2 \cdot 2H_2O$	Institute of General and Inorganic Chemistry of the national Academy of Sciences of Belarus	0.01–5 g L^{-1} $Sr(NO_3)_2$ solution	$0.1 \div 1.0 \times 10^3$ SEC = 10.9 mg g^{-1}	
Hydroxyapatite (HA) $Ca_{10}(PO_4)_6(OH)_2$	Institute of General and Inorganic Chemistry of the national Academy of Sciences of Belarus	0.01–5 g L^{-1} $Sr(NO_3)_2$ solution	$0.8 \div 3.2 \times 10^3$ SEC = 25.7 mg g^{-1}	

(continued)

Table 2 (continued)

Sorbent	Producer (developer)	Composition of treated water, pH	K_d, mL g^{-1} SEC	References
Magnesium hydrophosphate trihydrate (MHT) $MgHPO_4 \cdot 3H_2O$	Institute of General and Inorganic Chemistry of the national Academy of Sciences of Belarus	0.01–5 g L^{-1} $Sr(NO_3)_2$ solution	SEC = 280 mg g^{-1}	

1. *Ion exchange*. In this type of interaction, the solid phase changes its ions for equivalent amount of ions from the solution. Replacement of cation from the solid phase by cation from solution occurs:

$$\underline{RM_1} + M_2{}^+ \rightleftarrows \underline{RM_2} + M_1{}^+, \tag{5}$$

where

R – matrix polyanion
M_1 – cation of the matrix
M_2 – exchanged cation from solution

The matrix polyanion remains unchanged as a result of ion exchange, and the reaction is totally or at least partially reversible.

2. *Heterogeneous ion exchange reaction*. This is a reaction resulting in transformation of one chemical compound into another one:

$$\underline{\overset{+2}{M_1}A} + M_2{}^{2+} \rightarrow \underline{\overset{+2}{M_2}A} + M_1{}^{2+}, \tag{6}$$

where A is anion of the sorbent.

The compounds M_1A and M_2A have different crystal-chemical properties. Heterogeneous ion exchange reaction is irreversible; it has the direction to the formation of a compound with a lower solubility product. This mechanism is possible only for macroamounts of dissolved ions. In case of microconstituents such as radionuclides, concentration will not be enough for the formation of a new sparingly soluble phase.

3. *Electron-ion exchange reaction*

$$\underline{\overset{+2}{M_1}A} + M_2{}^+ \rightarrow \underline{\overset{+2}{M_2}A} + M_1{}^+ \tag{7}$$

In contrast to previous option, this process results in a change of oxidation state of a sorbate with further heterogeneous ion exchange reaction. Irreversibility of sorption is also typical for this mechanism.

4. *Molecular adsorption*

$$\underline{RM_1} + M_2A = \underline{RM_1 \cdot M_2A} \tag{8}$$

Consumption of a full molecule by a sorbent occurs in case of molecular adsorption. The mechanism of molecular adsorption implies any types of intermolecular interactions which do not result in the formation of chemical bonds between molecules of a sorbate and functional groups of a sorbent. This reaction is well reversible.

Other mechanisms of sorption of microconstituents from solutions are also described in literature. Based on the study of EPR spectra of the products of Ca^{2+} sorption from alkaline media by a hydrated titanium dioxide, it was found that calcium sorption cannot be described by the ion exchange mechanism [72]. The EPR spectrum of the hydrated titanium dioxide remains the same after sorption. It is supposed that sorption of bivalent ions by the hydrated titanium dioxide occurs due to the mechanism of sorption-hydrolytic interaction that was suggested for other sorption systems by Pechenyuk [73]. A bivalent ion forms a common hydroxide complex with Ti-OH groups according to the following reaction:

$$\equiv Ti - OH + Ca^{2+} + H_2O \rightarrow Ti - O - Ca - OH + 2H^+ \tag{9}$$

Natural adsorbents such as minerals and soils separate strontium from aqueous solutions mainly due to ion exchange mechanism [74, 75]. The appearance of isotherms of strontium sorption by illite allows suggesting at least two different types of sorption sites selective for strontium. Sorption of radioactive strontium by montmorillonite occurs due to the ion exchange mechanism; the sorption behavior of micro- and macroamounts of strontium does not differ [76]. Ion exchange mechanism of strontium sorption results in reversible sorption. Petrova et al. [77] showed that strontium is almost completely desorbed from the montmorillonite clay.

Humic acids presenting in natural waters and soil solutions may affect mechanisms of strontium sorption by natural minerals. The isotherms of cesium (Cs-137) and strontium (Sr-85) sorption by the K- and Ca-forms of montmorillonite from humate solutions have the appearance as a combination of Langmuir and Freundlich isotherms [78, 79]. Humic acids form complex compounds with strontium [80] and calcium [81, 82] affecting solubility of the minerals and playing an important role in strontium migration in the environment [12]. The rate of aluminosilicates dissolving increases in the presence of humic acids [83, 84] and alumina [85]. Humic acids presenting in natural waters and soil solutions can suppress sorption of radionuclides by natural aluminosilicates [86].

Modified natural minerals and synthetic inorganic sorbents show more variety of sorption mechanisms than raw natural minerals. For example, sorption of strontium ions by the mesoporous manganese oxide OMS-2 [66] is conditioned by heterogeneous ion exchange reactions and chemical transformation of the sorbent resulting in a high selectivity for strontium and irreversibility of the sorption process.

The mechanisms of strontium sorption by the hydrated titanium dioxide T-5 and the NPF-HTD sorbent based on it are studied. The obtained results indicate chemical transformation of the NPF-HTD sorbent after strontium sorption rather than simple ion exchange mechanism [69]. Exchange of strontium by H_3O^+ ions or H^+ ions in pair and end OH groups of the matrix of the hydrated titanium dioxide occurs depending on pH value of solution. The phase of the mixed nickel-potassium ferrocyanide also takes a participation in strontium sorption at high strontium concentrations more than 10^2 mg L^{-1}. A partial replacement of nickel (II) by strontium in the crystal lattice of the mixed nickel-potassium ferrocyanide occurs in the process of strontium sorption resulting in transformation of the mixed nickel-potassium ferrocyanide into the mixed nickel-strontium-potassium ferrocyanide. It is shown that the process of transformation of the ferrocyanide phase is also possible at lower strontium concentrations if its chemical analogue such as Ca^{2+} is present in the solution.

5 Conclusions

Increase of concentration of stable strontium in natural waters is conditioned by strontium leaching from rocks and soils, dissolution of strontium-containing minerals, and the presence of elevated strontium amounts in soils due to either natural processes or use of strontium-containing fertilizers. The maximal concentrations of strontium in natural water may reach up to 60 mg L^{-1}. Elevated concentration of strontium in drinking water may result in its accumulation in a human's body increasing fragility and deformations of bones. This effect is observed mainly in children in cases of combination of a high strontium intake and other negative factors such as deficiency of calcium and vitamin D, malnutrition, and violation of the ratio of trace elements.

Radioactive isotopes of strontium are released into the environment as a result of nuclear weapon tests, daily work of enterprises of the nuclear fuel cycle, use in industry, and radiation accidents. Activity concentrations of Sr-90 in natural waters may reach 10^5 Bq L^{-1}. Being a pure beta emitter, Sr-90 is very dangerous in case of uptake by an organism and internal irradiation. Consumption of contaminated water and food is the main source of radiostrontium intake to a human's body. Radionuclides of strontium are selectively accumulated in bone tissue resulting in long-term irradiation of bones and marrow. Therefore, it is necessary to eliminate radiostrontium from natural water and soils as well as decrease its mobility in the environment in order to provide radiation safety.

Sorption method is the most effective for strontium removal from aqueous media. The choice of the sorbents for decontamination is conditioned mainly by the chemical composition of solution to be treated. Modified natural sorbents are the most suitable for decontamination of natural waters due to their ecological safety in improved sorption characteristics as compared with raw natural sorbents. Both natural (raw and modified) and synthetic inorganic sorbents can be successfully

used for strontium separation from wastewater and liquid radioactive waste including radioactively contaminated seawater. Sorption characteristics of a number of sorbents presented in Tables 1 and 2 can help making the choice.

References

1. Karpova EA, Gomonova NF (2006) Strontium in an agrocenosis on a soddy-podzolic soil under conditions of the long-term effect and aftereffect of fertilizers. Eur Soil Sci 39:779–784
2. Gupta DK, Walther C (2018) Behaviour of strontium in plants and the environment. Springer, Cham
3. Alexeev LS, Gladkova EV (2012) Decontamination of drinking water from stable strontium. Environ Eng 2:56–58
4. SanPiN (2001) Russian sanitary norms and regulations. SanPiN 2.1.4.1074-01
5. GTD (2018) Strontium in drinking water - guideline technical document for public consultation. https://www.canada.ca/content/dam/hc-sc/documents/programs/consultation-strontium-drinking-water/document-eng.pdf. Accessed 14 Aug 2018
6. EPA (2018) Drinking water standards and health advisories tables. https://www.epa.gov/sites/production/files/2018-03/documents/dwtable2018.pdf. Accessed 14 Aug 2018
7. Council Directive 98/83/EC (1998) Council Directive 98/83/EC of 3 November 1998 on the quality of water intended for human consumption. https://eur-lex.europa.eu/legal-content/EN/TXT/PDF/?uri=CELEX:31998L0083&from=EN. Accessed 14 Aug 2018
8. Grazhdan PE (1961) Strontium in underground waters of Kopetdag. The role of microelements in the agriculture. The II conference on microelements. MSU, Moscow, pp 76–80
9. Kulsky LA, Goronovsky IT, Koganovskiy AM, Shevchenko MA (1980) Handbook on properties, analytical methods and decontamination of water. Naukova Dumka, Kiev
10. Voinar AO, Lazovskaya LI (1942) About biochemistry of strontium and barium. Biochemistry 7:244–246
11. Polyakov EV (2007) Behavior of ionic and colloid forms of microelements in colloidal chemical extraction from humic acid solutions. Radiochemistry 49:432–438
12. Polyakov EV, Volkov IV, Khlebnikov NA (2015) Competitive sorption of cesium and other microelements onto iron(III) hexacyanoferrate(II) in the presence of humic acids. Radiochemistry 57:161–171
13. Saenko EV, Leont'eva GV, Vol'khin VV (2005) Sorption elimination of strontium from natural water being formed in the region of strontium deposit. Proceedings of the conference "Ecological and economical problems of mineral resources development". PGTU, Perm, pp 203–204
14. Shcherbakov VI, Al'-Amri ZSA, Mikhaylin AV (2017) Ochistka pit'yevoy vody ot strontsiya fil'tratsionnym metodom s primeneniyem klinoptilolita [Drinking water purification from strontium by filtration method using clinoptilolite]. Vestnik MGSU [Proc Mosc State Univ Civ Eng] 12:457–463
15. Polyakova EV (2012) Strontium in drinking water sources of Archangelsk region and its influence on human's organism. Ecol Hum 2:9–14
16. Vinogradov AP (1957) Geochemistry of rare and trace elements in soils. Nauka, Moscow
17. Shacklette HT, Boerngen JG (1984) Element concentration in soils and other surficial materials of the conterminous United States. U.S. Geol Surv Prof Pap 1270
18. Sheudzhen AH (2003) Biogeochemistry. Kuban State Agricultural University, Maykop
19. Toikka MA, Perevozchikova EM, Levkina TI (1981) Strontium in soils and cities of Karelia. Microelements in the environment. Naukova Dumka, Kiev, pp 28–30
20. Koval'sky VV (1968) Geochemical ecology. Microelements in agriculture and medicine. Nauka, Moscow, pp 66–72

21. Pavlotskaya FI, Zatsepina LN, Tyuryukanova EB, Baranov VI (1966) On mobility and speciation of strontium-90, stable strontium and calcium in sol-podzol and chernozem soils. Radioactivity of soils and methods of its determination. Nauka, Moscow, p 65
22. Kabata-Pendias A, Pendias H (1979) Trace elements in the biological environment. Warsaw Yard Geology, Warsaw, p 300
23. Lavrischev AV (2000) Calcium and strontium in the soil-plant system in the process of soils liming by conversion chalk (on the example of JSC Acron, Novgorod). Ph.D. Thesis, Saint-Petersburg
24. Myasoedov BF (1997) Radioactive contamination of the environment and possibilities of modern radiochemistry in monitoring. Quest Rad Saf 1:4–16
25. Voronina AV, Betenekov ND, Semenishchev VS (2018) Water decontamination at radioactively contaminated lands. In: Gupta DK, Voronina AV (eds) Remediation measures for radioactively contaminated areas. Springer, Tokyo, pp 223–243
26. Voronina AV, Betenekov ND, Nedobukh TA (2010) Applied radioecology. USTU-UPI, Yekaterinburg
27. Lur'e YY (1979) Handbook on analytical chemistry. Khimiya, Moscow, pp 92–101
28. Plotnikov VI, Tamaeva K, Myasishchev AV (1989) Coprecipitation of strontium with individual and mixed hydroxides of transition metals. Radiochemistry 3:85–89
29. Avramenko VA, Egorin AM, Papynov EK, Sokol'nitskaya TA, Tananaev IG, Sergienko VI (2017) Processes for treatment of liquid radioactive waste containing seawater. Radiochemistry 59:407–413
30. Sanjieva DA (2005) Sorption concentration of strontium by natural mineral sorbents as a basis of decontamination of natural water and wastewater. Ph.D. thesis, Astrakhan State University, Astrakhan
31. Vajda N, Kim CK (2010) Determination of radiostrontium isotopes: a review of analytical methodology. Appl Radiat Isot 68:2306–2326
32. Makrlík E, Vaňura P (2011) Solvent extraction of some divalent metal cations into nitrobenzene by using a synergistic mixture of strontium dicarbollylcobaltate and nonactin. J Radioanal Nucl Chem 288:49–52
33. Makrlík E, Vaňura P, Selucký P (2008) Extraction distributions of micro amounts of strontium and barium in the two-phase water-HCl-nitrobenzene-dibenzo-21-crown-7-hydrogen dicarbollylcobaltate system. J Radioanal Nucl Chem 275:3–7
34. Smirnov IV, Stoyanov ES, Vorob'eva TP (2003) Nature of strontium extraction by synergistic mixtures of chlorinated cobalt dicarbollide and polyethers. Czechoslov J Phys 53:A501–A508
35. Makrlík E (2004) Solvent extraction of strontium picrate from water into nitrobenzene in the presence of benzo-15-crown-5. J Radioanal Nucl Chem 262:513–515
36. McLain DR, Mertz CJ, Sudowe R (2016) A performance comparison of commercially available strontium extraction chromatography columns. J Radioanal Nucl Chem 307:1825–1831
37. Horwitz P, Chiarizia R, Dietz M (1992) Acid dependency of the extraction of selected metal ions by a strontium-selective extraction chromatographic resin: calculated vs. experimental curves. Solvent Extr Ion Exch 10:337–361
38. Attrep M, Kahn B (2008) Determination of radio-strontium in water with a strontium-specific solid-phase extraction column. In: Attrep M, Kahn B (eds) Radioanalytical chemistry experiments. Springer, New York, pp 113–118
39. Sinharoy P, Banerjee D, Sharma JN, Kaushik CP, Shah JG, Agarwal K (2018) Separation of Sr(II) from Eu(III) across a supported liquid membrane using TEHDGA and 18-crown-6. J Radioanal Nucl Chem 317:919–923
40. Chernyavskaya NB (1985) Sorption of strontium on clinoptilolite and heulandite. Radiochemistry 27:618–621
41. Chernyavskaya NB, Konstantinovich AA, Andreeva NR, Vorobyeva GE, Skripak IY (1983) Use of clinoptilolite for decontamination of wastewater from cesium and strontium radionuclides. Radiochemistry 25:441–414
42. Kuznetsov YV, Shchebetkovsky VN, Trusov AG (1974) Basis of water decontamination from radioactive pollution. Atomizdat, Moscow

43. Milyutin VV, Gelis VM, Penzin RA (1993) Sorption and selective characteristics of inorganic sorbents and ion exchange resins with respect to strontium and cesium. Radiochemistry 35:76–82
44. Voronina AV (1995) Sorption of cesium and strontium from low-activity fresh waters. Radiochemistry 37:538
45. Voronina AV (1996) Synthesis, study of properties and applications of thin-layer inorganic sorbents based on non-woven filtering materials. Ph.D. Thesis. USTU, Yekaterinburg
46. Voronina AV, Blinova MO, Semenishchev VS, Gupta DK (2015) Returning land contaminated as a result of radiation accidents to farming use. J Environ Radioact 144:103–112
47. Milyutin VV, Gelis VM, Nekrasova NA, Kononenko OA, Vezentsev AI, Volovicheva NA, Korol'kova SV (2012) Sorption of Cs, Sr, U, and Pu radionuclides on natural and modified clays. Radiochemistry 54:75–78
48. Milyutin VV, Nekrasova NA, Yanicheva NY, Kalashnikova GO, Ganicheva YY (2017) Sorption of cesium and strontium radionuclides onto crystalline alkali metal titanosilicates. Radiochemistry 59:65–69
49. Ratko AI, Panasyugin AS (1996) Sorption of ^{137}Cs and ^{90}Sr by modified sorbents based on clinoptilolite. Radiochemistry 38:66–68
50. Fuks L, Herdzik-Koniecko I (2018) Vermiculite as a potential component of the engineered barriers in low- and medium-level radioactive waste repositories. Appl Clay Sci 161:139–150
51. Andryushchenko ND, Safonov AV, Babich TL, Ivanov PV, Konevnik YV, Kondrashova AA, Proshin IM, Zakharova EV (2017) Sorption characteristics of materials of the filtration barrier in upper aquifers contaminated with radionuclides. Radiochemistry 59:414–424
52. Ivanets AI, Shashkova IL, Kitikova NV, Drozdova NV, Saprunova NA, Radkevich AV, Kul'bitskaya LV (2014) Sorption of strontium ions from solutions onto calcium and magnesium phosphates. Radiochemistry 56:32–37
53. Makarov AV, Zharkova VO, Ershova YY, Tyupina EA, Krupskaya VV (2017) Sorption of Sr-90 and Cs-137 on monocationic forms of bentonite of Taganskoye deposit. Prog Chem Chem Technol 31:16–18
54. Galamboš M, Kufčáková J, Rajec P (2009) Sorption of strontium on Slovak bentonites. J Radioanal Nucl Chem 281:347–357
55. Kim Y, Kim YK, Kim JH, Yim M-S, Harbottle D, Lee JW (2018) Synthesis of functionalized porous montmorillonite via solid-state NaOH treatment for efficient removal of cesium and strontium ions. Appl Surf Sci 450:404–412
56. Tret'yakov SY (2002) Sorption of ^{90}Sr and ^{137}Cs on natural sorbents in model environmental systems. Radiochemistry 44:93–95
57. Zolotov YA, Dorokhova EN, Fadeeva VI (1999) Basis of analytical chemistry. Common questions. Separation methods, vol 1. High School, Moscow
58. Leontieva GV (1997) Structural modification of manganese (III, IV) oxides in synthesis of sorbents selective for strontium. Russ J Appl Chem 70:1615–1618
59. Kuznetsova VA, Generalova VA (2000) The study of sorption properties of iron, manganese, titanium, aluminum and silicone oxides with respect to ^{90}Sr and ^{137}Cs. Radiochemistry 42:154–157
60. Milyutin VV, Nekrasova NA, Kharitonov OV, Firsova LA, Kozlitin EA (2016) Sorption technologies in modern applied radiochemistry. Sorpt Chromatogr Process 16:313–322
61. Egorin A, Sokolnitskaya T, Azarova Y, Portnyagin A, Balanov M, Misko D, Shelestyuk E, Kalashnikova A, Tokar E, Tananaev I, Avramenko V (2018) Investigation of Sr uptake by birnessite-type sorbents from seawater. J Radioanal Nucl Chem 317:243–251
62. Koivula J, Harjula R, Lehto J (2005) NATO advanced research workshop (ARW). Combined and hybrid adsorbents: fundamentals and applications. Springer, Kiev
63. Milyutin VV, Nekrasova NA, Kozlitin EA (2015) Selective inorganic sorbents in modern applied radiochemistry. Proc Kola Sci Cent RAS 31:418–421
64. Dadachov MS, Rocha J, Fereira A, Lin Z, Anderson MW (1997) Ab initio structure determination of layered sodium titanium silicate containing edge-sharing titanate chains (AM-4) $Na_3(Na,H)Ti_2O_2[Si_2O_6]_2 \cdot 2H_2O$. Chem Commun 24:2371–2372

65. Decaillon JG, Andres Y, Mokili BM, Abbe JC, Tournoux M, Patarin J (2002) Study of the ion exchange selectivity of layered titanosilicate $Na_3(Na,H)Ti_2O_2[Si_2O_6]_2{\cdot}2H_2O$, AM-4, for strontium. Solvent Extr Ion Exch 20:273–291
66. Ivanets AI, Katsoshvili LL, Krivoshapkin PV, Prozorovich VG, Kuznetsova TF, Krivoshapkina EF, Radkevich AV, Zarubo AM (2017) Sorption of strontium ions onto mesoporous manganese oxide of OMS-2 type. Radiochemistry 59:264–271
67. Denton M, Manos M, Kanatzidis M (2009) Highly selective removal of cesium and strontium utilizing a new class of inorganic ion specific media. WM'2009 conference proceeding, Phoenix, USA, pp 1–8. http://www.wmsym.org/archives/2009/pdfs/9267.pdf
68. Manos MJ, Ding N, Kanatzidis MG (2008) Layered metal sulfides: exceptionally selective agents for radioactive strontium removal. Proc Natl Acad Sci USA 105:3696–3699
69. Voronina AV, Semenishchev VS (2016) Mechanism of strontium sorption by the mixed nickel–potassium ferrocyanide based on hydrated titanium dioxide. J Radioanal Nucl Chem 307:577–590
70. Voronina AV, Semenishchev VS (2013) Effect of surface modification of hydrated titanium dioxide on its selectivity to strontium. Radiochemistry 55:94–97
71. Mobtaker HG, Pakzad SM, Yousefi T (2018) Magnetic CuHCNPAN nano composite as an efficient adsorbent for strontium uptake. J Nucl Mater 504:55–60
72. Denisova TA (2009) State of proton-containing groups in sorbents based on oxyhydrate, heteropolymetallate and cyanoferrate phases. Chemistry Thesis, Yekaterinburg. URL: http://www.server/ihim.uran.ru/files/diss/avtoref/Denisova.pdf
73. Pechenyuk SI (1991) Sorption-hydrolytic precipitation of the platinum group metals on the surface of inorganic sorbents. Nauka, Leningrad
74. Bilgin B, Atun G, Keceli G (2001) Adsorption of strontium on illite. J Radioanal Nucl Chem 250:323–328
75. Konoplev AV, Bulgakov AA (2000) ^{90}Sr and ^{137}Cs exchange distribution coefficient in soil-water systems. Atom Energy 88:158–163
76. Spitsyn VI, Gromov VV (1958) A study of the systematic adsorption of radioactive strontium by montmorillonite and its fixation by roasting. Atom Energy 5:1341–1347
77. Petrova MA, Flowers AG, Krip IM, Shimchuk TV, Petrushka IM (2008) Sorption of Sr on clay minerals modified with ferrocyanides and hydroxides of transition metals. Radiochemistry 50:502–507
78. Shaban IS, Macasek F (1988) Influence of humic substances on sorption of cesium and strontium on montmorillonite. J Radioanal Nucl Chem 229:73–77
79. Sips R (1948) On the structure of a catalyst surface. J Chem Phys 16:490–495
80. Wenming D, Hongxia Z, Meide H, Zuyi T (2002) Use of the ion exchange method for the determination of stability constants of trivalent metal complexes with humic and fulvic acids – part I: Eu^{3+} and Am^{3+} complexes in weakly acidic conditions. Appl Radiat Isot 56:959–965
81. Pandey AK, Pandey SD, Misra V (2000) Stability constants of metal-humic acid complexes and its role in environmental detoxification. Ecotoxicol Environ Saf 47:195–200
82. Zhou P, Yan H, Gu B (2005) Competitive complexation of metal ions with humic substances. Chemosphere 58:1327–1337
83. Blake RE, Walter LM (1999) Kinetics of feldspar and quartz dissolution at 70–80 °C and near-neutral pH: effects of organic acids and NaCl. Geochim Cosmochim Acta 63:2043–2059
84. Huang WL, Keller WD (1970) Dissolution of rock-forming silicate minerals in organic acids: simulated first-stage weathering of fresh mineral surfaces. Am Mineral 55:2076–2094
85. Stumm W, Furrer G (1987) The dissolution of oxides and aluminium silicates; examples of surface-coordination-controlled kinetics. Aquatic surface chemistry. Chemical processes at the particle–water interface. Wiley, New York, pp 197–219
86. Malakhov AE, Voronina AV (2016) The influence of humic acids on sorption of cesium by natural and modified aluminosilicates. Proceedings of the 3rd international youth scientific conference "Physics, Technologies, Innovations. PTI-2016". Ural Federal University, Yekaterinburg, pp 308–309

Assessment of the Alkaline Earth Metals (Ca, Sr, Ba) and Their Associated Health Impacts

Pankaj Pathak, Rajiv Ranjan Srivastava, Gonul Keceli, and Soma Mishra

Contents

Abstract This chapter provides an outline of alkaline earth metals' contamination caused by the industrial and nuclear pollution. The assessment has been done for quantifying sources (viz. natural and anthropogenic) of the alkaline earth metals along with describing the physicochemical characteristics of calcium, strontium, and barium. The isotopes of strontium, calcium, and barium are found to have significant impact not only onto the human health but also the geoenvironment. In this view, estimation of risk assessment caused by these metals is mandatory and also described in this chapter. Notably, calcium is one of the most significant elements in human body in the form of bone skeleton. In contrast, strontium and barium are non-essential elements

P. Pathak (✉) · S. Mishra
Department of Environmental Science & Engineering, Marwadi University Rajkot, Gujarat, India
e-mail: pankajpathak18@gmail.com

R. R. Srivastava
Institute Research & Development, Duy Tan University, Da Nang, Vietnam

Department of Environmental Technology, Institute Research & Development, Duy Tan University, Da Nang, Vietnam

G. Keceli
Department of Chemistry, Faculty of Engineering, University of Istanbul, Istanbul, Turkey

P. Pathak, D. K. Gupta (eds.), *Strontium Contamination in the Environment*,
The Handbook of Environmental Chemistry 88,
https://doi.org/10.1007/978-3-030-15314-4_12

for human beings; however, due to their similar characteristics with calcium, they get managed to enter within the human body via accumulation onto the tissues and bones. Therefore, the quantification of strontium and barium is imperative that can be done by measuring ratios with respect to calcium (as, Ba:Ca and Sr:Ca).

Keywords Alkaline earth metals · Environment · Health impact · Metal pollution · Risk assessment

1 Introduction

The industrial activities in the areas of thermal, nuclear, chemical, pharmaceutical, medical, etc. are playing a significant role to meet the daily need of the people. However, in due course certain amounts of wastes are indispensable to be generated often laden with hazardous substances [1, 2]. This waste encompasses contaminants such as alkaline metals, heavy metals (including radionuclides), and organic and inorganic toxic substances in solid/liquid/gaseous forms or in the combination of all [3, 4]. Hence, it necessitates special attention for their disposal with an understanding of reaction mechanisms into the geoenvironment. The scope of the chapter is limited to the utility and adversity associated with alkaline earth metals due to the natural and anthropogenic activities of radionuclides and non-radionuclides. During the anthropogenic engagement due to industrial activities, the nature of the alkaline earth metals gets change and disturbs the natural environment [5, 6]. On the other hand, acid mine drainage is also a big concern for the countries involved in the mining process [7]. During the treatment process, an additional dosing of alkaline metals such as calcium carbonate and barium carbonate mixed into the soils for acid neutralization, which may cause environmental hazards. Henceforth, serious considerations have to be taken to deal with natural and anthropogenic activities.

Calcium and magnesium are the alkaline metals having significant abundance (2.5 and 3.6%, respectively) in the earth surface, while the other associated alkaline metals, viz. beryllium, barium, and radium, are of minute occurrence (0.001, 0.025, and 0.05%, respectively). These metals are usually present in sulphate, carbonate, hydroxide, and silicate forms; however, their solubility index is in variance with water, and their isotopes are radioactive in nature. The main chemical and nuclear characteristics of alkaline earth metals are shown in Table 1.

Such properties of the alkaline metals are used to find applications in nuclear industries. For example, beryllium (Be) is used for the containers storing the radioactive isotopes of uranium, ^{238}U, as Be does not easily accept the neutrons due to its shorter radioactivity (within seconds). Moreover, beryllium does not move deep into the soil and groundwater due to the partial solubility and causes less harm to the organisms. On the other hand, the magnesium (Mg) compounds are used as a refractory material in furnace linings for the metallurgical operations of various ferrous and non-ferrous metals, glass, cement, and agriculture industries as well [8]. Calcium (Ca) is one of the most important elements in the habitat as the bone skeleton, teeth,

Table 1 Chemical and nuclear properties of alkaline earth metals

Alkaline metals	Radio isotopes	Uses	Half-life	Solubility with SO_4^{2-} and MCO_3^{2-}	Solubility with OH^-	Solubility with NO_3^{3-}
Beryllium	^{6}Be, ^{7}Be, ^{8}Be, ^{9}Be, ^{10}Be, ^{11}Be, ^{12}Be, Be^{14}	Used as an alloy in spot welding, electrical contact, and nonsparking tools	4.9×10^{-22} s to 4.4 ms	Partial soluble	Partial soluble	Partial soluble
Magnesium	^{20}Mg, ^{22}Mg	Used to study the absorption and metabolism of Mg in the human body	90.8 ms–3.87 s	$MgSO_4$ commonly known as Epsom salts (used in pharmaceutical) is soluble in water and forms, but $MgCO_3$ is insoluble and forms white precipitate	Soluble in water and alcohol	Soluble
Calcium	^{41}Ca, ^{45}Ca, ^{48}Ca	Used extensively in clinical research and mainly in nutritional studies	162.7 days–6.4×10^{19} years	$CaSO_4$ and $CaCO_3$ are insoluble	Soluble in water and alcohol	Soluble
Strontium	^{82}Sr, ^{89}Sr, ^{90}Sr	Used in medicine and industry and is an *isotope* of concern in fallout from nuclear weapons and nuclear accidents	25.36 days−28.8 years	$SrSO_4$ and $SrCO_3$ are soluble	Soluble	Solubility decreases
Barium	^{116}Ba, ^{121}Ba, ^{128}Ba	Used in fire work for producing green colour, X-ray radiocontrast agents	1.3 s−2.4 days	$BaSO_4$ is insoluble in water	Soluble	Less soluble
Radium	^{223}Ra, ^{226}Ra, ^{228}Ra	Used to produce radon gas, in luminous paint, prostate cancer treatment	11.4 days–1,600 years	Insoluble	Insoluble	Insoluble

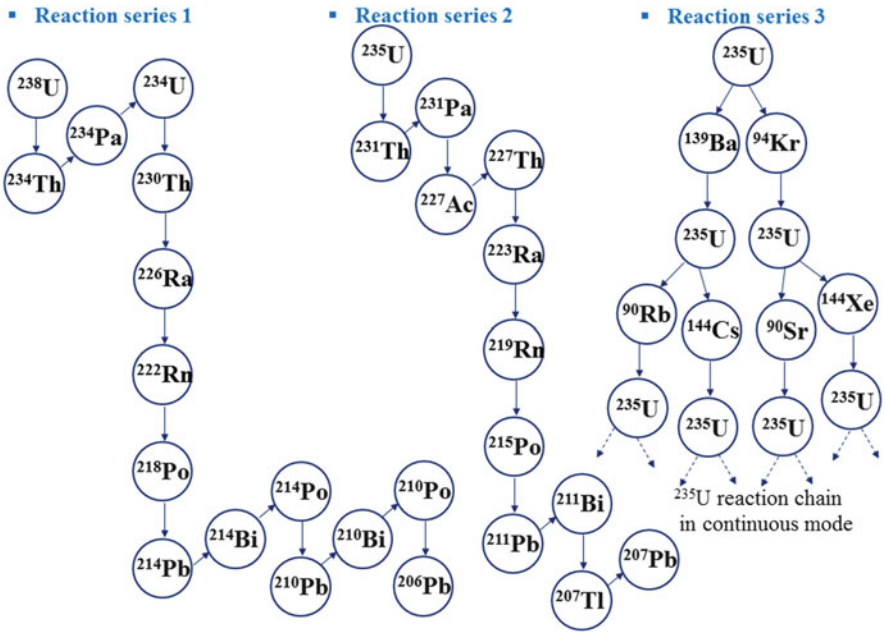

Fig. 1 Typical route of nuclear fission reaction producing the radionuclide fission by-products (with permission from the publisher [9])

and exoskeleton of some plants, as well. The plentiful occurrence of calcium in limestone, marble, gypsum, rock phosphate, and silicate rocks are due to its lesser reactivity as compared to other alkaline earth metals. In the nuclear industry, Ca-compound is used for chemical refining of thorium, uranium, and zirconium.

Strontium (Sr) is one of the most studied alkaline earth metal in radionuclear chemistry and its remediation from the environment as a contaminant kept under intermediate-level waste (ILW) of nuclear fission reaction producing ^{90}Sr (refer Fig. 1). Approximately 6% ^{90}Sr are supposed to be as a by-product of this fission reaction, while the nuclear fuel reprocessing of civilian and military interests are also contributing [3, 9]. It exhibits a half-life of ~28.8 years [3], and further it is converted into shorter-lived ^{90}Y daughter (half-life 64.2 h), and finally, it forms stable ^{90}Zr [10]. Naturally, strontium is found in the form of celestite ($SrSO_4$) and strontianite ($SrCO_3$). The properties of strontium are quite similar to calcium and barium. Nevertheless, if strontium and calcium are in trace amount together in a system, then their separation is very tedious work on contrary to its easier separation from barium (Tudorache et al. 2018). Notably, barium is naturally obtain in the form of barite ($BaSO_4$) and witherite ($BaCO_3$) and found to be consists in a mixture of 7 stable isotopes (^{138}Ba: 71.66 %, ^{137}Ba: 11.32%, ^{136}Ba: 7.81%, ^{135}Ba: 6.59, ^{134}Ba: 2.42%, ^{132}Ba: 0.097%, ^{130}Ba: 0.101%) besides its 13 known artificial radioactive isotopes. The ^{133}Ba isotope is employed in gamma spectroscopy as a standard and used as a carrier phase for chemically similar radium (Ra) that is produced during

radioactive decay of uranium and thorium. However, the concentration of Ra is very less in geomaterials (rocks and soil); the geologist finds a helpful relationship between uranium and radium to determine the age of rocks.

Nevertheless, the present chapter is focused on strontium; the physicochemical properties of calcium and barium are also included herein due to their strong relationship in quantification of strontium (as the ratios of Ba:Ca and Sr:Ca).

2 Physicochemical Characteristics of Alkaline Earth Metals

Due to their high reactivity, the alkaline earth metals do not occur in the free-state and often remain associated with silicate, sulphates, carbonates, and phosphates in the nature. The physicochemical properties of the concerned alkaline earth metals (Ca, Sr, and Ba) are given in Table 2 along with the major applications shown in Fig. 2. These metals form ionic salts by reaction with halogens (as Eq. 1), while reaction with water yields metal hydroxide (as Eq. 2), whereas they get reduced by hydrogen to form metal hydrides (as Eq. 3):

$$M_{(Solid)} + X_{2(Solid)} \rightarrow MX_2 \quad (1)$$

$$MO_{(Solid)} + H_2O \rightarrow M(OH)_{2(Solid)} \quad (2)$$

$$M_{(Solid)} + H_2 \rightarrow MH_{2(Solid)} \quad (3)$$

Table 2 Physicochemical properties of the main alkali earth metals (Ca, Sr, and Ba)

S. No.	Physicochemical properties	Calcium	Strontium	Barium
1	Atomic number	20	38	56
2	Relative atomic mass (g mol^{-1})	40.08	87.62	137.33
3	Melting point (°C)	842	777	727
4	Boiling point (°C)	1,448	1,382	1,897
5	Ionic radii (Å)	0.99	1.12	1.35
6	Electrode potential (E°/V at 298 K)	−2.87	−2.89	−2.90
7	Density (g cm^{-3})	1.55	2.64	3.34
8	Heat of fusion (kJ mol^{-1})	8.54	7.43	7.12
9	Heat of vaporization (kJ mol^{-1})	154.7	136	140.30
10	Crystal structure	Face centred cubic	Cubic closed packed	Body centred cubic
11	Metal concentration % (in the environment)	4–5	0.036–0.04	0.034–0.035

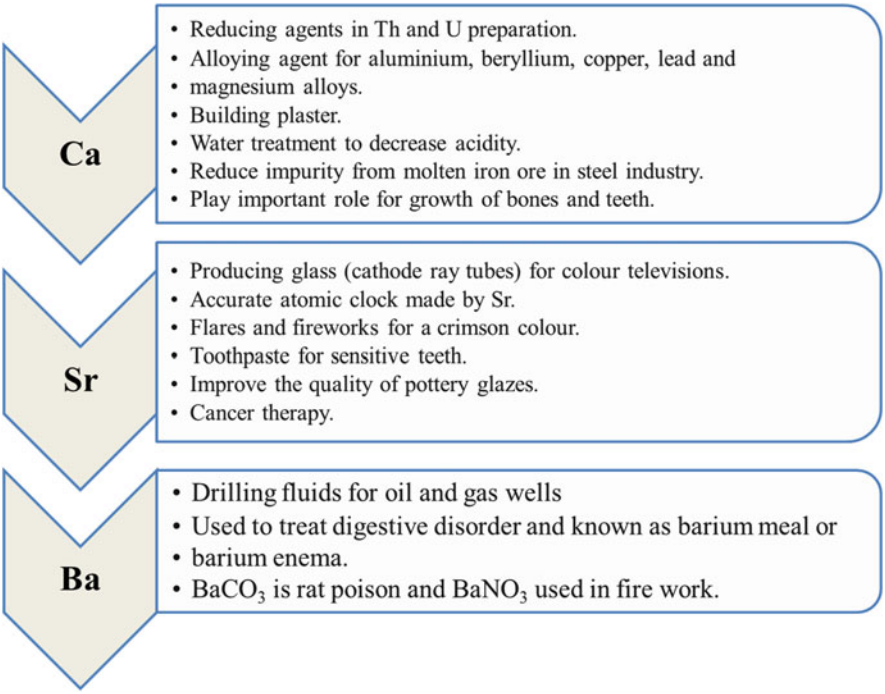

Fig. 2 Main applications of the compounds of calcium, strontium, and barium

2.1 Occurrence of Calcium

Calcium is the vital element in the earth surface with a wide range of concentration all over the terrestrially surface. It is found in grey silvery colour. Calcium is reported as the lightest amid all the alkali earth metals, and 4.15% calcium mainly occurs in the sedimentary rocks as limestone (as $CaCO_3$), chalk, and marble [11]. Amongst all, limestone ($CaCO_3$) and gypsum ($CaSO_4{\cdot}2H_2O$) are the important minerals of calcium and presented in Fig. 3.

The hygroscopic nature of calcium leads to the rapid formation of gaseous hydrogen even at room temperature when it comes in contact with water, whereas in presence of air, it forms white coating of calcium nitride (Ca_3N_2). It vigorously neutralizes acid by exothermic reaction and has capacity to absorb the moisture. It has five stable isotopes such as ^{40}Ca (96.941%), ^{42}Ca (0.647%), ^{44}Ca (2.086%), ^{46}Ca, and ^{48}Ca (0.187%) and has wide applications in industries and medical fields. There are several applications of $CaCO_3$ in the form of whitewashing, toothpaste, chewing gum gastric, anta-acids, and vitamins. Although it has crucial role in the human body as it helps in the blood clotting, the contraction of muscles, and the regulation of the heartbeat, however calcium phosphide is very toxic to aquatic organisms. It is widely found in green vegetables and dairy products and

(a) (b)

Fig. 3 Minerals of calcium: (**a**) limestone, (**b**) gypsum

recommended for the prevention of osteoporosis. The main sources of Ca are the dairy products, nuts, green vegetables. Moreover, it plays important role in mineral nutrition of plants which include cell wall stability and osmoregulation, and it has significant influence on soil properties, viz. pH, structural stability, cation exchange capacity, specific surface area, and bioaccumulation levels [2, 12, 13].

2.2 Occurrence of Strontium

Naturally, strontium is found as strontianite ($SrCO_3$) and celestite ($SrSO_4$) and shown in Fig. 4. It has four natural isotopes, i.e. ^{84}Sr, ^{86}Sr, ^{87}Sr, and ^{88}Sr, which are stable in nature [14]. It was reported that strontianite has higher Sr contents as compared to celestite. China, Spain, Russia, Mexico, Morocco, and the United States have higher strontium deposits and supplied in all over the world.

Strontium has high tendency to react with water and oxygen. When it reacts with water, it forms $Sr(OH)_2$ and hydrogen gas; however, when it burns in presence of air, then it produces Sr_3N_2 and SrO. Due to a high oxidative nature of metallic Sr^0, it is stored in kerosene. The isotopes of strontium are radioactive in nature (see Table 2), ^{90}Sr is the important one, and used as a tracer compound [3, 9]. It was stated that ^{90}Sr first gets decay into yttrium (^{90}Y) and eventually transform to zirconium (^{90}Zr) after completing their life cycle [15, 16]. Moreover, other isotope ratios, i.e. the ratio of ^{87}Sr:^{86}Sr, are mainly used in the geological investigations to determine the sediment areas especially in marine and fluvial environment [15, 17], and their ratio for the minerals and rocks is ranging from 0.7 to 4.0. Strontium has similar properties as calcium and barium due to which strontium can substitute these metals in the mineral compositions (Geeza et al. 2018). However, absorption of it in the body results to death as it substitutes calcium in the bone. In spite of that, strontium is also used as a

(a) (b)

Fig. 4 Minerals of Sr (**a**) strontianite and (**b**) celestite

pure metal in aluminium-silicon casting alloys composition modification. Other isotope like ^{89}Sr is used in the bone cancer treatment as an artificial radioisotope. ^{90}Sr is β-emitter and recognized as by-product of nuclear fission and widely used in SNAP (Systems for Nuclear Auxiliary Power) devices. These devices are used in remote weather stations, spacecraft, navigational buoys, etc.

2.3 Occurrence of Barium

Barium is found as fifth position in the alkaline earth metal series and highly reactive with air and water hence stored in oil. It constitutes 0.03% on the earth crust and mined as barites ($BaSO_4$) and witherite ($BaCO_3$) which are very insoluble in water and shown in Fig. 5. China, Australia, Germany, India, and Russia have large deposits of barite, and it mainly attributed during feldspar weathering in silicate rocks [11, 18].

Barium is a ductile and soft metal as compared to other alkaline earth elements and has a high density (3.51 g cm^{-3}). Naturally, barium has seven stable isotopes: ^{138}Ba (71.66%), ^{137}Ba (11.32%), ^{136}Ba (7.81%), ^{135}Ba (6.59%), ^{134}Ba (2.42%), ^{130}Ba (0.101%), and ^{132}Ba (0.097%). Barium and its compound are mainly used in metallurgy, petroleum mining, and radiology works. The elemental barium (Ba^0) is most importantly used as a scavenger for removing traces of oxygen and other gases in electronic tubes and television. Ba-containing solutions and medicines are also used in X-ray applications. Therefore, barium solutions and medicines are given to the X-ray tractors, especially for digestive system problems. The barium also acts as a carrier phase for radium, which is similar in chemical properties. Barium is found in some minerals in nature. Barium sulphate minerals are mostly formed in barite

(a) (b)

Fig. 5 Minerals of Ba (**a**) barytes, (**b**) witherite

mineral. Barite is the heaviest of non-metallic minerals. The other barium mineral is viterite, containing barium carbonate. Formation of strontium and calcium minerals, also known as baritone, barite, and barite calcite, and phosphate and silicate minerals is also observed. Moreover, ^{133}Ba isotope is used in nuclear physics studies as a standard source for the calibration of gamma-ray detector. In addition, Torres et al. [7] have used barium carbonate ($BaCO_3$) for reducing sulphate and divalent metal (viz. zinc, manganese, nickel, cobalt, cadmium, and thallium) amounts and also lowers its detection limit in the acid mining area.

3 Distribution of Ca, Sr, and Ba in the Environment

The geochemical mapping states the natural concentration (background) and anthropogenic contribution of metals on earth. Although strontium and barium have abundant background data in earth materials, it is one to two orders lesser as compared to calcium and magnesium. It was reported that these metals are less soluble than calcium and magnesium; therefore, when it presents in trace amount, then associated environmental risk are less due to less solubility. The wide applications of these metals are as an environmental tracer in geological operations and identification of groundwater contamination. Nigro et al. [19] have reported the use of strontium as an environmental tracer to identify groundwater contamination due to municipal solid waste landfill [15]. On the other hand, significant use of barium as a tracer is shown by Puroshotham et al. (2012) to determine the heavy metal contamination in the soil. Several researchers have also used ratios of Sr:Ca and Ba:Ca as a tracer to determine the geochemical reaction in the rock, soil, and groundwater [8, 20, 21]. The basic idea for selecting these metals as a tracer is because both the metals found in the environment with different minerals but release

in the soil solution during weathering process. Moreover, strontium and barium are found in trace amount; they do not react with each other and would not form any new mineral with their own. Hence, the ratio of these metals gives good background data for understanding the different environmental conditions. Strontium is a good substitute for calcium and/or potassium, whereas barium can generally replace potassium, though the potassium mineral is resilient to weathering process as compared to calcium mineral. Therefore, a rigorous weathering is required to release barium from the soil as compared to strontium discharge. It is known that weathering strength reduces with soil depth; hence concentrations of Ba:Sr are varying with depth. The concentration of K, Ca, Sr, and Ba in the soil solutions can precisely determine either by AAS or ICP-AES analysis, and further all the metals correlate with each other statistically to determine its distribution on earth surface [22, 23]. If it is strongly correlated with each other, then it is used to determine the geochemical reaction in the environment and also treat as environmental proxies in the estuarine waters [4, 8, 15, 21]. Land et al. [21] has demonstrated that Ba:Sr and Ca:Sr ratio can be used to determine the stream discharge in the soil water and ground. It was stated that both the ratios are analogous to each other and get differing with respect to the soil depth. Moreover, calcium and strontium are greatly found in granitic rock, and it has two imperative carriers, i.e. plagioclase and amphibole; however, strontium has much affinity with plagioclase as compared to amphibole. On the other hand, Carvalho et al. [24] have analysed the sediments which come out from mud volcanoes of the Gulf of Cadiz and found different types of major, minor, and trace elements into it. The barium front has been found in the upper sediments up to 50 cm in authigenic barite layers, while strontium and calcium were also found in significant values. Several factors, viz. pH, oxidation state (Eh), temperature, and reaction with other metals, have significant influence on Ca, Sr, and Ba compounds. Though these metals act as a tracer in the environment but due to the incessant anthropogenic activities it is possible that the background data of strontium and barium may increase in the natural environment then toxicity of other metals, viz. arsenic, cadmium, lead, and mercury will be increasing due to change in environmental conditions and causes severe impacts to the environment [6, 25]. Henceforth, it necessitates understanding the distribution pattern of these metals along with its reaction mechanism. In this view, the Eh-pH diagram of these metals have been constructed by using Medusa software at 25 °C with 10 μM concentration, and obtained results are shown in Fig. 6a, b. Both the metals exhibit similar Eh-pH diagram and reveal the ionic species of the metals with changing pH and Eh. It also helps to understand the reaction mechanism with other toxic metals. Furthermore, Vinograd et al. [26, 27] have reported that effect of strontium and barium for the uptake of isotopic radium during failure of nuclear container. The thermodynamic parameters of $SrSO_4$, $BaSO_4$, and $RaSO_4$ were determined by the solubility of soil solution and aqueous solution at 25 °C [27]. It was also reported that high concentration ratio of Sr:Ba in barite have a negative effect on radium retention. Consequently, higher solubility of celestite mineral and higher concentration of sulphate ion in the aqueous phase may increase the Sr:Ba ratio, which helps to keep Ra^{2+} in the soil [26, 27].

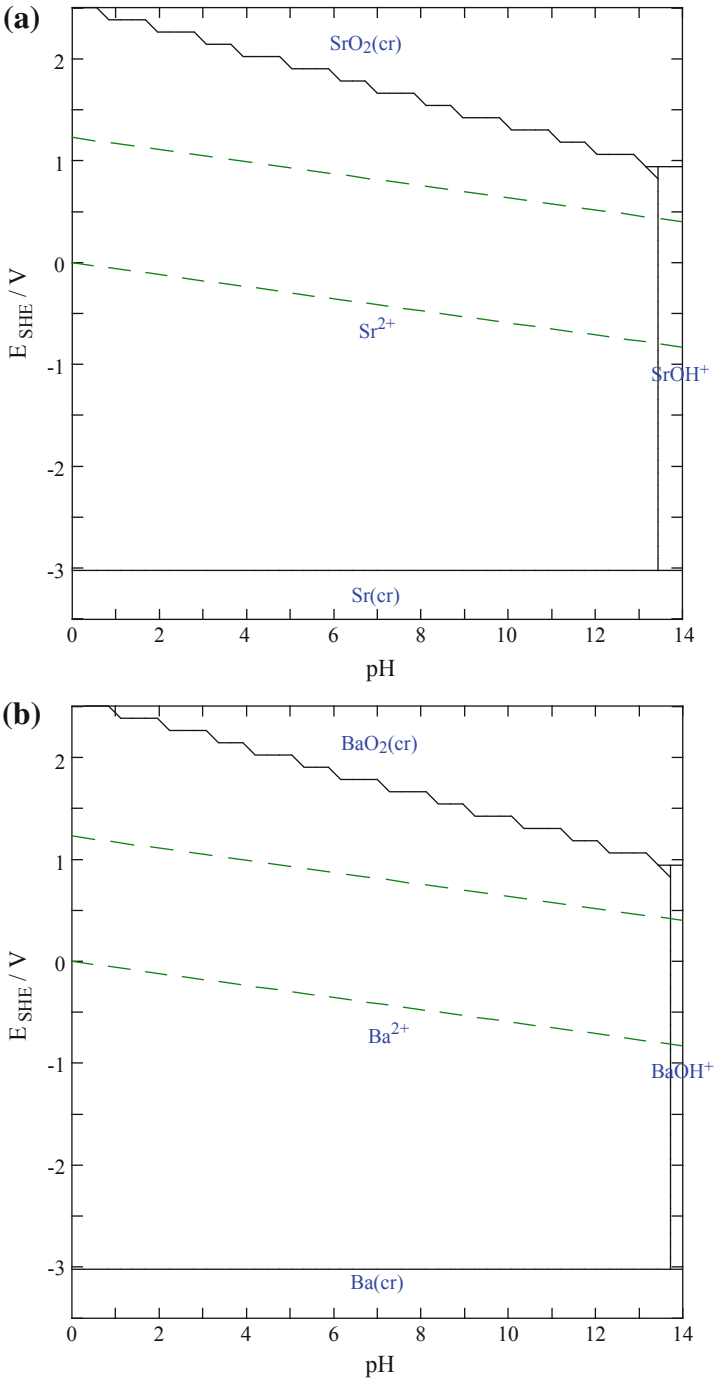

Fig. 6 (**a**) The Eh-pH diagram of Sr at 25 °C with 10 μM concetration. (**b**) The Eh-pH diagram of Ba at 25°C with 10 μM concetration

4 Assessment of Metal Pollution in the Environment

The anthropogenic metal pollution can be determined by using an enrichment factor (EF) in the soil/sediments. It normalizes the metals in order to lessen the variations produced by heterogeneous soils/sediments, whereas the reference metal is designated to have a minimum variation of occurrence in the environment that is neither small concentration variations nor synergistic or opposite effects towards the sampled metals. Two equations have been proposed to determine the enrichment factor as shown in the following [1, 28]:

$$\mathrm{EF}\% = \frac{C - C_{\min}}{C_{\max} - C_{\min}} \times 100 \tag{4}$$

$$\mathrm{EF} = \frac{(C_i/C_{\mathrm{Fe}})_s}{(C_i/C_{\mathrm{Fe}})_r} \tag{5}$$

where C is the mean concentration of metal in the soil, $C_{\max}$ is the maximum concentration, $C_{\min}$ is the minimum concentrations, $(C_i/C_{\mathrm{Fe}})_s$ is the ratio of the concentration of a polluted metal with that of iron at each sample, and $(C_i/C_{\mathrm{Fe}})_r$ is the same ratio of the concentration for the reference soil. Iron (Fe) was selected as reference material because it is less affected by anthropogenic pollution in the soil. Further, based on EF factor, soils were classified into seven classes: (1) if EF < 1 no enrichment, (2) EF < 3 slight enrichment, (3) EF $= 3$ to 5 moderate enrichment, (4) EF $= 5$ to 10 moderate-to-severe enrichment, (5) EF $= 10$ to 25 severe enrichment, (6) EF $= 26$ to 50 very severe enrichment, and (7) EF > 50 extremely severe enrichment [29, 30]. This factor indicates the extent of pollutant in the environment and estimates the geo-accumulation (metal retained) in the soil environment. However, a geo-accumulation index was already calculated by Muller [31] using Eq. 6:

$$\mathrm{I}_{\mathrm{geo}} = \log_2 \frac{C_n}{1.5B_n} \tag{6}$$

where C_n is the metal concentration in the soil sample and B_n is the background concentration in the soil. Further, metal pollution index (MPI) and pollution load index (PLI) can estimate the pollution load in the environment and help in assessing risk at polluted site. The MPI and PLI equations are shown in the following:

$$\mathrm{MPI} = (Cf_1 \times Cf_2 \times Cf_3 \ldots . Cf_n)^{1/n} \tag{7}$$

$$\mathrm{PLI} = \sqrt[n]{Cf_1 \times Cf_2 \times Cf_3 \times \ldots .. Cf_n} \tag{8}$$

$$\mathrm{CF}_{\mathrm{metal}} = \frac{C_{\mathrm{metal}}}{C_{\mathrm{background}}} \tag{9}$$

where *Cf* is the metal concentration in the soil sample, CF is contamination factor, n is number of metals, and C_{metal} and $C_{background}$ are metal concentration in the soil and background [29].

5 Effect of Alkaline Earth Metals (Ca, Sr, Ba) on Human Health

Metal toxicity has shown to be a major threat to the environment due to severe risk associated with human health and plants, though alkaline metals and alkaline earth metals play major role for the development and growth of biota. Nevertheless, when the concentration of these metals increases beyond the permissible limits either due to natural or anthropogenic activities, it may cause severe environmental and health issues [32] (Valido et al. 2018).

An overview of metal pollution in a different environment is given in Fig. 7. It states that Ca^{2+} and Ba^{2+} are found in all environments, i.e. air, water, and soil; further through dust particle, groundwater contamination, and leaching process, these metals interact either with plants or directly to human being and cause a severe impact to the biotic environment.

The concentration of these metals increases in the air, water, and soil environment via mining. In this section, the toxicity of three metals (viz. Ca, Sr, and Ba) along with its associated risk is being discussed in detail. It has been reported that calcium is an important segment in the cellular body of an organism. The free Ca^{2+} initiates the cellular actions, viz. movement, secretion, transformation, and division [33], but if the concentration of calcium increases in the body, it starts disintegrating the cells, and this phenomenon is known as decalcification. An excessive amount of calcium

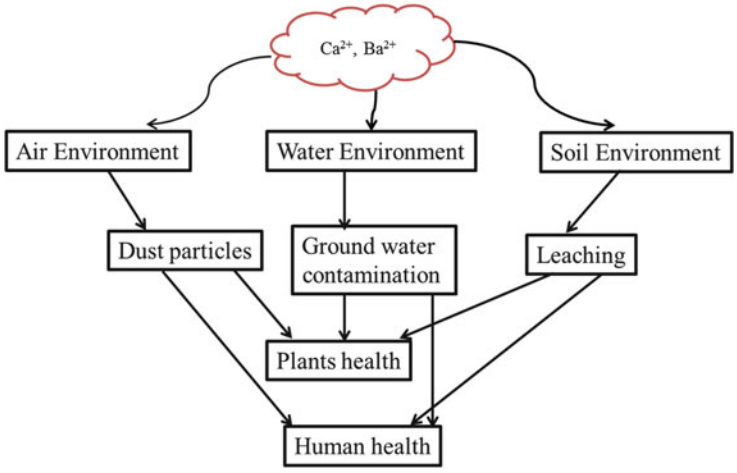

Fig. 7 An overview of metal contamination in different environment

Table 3 Impact on human health due to excessive exposure of Ca, Sr, and Ba

Metals	Permissible limit (ppm)	Impacts	References
Ca	18.50	Hypercalcemia, renal cyst, kidney failure, gall-bladder stones	Mannstadt et al. [34]; Gautam et al. [35]
Sr	1.50	Somatic and genetic changes causes cancer in the bone, nose, lungs, skin	Pathak [3]; CGWB Report [16]
Ba	<100	Cause cardiac arrhythmias, respiratory failure, brain swelling, gastrointestinal dysfunction, muscle twitching, and elevated blood pressure	Pathak et al. [36]

found in blood is known as hypercalcemia, and it causes renal insufficiency, vascular and soft tissue calcification, and kidney stone as mentioned in Table 3. On the other hand, plants uptake the calcium from the soil, and high concentration of calcium increases the pH of soil that alters the soil fertility.

In the case of strontium, the radioactive ^{90}Sr gets produced from nuclear fallout of weapon testing and fission reaction, which has the biological half-life of ~18 years that presents a high health risk in comparison to the stable (non-radioactive) strontium [3]. Although the concentrations of radioactive strontium in the environment are extremely low, eventually the particles will always end up in soils or water-bottoms where they mix with other strontium particles. Naturally, strontium concentration increases through soil and rock weathering but not likely to end up in drinking water. A very small fraction of strontium comes through dust particles from the air during firework burning [36, 37]. In contrast, a large fraction of strontium can get dissolved in the water due to a good solubility. Sources of strontium for a human being can be corn, orange, cabbage, onions, and lettuce. However, intake of 0.8–5.0 mg day^{-1} is considered harmless (CGWB 2014); a higher uptake may cause severe damage to bones (often due to being an analogous to calcium), anaemia, oxygen shortages and at last leads to cancer due to the damaged genetic materials in cells. Strontium chromate is one compound that causes severe impact to human health amongst all chemical compounds of strontium, which is basically due to the combined toxicity of chromium anions.

In connection to this, barium is also an active alkaline earth metal that easily reacts with oxygen, nitrogen, sulphur, hydrogen, ammonia, halogens, acids and able to form aqueous species by dissolving its compounds into water. In presence of air and other oxidizing gases, it emits toxic gases dangerous to human health. In presence of nitrogen at higher temperatures, the yield of barium nitrides can be used to vaporize oxygen, which eliminates nitrogen and carbon dioxide from a system. The sulphide of barium called as black ash, is used to derive many compounds from the geomaterials. It is a highly susceptible metal that can replace potassium and causes kidney and heart disorders. The small amounts of water-soluble barium in the mouth can cause difficulty in breathing, high blood pressure, changes in heart rhythm, gastric irritation, muscle weakness, changes in nerve reflexes, and brain and liver disorders. A high intake of water-soluble barium may also lead to death.

6 Conclusions

The alkaline earth metals play a significant role in the environment, whereas isotopes of calcium, strontium, and barium are used as environmental tracer. Due to natural or anthropogenic activities, the concentration of these metals increases in the environment and causes severe impacts. In this context, risk assessment can be done by estimating enrichment factor (EF), geo-accumulation, contamination factor, metal pollution index (MPI), and pollution load index.

References

1. Dantu S (2009) Heavy metals concentration in soils of South East Ranga Reddy district, Andhra Pradesh, India. Environ Monit Assess 149:213–222
2. Pathak P (2014) Determination of distribution coefficient of soil-contaminant system. PhD thesis, Department of Civil Engineering, Indian Institute of Technology Bombay, Mumbai, India
3. Pathak P (2017) An assessment of strontium sorption onto bentonite buffer material in waste repository. Environ Sci Pollut Res 24:8825–8836
4. Pathak P, Singh DN, Apte PR, Pandit GG (2016) Statistical analysis for prediction of distribution coeffiecient (k_d) of soil-contaminant system. J Environ Engg 142:1–11
5. Wiederhold JG (2015) Metal stable isotope signatures as tracers in environmental geochemistry. Environ Sci Technol 49:2606–2624
6. Yang YY, Liu LY, Guo LL, Lv YL, Zhang GM, Lei J, Liu WT, Xiong YY, Wen HM (2015) Seasonal concentrations, contamination levels, and health risk assessment of arsenic and heavy metals in the suspended particulate matter from an urban household environment in a metropolitan city, Beijing, China. Environ Monit Assess 187:409–423
7. Torres E, Lozano A, Macias F, Gomez-Arias A, Castillo J, Ayora C (2018) Passive elimination of sulfate and metals from acid mine drainage using combined limestone and barium carbonate systems. J Clean Prod 182:114–123
8. Poulain C, Gillikin DP, Thebault J, Munaron JM, Bohn M, Robert R, Paulet YM, Lorrain A (2015) An evaluation of Mg/Ca, Sr/Ca, and Ba/Ca ratios as environmental proxies in aragonite bivalve shells. Chem Geol 396:42–50
9. Pathak P, Sharma S (2018) Sorption isotherms, kinetics, and thermodynamics of contaminants in Indian soils. J Environ Eng 10:1–9
10. Wallace SH, Shaw S, Morris K, Small JS, Fuller AJ, Burke IT (2012) Effect of groundwater pH and ionic strength on strontium sorption in aquifer sediments: implications for ^{90}Sr mobility at contaminated nuclear sites. Appl Geochem 27:1482–1491
11. Park G (2015) Introducing natural resources. Dunedin Academic Press, Dunedin
12. Amoros JA, Bravo S, Perez-de-los-Reyes C, Garcia-Navarro FJ, Campos JA, Sanchez-Ormeno M, Jimenez-Ballesta R, Higueras P (2018) Iron uptake in vineyard soils and relationships with other elements (Zn, Mn and Ca). The case of Castilla-La Mancha, Central Spain. Appl Geochem 88:17–22
13. Bravo S, Amoros JA, Perez-de-los-Reyes C, Garcia-Navarro FJ, Moreno MM, Sanchez-Ormeno M, Higueras P (2017) Influence of the soil pH in the uptake and bioaccumulation of heavy metals (Fe, Zn, Cu, Pb and Mn) and other elements (Ca, K, Al, Sr and Ba) in vine leaves, Castilla-La Mancha (Spain). J Geochem Explor 174:79–83

14. Shand P, Darbyshire DPF, Love AJ, Edmunds WM (2009) Sr isotopes in natural waters: applications to source characterisation and water–rock interaction in contrasting landscapes. Appl Geochem 24:574–586
15. Bu W, Zheng J, Liu X, Long K, Hu S, Uchida S (2016) Mass spectrometry for the determination of fission products ^{135}Cs, ^{137}Cs and ^{90}Sr: a review of methodology and applications. Spectrochim Acta B Atom Spectros 119:65–75
16. CGWB Report (2014) Concept note on geogenic contamination of ground water in India. Central Ground Water Board. Ministry of Water Resources, Govt. of India, Delhi
17. Ryan SE, Snoeck C, Crowley QG, Babechuk MG (2018) ^{87}Sr/^{86}Sr and trace element mapping of geosphere-hydrosphere-biosphere interactions: a case study in Ireland. Appl Geochem 92:209–224
18. Purushotham D, Lone MA, Rashid M, Rao AN, Ahmed S (2012) Deciphering heavy metal contamination zones in soils of a granitic terrain of southern India using factor analysis and GIS. J Earth Syst Sci 121:1059–1070
19. Nigro A, Sappa G, Barbieri M (2017) Strontium isotope as tracers of ground water contamination. Procedia Earth Planetary Sci 17:352–355
20. Horta-Puga G, Carriquiry JD (2012) Coral Ba/Ca molar ratios as a proxy of precipitation in the northern Yucatan Peninsula, Mexico. Appl Geochem 27:1579–1586
21. Land M, Ingri J, Andersson PS, Ohlander B (2000) Ba/Sr, Ca/Sr and ^{87}Sr/^{86}Sr ratios in soil water and groundwater: implications for relative contributions to stream water discharge. Appl Geochem 15:311–325
22. Amr MA, Helal AFI, Al-Kinani AT, Balakrishnan P (2016) Ultra-trace determination of ^{90}Sr, ^{137}Cs, ^{238}Pu, ^{239}Pu, and ^{240}Pu by triple quadruple collision/reaction cell-ICP-MS/MS: establishing a baseline for global fallout in Qatar soil and sediments. J Environ Radioact 153:73–87
23. Reimann C, Filzmoser P, Hron K, Kynclova P, Garrett RG (2017) A new method for correlation analysis of compositional (environmental) data – a worked example. Sci Total Environ 607–608:965–971
24. Carvalho L, Monteiro R, Figueira P, Mieiro C, Almeida J, Pereira E, Magalhaes V, Pinheiro L, Vale C (2018) Vertical distribution of major, minor and trace elements in sediments from mud volcanoes of the Gulf of Cadiz: evidence of Cd, As and Ba fronts in upper layers. Deep-Sea Research Part I 131:133–143
25. Giri S, Singh AK (2015) Human health risk assessment via drinking water pathway due to metal contamination in the groundwater of Subarnarekha River Basin, India. Environ Monit Assess 187:63
26. Vinograd VL, Kulik DA, Brandt F, Klinkenberg M, Weber J, Winkler B, Bosbach D (2018) Thermodynamics of the solid solution-Aqueous solution system (Ba, Sr, Ra)SO_4 + H_2O: I. The effect of strontium content on radium uptake by barite. Appl Geochem 89:59–74
27. Vinograd VL, Kulik DA, Brandt F, Klinkenberg M, Weber J, Winkler B, Bosbach D (2018) Thermodynamics of the solid solution – aqueous solution system (Ba, Sr, Ra) SO_4 + H_2O: II Radium retention in barite-type minerals at elevated temperatures. Appl Geochem 93:190–208
28. Zonta R, Zaggia L, Argrse E (1994) Heavy metal and grain size distributions in estuarine shallow water sediments of the Cona Marsh (Venice Lagoon Italy). Sci Total Environ 151:19–28
29. Ali Z, Malik RN, Shinwari ZK, Qadir A (2015) Enrichment, risk assessment, and statistical apportionment of heavy metals in tannery-affected areas. Int J Environ Sci Technol 12:537–550
30. Saleem M, Iqbal J, Shah MH (2015) Geochemical speciation, anthropogenic contamination, risk assessment and source identification of selected metals in freshwater sediments – a case study from Mangla Lake, Pakistan. Environ Nanotech Monit Manag 4:27–36
31. Muller G (1979) Schwermetalle in den sedimenten des Rheins Veranderungen seitt 1971. Umschau 79:778–783. (in German with English abstract).
32. Jaishankar M, Tseten T, Anbalagan N, Mathew BB, Beeregowda KN (2014) Toxicity, mechanism and health effects of some heavy metals. Interdis Toxicol 7:60–72

33. Carafoli E (1987) Intracellular calcium homeostasis. Annu Rev Biochem 56:395–433
34. Mannstadt M, Bilezikian JP, Thakker RV, Hannan FM, Clarke BL, Rejnmark L, Mitchell DM, Vokes TJ, Winer KK, Shoback DM (2017) Hypoparathyroidism. Nat Rev Dis Primers 3:17055. https://doi.org/10.1038/nrdp.2017.55
35. Gautam S, Talatiya A, Patel M, Chabhadiya K, Pathak P (2018) Personal exposure to air pollutants from winter season bonfres in Rural areas of Gujarat, India. Expo Health. https://doi.org/10.1007/s12403-018-0287-9
36. Pathak P, Srivastava RR, Ojasvi (2017) Assessment of legislation and practices for the sustainable management of WEEE in India. Renew Sustain Energy Rev 78:220–232
37. Feng J, Yu H, Su X, Liu S, Li Y, Pan Y, Sun JH (2016) Chemical composition and source apportionment of PM 2.5 during Chinese Spring Festival at Xinxiang, a heavily polluted city in North China: fireworks and health risks. Atmos Res 182:176–188

Index

P. Pathak, D. K. Gupta (eds.), *Strontium Contamination in the Environment*,
The Handbook of Environmental Chemistry 88,
https://doi.org/10.1007/978-3-030-15314-4